



TECHNISCHE UNIVERSITÄT MÜNCHEN

Wissenschaftszentrum Weihenstephan für Ernährung, Landnutzung und Umwelt

Lehrstuhl für Analytische Lebensmittelchemie

Mass spectrometry based metabolomics to follow the prebiotic and probiotic impact on the human gut microbiome

Tanja Verena Maier

Vollständiger Abdruck der von der Fakultät für Wissenschaftszentrum Weihenstephan für Ernährung, Landnutzung und Umwelt der Technischen Universität München zur Erlangung des akademischen Grades eines

Doktors der Naturwissenschaften

genehmigten Dissertation.

Vorsitzender: Prof. Dr. M. Klingenspor

Prüfer der Dissertation:

1. apl. Prof. Dr. P. Schmitt-Kopplin
2. Prof. Dr. M. Rychlik
3. Prof. Dr. D. Haller

Die Dissertation wurde am 04.05.2017 bei der Technischen Universität München eingereicht und durch die Fakultät Wissenschaftszentrum Weihenstephan für Ernährung, Landnutzung und Umwelt am 12.10.2017 angenommen.

*„Habe dich sicher
In meiner Seele
Ich trage dich bei mir
Bis der Vorhang fällt“*

Herbert Grönemeyer, Der Weg

For my father

Acknowledgements

First of all, I would like to thank my supervisor Prof. Dr. Philippe Schmitt-Kopplin. Thank you very much for your support and trust, believing in me and giving me the opportunity working on fascinating and incredible projects. I had an incredibly great and memorable time during the past years and I am very grateful that I was part of your exceptional group.

I thank Prof. Dr. Janet Jansson for her exceptional cooperation, lead and support in the dietary study project. I'm also very grateful for the opportunity to spend enjoyable, informative and productive weeks at the Pacific Northwest National Laboratory (PNNL) in Richland, WA. Thank you very much to everyone who was involved and participated in the dietary study project. Only the close cooperation made the high quality results and the paper possible. I want to thank Dr. Jörg Bernhardt and Prof. Dr. Katharina Riedel for the magnificent opportunity to avail their Voronoi TreeMaps visualization technique. It was a great gain for the dietary study.

I thank the Töpfer GmbH, Prof. Dr. Dirk Haller, Monika Bazanella and the whole team behind it for lining up such an incredible interesting, exciting and simultaneously challenging project. Thank you for all informative and productive project meetings, which always pushed forward our goals up to our marvelous paper. Thank you, Monika for an exceptional cooperative work and the mutual support in this study. It was my pleasure work together with you and being part of this study.

I would like to thank Brigitte Look for her support in the laboratory. Thank you very much Brigitte for spending plenty of time in the lab to prepare my samples. Your brilliant sample preparation made these great results in my thesis possible. A big thank you goes also to Dr. Marianna Lucio for always having time for me, having great ideas, good discussions, as well as for encouraging me to deal with the most helpful R and of course for her support in statistics. I also want to thank Dr. Basem Kanawati for his support at the FT-ICR-MS. Thank you to my seatmate Kirill Smirnov for his support in programming and help with statistical issues, as well as for several funny moments in our office. Similarly, I would like to thank all people in our office, where we spend lots of time together and share the one or the other inspiring discussion, as well as special and funny moment: Theresa Bader, Sabine Dvorski, Kirill Smirnov, Yan Li and Dr. Chloé Roullier-Gall. Many thank you to Dr. Michael Witting and Dr. Alesia

Walker for enlightening discussions and their briefing and support at the maXis and data processing, especially at the beginning of my thesis. Thanks to Wendelin Koch and Daniel Hemmler when I once again needed a strong man at the maXis. A special thank you goes to Dr. Silke Heinzmann for being an important member of my thesis committee, for her support and inspiring and enlightening discussions, as well as for proof-reading. I also want to thank Astrid Bösl for her strenuous efforts and support in various matters. It's my pleasure knowing you. I am grateful to know Hans-Christian Rudloff, with whom I could entrust and talk about many things and who was a great support for this thesis.

A very special thank you goes to Sabine Dvorski, Jenny Uhl and Dr. Constanze Müller for incredibly wonderful and funny past years, memorable moments and very revealing discussions. I am very grateful and happy I met each one of you and to call you my friends. I am unspeakably thankful that you were there for me in bad times and that I could always rely on you in good and bad times. Thank you that I can be the one I am. I look forward to many, many more splendid years of this friendship. Thank you, Sabine for your motivation, your everlasting support, our talks and for always having an open ear for me. Thank you, Jenny for your support and motivation and being always there for me. Thank you Constanze for giving me the opportunity to get away from everyday life during thesis writing and to spend incredible lovely times with you and your kids.

A great thank you goes to Maren Locher for being my friend for already such a long time, who had to listen to one or the other scientific problem. Thank you for the necessary distraction during my studies and the doctoral thesis.

Zu guter Letzt gilt ein unbegrenzt großer Dank meiner Familie, die immer an mich geglaubt und mich mein ganzes Leben lang in all meinen Entscheidungen und Vorhaben unterstützt hat, was letztendlich diese Arbeit ermöglicht hat. Danke Mama, dass du immer für mich da bist! Hab dich lieb.

Auch wenn du nicht mehr da bist und das hier nie lesen wirst: Danke Papa, für eine wundervolle Kindheit. Dein Tod und meine Trauer hatten mich in ein tiefes Loch gerissen. Dieser frühe Verlust jedoch hat mich stärker gemacht. Ich habe gelernt nicht aufzugeben, meine Ziele nicht aus den Augen zu verlieren und dass es sich lohnt für das was man wirklich möchte zu kämpfen. All dies hat diese Arbeit ermöglicht und ich bin mir sicher, wenn du noch hier wärst, dann wärst du stolz auf mich.

Summary

The human gastrointestinal tract and its microbiome is a complex ecosystem. It is involved in several nutritional, physiological, immunological, and protective functions in the human body and is central to understand the dynamics of health and disease. Nutrition affects the intestinal microbial community, whereas the metabolism is strongly affected as well. Healthy nutrition can prevent diseases, whereas malnutrition can promote them, such as inflammation and infections, gastrointestinal diseases, as well as diabetes and obesity. Food additives, such as prebiotics or probiotics are of vast interest to induce health-promoting effects on the human gut microbiome. In order to understand how diet affects the gut microbiome, the comprehensive global metabolome is studied. Therefore, the aim of this thesis was to evaluate the impact of pre- and probiotics on the fecal metabolome by comprehensive analytical techniques, including ultra-high performance liquid chromatography and ultra-high resolution mass spectrometry. Through metabolomics analyses, the gut microbiota can be directly compared to the metabolic outcome in the host. For that reason, different non-targeted metabolomics methods were applied and results used to guide a subsequent series of targeted metabolite analyses. In order to unravel the complex interplay between organisms, metabolites and functional processes, additional 16S sequencing and shotgun proteomics complemented the analysis. Fecal samples of adults suffering from insulin resistance were analyzed after diets with varying amounts of resistant starch. Metabolites of various chemical classes were strongly affected by digestion of different prebiotics, including lipids, specific fatty acids, bile acids, oxylipins and several compounds of the lipid metabolism. Genomics and proteomics revealed microbes and a number of proteins altered through dietary starch arising as high abundant levels of *Firmicutes* and characteristic proteins of the lipid metabolism as well. In the second study, the impact of probiotics on infants' gut microbiome in the first year of life was studied. Metabolomics revealed different metabolite profiles between breastfed and formula-fed infants converging over time, which was not only seen in the differently affected bile acids, but also in carboxylic acids and numerous fatty acids, varying in chain length and saturation degree. Several distinct metabolic effects were seen that made the use of formula feeding more similar to breast milk. This finding lead to the assumption that probiotic supplementation may help to approximate breast milk, which strengthened the use of probiotics. However, these results cannot yet be explained, but for the moment were suggestively an initial sign for the effects of probiotics. Both studies impressively demonstrated the impact of pre- and probiotics and emphasized mass spectrometry based fecal metabolomics as a powerful tool to evaluate the status of the gut microbiome, but also to discover the impact of diet.

Zusammenfassung

Der menschliche Magen-Darm-Trakt und sein Mikrobiom sind ein komplexes Ökosystem, das in mehreren ernährungsbedingten, physiologischen, immunologischen und schützenden Funktionen im menschlichen Körper involviert ist. Um die Dynamik zwischen Gesundheit und Krankheit zu verstehen ist es von zentraler Bedeutung. Der Stoffwechsel und die Ernährung sind stark an die mikrobielle Darmgemeinschaft gekoppelt. Gesunde Ernährung kann Krankheiten verhindern, während Fehlernährung sie fördern kann, wie z.B. Entzündungen und Infektionen, Magen-Darm-Erkrankungen, sowie Diabetes oder Fettleibigkeit. Um eine gesunde Entwicklung des menschlichen Darmmikrobioms zu erreichen, ist der Verzehr von Lebensmittelzusatzstoffen, wie Präbiotika oder Probiotika von großem Interesse. Ziel dieser Arbeit war es daher, durch umfassende analytische Techniken, einschließlich Ultra-Hochleistungs-Flüssigkeitschromatographie und hochauflösender Massenspektrometrie, die Einflüsse von Prä- und Probiotika anhand von Metaboliten in Stuhlproben zu bewerten. Durch Metabolomikanalysen kann die Darmmikrobiota direkt mit der metabolischen Auswirkung im Wirt verglichen werden. Aus diesem Grund wurden verschiedene nicht-zielgerichtete Metabolom-Methoden angewendet und deren Ergebnisse dazu verwendet, nachfolgende zielgerichtete Metaboliten-Analysen durchzuführen, um erhaltene Ergebnisse zu validieren. Um das komplexe Zusammenspiel von Mikroorganismen, Metaboliten und funktionalen Prozessen zu untersuchen, wurde die Studie durch zusätzliche 16S-Sequenzierung und „Shotgun“ Proteomik ergänzt. Stuhlproben von Erwachsenen, die an Insulinresistenz leiden, wurden nach verschiedenen Diäten mit unterschiedlichen Mengen an resistenter Stärke (Präbiotika) untersucht. Metabolite verschiedener chemischer Klassen wurden durch die Verdauung verschiedener Präbiotika stark beeinflusst, darunter waren unter anderem Lipide, spezifische Fettsäuren, Gallensäuren, Oxylipine und mehrere Metabolite des Lipidstoffwechsels. Auf Grund der Einnahme von resistenter Stärke zeigten die Genomik und Proteomik Analysen ein erhöhtes Auftreten von *Firmicuten* und eine Vielzahl an Proteinen des Lipidstoffwechsels. In der zweiten Studie wurde der Einfluss von Probiotika auf das Darmmikrobiom der Kinder im ersten Lebensjahr untersucht. Metabolomikanalysen zeigten verschiedene Metabolitenprofile zwischen gestillten Kindern und denen, welche mit Muttermilchersatzmilch gefüttert wurden. Die Metabolitenprofile konvergierten im Laufe der Zeit, was sich nicht nur in den unterschiedlichen Profilen verschiedener Gallensäuren gezeigt hat, sondern auch in Carbonsäuren und zahlreichen Fettsäuren mit unterschiedlicher Kettenlänge und Sättigungsgrad. Darüber hinaus zeigten mehrere Metabolite in der Probiotika-Gruppe ein ähnliches Verhalten, wie in der Gruppe in der die Kinder gestillt wurden. Dieses Ergebnis führte zu der Annahme,

dass Probiotika ähnliche charakteristische Merkmale wie die Muttermilch aufweisen könnten, was die Einnahme von Probiotika bestärkt. Allerdings können diese Ergebnisse noch nicht erklärt werden, sind aber für den Augenblick erste Hinweise für die Auswirkungen von Probiotika. Beide Studien zeigten eindrucksvoll die Einflüsse von Prä- und Probiotika und dass die Massenspektrometrie basierte Metabolomik von Stuhlproben sich besonders dazu eignet, die Auswirkungen der Ernährung auf das menschliche Darmmikrobiom zu untersuchen.

Table of Contents

Acknowledgements	iv
Summary	vi
Zusammenfassung	vii
Table of Contents.....	ix
List of Tables.....	xiii
List of Figures	xv
Abbreviations and Symbols	xvii
1 Introduction	1
1.1 The Metabolome, Metabolomics and their key roles in biochemical processes in the “omics”-family	1
1.1.1 Non-targeted vs. targeted metabolome analysis – dealing with the unknown	2
1.1.2 Lipidomics as part of systems biology	3
1.2 Methods, sample preparation and analytical techniques in Metabolomics	5
1.2.1 Chromatography.....	5
1.2.2 Mass Spectrometry	7
1.2.2.1 Electrospray ionization	8
1.2.2.2 Fourier transform ion cyclotron resonance mass spectrometry	8
1.2.2.3 Ultra-high resolution Time-of-Flight mass spectrometry	10
1.2.2.4 Tandem mass spectrometry (MS/MS).....	12
1.2.3 UV-Vis spectroscopy	13
1.3 More about other „omics“-sciences	13
1.3.1 Genomics – Deoxyribonucleic acid and the Genome.....	13
1.3.2 Proteomics – Proteins and the Proteome.....	14
1.4 The human intestinal tract, the gut microbiota in health and disease	15
1.4.1 Nutritional impact on the human gut microbiome	17
1.4.1.1 Impact of prebiotics and probiotics on the human gut microbiome.....	18
1.4.2 Nutritional impact on the metabolome, including metabolite classes and their diversity.....	19
1.5 Data handling, processing and statistical evaluation – a metabolomics workflow	22
1.5.1 Unsupervised and supervised methods in multivariate data analysis.....	22
1.6 Thesis structure	25
2 Effect of resistant starch on the gut microbiome.....	28
2.1 Introduction	28
2.2 Study design and objective.....	30
2.3 Material and Methods	32

2.3.1	Metabolomics	32
2.3.1.1	Metabolite extraction	32
2.3.1.2	Metabolomics using direct infusion FT-ICR-MS analysis	32
2.3.1.3	Data processing	33
2.3.1.4	Multivariate Data Analysis: unsupervised and supervised techniques	33
2.3.1.5	Significance testing, data handling and visualization.....	34
2.3.1.6	Lipidomics approach by UHPLC-ToF-MS for MS/ MS analysis.....	34
2.3.1.7	Short-chain fatty acid analysis.....	35
2.3.2	Genomics analysis	37
2.3.2.1	DNA extraction, library preparation, and sequencing	37
2.3.3	Proteomics analysis	38
2.3.3.1	Protein extraction	38
2.3.3.2	Metaproteomics approach.....	38
2.3.4	Multi-omics statistical analyses	38
2.3.4.1	Network analysis: context likelihood of relatedness (CLR) method.....	38
2.3.4.2	Supervised ordination approach for multi-omics correlation.....	39
2.3.5	Visualizing complex genomic and proteomic data via Voronoi Treemaps.....	39
2.4	Results and Discussion	41
2.4.1	Metabolomics perspective of positive and negative ionization techniques	41
2.4.1.1	Global fecal metabolome analysis due to different diets	41
2.4.1.2	OPLS-DA for metabolite discrimination applied on different classification models	46
2.4.1.3	Correlation studies: metabolome and the amount of resistant starch.....	53
2.4.1.4	Lipid metabolism affected by high resistant starch.....	57
2.4.1.5	Different compound classes affected through baseline, HRS or LRS diet.....	61
2.4.1.5.1	Lipid patterns changed through baseline, HRS and LRS diet	61
2.4.1.5.2	Importance and differences of fatty acids in the human fecal metabolome.....	67
2.4.1.5.3	Oxylipins, Hydroxy Fatty Acids and Octadecanoids.....	72
2.4.1.5.4	Short-chain fatty acid profile though dietary starch intake.....	75
2.4.2	Impact of resistant starch on the microbiome: genome and proteome level.....	77
2.4.2.1	Dynamics of the human microbiome in response to a resistant starch diet: genome level.....	77
2.4.2.2	Dynamics of the human microbiome in response to a resistant starch diet: proteome level	79
2.4.3	Multi-omics data integration	83
2.4.3.1	Supervised ordination approach for multi-omics correlation.....	84
2.4.3.2	Mass-difference network analysis	85
2.5	Summary and Conclusion	88
3	Impact of breast feeding and bifidobacteria-supplemented formula on the infant fecal metabolite profile in the first year of life	92
3.1	Introduction	92
3.2	Objective and Goals	94
3.2.1	Study design	95
3.3	Materials and Methods	97
3.3.1	Metabolite extraction of fecal samples	97
3.3.2	Non-targeted UHPLC-ToF-MS metabolite analysis of fecal methanol extracts	97

3.3.3	Automated data processing of high throughput samples.....	98
3.3.4	Data filtering, metabolite annotation and classification.....	100
3.3.5	Fatty acid analysis, focusing on SCFA and MCFA, lactic acid and pyruvic acid	100
3.3.6	Standard operation procedure: metabolite profiling using RP- UHPLC-MS	101
3.3.7	Tandem mass spectrometry (RP- UHPLC-(+/-)-ToF-MS/MS)	101
3.3.8	Visualization, software and statistical evaluation.....	102
3.4	Results and Discussion	103
3.4.1	Comparison of exclusively breastfed and formula-fed, respectively and mixed fed infants	103
3.4.2	Differences in the fecal metabolome of exclusively fed (breastfed vs. formula-fed) infants.....	104
3.4.2.1	In the first year of life	104
3.4.2.2	Breastfed vs. interventional formula fed (F+) vs. placebo formula-fed (F-) by the month	109
3.4.2.3	Pathway analysis - affected by nutrition - KEGG metabolic pathway analysis	111
3.4.2.4	Impact on the bile acid metabolism through breast- and formula feeding	113
3.4.2.5	Intermediates of the tocopherol metabolism increased in formula fed infants	121
3.4.2.6	Fatty acids and derivatives altered in breastfed and formula-fed infants.....	124
3.4.2.7	Impact of different feeding types on the SCFA profile (breastfed vs. formula-fed)	130
3.4.3	Differences in non-probiotic fed and probiotic fed infants.....	137
3.4.4	Correlation studies between OTUs and fecal metabolites of breast- and formula-fed infants	142
3.4.5	Delivery effects on the infant fecal metabolome	148
3.5	Summary and Conclusion	150
4	Thesis summary and concluding remarks	152
5	Supplementary data	156
5.1	Dietary study.....	156
5.1.1	MS/MS identification experiments	156
5.2	InfantBio-study.....	158
5.2.1	MS/MS identification experiments	158
5.2.1.1	Bile acids.....	158
5.2.1.2	Fatty acids altered in either breastfed or formula-fed infants.....	159
5.2.1.3	Unknowns, but highly significant affected by either breast milk or formula.....	160
5.2.1.3.1	(+) ToF-MS	161
5.2.1.3.2	(-) ToF-MS	162
5.2.1.4	Differences in F+ and F-, MS/MS spectra of discriminating features.....	163
6	Appendix.....	164
6.1	Tables of the dietary study	164
6.1.1	Chemicals and other consumable material	164
6.1.2	Instrument Setup.....	164
6.1.2.1	FT-ICR-MS.....	164
6.1.2.2	UHPLC-ToF-MS conditions.....	165
6.1.2.3	Other Instruments.....	166
6.1.3	OPLS-DA for metabolite discrimination applied on different classification models	166
6.1.4	Correlation studies: impact of the amount of RS on the metabolite profile.....	167
6.1.5	Lipid metabolism affected by high resistant starch	170

6.1.6	Metabolite classes impacted through baseline, HRS and LRS diet.....	172
6.1.6.1	Phosphatidic acids impacted through diet	172
6.2	Tables of the InfantBio Study	177
6.2.1	Chemicals and other consumable material	177
6.2.2	Instrument Setup	178
6.2.2.1	UHPLC-ToF-MS conditions	178
6.2.2.2	Other Instruments.....	180
6.2.3	Extrapolated metabolites for the discrimination of feeding and over time.....	181
6.2.4	Impact on the bile acid metabolism through breast- and formula-feeding	184
6.2.5	Intermediates of the tocopherol metabolism increased in formula fed infants	186
6.2.6	Fatty acids altered in breastfed and formula-fed infants.....	187
6.2.7	Impact of different feeding types on the SCFA profile (breastfed vs. formula-fed)	189
6.2.8	Differences in exclusively non-probiotic fed and probiotic fed infants.....	190
6.2.9	Correlations between OTUs and Metabolites	190
	Literature	195
	Curriculum vitae.....	215
	Scientific Communications	216
	Eidesstattliche Erklärung	219

List of Tables

Table 2.3-1: External calibration results of the SCFA analysis.....	36
Table 2.4-1: OPLS-DA models to compare different diet set-ups.....	47
Table 2.4-2: Lipids changed due to baseline and dietary starch diets.....	66
Table 3.2-1: InfantBio study population characteristics.....	96
Table 3.3-1: SCFA results of the external calibration.....	101
Table 3.4-1: Core metabolites over time in all infants independent from feeding.....	108
Table 3.4-2: List of bile acid analyzed by UHPLC-(-)-ToF-MS.....	115
Table 3.4-3: Correlations between tocopherol and tocotrienol and the amount of formula fed.....	123
Table 3.4-4: Mean and individual range of SCFA, pyruvic and lactic acid concentrations (in $\mu\text{mol/L}$).....	131
Table 3.4-5: Pyruvic acid, lactic acid and SCFA significantly changed through diet.....	133
Table 3.4-6: Correlation between SCFA and OTUs of month 1, 7 and 12 in the different feeding groups.....	136
Table 3.4-7: Orthogonal signal corrected OPLS/O2PLS-DA results from different model comparison.....	142
Table 3.4-8: Correlation between feeding cohort specific metabolites and OTUs.....	145
Table 3.4-9: Correlation between feeding cohort specific metabolites and OTUs.....	147
Table 6.1-1: Chemicals.....	164
Table 6.1-2: Columns.....	164
Table 6.1-3: FT-ICR-MS: solarix™ Bruker Daltonik GmbH.....	164
Table 6.1-4: SCFA Analysis.....	165
Table 6.1-5: Lipidomics Approach.....	165
Table 6.1-6: Other Instruments.....	166
Table 6.1-7: Mass signals differed between the HRS diet at day 28 and day 56.....	166
Table 6.1-8: Top 50 metabolites highly correlated with resistant starch.....	167
Table 6.1-9: Top 50 metabolites negatively correlated with resistant starch.....	168
Table 6.1-10: Top 50 metabolites highly correlated with resistant starch analyzed in (+) FT-ICR-MS.....	169
Table 6.1-11: Metabolites of the lipid metabolism altered through baseline, HRS or LRS diet.....	170
Table 6.1-12: Phosphatidic acid altered in baseline diet.....	172
Table 6.1-13: Phosphatidic acids altered through LRS diet.....	172
Table 6.1-14: Phosphatidic acids altered through dietary starch intake.....	173
Table 6.1-15: Cyclic phosphatidic acids altered in baseline diet.....	173
Table 6.1-16: Fatty acids altered through the baseline, HRS or LRS diet.....	174
Table 6.1-17: Dicarboxylic acids significantly increased in HRS diet samples.....	175
Table 6.1-18: Oxylipins, Hydroxy Fatty acids and Octadecanoids significantly increased in HRS diet samples.....	175
Table 6.1-19: Sulfated Oxylipins, Hydroxy Fatty acids and Octadecanoids significantly increased in HRS diet samples.....	176
Table 6.1-20: SCFA profile in baseline, HRS and LRS diet samples.....	177
Table 6.2-1: Chemicals.....	177
Table 6.2-2: Consumable material.....	178
Table 6.2-3: Columns.....	178
Table 6.2-4: Non-targeted metabolomics analyses of fecal samples.....	179
Table 6.2-5: SOP: Metabolite Profiling using RP- UHPLC-MS.....	179
Table 6.2-6: SCFA Analysis.....	180

<i>Table 6.2-7: Other Instruments</i>	180
<i>Table 6.2-8: Significant features for all exclusively breastfed infants changed over time.</i>	181
<i>Table 6.2-9: Significant features for all exclusively formula-fed infants changed over time.</i>	181
<i>Table 6.2-10: Significant features for all exclusively breastfed infants changed over time.</i>	182
<i>Table 6.2-11: Significant features for all exclusively formula-fed infants changed over time.</i>	183
<i>Table 6.2-12: Bile acids altered through breast- and formula-feeding over time</i>	184
<i>Table 6.2-13: Bile acids differently altered through interventional formula and placebo formula.</i>	185
<i>Table 6.2-14: Metabolites of the tocopherol metabolism altered in formula-fed infants.</i>	186
<i>Table 6.2-15: Fatty acids altered between F+ and F- vs. breastfed</i>	187
<i>Table 6.2-16: Metabolites, altered between F+ and F- vs. breastfed.</i>	188
<i>Table 6.2-17: SCFA, pyruvic acid and lactic acid altered through either breastfeeding or formula feeding; *Mann-Whitney Test, ° post hoc Kruskal-Nemenyi test.</i>	189
<i>Table 6.2-18: Differences in exclusively non-probiotic fed and probiotic fed infants.</i>	190
<i>Table 6.2-19: Feeding Cohort Specific Metabolites and Correlation to OTUs of Month 1.</i>	190
<i>Table 6.2-20: Feeding Cohort Specific Metabolites and Correlation to OTUs of Month 7.</i>	191
<i>Table 6.2-21: Feeding Cohort Specific Metabolites and Correlation to OTUs of Month 12.</i>	192
<i>Table 6.2-22: Feeding Cohort Specific Metabolites and Correlation to OTUs of Month 1.</i>	192
<i>Table 6.2-23: Feeding Cohort Specific Metabolites and Correlation to OTUs of Month 7.</i>	193
<i>Table 6.2-24: Feeding Cohort Specific Metabolites and Correlation to OTUs of Month 12.</i>	193

List of Figures

Figure 1.1-1: Structural overview of the various lipid classes.....	4
Figure 1.2-1: Schematic over of principles of FT-ICR-MS.....	9
Figure 1.2-2: Schematic setup and principles of an orthogonal hybrid Q-ToF-MS (reflectron analyser) (adapted from the maXis™ user manual).....	11
Figure 1.6-1: Thesis structure	25
Figure 2.2-1: Study design to investigate the impact of resistant starch on the human gut microbiome.	31
Figure 2.4-1: Over view of the fecal metabolome visualized in unsupervised PCA scores scatter plots.	41
Figure 2.4-2: Unsupervised PCA scores scatter plots comparing the fecal metabolome	43
Figure 2.4-3: Unsupervised PCA scores scatter plots comparing the fecal metabolome due to different order. ...	44
Figure 2.4-4: Unsupervised PCA scores scatter plots comparing the fecal metabolome.	45
Figure 2.4-5: OPLS-DA scores scatter plot of fecal metabolome of HRS diet vs. LRS diet.	48
Figure 2.4-6: Differences between baseline and HRS diet at different time points	49
Figure 2.4-7: Overview of significant mass signals obtained through OPLS-DA.....	50
Figure 2.4-8: Mass signals classified into (A) number of compound classes and (B) main pathways.	52
Figure 2.4-9: OPLS-DA scores scatter plot of fecal metabolome comparing baseline and RS diets.....	53
Figure 2.4-10: Top 50 metabolites positively correlated with HRS, analyzed in (-) FT-ICR-MS.	54
Figure 2.4-11: Top 50 highly correlated metabolites analyzed in (+) FT-ICR-MS.	55
Figure 2.4-12: Top 50 metabolites negatively correlated with HRS, analyzed in (-) FT-ICR-MS.....	56
Figure 2.4-13: Metabolites of the lipid metabolism impacted through diet.....	59
Figure 2.4-14: Phosphatidic acids significantly decreased through dietary starch intake.....	62
Figure 2.4-15: Phosphatidic acids altered through LRS diet.	63
Figure 2.4-16: Phosphatidic acids increased through dietary starch intake.	64
Figure 2.4-17: Cyclic phosphatidic acids significantly increased in baseline diet.	64
Figure 2.4-18: Fatty acids significantly changed through diet.	68
Figure 2.4-19: Unsaturated fatty acids increased in baseline diet	69
Figure 2.4-20: Saturated fatty acids significantly increased in samples of LRS diet.....	70
Figure 2.4-21: Dicarboxylic acids significantly increased in the HRS diet.	71
Figure 2.4-22: Oxylipins and their sulfated conjugates significantly increased in the HRS diet.....	73
Figure 2.4-23: Hydroxy fatty acids and octadecanoids significantly increased in the HRS diet.....	74
Figure 2.4-24: Sulfated hydroxy fatty acids and octadecanoids significantly increased in the HRS diet.	75
Figure 2.4-25: SCFA profiles altered in participants consumed the baseline, HRS or LRS diet.....	76
Figure 2.4-26: Taxonomic treemap of 16S rRNA OTUs.....	78
Figure 2.4-27: Voronoi Treemaps at experimental stage „baseline“ with their specific microbiomes.	80
Figure 2.4-28: Taxonomic treemap of averaged species specific summarized protein counts.	81
Figure 2.4-29: Treemap of averaged bacterial protein specific counts.....	82
Figure 2.4-30: Multi-Omics integration through supervised ordination approach.	84
Figure 2.4-31: Multi-Omics integration displayed as CLR network.....	86
Figure 3.2-1: Study design of the InfantBio study.....	95
Figure 3.3-1: Genedata Expressionist® Refiner MS for Mass Spectrometry Workflow.....	99
Figure 3.4-1: Unsupervised PCA scores scatter plots comparing exclusively and mixed fed infants.....	103

Figure 3.4-2: Unsupervised PCA scores plots of exclusively fed infants over time.	105
Figure 3.4-3: Heatmap of the most abundant and discriminating metabolites over time.	106
Figure 3.4-4: Unsupervised PCA scores plots of exclusively fed infants month by month.	109
Figure 3.4-5: Unsupervised PCA scores plots of exclusively fed infants month by month.	110
Figure 3.4-6: Significantly changed main pathways of KEGG metabolic pathways by month.	112
Figure 3.4-7: Extracted Ion Chromatogram of bile acids.	115
Figure 3.4-8: Schematic overview of the primary bile acid biosynthesis adapted from KEGG pathway (Kanehisa and Goto 2000).	116
Figure 3.4-9: C24 bile acids changed over time in exclusively fed infants.	118
Figure 3.4-10: Differences in the bile acid profile between B, F- and F+ in month 1, 3 and 5.	120
Figure 3.4-11: Vitamin E metabolite patterns in breastfed and formula-fed infants.	121
Figure 3.4-12: Over time patterns of intermediates of the biosynthesis of tocopherols.	122
Figure 3.4-13: Saturated fatty acids increased in breast fed infants up to month 5.	125
Figure 3.4-14: Unsaturated long-chain fatty acids significantly increased in breastfed infants.	127
Figure 3.4-15: Dodecenedioic acid (A) and dihydroxyoleic acid (B) increased in formula-fed infants.	128
Figure 3.4-16: Hydroxyphenyllactic acid increased in breastfed infants over time.	129
Figure 3.4-17: Extracted ion chromatogram of SCFA, lactic and pyruvic acid.	130
Figure 3.4-18: Pyruvic acid, lactic acid and SCFA impacted through diet.	132
Figure 3.4-19: Correlation between SCFA and OTUs of month 1, month 7 and month 12.	135
Figure 3.4-20: Lysophosphatidylethanolamine LysoPE(15:0) significantly increased in F- infants.	138
Figure 3.4-21: Mass signals at early life significantly changed through placebo or interventional formula.	139
Figure 3.4-22: Mass signals at month 1 significantly changed through placebo or interventional formula.	140
Figure 3.4-23: Mass signals significantly changed through placebo or interventional formula later in life.	141
Figure 3.4-24: Correlation studies between metabolites and OTUs at month 1, 7, and 12.	143
Figure 3.4-25: Correlation studies between metabolites and OTUs at month 1, 7, and 12.	144
Figure 3.4-26: Correlation studies between metabolites and OTUs at month 1, 7, and 12.	146
Figure 3.4-27: Differences in the metabolite profile due to cesarean or vaginal delivery in month 1.	149
Figure 5.1-1: Identification of (A) decanoic acid, (B) dodecanoic acid, and (C) tetradecanoic acid.	156
Figure 5.1-2: Fatty acids in the human fecal metabolome significantly increased in the baseline diet.	157
Figure 5.2-1: Experimental (-)-ToF-MS/MS spectra of bile acid sulfate conjugates.	158
Figure 5.2-2: Experimental (-)-ToF-MS/MS spectra of primary bile acids.	158
Figure 5.2-3: Experimental (-) ToF-MS/MS spectra of bile acid glycine conjugates.	159
Figure 5.2-4: Experimental (-)-ToF-MS/MS spectra of metabolites increased in breastfed infants.	159
Figure 5.2-5: Experimental (-)-ToF-MS/MS spectra of fatty acids increased in formula-fed infants.	160
Figure 5.2-6: Experimental (+) ToF-MS/MS spectra of unknown features increased in formula-fed infants.	161
Figure 5.2-7: Experimental (+) ToF-MS/MS spectra of unknown features increased in breastfed infants.	162
Figure 5.2-8: Experimental (-)-ToF-MS/MS spectra of unknown features increased in formula-fed infants.	162
Figure 5.2-9: Experimental (-)-ToF-MS/MS spectra of unknown features increased in formula-fed infants.	163
Figure 5.2-10: Experimental (+) ToF-MS/MS spectra of unknown features increased in F+.	163

Abbreviations and Symbols

ACN	Acetonitrile
AMP ⁺	positively charged reagent for the derivatization of free carboxylic acids
ASCII	American Standard Code for Information Interchange (data format)
BA	Bile acids
bar	SI unit for pressure
CA	Cholic acid
CDCA	Chenodeoxycholic acid
CID	Collision-induced dissociation
CLR	Context likelihood of relatedness
COG	Cluster of Orthologous Groups of proteins
CPA	Cyclic phosphatidic acid
CS	Cesarean section
CV-ANOVA	Cross validation analysis of variance
CVD	Cardiovascular disease
δ	Chemical shift
Da	Dalton
DDA	Data dependent acquisition
df	Degrees of freedom
DG	Diradylglycerols
DI-MS	Direct infusion-MS
DNA	Deoxyribonucleic acid
EIC	Extracted ion chromatogram
ESI	Electrospray ionization
(+) ESI	Positive electrospray ionization
(-) ESI	Negative electrospray ionization
eV	Electron volt
FA	Fatty acyls/Fatty acids
FC	Fold change
FSH	Follicle-Stimulating Hormone
FID	Free induction decay
FT-ICR-MS	Fourier Transform Ion Cyclotron Resonance Mass Spectrometry
FWHM	Full width at half maximum
GC	Gas Chromatography
GCA	Glycocholic acid
GCDCA	Glycochenodeoxycholic acid
GC-MS	Gas chromatography-mass spectrometry
GIT	Gastrointestinal tract
GHz	Gigahertz
GL	Glycerolipids
GP	Glycerophospholipids
HC	High carbohydrate
HMDB	Human Metabolome Database
HMO	Human milk oligosaccharide
HOMA-IR	Homeostatic model assessment insulin resistance

<i>HPLC</i>	<i>High performance liquid chromatography</i>
<i>HRS</i>	<i>High resistant starch</i>
<i>IBD</i>	<i>Inflammatory bowel disease</i>
<i>IPA</i>	<i>Isopropyl alcohol</i>
<i>IT-MS</i>	<i>Ion trap-MS</i>
<i>KEGG</i>	<i>Kyoto Encyclopedia of Genes and Genomes</i>
<i>LAB</i>	<i>Lactic acid bacteria</i>
<i>LC</i>	<i>Liquid Chromatography</i>
<i>LCFA</i>	<i>Long-chain fatty acids</i>
<i>LC-MS</i>	<i>Liquid chromatography-mass spectrometry</i>
<i>LCPUFA</i>	<i>Long-chain polyunsaturated fatty acid</i>
<i>LRS</i>	<i>Low resistant starch</i>
<i>LDL</i>	<i>Low Density Lipoprotein</i>
<i>LOG2 FC</i>	<i>Binary logarithm fold change</i>
<i>MCFA</i>	<i>Medium-chain fatty acids</i>
<i>MeOH</i>	<i>Methanol</i>
<i>mL</i>	<i>Milliliter</i>
<i>mL/min</i>	<i>Milliliter/Minute</i>
<i>MS</i>	<i>Mass Spectrometry</i>
<i>MHz</i>	<i>Megahertz</i>
<i>MS/MS</i>	<i>Tandem mass spectrometry</i>
<i>min</i>	<i>Minutes</i>
<i>m/z</i>	<i>Mass-to-charge ratio</i>
<i>nm</i>	<i>Nanometer</i>
<i>NMR</i>	<i>Nuclear magnetic resonance</i>
<i>OPLS-DA</i>	<i>Orthogonal partial least squares – discriminant analysis</i>
<i>OTU</i>	<i>Operational taxonomic unit</i>
<i>PA</i>	<i>Glycerophosphates/phosphatidic acid</i>
<i>PC</i>	<i>Phosphatidylcholine</i>
<i>p-corr</i>	<i>Correlation significance</i>
<i>PCA</i>	<i>Principal component analysis</i>
<i>PDA</i>	<i>Photodiode array detector</i>
<i>PE</i>	<i>Phosphatidylethanolamine</i>
<i>PG</i>	<i>Glycerophosphoglycerols</i>
<i>PK</i>	<i>Polyketide</i>
<i>PLD2</i>	<i>Phospholipase D2</i>
<i>PLS-DA</i>	<i>Partial least squares – discriminant analysis</i>
<i>PPARγ</i>	<i>peroxisome proliferator-activated receptor-gamma</i>
<i>ppm</i>	<i>Parts per million</i>
<i>PR</i>	<i>Prenol lipids</i>
<i>PS</i>	<i>Phosphatidylserine</i>
<i>psi</i>	<i>Pound-force per square inch</i>
<i>PUFA</i>	<i>Polyunsaturated fatty acid</i>
<i>Q²(Y)</i>	<i>Goodness-of prediction</i>
<i>Q-MS</i>	<i>Quadrupole-MS</i>
<i>QQQ-MS</i>	<i>Triple quadrupole-MS</i>
<i>Q-ToF-MS</i>	<i>quadrupole time-of-flight-MS</i>
<i>R²(Y)</i>	<i>Goodness-of-fit</i>
<i>RP</i>	<i>Reversed phase</i>

<i>rRNA</i>	<i>Ribosomal ribonucleic acid</i>
<i>RS</i>	<i>Resistant starch</i>
<i>SL</i>	<i>Saccharolipids</i>
<i>SCFA</i>	<i>Short-chain fatty acid</i>
<i>SOP</i>	<i>Standard operation procedure</i>
<i>SP</i>	<i>Sphingolipids</i>
<i>ST</i>	<i>Sterol lipids</i>
<i>T</i>	<i>Tesla</i>
<i>TG</i>	<i>Triacylglycerol</i>
<i>TMS</i>	<i>Tetramethylsilane</i>
<i>TOC</i>	<i>Total organic carbon</i>
<i>ToF</i>	<i>Time-of-Flight</i>
<i>TZD</i>	<i>Thiazolidinedione</i>
<i>UHR-qToF-MS</i>	<i>Ultrahigh resolution quadrupole time-of-flight mass spectrometry</i>
<i>UHPLC-MS</i>	<i>Ultrahigh-performance liquid chromatography – mass spectrometry</i>
<i>UHPLC-ToF-MS</i>	<i>Ultrahigh-performance liquid chromatography time-of-flight mass spectrometry</i>
<i>UV</i>	<i>Unit variance</i>
<i>UV-Vis</i>	<i>Ultraviolet-visible</i>
<i>VD</i>	<i>Vaginal delivery</i>
<i>WHO</i>	<i>World health organization</i>

Chapter I

1 Introduction

1.1 The Metabolome, Metabolomics and their key roles in biochemical processes in the “omics”-family

The metabolome is the final succeeding product of the genome (Dunn et al. 2005, Lattimer and Haub 2010) and represents the total amount of small molecules – the metabolites - in a living cell (Nicholson et al. 1999). The resulting scientific discipline called “Metabolomics” and the related “Metabonomics” term were defined by Fiehn and Nicholson (Nicholson et al. 1999, Fiehn 2002, Nicholson and Wilson 2003)

Alongside the other “omics” approaches, like genomics, transcriptomics and proteomics, metabolomics is one of the “omics”-disciplines in systems biology applied not only to investigate the metabolome. Metabolomics enables to complete the information received from the genome and proteome on a functional level, to characterize the phenotype and to study the complex function of the metabolites in many different regulatory processes inside or outside the cell (Villas-Boas et al. 2005). Further, metabolites are intermediates of biochemical processes and thus play a very important role in connecting different pathways in organisms (Villas-Boas et al. 2005).

The metabolome varies in response to different influences (e.g. nutrition, medication and physiology), individual influences in health and disease and the involvement of the gut microbiota in the biological processes and thus reveals the complexity of the metabolome. Metabolomics plays a role in several research areas such as medical and clinical research (e.g. cancer, nutrition, obesity and diabetes), fundamental research and environmental interests. Therefore, metabolomics is applied to many sample origins, comprising different body fluids (plasma, urine), microbiome (gut microbiota, feces), cells, tissues or aquatic samples. To give a small abstract of the complexity of the metabolome, it may consist of hydrophilic compounds, carbohydrates, alcohols, ketones, amino acids, fatty acids, lipids and many others, but in many cases the identity of several metabolites remains unknown. This complexity makes it nearly impossible to study the whole metabolome simultaneously (Villas-Boas et al. 2005). In metabolome analyses, mostly metabolites with a molecular mass < 1000 Dalton (Da) are analyzed. In this context, in metabolomics another distinction is made between non-targeted and targeted analysis.

1.1.1 Non-targeted vs. targeted metabolome analysis – dealing with the unknown

The aim of non-targeted or also called untargeted analyses is to get a global overview of the variety of metabolites and metabolite classes present in a biological system. Hereby, identification and/or quantification of the metabolites is not needed (Fiehn 2002). The dominating focus here is the characterization of the biological samples and the identification of the overall metabolite profiles in the given objective. Here, it is possible to combine various analytical techniques to analyze the metabolome (Villas-Boas et al. 2005).

The non-targeted approach is faced with many unknown metabolites, whose identification is time-consuming and costly (Bowen and Northen 2010). Furthermore, identification of metabolites is difficult and demanding, which poses many challenges of experimental and analytical nature (Peironcely et al. 2013). Even if the modern analytical techniques allow detecting hundreds or thousands of features within one analysis, it's nearly impossible to identify each detected feature. Currently available databases are not comprehensive and cover only a proportion of metabolites, which can be assigned to potential metabolites. Many metabolites in a complex matrix remain unknown, which correspond to either adducts, fragments, dimers or trimers or possibly new metabolites (Witting et al. 2015). Therefore, usually the most discriminant features obtained by statistical analyses will be selected for identification (Bowen and Northen 2010). In practice, not always well-known metabolites are responsible for class discrimination, but also the unknown ones. Therefore, different approaches for metabolite identification can be performed, whereas tandem mass spectrometry (Chapter 1.2.2.4) is widely used.

Conversely, in the targeted analyses a pre-defined set of metabolites is analyzed and quantified. These pre-defined metabolites usually belong to one class of metabolites (Fiehn 2002) as carbohydrates, fatty acids or lipids and usually comprise further sample preparation. Nowadays, for this characterization of metabolites further termini for the individual metabolite class analysis, including lipidomics for lipids (the lipidome) or glycomics for glycans (the glycome) were defined (Griffiths and Wang 2009). In general, there is no universal metabolomics approach for both types of analyses.

Additionally, many other periphrases of targeted and non-targeted analysis already exist, such as metabolite profiling and metabolic fingerprinting. Therefore, in 2007 Goodacre summarized the most common used analytical techniques for differently applied metabolome analysis (Goodacre 2007). Hereafter, an abstract of the table is summarized. For targeted metabolite analysis, high-performance

liquid chromatography (HPLC), gas chromatography mass spectrometry (GC-MS) and liquid chromatography mass spectrometry (LC-MS) are widely used, whereas for the non-targeted approaches, techniques with high, even ultra-high resolution and high performance, such as quadrupole time-of-flight mass spectrometry (Q-ToF-MS) or Fourier transform ion cyclotron resonance mass spectrometry (FT-ICR-MS) are used. In summary, the requirements to investigate the metabolome comprises the sample collection and preparation, the adequate analytical approach with appropriate sensitivity and selectivity (Fiehn 2002), which will further be described in detail in chapter 1.2.

1.1.2 Lipidomics as part of systems biology

Lipidomics became a biologically and analytically attractive technique to analyze the lipid content in a biological system and is able to complete the metabolome analyses. Lipids play important roles in many biological processes such as in energy storage, membrane lipids or as signal molecules (Witting et al. 2014) and even play a central role in gut physiology (Gregory et al. 2013). Thus, various classes of lipids are present in biological samples and already were classified by the Lipid Maps consortium (www.lipidmaps.org) into the following main classes with several subclasses: fatty acyls (FA), glycerolipids (GL), glycerophospholipids (GP), sphingolipids (SP), sterol lipids (ST), prenol lipids (PR), saccharolipids (SL) and polyketides (PK) (Fahy et al. 2005, Fahy et al. 2009). Another category of GP are lysolipids, emerging through the loss of one or both acyl groups (Gregory et al. 2013).

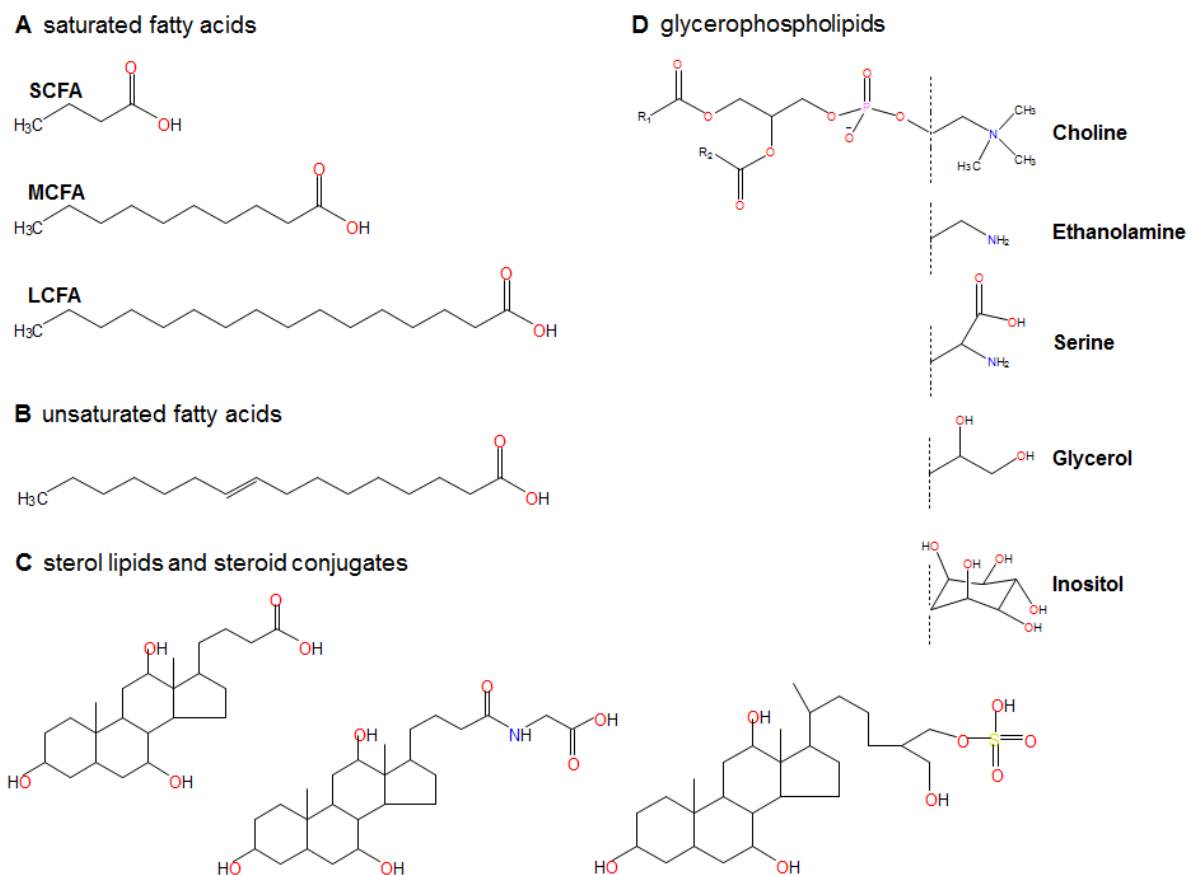


Figure 1.1-1: Structural overview of the various lipid classes.

A: saturated fatty acids differentiating in chain length in SCFA (C1:0 – C5:0), MCFA (C6:0 – C12:0) and LCFA (C13:0 – C22:0). B: unsaturated fatty acids (different chain length, mono-unsaturated and poly-unsaturated fatty acids possible). C: Sterol lipids and steroid conjugates with glycine or sulfate conjugation. D: Various classes of Glycerophospholipids with changing head groups, R1 and R2 can be fatty acids (with various chain length, double bonds and branches) bound by an ether or ester bond.

The variety and complexity of the lipids are impressive, as the combinations in lipids with different chain lengths, branches, side chains, double bonds, head groups, functional groups and other modifications are almost never-ending. To illustrate the complexity, Figure 1.1-1 shows some structural information of the various lipid classes (e.g. saturated/unsaturated fatty acids, STs and GPs). However, this complexity coincidentally poses difficulties in the analysis and differentiation of lipids with respect to isomeric and isobaric lipid species. The analytical technique is not only required to separate isomers, but also to sensitively detect and identify lipids from different classes. Therefore, a chromatographic separation with high performance coupled to a mass spectrometer with high resolution is one of the analytical approaches for lipidomics or lipid profiling applied, wherefore reversed phase (RP) columns using an acetonitrile (ACN) and isopropyl alcohol (IPA) gradient are commonly used (Bird et al. 2011,

Witting et al. 2014). In addition to lipid profiling, another method, called “shotgun lipidomics” is applied. Here, the crude lipid extract is analyzed by direct infusion into the MS (DI-MS) (Han and Gross 2005), without prior chromatographic or other separation methods. The major disadvantage of this method is the impossibility to separate closely related isomers (Witting et al. 2014), due to their similar physicochemical properties. Even if shotgun lipidomics is still at its early stage, it provides a convincing basis to investigate the lipidome in biological samples and shows its increasing potential to analyze thousands of lipid species (Han and Gross 2005).

1.2 Methods, sample preparation and analytical techniques in Metabolomics

Biological samples are complex by nature, with thousands of metabolites present and thus are characterized through their high chemical diversity. To analyze biological samples in a metabolomics manner, it requires not only the adequate sample collection and sample preparation, but also the appropriate analytical method. Current analytical techniques applied in Metabolomics are shortly described in the following chapters.

1.2.1 Chromatography

Chromatography is a powerful analytical technique and enables the separation of analytes of a complex mixture. It can be used for both, qualitative and quantitative analyses, wherefore typically, liquid chromatography (LC) and gas chromatography (GC) are used in metabolomics analyses. In LC, the sample is dissolved in a mobile phase. The mobile phase might be either liquid, gaseous or a supercritical fluid. The sample-mobile phase mix is carried over a stationary phase through either a pump (LC) or by overpressure (GC). Depending on their physicochemical properties, interactions between the analytes in the sample and the mobile/stationary phase takes place through e.g. hydrogen-bridges, van-der-Waals-forces, dipol-dipol interactions or hydrophobic interactions. This leads to a separation of the analytes. Afterwards, the analytes are detected by a suitable detector, such as a mass spectrometry (Chapter 1.2.2), fluorescence or UV-Vis spectrometer (Chapter 1.2.3).

One of the most commonly used methods in metabolomics is HPLC. This technique protrudes through its sensitivity, selectivity and its ability to separate non-volatile and thermal instable compounds (Skoog et al. 2013). Further, its application fields are extensive, comprising the analysis of amino acids, proteins, carbohydrates, steroids, lipids, pharmaceuticals and many more organic compounds. Since

every analyte has a different retention behavior, the choice of the stationary phase depends on the class of analytes that needs to be separated. In LC, nowadays most of the analyses in metabolomics are performed as RP chromatography (Dettmer et al. 2007), where non-polar functional groups are bonded on the silica surface, which acts as the stationary phase. Therefore, commonly used stationary phases in RP chromatography are modified silica particles with octyl (C8) or octadecyl (C18) chains covalently joined on the surface of silica. Usually, particle sizes from 3 μm to 10 μm see use in HPLC. In RP chromatography, polar mobile phases (e.g. methanol, isopropanol, ACN, water etc.) are used. In general, by applying a mobile phase gradient, changing the solvent composition from polar to a more organic rate within a run, medium polar to non-polar analytes get separated (Dettmer et al. 2007).

In addition to the classical HPLC, another method, the ultrahigh-performance liquid chromatography (UHPLC) gained a very strong market and has several benefits in contrast to HPLC. It stands out through its high resolution, efficiency and analysis time (Novakova et al. 2006, Lenz and Wilson 2007). To reduce the analysis time and improve the resolution, UHPLC is usually performed at pressures up to 1000 bar) and columns packed with particle sizes < 2 μm (Dunn et al. 2005, Griffiths and Wang 2009) are used. These benefits enable the UHPLC as the suitable analytical technique for complex biological samples as present in metabolome analyses.

There are several detection possibilities in chromatography, but the widely used technique in analytical chemistry is mass spectrometry (MS). Typically, mass spectrometers, quadrupole mass spectrometer (Q-MS), triple-quadrupole mass spectrometer (QQQ-MS), ion trap mass spectrometer (IT-MS) and quadrupole time-of-flight mass spectrometer (Chapter 1.2.2.3) are coupled to HPLC and UHPLC in metabolome analyses. A further possibility is the injection of the sample directly into the MS, without prior separation applied, as it is mainly the case in FT-ICR-MS, also known as DI-MS. Nevertheless, prior chromatographic separation of the analytes has four important advantages in contrast to DI-MS. First, it allows the separation of isomeric and isobaric compounds. Second, LC enables the analysis of complex mixtures and allows analyzing a broad range of metabolites without prior derivatization of the metabolites (Khakimov et al. 2014). Third, matrix effects and ionization suppressions are reduced due to prior separation of the analytes. Fourth, additional data is provided (e.g. retention time) (Lin et al. 2010, Lei et al. 2011, Muller et al. 2013). On the downside, one major drawback of LC remains the

moderate throughput, wherefore the analysis of hundreds or even thousands of samples, such as present in high cohort metabolomics studies, utilizes some time.

1.2.2 Mass Spectrometry

Mass spectrometry (MS) enables the analysis of complex biological samples, as it is required in metabolomics, wherefore it became the most used technique in metabolome research. In general, a mass spectrometer consists of three basic components: an ion source, a mass analyzer and a unit for detecting the ions. Hereto, details about the electrospray ionization (ESI) technique are given in Chapter 1.2.2.1. Further, in the following chapters, two mass analyzers will be described in detail: FT-ICR-MS and the high resolution Time-of-Flight mass spectrometer (UHR-ToF-MS). Both mass analyzers are highly suitable for non-targeted metabolomics and metabolite identification due to their high mass resolving power (Gowda and Djukovic 2014). MS has the potential to detect and identify metabolites based on their mass-to-charge ratio (m/z); it offers high sensitivity, high accuracy and a wide dynamic range (Lin et al. 2010). This is displayed by highly specific chemical information, accurate masses, resolving power and mass resolution, as well as the detection of isotope patterns, provided through the MS analyses.

Mass resolving power, mass resolution and mass accuracy, are important terms, which play notable roles in MS. The resolving power of an instrument is a performance parameter and usually is given as full width at half maximum (FWHM). The mass resolution (R) describes the ability to separate two closely neighbored mass signals, which gets very important dealing with complex samples. The mass accuracy is defined as the difference between the experimental mass and the exact calculated mass. The relative mass accuracy or mass error is given in parts per million (ppm), calculated as follows (Equation 1.2.2-1) (Gross 2011).

$$\text{relative mass error [ppm]} = \frac{m/z_{\text{experimentell}} - m/z_{\text{calculated}}}{m/z} \cdot 10^6$$

Equation 1.2.2-1: relative mass error calculation in ppm to characterize the mass accuracy, used in mass spectrometry.

According to current state-of-the-art in mass spectrometry, the FT-ICR-MS shows the highest resolving power with over 1,000,000 (Ghaste et al. 2016) and a mass accuracy < 0.2 ppm (Schmitt-Kopplin et al. 2010).

1.2.2.1 Electrospray ionization

The ESI technique is one of the well-known and frequently used ionization methods in metabolomics research. This technique is highly suitable for compounds with medium to high molecular weights, non-volatile and easily ionizable compounds, including a wide range of polar, unpolar and ionic compounds. ESI is a soft ionization technique, as the ionic analytes, dissolved in a volatile solvent, get evaporated at atmospheric pressure (Gross 2011). With the help of nebulizer gas (nitrogen) and through electrostatic nebulization, the sample is transferred into an aerosol. This is performed by applying high voltage on the ESI needle, which results in electrophoretic charge separation of the ions. Due to the evaporation of the solvent droplets, which is supported by a dry gas (nitrogen), the charge density is increasing. In consequence, smaller droplets are built through coulomb forces. This process of solvent evaporation and split-up of the droplets is repeating several times and highly charged micro droplets arise, which get conducted into the mass analyzer.

In ESI, two different polarities can be applied: positive (+) ESI and negative (-) ESI. Each polarity enables the ionization of different, but also identical compounds, which is depending on their functional groups and ability to be ionized. In positive ionization mode, compounds usually get protonated, with adduct formation (e.g. sodium or potassium) possible, and in negative mode they get deprotonated.

1.2.2.2 Fourier transform ion cyclotron resonance mass spectrometry

Fourier transform ion cyclotron resonance mass spectrometry (FT-ICR-MS) is a benefitting analytical approach for metabolomics research. The ultra-high resolving power up to 1,000,000, the high mass accuracy (< 0.2 ppm) (Schmitt-Kopplin et al. 2010) and its high mass range (Marshall et al. 1998), enables the FT-ICR-MS as highly suitable for complex biological samples as given in metabolome research. The fundamental principle behind, is the motion of a charged analyte in a magnetic field. Classically, ICR-MS enables ions to be excited to a higher trajectory and measures the absorption of energy of an excited oscillator (Gross 2011).

The main components of an FT-ICR-MS are: ion source, optical lenses, ion traps and guides (quadrupole, octapole and/or multipole), a superconducting magnet and the core part, the ICR cell. Figure 1.2-1 schematically illustrates the principle and the setup of an FT-ICR mass spectrometer.

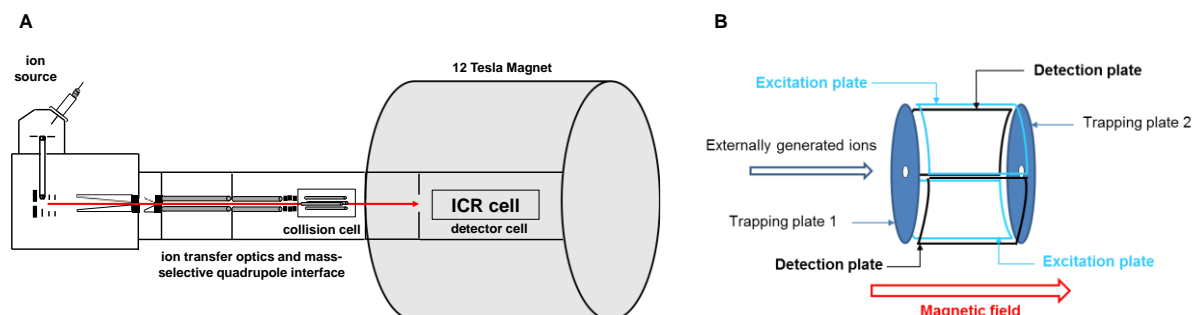


Figure 1.2-1: Schematic overview of principles of FT-ICR-MS.

A: Schematic setup, including ion source, ion optics, quadrupole, octapole, ICR cell (plus superconducting cryomagnet). B: ICR cell

First, ions get generated by an ion source, predominately with ESI and are perpendicularly focused by optical lenses into a spatial uniform magnetic field (caused by a superconducting magnet), where an octapole ion guide and the ICR cell are located.

In the magnetic field, so in the ICR cell, the ions have to undergo the perpendicular Lorentz force, which bends the ion's velocity into a circular path, the ion cyclotron motion (Marshall et al. 1998). According to the mass and the strengths of the magnetic field, the ions have different radii circulating in the ICR cell. The masses get resolved by increasing the radii of the circulating ions and can further be detected. This is conducted by applying an electric field, which forces the ions to increase their movements and allows the excitation to a higher trajectory (Gross 2011). After the excitation, the circulating ions can be detected by additional conductive parallel electrodes (detector plates). Going through the detector plates, the ions induce a current, which is recorded as free induction decay (FID) due to the ion cyclotron motion. Fourier transformation converts it into a mass signal (Marshall et al. 1998, Gross 2011). Further descriptions of FT-ICR-MS with excellent and informative physical chemistry background are presented in (Marshall et al. 1998, Marshall 2000).

The outstanding advantage of ultra-high resolution and high mass accuracy allows the assignment of molecular formulas and further the classification of the elemental and molecular composition. Further,

FT-ICR-MS benefits in its low detection limits in the attomole to femtomole range (Dettmer et al. 2007). However, the separation of isomeric and isobaric compounds remains an issue, because the sample is infused all at once. Even if no prior chromatographic separation is needed for the analysis and it is mainly used in DI mode, the difficulty with matrix effects and ion suppression are increased, which may cause less sensitivity (Lin et al. 2010). However, FT-ICR-MS has been established as a high throughput technique with high sensitivity, being the ideal method for non-targeted metabolomics, due to the reasons mentioned above.

1.2.2.3 Ultra-high resolution Time-of-Flight mass spectrometry

Time-of-Flight mass spectrometry (ToF-MS) offers with its resolving power of up to 60,000 and a mass accuracy < 5 ppm (Zhang et al. 2012) a further analysis technique and appropriate solution in metabolome research. Here, the advantage is in coupling with chromatographic systems, whereas mainly LC instruments are used, which is often used for non-targeted metabolomics. The fundamental principle of ToF-MS is simple: the separation of ions (prior generated by ESI) is conducted by the time of flight of the ions with different m/z . The smaller/lighter the ion, the shorter is its flight time and therefore it gets detected first, compared to ions with higher/heavy size.

The main components of a ToF-system are: ion source, ion transfer and focusing funnels, quadrupole as mass filter, followed by a quadrupole as collision cell and the ToF mass analyzer. This is schematically demonstrated in Figure 1.2-2 using the example of a reflectron time-of-flight mass analyzer, the orthogonal hybrid quadrupole-ToF-MS (Q-ToF-MS), which was used in this thesis.

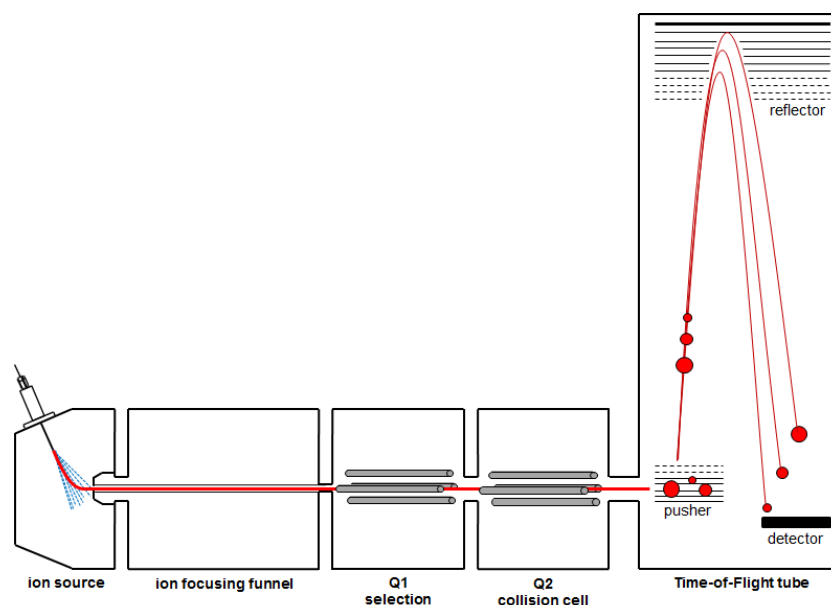


Figure 1.2-2: Schematic setup and principles of an orthogonal hybrid Q-ToF-MS (reflectron analyser) (adapted from the maXis™ user manual).

After the ionization, the ions are transferred and focused by a funnel system and a multipole into the following quadrupole units. The first quadrupole serves as mass filter and allows the selection of single m/z or m/z ranges. The second one is the collision cell and used differently according to the selected analysis mode. Here, the MS experiments can be applied in full scan mode, while the collision cell serves as a further transfer unit, leading the ions into the ToF analyzer. Further, MS/MS experiments can be performed by using collision-induced dissociation (CID) with an inert gas, which can be either nitrogen or noble gases. More details about MS/MS experiments, also known as tandem mass spectrometry (MS/MS) are given in chapter 1.2.2.4.

The last part is the ToF mass analyzer, which is composed of a pusher, a reflector and the detector. Separation takes place due to the different velocities of the different accelerated m/z (ions) and their corresponding flying time. In detail, the pusher shoves and accelerates the incoming ions from the collision cell orthogonally onto the reflector. Here, also the determination of the masses (m/z) takes place by measuring the drift time of the ions after the acceleration until their contact onto the detector unit. After the acceleration the potential energy of the ions is converted into kinetic energy. The reflector acts as a mirror for ions to which ions with different kinetic energy are focused (Gross 2011), improves the resolution and leads the ions back to a detector, which is converting the ion signal into an electrical signal. These signals are transmitted to a digitizer card and after several conversional steps, the signal results in a mass spectrum.

1.2.2.4 Tandem mass spectrometry (MS/MS)

For tandem-MS (MS/MS) experiments, the collision cell serves as a collision chamber for prior mass selected ions to be fragmented by applying different collision energies, where 10 eV to 50 eV are mainly applied. In other words, MS/MS allows the analysis and interpretation of the product ion mass spectra, through the prior m/z -selected precursor ions. Therefore, a commonly applied activation method in tandem-MS is CID, which allows the fragmentation of ions in a gas phase. This technique is highly suitable for structural analysis and/or especially in metabolomics for biomarker identification or metabolite classification of unknown metabolites.

In principle, the ions in a collision cell collide with the gas atoms of the inert collision gas. The collision causes a conversion of the ions' translational energy into internal energy and an excited stage (de Hoffmann and Stroobant 2007). Through statistical allocation of the internal energy in the ion, dissociation of the ion occurs (Gross 2011) and fragments are formed. The interpretation of the resulted mass spectra of those fragments is the primary step for the structural analysis of the metabolite and for metabolite identification. Usually, in an MS/MS experiment it is advisable to start with low collision energies (e.g. 10 eV or 20 eV), where the prior m/z -selected precursor ion is still visible and then increases the collision energies to 30 eV, 40 eV or even higher, which enables greater fragmentation. This step-wise increase of the collision energy results in a higher amount of fragment ions in relation to the precursor ion and provides additional information for the structural analysis.

Several MS/MS databases for the identification of compounds based on their fragmentation pattern are available, which are of great assistance in metabolite identification. To name but a few of the available MS/MS spectral databases: Metlin (Smith et al. 2005) or HMDB (Wishart et al. 2007) offer thousands of comprehensive MS/MS metabolite data. As a first classification, the experimental fragmentation pattern can be compared with database spectra of different collision energies and ionization modes. For further certainty in identification, the experimental fragmentation pattern of an analyte in a complex sample is compared to the experimental fragmentation pattern of one single standard measured exactly identical. However, the identification of metabolites remains challenging; especially since many metabolites are not listed in the MS/MS spectral databases and not always commercially available.

1.2.3 UV-Vis spectroscopy

In spectroscopy, molecules/atoms/nuclei are transferred from a low-energy ground state into a higher energy condition, whereby energy in the form of electromagnetic radiation or as electromagnetic waves is introduced. The absorbed frequency corresponds to the different energy levels of the molecule, which allows drawing inferences about the structure. The absorption of ultraviolet (UV) or visible (Vis) radiation is a two-stage process. In UV-Vis spectroscopy firstly, electronic transitions are excited, which means the irradiated energy is sufficient enough to lift electrons from an occupied to an unoccupied orbital. Secondly, wave lengths from 200 – 800 nm are consecutively shined in and the extinction of wave lengths is measured (Skoog et al. 2013). UV-Vis spectroscopy is especially applicable for valence electrons consisting of π -bonds and non-binding electron pairs. The presence of valence electrons, which can be excited to higher energy levels able all organic compounds to absorb radiation (Skoog et al. 2013). An UV-Vis detector mainly detects compounds, which display conjugated double-bond systems, double- and multiple bonds, as well as carbonyl groups. Therefore, UV-Vis spectroscopy is only applied for structural elucidation as a supplemental method to nuclear magnetic resonance (NMR) or MS and is usually used as a detector in chromatography.

1.3 More about other „omics“-sciences

The full range of the “omics”-sciences consist of four main research fields, including genomics (Chapter 1.3.1), transcriptomics, proteomics (Chapter 1.3.2) and metabolomics. Numerous network and feedback loop interactions coexist between the genome, transcriptome, proteome and metabolome and therefore they mutually affect the specific behavior of a biological system (Goodacre 2005, Bujak et al. 2015). The network of all those “omics”-sciences allows to get a global picture of the microbial community structure, the metabolic status and characterizing the personal phenotype (characteristics of an organism), and to unravel the dynamics and mechanisms in a given ecosystem (Perez-Cobas et al. 2013).

1.3.1 Genomics – Deoxyribonucleic acid and the Genome

Genomics is the study of an organism’s complete set of deoxyribonucleic acid (DNA - the genome). This allows gaining a deeper insight into the microbial community in a given biological system. Nowadays, this technique allows studying the DNA of several organisms at the same time and enables

the consideration about the relationship between microbial and human life (Rhodes et al. 2013). Genomics can also be taken from specific environments, such as the gut in order to investigate the genome of microorganisms (=metagenomics). The genome is investigated through sequencing techniques, which allow the assembling and analysis of the genomes' function and structure, while the exact order of the nucleobases (Adenine, Cytosine, Guanine, Thymine) in the DNA can be examined. The modern sequencing techniques, also called next generation sequencing, offer a wide spectrum for DNA-sequencing, including the 16S ribosomal ribonucleic acid (rRNA) sequencing, pyrosequencing or shotgun sequencing (shotgun metagenomics) (Erickson et al. 2012). The 16S rRNA sequences are often analyzed, because they serve as a proxy for the entire genome (Rhodes, Gligorov et al. 2013). It is widely used and enables the estimation of relationships among bacteria and the identification of unknown bacteria on the genus or species level (Sacchi et al. 2002).

In the study of complex microbial communities and their interactions in a host (e.g. in the human gut) (Smirnov et al. 2016), the DNA first is directly extracted from the environment, followed by a metagenomics analysis, which can be performed by using either 16S rRNA sequencing or as randomly environmental DNA sequencing (Rhodes et al. 2013). Afterwards, the obtained sequences can be retrieved in several databases and assigned to a specific taxonomic rank up to the species level. Further, the genes of the genome first are transcribed and translated to produce proteins (Verberkmoes et al. 2009), where one gene can encode more than one protein, which increases the complexity of the proteome in an organism as follows in the next chapter.

1.3.2 Proteomics – Proteins and the Proteome

Proteomics is the study of the entire complement of proteins, produced in an organism (the proteome). The proteome is a dynamic system and reflects the gene and the environment (Horgan and Kenny 2011). Therefore, it varies from time to time through different stresses that an organism is exposed to. Proteomics offers information on protein abundances, including their variations and modifications. It is applied to investigate for example the involvement of proteins in metabolic pathways, time and place of protein expression and the rates of protein production or degradation.

A relatively new method in proteomics analyses is shotgun metaproteomics, which is applicable for complex and highly diverse microbial communities, just as present in the human gut (Erickson et al.

2012) and in one of the most complex biological sample types until now: Feces (Verberkmoes et al. 2009). Additionally, it was demonstrated that microbial and human proteins can be differentiated and monitored simultaneously by applying shotgun proteomics (Young et al. 2015).

Among the several high-throughput techniques for proteome studies, the most commonly applied technique is MS, like tandem-MS (Horgan and Kenny 2011). MS based techniques allow further the characterization and quantification of thousands of proteins within a complex microbial community (Young et al. 2015). Furthermore, approaches with LC coupled to MS (e.g. 2D-LC-MS/MS) are, especially for shotgun metaproteomics, often applied. In proteomics analysis, thousands of ions are measured, whose peptide mass information afterwards need to undergo complex algorithms to search against protein database for identification (Horgan and Kenny 2011) (Verberkmoes et al. 2009). The human gut microbiota functions and metabolic activities can be characterized by applying microbial proteomics. This enables to reveal information about the microbiome development and their interactions with the human host (Xiong et al. 2015). The biological complexity, the function and the entirety of impacts (e.g. nutrition) on the human intestinal tract with respect to microbial communities, the genes, the metabolic activities and their role in the human immune system for the prevention and development of diseases is described in the following chapters.

1.4 The human intestinal tract, the gut microbiota in health and disease

The human gastrointestinal tract (GIT) and its microbiome is a complex ecosystem (Heintz-Buschart et al. 2016), which is central to understand the dynamics of health and disease. In numbers, more than 100 trillion microbes (10^{14}) are located in the GI (Lin et al. 2014), including 300 to 500 different bacterial species, with more than 2 million genes (Quigley 2013). Therefore, the bacterial genome is enormous (approximately 150–fold) in contrast to the human genome (Quigley 2013, Ursell et al. 2014). Amongst, the human intestine is one of the areas within the human body that is highly populated by microorganisms (mainly bacteria) (Rhodes et al. 2013). In mammals, four dominating bacterial phyla inhabit the gut: *Firmicutes*, *Bacteroidetes*, *Actinobacteria* and *Proteobacteria* (Qin et al. 2010). The entirety of living microorganisms in the human being, including bacteria, viruses, and fungi and their genetic material is referred to as the human microbiome (Lederberg 2003). In the gut or intestine, the gut microbiome comprises all gut inhabiting microorganisms, including their genes and genomes, as well as the microbiota and host metabolites (Whiteside et al. 2015). The gut microbiota (former: flora)

only refers to the microbial community. Up to now, feces is the most investigated material in examining the microbial composition and the metabolic interactions of the gut (Gerritsen et al. 2011). Additionally, each individual is characterized by its specific gut microbial composition, which therefore also could be used as an alternative way of individual fingerprinting (Quigley 2013). The intestinal microbial community strongly influences the metabolism and nutrition, the development of the immune system and prevents the colonization through pathogens (Pop et al. 2016).

At birth, the development and the population of the gut microbiome is initiated through the maternal and environmental bacteria. Subsequently, the population in the gut grows and assembles through different extraneous influences. This is induced by nutrition, genetics (Benson et al. 2010), contact to humans/animals (Song et al. 2013) and further environmental contacts. Later on in life, the population in the gut remains relatively constant (Quigley 2013). In this context, the impact of nutrition, with respect to prebiotics, and probiotics or breast milk on the human gut microbiome will be reviewed in detail in Chapter 1.4.1. However, even if the population in the gut remains relatively constant later in life, the gut microbiome is very plastic and is relatively susceptible to several factors, including diet, physiology, drugs, probiotics and microbial metabolites (Ursell et al. 2014).

Different gut microbes can alter metabolites throughout their host (Ursell et al. 2014), and their participation in various metabolic processes beneficially influence both, the host and the microbes (Quigley 2013). Through metabolomics analyses, the gut microbiota can be directly compared to the metabolic outcome in the host (Ursell et al. 2014). To discover this, several studies were designed, e.g. analyzing and comparing plasma samples from germ-free and conventionally raised mice. Wikoff et al. thereby investigated the impact of the gut microbiota on the host and found differed plasma metabolites between the two types of mice (Wikoff et al. 2009). Central importance of this beneficial interaction between the microbiota and host is the communication of bacteria inhabiting the gut and microorganisms with the host's immune system (Quigley 2013), which already develops at birth (Nicholson et al. 2012). Additionally, several microbe-derived metabolites have been found to influence health through effects on gut immune system. An overview of gut bacteria and their contributing metabolites with respect to potential biological functions in human health and disease is presented by Nicholson et al. (Nicholson et al. 2012).

Therefore, over the last decades, several studies were investigated the impact of the gut microbiome and/or the host-microbe interactions on the prevention and development of diseases. Just to cite a few, Hullar et al. investigated the impact of the gut microbiota on cancer and presented epidemiological evidence for the mutual impact of gut microbes, diet and cancer risk. The potential impact on cancer risk from gut microbial metabolism of specific metabolites was tabular illustrated (Hullar et al. 2014). As obesity, insulin resistance, and diabetes and thus metabolic disorders, reached worrying levels all over the world, lots of research to prevent, cure or regulate those diseases was accomplished - as presented in chapter 2.1. Bäckhed et al. studied the regulation of the host energy metabolism and fat storage in colonized pre-germfree mice and thereby highlighted the importance of the gut microbiota and its function in obesity and insulin resistance (Backhed et al. 2004). Moreover, Caricelli et al. studied the role of the gut microbiota on insulin resistance and obesity, and detected an increase of Firmicutes in the obese mice, compared to lean ones, which could be associated with insulin resistance (Caricilli and Saad 2013). The impact of the gut microbiota on inflammation, obesity, insulin resistance and metabolic disease is explicitly and nicely presented in several reviews (Shen et al. 2013, Boulange et al. 2016, Saad et al. 2016).

1.4.1 Nutritional impact on the human gut microbiome

Nutrition is important to ingest essential nutrients. However, the choice of food is sensitive, since over- and undernutrition as well as the selection of poor food compositions can trigger diseases. Nutrition can promote and prevent diseases (McNiven et al. 2011), such as inflammation and infections, gastrointestinal diseases, as well as diabetes or obesity (Flint et al. 2012). The human gut microbiota is involved in several nutritional, physiological, immunological, and protective functions in the human body (Salonen and de Vos 2014). Through fermentation of indigestible compounds, such as dietary fiber (e.g. resistant starch), the microbial community contributes nutrients and energy to the host (Flint et al. 2012, Ursell et al. 2014). For instance, humans are unable to produce metabolites, such as short-chain fatty acids (SCFA), some vitamins and also amino acids (Wong et al. 2006, Hamer et al. 2008). It was shown that short- and long term exposure to diets changes the microbial community composition (Flint et al. 2012). However, most of the microbial functions still remain unknown, but recently it was established that some bacteria in the human intestine are involved in food metabolism (Salonen and de Vos 2014). This comprises phyla of *Firmicutes* and *Bacteroidetes*, which predominantly affect the

nutrition and the corresponding nutritional metabolism (Ramakrishna 2013). Due to the current medical and nutritional interests, several studies in nutritional research in health and disease were accomplished in the last decades. They focused especially on the dietary modulation of the intestinal microbiota through prebiotics, such as dietary fiber. Also, the impact of probiotics on the human gut microbiome in all stages of life, ranging from infancy to childhood and adults is of vast interest.

1.4.1.1 Impact of prebiotics and probiotics on the human gut microbiome

Prebiotics are food additives and dietary non-digestible or slowly digestible, but partially fermented oligosaccharides. They are said to promote the growth, composition and activity of health-beneficial bacteria (e.g. bifidobacteria) in the intestine (Gibson and Roberfroid 1995, Walker et al. 2011, Thomas et al. 2014). Prebiotics supply the gut microbes, which further supply the host with energy and essential nutrients (Topping et al. 2007). It is expected, that the dietary intake in the form of prebiotics can prevent human diseases, such as IBD, obesity and diabetes (Holmes et al. 2012, Birt et al. 2013). Nowadays, numerous non-digestible carbohydrates, which serve as prebiotic food additives, are available, such as resistant starch (RS). RS consist up to 70 per cent predominately of amylopectin and amylose. High-amylose containing starches are resistant to the enzymatic digestion by amylase (Topping et al. 2007). Especially in the form of amylose and amylopectin, RS is qualified as a prebiotic (Topping et al. 2007). Already in the late '90s, Brown et al. demonstrated the effects of RS as prebiotic (Brown et al. 1997, Brown et al. 1998). They studied the potential of high-amylose starch in pigs and in mice. They found higher fecal concentrations and excretion of *Bifidobacterium longum* in fecal samples of pigs fed a conventional starch (Brown et al. 1997). In another study, mice were fed with high-amylose starch, whereas an increase of lactic acid bacteria (LAB) numbers was observed in the fecal samples (Brown et al. 1998). Also, the increase of *B. longum* in the pigs was similar to the impact of other prebiotics reported in several human studies. Bifidobacteria have potential benefits on the health of mammals (Conway 2001). Additionally, it could be observed that bifidobacteria were enhanced in breast fed infants. Therefore, the supplementation of bifidobacteria in infant formula is reasonable to induce health-promoting effects.

The world health organization (WHO) and the food and agriculture organization of the United Nations (FAO) defined probiotics as “*Live microorganisms which when administered in adequate amounts confer a health benefit on the host*” (WHO and FAO 2002, Bergmann et al. 2014). Probiotics promote

specific changes in the gut microbiota and then are integrated into the gut ecosystem (Delzenne et al. 2011). Several microorganisms serve as probiotics, whereas most of them are already naturally occurring in the human GIT, such as *Lactobacillus* and *Bifidobacterium*, including their multitude of species and strains (Holzapfel et al. 1998, Gerritsen et al. 2011). Also microorganisms of the genera *Streptococcus*, *Enterococcus*, *Propionibacterium*, as well as *Bacillus* strains, the *E. coli* strain Nissle 1917 and *Saccharomyces* strains (e.g. *S. boulardii*) (Holzapfel et al. 1998, Gareau et al. 2010) can be used as probiotics. However, not all probiotics provide the same beneficial effects and therefore need to be selected carefully according to the desired impact on the gut microbiome and their clinical use (Mileti et al. 2009). Further, bacteria envisaged as probiotics need to fulfill some criteria. These comprise the nonpathogenicity, being cultivable in industrial scale and having a health enhancing impact on the human gut microbiome (Holzapfel et al. 1998).

At birth, only facultative anaerobic bacteria can grow in the intestine of newborns (e.g. *Enterobacteriaceae*). After a while, anaerobic bacteria colonize the gut. Those are *Bifidobacterium*, *Clostridium* and *Bacteroides*. In the first few months, the diet of infants is either breast milk or formula. The diet of infants influences the bacterial composition of the gut, while breastfed infants have a bifidobacteria enriched gut microbiota, the gut microbiota of formula-fed ones is more diverse colonized (Hascoet et al. 2011). In breastfed infants, especially the wholesome bifidobacteria is stimulated to grow, through the in breast milk containing milk oligosaccharides. Metatranscriptomic analyses already revealed differences in the bifidobacteria abundance between breastfed and formula-fed infants (Gerritsen et al. 2011). Therefore, several formulas (non-probiotic and bifidobacteria-supplemented) were designed to reflect the composition and impact of breast milk on the infant gut microbiome for *bifidobacterium* growth and thus the health-promoting profit.

1.4.2 Nutritional impact on the metabolome, including metabolite classes and their diversity

Many studies were accomplished for the analysis of urine, tissue material and plasma (Matysik et al. 2016). From a metabolomics perspective, relatively little attention was paid to the impact of diets on the fecal metabolome (Chow, Panasevich et al. 2014). Digestion of pre- and probiotics are best observed in the gut, wherefore predominantly fecal samples are collected to study the impact of diet on the metabolome. Fecal material not only contains unabsorbed metabolites, but also contains bacteria, host metabolites and gut metabolites, which enable to link the impact of diet and gut microbiota metabolic

interactions (Matysik et al. 2016). This in turn allows multi-omics analysis and links the metabolism of host and bacteria.

Nutritional metabolomics is able to comprehend the entire metabolome through dietary changes and to map metabolic regulation problems with diet (McNiven et al. 2011). The gut metabolome and the microbiome are strongly connected, as already changes and differences in the microbial community can change the metabolome (Xie et al. 2013). Hereto, the Kyoto Encyclopedia of Genes and Genomes (KEGG) database (Kanehisa and Goto 2000, Kanehisa et al. 2008) offers a wide range of metabolites, linked to genomic and proteomic (enzyme-related) information, presenting the complexity of the metametabolome in relation to metabolic pathways (e.g. carbohydrate metabolism, energy metabolism and lipid metabolism) involved in health and disease.

When investigating the gut metabolome, metabolomics helps tracking the interactions between nutritional metabolites and the human metabolism (McNiven et al. 2011). The gut metabolome is predominately investigated through the analysis of fecal samples. Particularly, metabolomics of feces can reveal valuable knowledge about health and nutrition (Deda et al. 2015) and provide a better understanding of the complex interactions of microbes, diets, and the host (Chow et al. 2014).

Further, metabolome analyses allow drawing inferences from the relationship between the metabolism of the gut microbiota and the metabolic outcomes in the host (Aw and Fukuda 2015). These metabolites originating from the gut microbiome serving as nutrients for cells and tissues comprise complex interactions between the gut microbiome, the gut microbiota-derived metabolites and the host. Some of the main metabolite classes involved in the host microbiome are, among others, choline, bile acids and/or SCFAs, which are essential for human health. Even more compound classes and interactions are present in the gut microbiota, due to the variety of gut microbial genes with yet unknown function (Xie et al. 2013). Especially metabolite classes, such as the carbohydrates, lipids/fat, proteins and metabolites of the energy metabolism, play a major role in the nutritional metabolome and therefore are relevant for human nutrition (Gibney et al. 2005). Moreover, the differentiation between microbial or host-derived metabolites mainly still remains mainly indistinguishable and is a challenge in metabolomics analyses.

Through bacterial fermentation processes, the major end products are SCFA, which serve as an energy source for the host and enable linking microbiota and the host (Cummings 1981, Xie et al. 2013).

Through prebiotics intake and if the dietary fiber passes the digestion in the upper intestine, it is fermented through bacteria into bacterial metabolites. One important metabolite class, SCFA are produced (Scott et al. 2011), which can be detected in fecal samples. These dietary changes influence the health of the host and are responsible for the changing proportion of SCFA, which are predominantly acetate, propionate and butyrate. Further, formate, fumarate, malonate, succinate, caproate and valerate are produced through bacterial fermentation after the dietary fiber intake, but occur less abundant (Xie et al. 2013). The production and the activity in the human gut of SCFA have numerous pivotal impacts on humans' health for metabolic diseases (e.g. obesity and diabetes) and gastrointestinal disorders (e.g. IBD or cancer).

Bile acids are sterols, which are classified in primary (Cholic acid, CA and Chenodeoxycholic acid, CDCA) and secondary bile acids (deoxycholic acid and lithocholic acid). Primary bile acids are formed in the liver from the conversion of cholesterol and are further conjugated by either taurine or glycine. In general, in the human gut, where the bile acids undergo bacterial metabolism with conversions as e.g. deconjugation, esterification and desulfatation, the secondary bile acids are formed, which appear very early in life and which were already identified in meconium. These bacterial conversions result in more than 20 different secondary bile acids in adult human feces (Gérard, 2014). Bile acids play an important role especially in the modulation of lipids, glucose and the energy metabolism. *Bacteroides*, *Eubacterium*, *Clostridium* and *Escherichia coli* are mainly involved in generating secondary bile acids (Xie et al. 2013, Aw and Fukuda 2015).

SCFA and bile acids and further metabolite classes (e.g. lipids, fatty acids, vitamins etc.) play an important role in the nutritional impact on the human metabolome and microbiome and therefore in the dietary intake of pre- and probiotics. Hence, the role of metabolomics, including SCFA and bile acids in relation to insulin resistance (prebiotics) and to the development of the infant gut microbiome differing between formula (with and without probiotics) and breast milk will be reviewed, experimentally illustrated and explicitly described in chapter 2 (Effect of resistant starch on the gut microbiome) and chapter 3 (Impact of breast feeding and bifidobacteria-supplemented formula on the infant fecal metabolite profile in the first year of life).

1.5 Data handling, processing and statistical evaluation – a metabolomics workflow

In metabolomics, one of the challenges is the data handling due to the enormous output of spectral data in biological samples obtained through an appropriate analytical system.

The obtained spectral data need to be processed, i.e. aligned, filtered (e.g. raw data filtration, mass defect and isotopic peaks) and normalized, followed by molecular formula calculation and metabolite annotation. Metabolite annotation can be carried out through several available metabolite databases and annotation tools, such as Metlin (Smith et al. 2005) or MassTRIX (Suhre and Schmitt-Kopplin 2008, Wagele et al. 2012). The MassTRIX webserver enables the metabolite annotation through HMDB (Wishart et al. 2007, Wishart et al. 2009, Wishart et al. 2013), KEGG (Kanehisa and Goto 2000, Kanehisa et al. 2008) and LipidMaps (Fahy et al. 2005, Fahy et al. 2009). It is a challenge to deal with the relatively small number of known metabolites in databases in contrary to the huge number of non-assigned metabolites. Therefore, data processing is an important step, especially in non-targeted metabolomics analyses to obtain meaningful data matrices. Lastly, the data is scaled and then undergoes different statistical analyses to provide a funded base for further data interpretation and identification of novel metabolites. In metabolomics, multivariate tools, such as unsupervised (e.g. principal component analysis, PCA) or supervised (e.g. partial least squares discriminant analysis, PLS-DA) techniques are widely used.

1.5.1 Unsupervised and supervised methods in multivariate data analysis

Principal component analysis (PCA) is one of the most frequently applied unsupervised methods in multivariate data analysis for statistical evaluation of the metabolomics data set to represent multidimensional data (Dettmer et al. 2007). The in a metabolomics data matrix containing information is compressed into principal components, while the information of the majority of the total variance existing in the data can be projected, mainly as first and second component.

In PCA, the correlation between the dependent variable and the independent variables are not considered, while only the characteristics of the X-vector or the predictive variables are captured. The principle of PCA is as follow: a few linear combinations of the variables get detected and are used to summarize the data to project them into a scores scatter plot (Maitra and Yan 2008). Therefore, PCA enables getting a first hint of possible patterns in the data set. Partial least squares discriminant analysis

(PLS-DA) is an alternative approach to PCA. It accounts as much information for the analysis in the raw predictive variables and in the relationship between the predictive and target variables to maximize inter-class variance. Here, one variable is treated as the dependent variable and tries to reduce the dimension while maximizing the separation of classes (Maitra and Yan 2008). OPLS-DA is performed to discriminate different classes or groups involved in a study and to extract variables (loadings) (e.g. metabolites) responsible for the class discrimination. To conclude, PCA is first performed to get an overview of the metabolomics data and can be extended through an PLS-DA/OPLS-DA method to classify the data. The application of PCA and OPLS-DA on an experimental metabolomics data set of fecal samples is explicitly described and illustrated below in the following chapters 2 and 3.

1.6 Thesis structure

The presented thesis is structured into two main chapters of nutritional studies, including mass spectrometry based metabolomics analyses to investigate the prebiotic and probiotic impacts on the human fecal metabolome. A general overview of the structure in this thesis is illustrated in Figure 1.6-1. In the first nutritional study, the impact of resistant starch on the human gut microbiome and fecal metabolome of participants with reduced insulin sensitivity was discussed (Chapter II). Further, shotgun proteomics and 16S rRNA sequencing analyses were performed. The integration of all three “omics”-datasets finally provided insights into a global systems-level understanding of host, including microbial metabolism and protein expression. The main effects of the resistant starch diet on the human gut microbiome and on the functions that each “omics”-discipline carried out was discussed. Chapter III reviewed the impact of early life intervention with bifidobacteria-supplemented formula on the infant fecal metabolite profile with in the first year of life, in contrast to breastfed and non-interventional formula fed infants. It was demonstrated, that diet can influence the composition of the human fecal metabolome differently, wherefore the overall results discussed in this thesis are summarized in chapter IV.

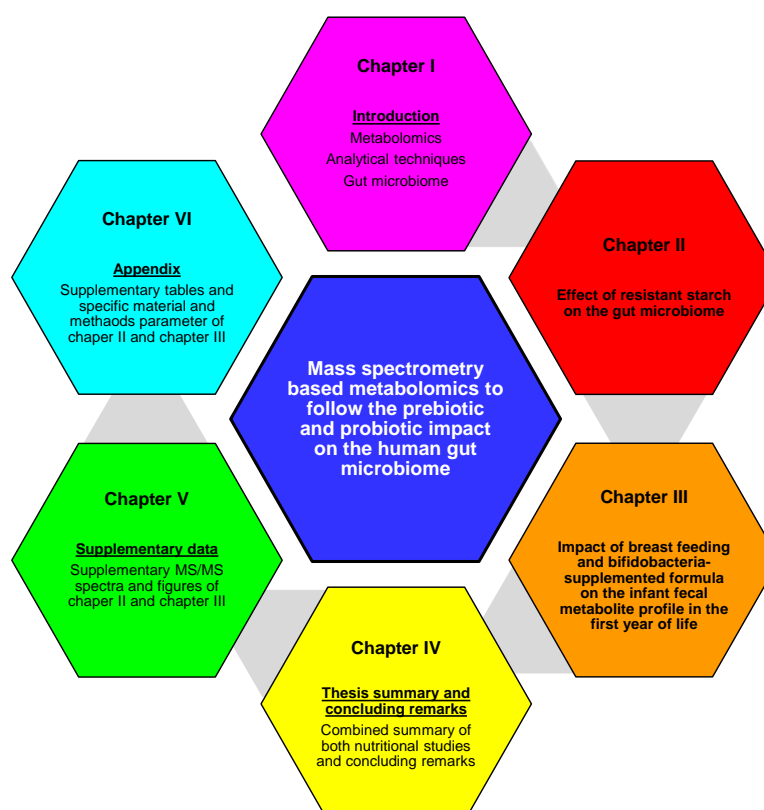
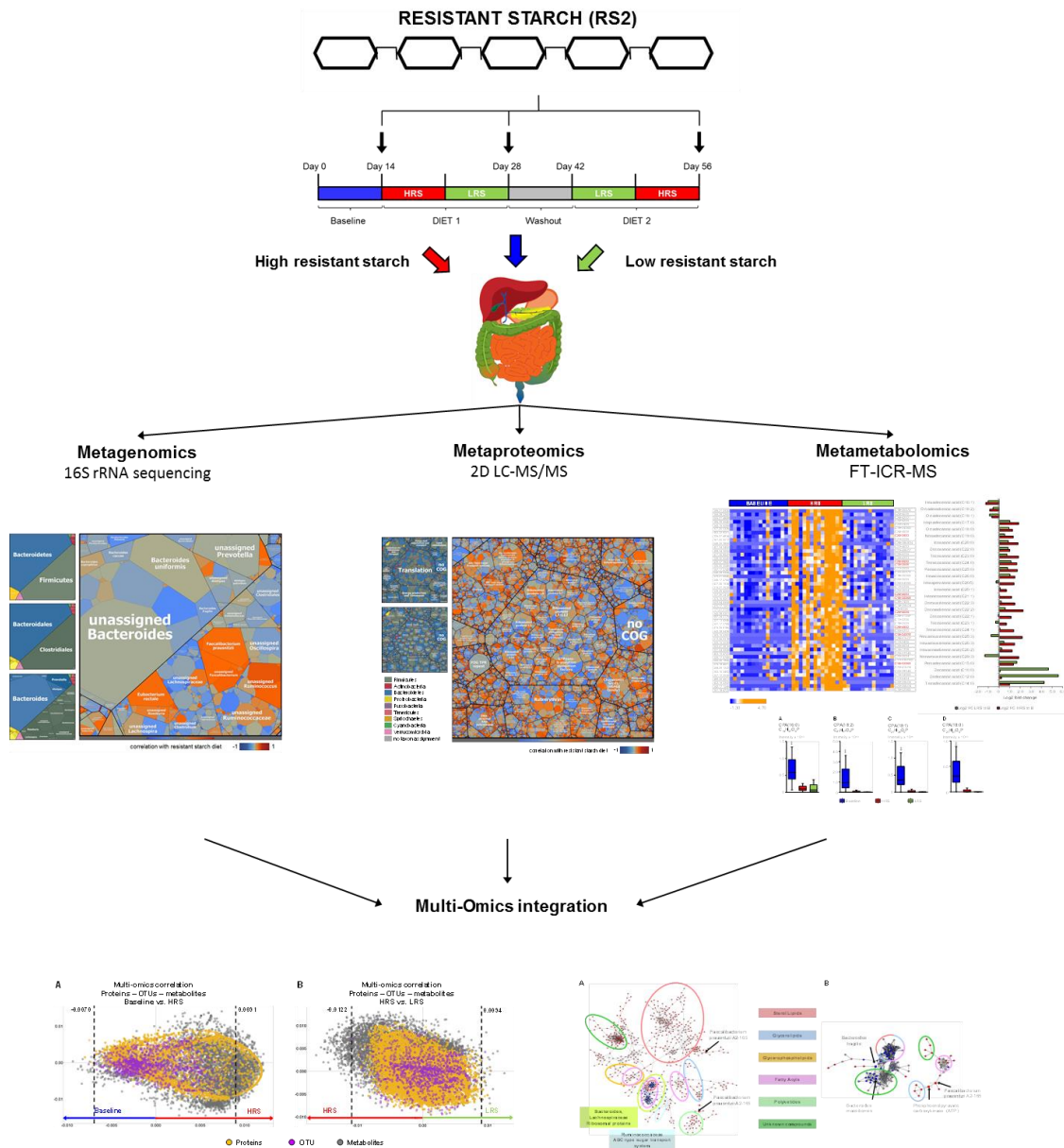


Figure 1.6-1: Thesis structure

Additional information is given in the supplement (chapter V), including MS/MS spectra of MS/MS experiments performed in both studies, described in chapter 2 or chapter 3, respectively. The appendix (chapter VI) contains specific and detailed material and methods parameter, as well as tables of the discussed findings of the results and discussion sections of chapter II and III.

Chapter II

Effect of resistant starch on the gut microbiome



Parts of this chapter (chapter II - Effect of resistant starch on the gut microbiome) are published in:

Maier, T. V.; Lucio, M.; Lee, L. H.; VerBerkmoes, N. C.; Brislaw, C. J.; Bernhardt, J.; Lamendella, R.; McDermott, J. E.; Bergeron, N.; Heinzmann, S. S.; Morton, J. T.; González, A.; Ackermann, G.; Knight, R.; Riedel, K.; Krauss, R. M.; Schmitt-Kopplin, P.; Jansson, J. K.: Impact of Dietary Resistant Starch on the Human Gut Microbiome, Metaproteome, and Metabolome. *mBio* vol. 8 no. 5 e01343-17 (2017). (Maier et al. 2017).

Copyright (2017) Maier et al.

(The original article is available: <http://mbio.asm.org/content/8/5/e01343-17.full>)

Licence notice: <https://creativecommons.org/licenses/by/4.0/>

Chapter II

2 Effect of resistant starch on the gut microbiome

2.1 Introduction

Excessive body weight and its associated metabolic disorders, including diabetes and cardiovascular disease (CVD) (Chang et al. 2016), reached epidemic proportions over the last few decades. Identification of effective strategies for prevention and management of these chronic conditions is a matter of urgency. Therefore, the objective of this study was to assess the effects of diets varying in digestibility of carbohydrates (prebiotics) on metabolism and the gut microbiome of individuals suffering from insulin resistance, the antecedent of diabetes type II.

The main function of insulin is to reduce the blood sugar level (Stryer 1995). In healthy individuals, insulin is released to reduce the blood sugar level. After the blood sugar level is normalized the level of insulin in the blood is decreased as well. Further, insulin is responsible for the uptake of glucose in the cells, especially of liver, muscles and fat tissue (Stryer 1995). Participants suffering from insulin resistance already show higher blood sugar levels (Shahidi and de Camargo 2016) and higher levels of insulin in the blood (hyperinsulinaemia) (Shanik et al. 2008); the cells are not capable to react to insulin and the blood sugar level cannot be reduced, which leads to an increased release of glucose in the urine. Recent evidence suggests that diet, lifestyle and drugs interact with and modify the gut microbiome (Turnbaugh et al. 2009, Bergeron et al. 2016, Ussar et al. 2016) in a manner that may influence metabolic regulation and disease susceptibility (Conlon and Bird 2014). One of the properties of the gut microbiome is its capacity to influence energy recovery through catabolism of poorly digestible nutrients, such as RS and other polysaccharides, operating as prebiotics (Conlon and Bird 2014) .

In general, prebiotics are food additives and dietary non-digestible or slowly digestible, but partially fermented oligosaccharides, promoting the growth, composition and activity of health-beneficial bacteria in the intestine (Gibson and Roberfroid 1995, Thomas et al. 2014), such as bifidobacteria (Walker et al. 2011). Further, prebiotics modulate the abundance of *Faecalibacterium prausnitzii* (Miquel et al. 2013). Prebiotics serve as nourishment for the gut microbes, which anon supply the host with energy and essential nutrients (Topping et al. 2007). Prebiotic food additives are represented by numerous non-digestible carbohydrates (e.g. RS). In general, RS is resistant to pancreatic amylase

digestion and is not absorbed in the intestine (Fuentes-Zaragoza et al. 2011). Furthermore, several health-promoting and gut microbes' beneficial applications of RS can be summarized. First, RS acts as substrate to influence the growth of definite microbes (e.g. lactobacilli and bifidobacteria). Second, it acts as dietary fiber to promote health and metabolic diseases (Fuentes-Zaragoza et al. 2011). Based on the nutritional characteristics, it is classified into four main types: RS 1 is a physically inaccessible starch, present in milled grains and seeds. RS 2 occurs in a granular form (e.g. high amylose corn) and cannot be digested through enzymes but is digestible very slowly in the small intestine. RS 3 is a retrograded starch and the most RS form, which resists enzyme digestion. The last type, RS 4 is chemically modified starch ((Fuentes-Zaragoza et al. 2011).

The most common RS in food are, with up to 70 percent, predominately amylopectin and amylose. High-amylose containing starches are resistant to amylolytic processes through the enzymatic digestion by amylase (Topping et al. 2007). The prebiotic potential of high-amylose starch was already studied in pigs and in mice. It was found, that fecal concentrations and excretion of *Bifidobacterium longum* were higher when RS was fed, than in fecal sample of pigs fed a conventional starch (Brown et al. 1997). In fecal samples of mice fed with high-amylose starch an increase of LAB numbers was observed (Brown et al. 1998). The detected increases of *B. longum* in pigs are similar to the impact of other prebiotics reported in several human studies. Both studies revealed, that RS, especially in the form of amylose/amylopectin qualifies as a prebiotic (Topping et al. 2007). However, the impact of RS on the fecal metabolite profile (non-targeted and targeted), except SCFA, is not clearly investigated yet, which further reveals the relatively low number of studies conducted to investigate the impact of RS in the gut microbiome in a metabolomics matter, in contrast to the high number of studies dealing with bacterial species. Therefore, this chapter mainly focused on the metabolomics perspective of the impact of RS on the fecal metabolite profile.

2.2 Study design and objective

The effects of resistant (amylose) vs. rapidly digested (amylopectin) starches were studied in a controlled, randomized, within-subjects' crossover dietary intervention trial in 16 subjects with reduced insulin sensitivity. In this study, 26 women and 13 men were enrolled, with 23 participants being assigned to the high carbohydrate arm (HC), containing 60% of total carbon and 16 participants being assigned to the low carbohydrate arm (LC), containing 40% of total carbon in the diet. In general for both diet arms, several criteria were set for participation, including being insulin resistant with a homeostatic model assessment insulin resistance parameter (HOMA-IR) > 50th percentile for sex, overweight or obese (BMI between 27 and 35 kg/m²), Other eligibility criteria were as follows: Male participants were older than 20 and post-menopausal female participants older or equal to 43 years, having no menses for ≥3 years or ≥1 year < 3 years, and an appropriate follicle-stimulating hormone (FSH) plasma concentration. Additionally, participants did not take any drugs, were non-smokers and had no record of chronic diseases and were healthy apart from their insulin resistance (Maier et al. 2017). Furthermore, clinical criteria for participation were fasting glucose (<126 mg/dL), fasting triglycerides (<500 mg/dL), blood pressure (<150/90), low density lipoprotein (LDL) and total cholesterol (≤ 90th percentile for age and gender) and having a stable weight with <3% change 3 months prior to the study. Additionally, participants avoided consuming alcohol and any other dietary supplements over the period of the study. Further details of the study design are given in Bergeron et al. (Bergeron et al. 2016) and Maier et al. (Maier et al. 2017). The study protocol was approved by the Institutional Review Board of Children's Hospital and Research Center of Oakland (CHORI). All participants gave written informed consent to take part in the study. The study protocols were approved by the Human Subjects Committee of both Children's Hospital Oakland Research Institute and Lawrence Berkeley National Laboratory. Written informed consent was obtained from each subject (Maier et al. 2017).

Within this thesis, the focus was on the LC diet arm, wherefore the study design is presented in Figure 2.2-1. The first two weeks all participants consumed the same baseline diet (n= 14) and were then assigned to a sequence of the two experimental diets: a high resistant starch (HRS) diet containing 38 grams of RS and a low resistant starch (LRS) diet containing 2 grams of RS. Each diet period lasted 14 days with a 7 days home diet and 7 days baseline diet in between. Within each diet group the participants first consumed the diet 1 (either HRS or LRS) for 2 weeks. Afterwards, participants consumed diet 2 (opposite to diet 1) for another 2 weeks (Maier et al. 2017). The baseline diet and both

RS diets contained similar macronutrient distribution. However, the baseline diet was low in foods containing naturally-occurring RS. Both diets contained a type 2 resistant starch (RS2), which was a granular form of high amylose cornstarch. In the HRS diet, Hi-maize 260 cornstarch (42g RS/100g starch, National Starch and Chemical Co., Bridgewater, NJ) was used, whereas for the LRS diet Melojel (2g RS/100g starch, National Starch and Chemical Co., Bridgewater, NJ) was used. Participants assigned to the LRS diet consumed Melojel predominately in baked goods, which was mostly cooked. Participants assigned to the HRS diet consumed 50% of the Hi-Maize starch raw. Here the starch was mixed with other food in fruit purees, soups and beverages (Bergeron et al. 2016).

Fecal samples were collected from 16 participants of the LC diet arm over three time points: day 14: after baseline diet; day 28: after the first diet period (DIET 1); and day 56: after the second diet period (DIET 2) and divided into 5 groups: G1: Baseline diet; G2: HRS diet (Day 28); G3: LRS diet (Day 28); G4: LRS diet (Day56) and G5: HRS diet (Day 56) as seen below (Figure 2.2-1). Fecal samples were collected for metabolite analysis by (-/+) FT-ICR-MS (metabolomics), 16S rRNA sequencing (genomics) and for protein analysis using 2D LC-MS/MS (proteomics).

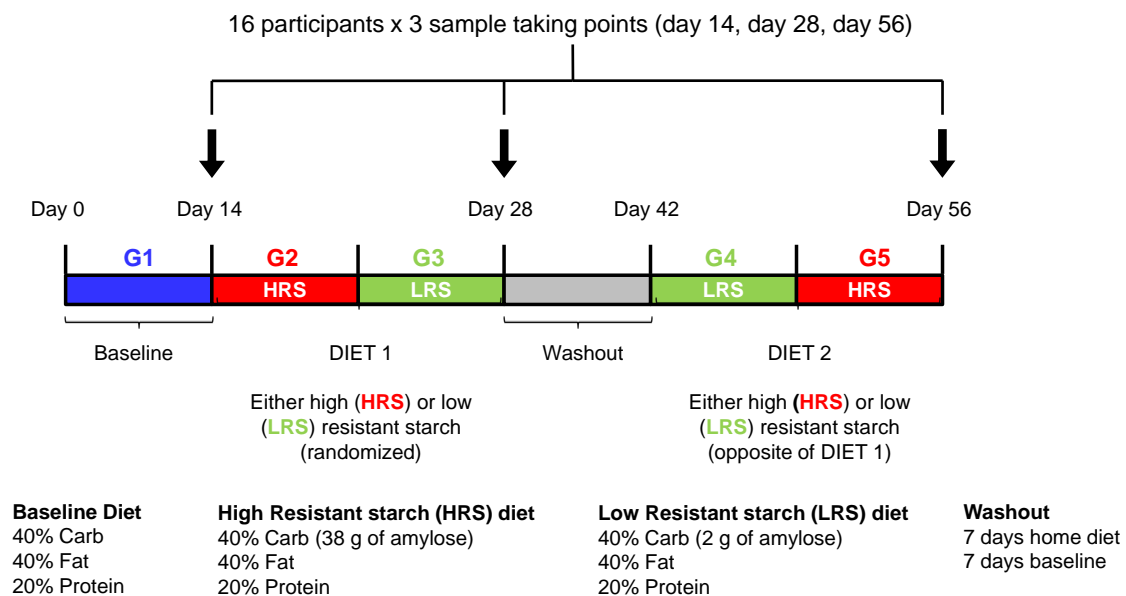


Figure 2.2-1: Study design to investigate the impact of resistant starch on the human gut microbiome.

From Maier, T. V.; Lucio, M.; Lee, L. H.; VerBerkmoes, N. C.; Brislawn, C. J.; Bernhardt, J.; Lamendella, R.; McDermott, J. E.; Bergeron, N.; Heinzmann, S. S.; Morton, J. T.; González, A.; Ackermann, G.; Knight, R.; Riedel, K.; Krauss, R. M.; Schmitt-Kopplin, P.; Jansson, J. K.: Impact of Dietary Resistant Starch on the Human Gut Microbiome, Metaproteome, and Metabolome. *mBio* vol. 8 no. 5 e01343-17 (2017). Illustration modified from (Maier et al. 2017), Copyright (2017) Maier et al., Information about the creator and respective contributions, as well as the original material are available: <http://mbio.asm.org/content/8/5/e01343-17.full> with the original title: Crossover study design. Licence notice: <https://creativecommons.org/licenses/by/4.0/>.

2.3 Material and Methods

2.3.1 Metabolomics

2.3.1.1 *Metabolite extraction*

Fecal sample collection and the metabolite extraction was performed in the Lamendella lab (contact: Dr. Regina Lamendella) from the Biology Department at the Juniata College in Huntingdon, Pennsylvania, USA. Fecal water and methanol (MeOH) extracts were prepared of the fecal samples and all extraction steps were performed on ice. For fecal water extraction, approximately 15 g of each stool sample was homogenized with 20 mL cold sterile water in a conical 50 mL Falcon tube, by using a hand-held homogenizer (VDI 12 Homogenizer 115V VWR #82027-184) at full speed (30,000 rpm) for 2 x 30 s, with cooling on ice in between homogenization periods. The homogenate was split into four 50 mL conical Falcon tubes, of which two tubes were prepared for metabolite extraction and the other two for proteomics (Chapter 2.3.3.1). For fecal water, the homogenate was centrifuged at 4 °C, 14,000 x g for 10 minutes and the aqueous supernatant was decanted and stored at -80 °C, whereas the remaining cell pellet was used for MeOH extraction. For MeOH extraction, 1.2 mL of cold (-20 °C) MeOH was added to each of both tubes of the fecal water extraction and briefly mixed by vortexing. Further, the cells were lysed by pressure cycling at 30,000 psi with 30 cycles using the Barocycler NEP3229 (Pressure Biosciences, Easton, MA, USA). Afterwards, the lysates were centrifuged for 10 minutes (4 °C, 14,000 x g). Both supernatants of the MeOH extract were combined into a fresh microcentrifuge tube and stored at -80 °C prior to the analysis by FT-ICR-MS (Maier et al. 2017).

2.3.1.2 *Metabolomics using direct infusion FT-ICR-MS analysis*

Each MeOH extract was diluted 1:4 with ice cold MeOH. Samples were measured randomized in negative and positive ESI mode using an ultrahigh resolution solariX™ FT-ICR-MS (Bruker Daltonik GmbH) with a 12 T superconducting magnet and an Apollo II ESI source. The instrument was calibrated using a 5 ppm arginine solution. In both ionization modes, 500 scans for each sample were acquired in single MS mode within a mass range from m/z 122.9 to m/z 1000 in (-) ESI and from m/z 147.4 - m/z 2000 in the (+) ESI mode. The MS parameters were as follows: capillary: -3600 V/3700 V (-/+), nebulizer pressure = 2.0 bar, dry gas = 4.0 L/min and dry temperature = 180 °C (Maier et al. 2017). Further parameters are listed in Table 6.1-3. A detailed list of chemicals is given in Table 6.1-1.

2.3.1.3 Data processing

Ultra-high resolution mass spectra were processed using DataAnalysis 4.0 SP2 (Bruker Daltonik GmbH). The (-) FT-ICR-MS mass spectra were calibrated internally using a reference list of known masses (fatty acids) with an error below 0.075 ppm. The (+) FT-ICR-MS spectra were calibrated with an error below 1 ppm. All mass spectra were exported as ASCII files with a signal-to-noise ratio above 4 and a relative intensity threshold of 0.001% of the base peak using the AutomationEngine 4.0 (Bruker Daltonik GmbH). ASCII files were converted to ASC files by in-house software, before all spectra were aligned to a data matrix with an error of 1 ppm by in-house software. Through the alignment step the data matrix of the (-) FT-ICR-MS mode resulted in 97 483 mass signals, whereas the data matrix of the (+) FT-ICR-MS mode contained 115 287 mass signals. Firstly, both aligned data matrices were filtered by mass signals counted < 5 times in $n = 45$ mass spectra and a mass defect above 0.8, which resulted in 14 167 mass signals for (-) ESI mode and 19 652 mass signals for (+) ESI mode. Further filtration steps were applied, where the mass signals were assigned to molecular formulas using Netcalc (Tziotis et al. 2011) (network tolerance = 0.2 ppm; NetCalc tolerance = 0.2 ppm). Additionally, the mass signals were searched against the KEGG (Kanehisa and Goto 2000, Kanehisa et al. 2008), Human Metabolome Database (HMDB) (Wishart et al. 2007) and Lipid Maps (www.lipidmaps.org) databases using homo sapiens (*hsa*) as reference organism using the MassTRIX web server (Wagele et al. 2012) with a maximum error of 1 ppm. The final matrices for all data analysis steps within this thesis contained 5552 mass signals for the (-) FT-ICR-MS mode and 14 891 mass signals for the (+) FT-ICR-MS mode, consisting of mass signals which further could be assigned to a molecular formula and to compounds listed in databases (Maier et al. 2017).

2.3.1.4 Multivariate Data Analysis: unsupervised and supervised techniques

The data sets were evaluated through unsupervised (e.g. PCA) and supervised techniques (e.g. OPLS-DA). The PCA was applied by using SIMCA-P 9.0 (Umetrics, Umeå, Sweden) and the OPLS-DA was performed by SIMCA-P 13.0.3.0 (Umetrics, Umeå, Sweden). For the PCA analysis, the dataset was unit variance (UV) scaled. For OPLS-DA of the metabolomics data, the dataset was UV scaled. For each classification model, CV-ANOVA was applied in order to verify the robustness of each model. Indicators, such as the p-value, the goodness-of-fit $R^2Y(\text{cum})$ and the goodness-of prediction $Q^2(\text{cum})$ were reported (Maier et al. 2017).

2.3.1.5 Significance testing, data handling and visualization

The level of significance was tested by applying the *post hoc* Kruskal-Nemenyi test for pairwise test of multiple comparisons of mean rank sums in R (Computing 2014) (package: 'PMCMR' version 4.1) (Pohlert 2014). Heatmaps were generated by Hierarchical Clustering Explorer version 3.5 (Seo and Shneiderman 2002) (Human-Computer Interaction Lab. University of Maryland, College Park). Therefore, the data was normalized ($(X-m)/\sigma$) and clustered by rows (Euclidean distance) (Maier et al. 2017). Boxplots and the log₂ fold change were calculated and visualized in Microsoft Office Excel 2010. Correlation studies were conducted by Pearson correlation in Microsoft Office Excel 2010, whereas correlation coefficients were reported. The significance for the correlation (p-corr) was calculated in Microsoft Office Excel 2010 by applying the data analysis function "Regression".

2.3.1.6 Lipidomics approach by UHPLC-ToF-MS for MS/MS analysis

Fecal samples also were analyzed by a lipidomics-MS/MS approach (Witting et al. 2014) using an ACQUITY-UPLC[®] system (Waters GmbH, Eschborn, Germany) coupled to a Bruker maXis[™] UHR-qToF-MS (Bruker Daltonik GmbH, Bremen, Germany) with an Apollo II ESI source. Extracted methanolic fecal samples were measured in positive and negative ionization mode. Nitrogen was used as dry and nebulizer gas. Following parameters were applied: End plate Offset = -500V, Capillary = -4500 V (positive mode)/4000 V (negative mode), Nebulizer pressure = 2.0 bar, Dry gas = 8.0 L/min, Dry Temperature = 200 °C. Data was acquired also in MS/MS mode (data dependent acquisition, DDA) using the Bruker AutoMSn mode with alternating collision energies (collision energy ramp) and set default parameters for the isolation windows. Further details are listed in Table 6.1-5.

A Cortecs C18 column [150 mm x 2.1 x 1.6 μm] (Waters GmbH, Eschborn, Germany) was used for separation, which was performed with a gradient consisting of Eluent A (60% ACN, 40% MilliQ water, 10 mM ammonium formiate and 0.1% formic acid) and Eluent B (90% IPA, 10% ACN, 10 mM ammonium formiate and 0.1% formic acid). First, an isocratic step with 32% B was initiated for 1.5 minutes. Until the 21st minute Buffer B was increased to 97% B and held for 4 minutes. Within 0.1 minutes the gradient was set to initial conditions for 4.9 minutes to re-equilibrate the column. The flow rate was 250 μL/min. Five μL of each sample was injected by partial loop. Between 0.1 and 0.3 minutes a 1:4 diluted Low Concentration Tune Mix (Agilent, Waldbronn, Germany) was injected in order to

recalibrate each chromatogram. Chromatograms of both ionization modes were processed and aligned automatically as an end-to-end automation by using the Genedata Expressionist® Refiner MS for MS-based metabolomics data from the Genedata AG. The adequate UHPLC-ToF-MS data processing workflows of both ionization modes were designed and provided by Dr. Michael Witting from the research unit Analytical BioGeoChemistry, Helmholtz Zentrum München, Germany and adjusted as required for data processing.

The lipidomics-MS/MS approach was considered for metabolite classification or identification of significantly impacted mass signals through the baseline, HRS or LRS diet. Therefore, mass spectra were processed and calibrated using Data Analysis 4.1 SR 1 (Bruker Daltonik GmbH). Chromatograms of the standards used for the MS/MS experiment were averaged, standard-dependent and calibrated with an error of less than 0.5 ppm using a reference list of standards of the injected calibration standard mix (G1969-85000, Agilent, Waldbronn, Germany). The mass spectra and extracted ion chromatograms (EIC) were extracted from each standard and representative sample with an error of ± 0.01 Da (Maier et al. 2017).

2.3.1.7 Short-chain fatty acid analysis

For the SCFA analysis, the fecal MeOH extracts and chemical standards (i.e. propionic acid, butyric acid, valeric acid and isovaleric acid) were prepared and derivatized on ice as instructed in the AMP+ Mass Spectrometry Kit (Caymen Chemicals) product insert. AMP+ is a positively charged reagent for the derivatization of carboxylic acids. This resulted in a total amount of 88 μ L derivatized solution per sample and standard, which was further diluted with 352 μ L of a mixture of solvents used for the analysis in the ratio 99:1 A:B (5 mM CH₃COONH₄ + 0.1% acetic acid:ACN (Bazanella et al. 2017, Maier et al. 2017)).

The SCFA analysis was performed on an UHPLC-ToF-MS in (+) ESI mode. Gradient separation – with a total runtime of 22 minutes plus 2 minutes pre-run – of 1 μ L each took place on a Waters BEH C8 column (1.7 μ m, 2.1mmx150mm) with A as 5 mM CH₃COONH₄ and 0.1% acetic acid and B with 100% ACN. Starting conditions of the gradient separation were 99% A, hold for 1 minute. Within 16 minutes %A was decreased from 99% A to 1% A and hold for further 2 minutes, followed by an increase to 99% A, which was hold for further 2.8 minutes. The flow rate of the mobile phase was constantly set to 0.3

2. Effect of resistant starch on the gut microbiome

mL/min and column temperature was set to 40 °C. At the first 0.1 minutes of each analysis, a 1:4 diluted ESI-L Low Concentration Tuning Mix (Agilent, Waldbronn, Germany) was injected for calibration purposes. The respective MS parameters were as follows. Mass range: m/z 50 – 1200, spectra rate: 2.0 Hz, capillary: 4500 V, end plate offset: -500 V, nebulizer gas: 2.0 bar, dry gas: 8 l L/min, dry temperature: 200 °C. The photodiode array detector (PDA) was operated at an UV range from 190 – 500 nm (Bazanella et al. 2017, Maier et al. 2017). Further details are given in Table 6.1-4.

Prior to the extraction of the mass signals, the [M+H]⁺ adducts of the derivatized products, including the AMP⁺ reagent (185.11 amu) were calculated as follows:

$$(M)\text{Monoisotopic mass (metabolite)} - H_2O + AMP^+(C_{12}H_{13}N_2^+) = M - AMP^+$$

Equation 2.3.1-1: Calculation of the monoisotopic mass of the SCFA AMP⁺ derivate.

Subsequently, retention time (RT) was extracted using DataAnalysis Version 4.1 (Bruker Daltonik GmbH, Bremen, Germany). The peak areas were extracted using QuantAnalysis Version 2.1 (Bruker Daltonik GmbH, Bremen, Germany) and evaluated. The peak areas of the respective compounds were extracted and quantified externally by using 8 calibration points via the calculated calibration function (Table 2.3-1). For significance testing of the SCFA, pyruvic acid and lactic acid in the different feeding groups, the *post hoc* Kruskal-Nemenyi test (package: 'PMCMR' version 4.1) (Pohlert 2014) was applied by using R Studio Version 0.99.489 (Bazanella et al. 2017, Maier et al. 2017).

Table 2.3-1: External calibration results of the SCFA analysis.

From Maier, T. V.; Lucio, M.; Lee, L. H.; VerBerkmoes, N. C.; Brislawn, C. J.; Bernhardt, J.; Lamendella, R.; McDermott, J. E.; Bergeron, N.; Heinzmann, S. S.; Morton, J. T.; González, A.; Ackermann, G.; Knight, R.; Riedel, K.; Krauss, R. M.; Schmitt-Kopplin, P.; Jansson, J. K.: Impact of Dietary Resistant Starch on the Human Gut Microbiome, Metaproteome, and Metabolome. *mBio* vol. 8 no. 5 e01343-17 (2017). Reprinted from (Maier et al. 2017). Copyright (2017) Maier et al.

name	m/z (derivatized)	RT [min]	calibration function	coefficient of determination	method
Propionic acid	241,1341	4.0	y = 1,2119x - 0,5784	R ² = 0,9990	UV
Butyric acid	255,1497	4,6	y = 59940x + 16956	R ² = 0,9981	MS
Isovaleric acid	269,1654	5,3	y = 82730x + 6202,9	R ² = 0,9993	MS
Valeric acid	269,1654	5,5	y = 92248x + 4883	R ² = 0,9998	MS

2.3.2 Genomics analysis

2.3.2.1 DNA extraction, library preparation, and sequencing

DNA extraction, sequencing, library preparation, data processing and interpretation was performed in the Lamendella Lab (contact: Dr. Regina Lamendella) from the Biology Department at the Juniata College in Huntingdon, Pennsylvania, USA and in the Children's Hospital Oakland Research Institute, Oakland, CA 94609, USA, as well as by Gail Ackermann, Antonio González Peña and Rob Knight from the University of California, San Diego, USA. DNA from fecal samples were extracted in duplicate from 0.25 g samples using the PowerSoil DNA extraction kit (MoBio, Carlsbad, CA) according to manufacturer's instructions, including an additional heat lysis step for 5 minutes at 60°C (Maier et al. 2017).

PCR amplification of the DNA was performed using an F515/R806 primer to target the V4-V6 region of the 16S rRNA gene and barcoded with a 12-base error-correcting Golay code as previously described by Caporaso et al. (Caporaso et al. 2011). Sequencing was performed on the Illumina HiSeq2000 platform as previously described (Caporaso et al. 2012). Sequence data were analyzed using the Quantitative Insights into Microbial Ecology (QIIME) pipeline. Sequences were quality filtered and clustered into operational taxonomic units (OTUs) using the closed-reference OTU picking protocol at 97% sequencing identity (Caporaso et al. 2010, Bergeron et al. 2016). Further, the taxonomy of each associated OTU was calculated as previously described (Lozupone and Knight 2005). Subsequently, the raw OTU data table was filtered, normalized and imported into R using the 'phyloseq' package (McMurdie and Holmes 2013). Further filtering steps were applied, including retaining samples if they contain more than 5000 reads and retaining OTUs if they appeared more than five times in more than 5 samples, resulting in 1107 OTUs. To control for sequencing depth, OTU counts in each sample were proportionally scaled to an even depth of 5000 reads per sample. Using the raw biom table, the 'DESeq2' package (Love et al. 2014) was used to identify OTUs which were differentially abundant between groups (Maier et al. 2017).

2.3.3 Proteomics analysis

2.3.3.1 Protein extraction

Protein extraction was performed in the Lamendella lab (contact: Dr. Regina Lamendella) from the Biology Department at the Juniata College in Huntingdon, Pennsylvania, USA. Following the metabolite extraction (chapter 2.3.1.1), for protein extraction, 5 mL of PBS were added to the remaining two tubes of homogenized fecal material, which were briefly vortexed. Afterwards, the mixture was centrifuged at 4000 g, for 5 minutes (4 °C) to pellet larger debris, and the supernatants were transferred into a new 50 mL conical Falcon tubes. Another 4 mL of cold PBS were added to the cell pellet/debris and homogenized again (full speed for 2 x 30 s), followed by centrifugation (10 minutes at 10,000 x g, 4 °C). The supernatants were discarded. The cell pellet was washed with cold PBS and re-suspended in 600 µl of cold PBS, vortexed and centrifuged at 14,000 g for 10 min. The supernatant was discarded and the sample was stored at -80 °C prior to proteomics analysis (Maier et al. 2017).

2.3.3.2 Metaproteomics approach

The metaproteomics approach, including analyses and interpretation of the proteomics data was carried out by Lang Ho Lee from the Department of Genome Science and Technology, University of Tennessee, Knoxville, Tennessee, USA and Nathan VerBerkmoes from the University of Texas, El Paso, Texas, USA. Further information on the metaproteomics approach is given in (Maier et al. 2017).

2.3.4 Multi-omics statistical analyses

2.3.4.1 Network analysis: context likelihood of relatedness (CLR) method

Network analysis using the context likelihood of relatedness (CLR) method was performed by Dr. Jason McDermott from the Biological Sciences Division at the Pacific Northwest National Laboratory (PNNL) in Richland, Washington, USA.

In order to provide maximum overlapping, datasets between 16S and proteome, proteome and metabolome, as well as metabolome and 16S, pairs of datasets were assembled by matching participants from each individual dataset (16S, proteomics, and metabolomics). Afterwards, the combined data matrix was filtered to exclude those rows (OTU, protein, or metabolite, respectively) that

had more than 50% of values missing. On the filtered data matrix, the CLR method was applied, in order to determine shared information (Faith et al. 2007, McDermott et al. 2012). Six individual networks were constructed by applying a Z score filter of 6.5 to each dataset. Edges from individual networks were combined into a single network taking interactions from within a dataset (e.g. protein to protein) from the networks inferred from single datasets (e.g. proteomics) and inter-dataset edges from the appropriate combined datasets (e.g. protein to metabolite edges from the proteomics+metabolomics dataset). Differential expression was calculated as the fold change between mean abundance of each component (16S, protein, and metabolite) between participants of the HRS diet versus the baseline diet. Calculations also were performed between participants consuming the LRS diet versus those, consuming the baseline diet. The p-value was calculated using a two-sided Student's t test. Networks were represented in Cytoscape (Shannon et al. 2003) and annotations from the individual data types were used to highlight clusters of components enriched in particular labels as indicated in the figures (Maier et al. 2017).

2.3.4.2 Supervised ordination approach for multi-omics correlation

Multi-omics integration as supervised ordination approach was done using SIMCA-P 13.0.3.0 (Umetrics, Umea, Sweden). In order to study the three combined datasets, two different OPLS-DA models were built: the baseline diet to the HRS diet, and the HRS diet to the LRS diet. For integration of all different omics datasets, the samples were aligned in one matrix and were UV scaled. OPLS-DA loading plots were constructed to simultaneously visualize features of the genome, proteome and metabolome impacted by baseline, LRS or HRS diet. The loadings were extracted and visualized as loading plots using RStudio (Computing 2014) (Version 0.99.489). For each classification model, CV-ANOVA was applied in order to verify the robustness of each model. Indicators, such as the p-value, the goodness-of-fit $R^2Y(\text{cum})$ and the goodness-of prediction $Q^2(\text{cum})$ were reported (Maier et al. 2017).

2.3.5 Visualizing complex genomic and proteomic data via Voronoi Treemaps

Voronoi Treemap visualization of genomic and proteomic data was performed by Dr. Jörg Bernhardt from the department for Microbial Physiology and Molecular Biology at the Institute for Microbiology at the Ernst Moritz Arndt University of Greifswald and were developed and adapted for biological applications (Bernhardt et al. 2009, Otto et al. 2010, Mehlan et al. 2013) based on the originate work of

Ben Shneiderman (Shneiderman 1992), followed by an improvement to Voronoi treemaps performed by Balzer and Deussen (Balzer and Deussen 2005). Participant specific Pearson correlations of the genomic data with the RS regime assigned values of 0; 0.05 and 1 for baseline; LRS and HRS diets, respectively was performed. The participant's correlation values were averaged and visualized by using the following color code: -1: dark blue; -0.5: light blue; 0: medium grey; 0.5: orange; 1: dark red). The treemap polygon sizes correspond to the average count of OTUs calculated over all samples (Maier et al. 2017).

The proteome data was normalized vertically. Baseline, HRS and LRS diets were considered for the data analysis. The taxon assignments were extracted from the original proteome data table and entries without assignments were extracted from UniProt, if possible. Still unassigned proteins were classified as “unassigned” or similarly. The proteome data of each participant was calculated as z-scores, which simplified color coding, since z-scores are symmetric around 0 and can be transformed easily to a color code. Additionally, the differences from participant to participant are still comparable, since z-scoring was applied for each single participant. Furthermore, the proteome data were condensed to the microbial species level and the Voronoi treemaps were colored accordingly to species. In order to assign the proteins to functional classes, all proteins were analyzed separately (microbial to COG and human to KEGG BRITE (Kanehisa et al. 2012)). Pearson correlation was applied with the RS regime assigned values of 0; 0.05 and 1 for baseline; LRS and HRS diets, respectively. Correlation values were colored with the same color code described above for the genomic data (Maier et al. 2017).

2.4 Results and Discussion

2.4.1 Metabolomics perspective of positive and negative ionization techniques

2.4.1.1 Global fecal metabolome analysis due to different diets

In order to get an overview how the fecal metabolome was impacted by the baseline, HRS and LRS diet and how they interacted with each other, the fecal metabolite profiles of all participants of all diet periods were analyzed through PCA. Both ionization modes were considered separately, including metabolomic data analyzed in (-) FT-ICR-MS (Figure 2.4-1 A) and (+) FT-ICR-MS (Figure 2.4-1 B). The scores scatter plot of the (-) FT-ICR-MS mode data revealed a slight separation between the HRS diet and the baseline diet, as well as between the HRS and LRS diet. On the contrary, the LRS diet and the baseline diet seemed to have a similar pattern and appeared to be mainly clustered together in the scores scatter plot. In the (+) FT-ICR-MS mode, the scores scatter plot revealed a slight separation between the baseline diet and both RS diets, whereas the HRS diet and the LRS diet did not show a separation at all.

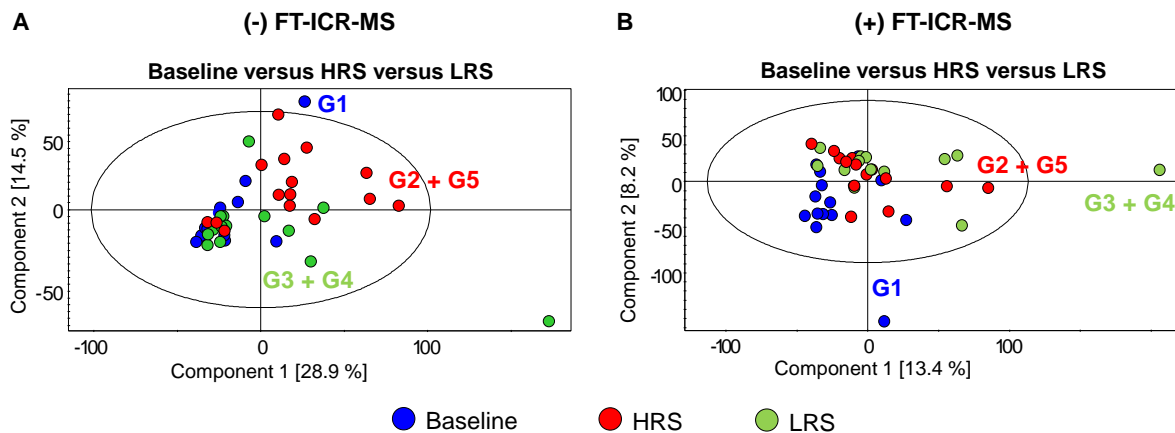


Figure 2.4-1: Over view of the fecal metabolome visualized in unsupervised PCA scores scatter plots.

Comparison of different groups through PCA (UV scaling) of participants of the baseline (blue), HRS (red) and LRS (green) diet with respect to different amounts of dietary starch, analyzed in (-) FT-ICR-MS (A) and (+) FT-ICR-MS (B) mode. All participants of all of dietary stages, including both time points of the dietary starch intake are illustrated.

Afterwards, the fecal samples of participants at different dietary stages and different time points were investigated, wherefore several interrogations were of interest: 1. The impact of varying amounts of RS. 2. The order of RS consumption and 3. The time effect of dietary starch intake. Therefore, the

participants were divided into 5 main groups, namely the baseline diet (G1), the RS groups at day 28 with HRS diet (G2) and LRS diet (G3), as well as the RS groups at day 56, consuming LRS (G4) and HRS (G5) diet. The baseline (G1) was compared to HRS (G2) or LRS (G3) to investigate the impact of varying amount of RS, after the baseline diet, where no RS was given and individuals were fed the same diet. Further, the HRS diet at day 28 (G2) was compared to the LRS diet at day 28 (G3) to investigate the impact of HRS or LRS at the same time point, as given in the models comparing G4 and G5 at day 56, too. There, it will be investigated if the time metabolite profile comparing the HRS and LRS diet differs between day 28 and day 56. Therefore, the individuals were fed again with the baseline diet for 7 days, followed by the second diet period at day 56 to create a comparable base between the starting point of the study and the second diet period. Another interrogation was, if the fecal metabolite profiles of the same diet at different time points were similar, wherefore the metabolite profiles between both HRS diets (G2 and G5), as well as both LRS diets (G3 and G4) were compared.

To investigate this, the fecal metabolome measured either in (-) FT-ICR-MS or (+) FT-ICR-MS mode was investigated through PCA. The scores scatter plots of the fecal metabolome measured in (-) FT-ICR-MS mode (Figure 2.4-2) showed a clear separation between baseline diet (G1) and HRS diet at day 28 (G2), but no separation could be achieved comparing samples of the baseline diet and LRS diet at day 28 (G3). Further, a separation between HRS (G2) and LRS (G3) at day 28, between HRS (G4) and HRS (G5) at day 56 as well as in the merged HRS (G2, G5) and merged LRS (G3, G4) diet groups could be observed in the scores scatter plots.

Principal Component Analysis comparing the fecal metabolome through dietary starch intake, analyzed in (-) FT-ICR-MS

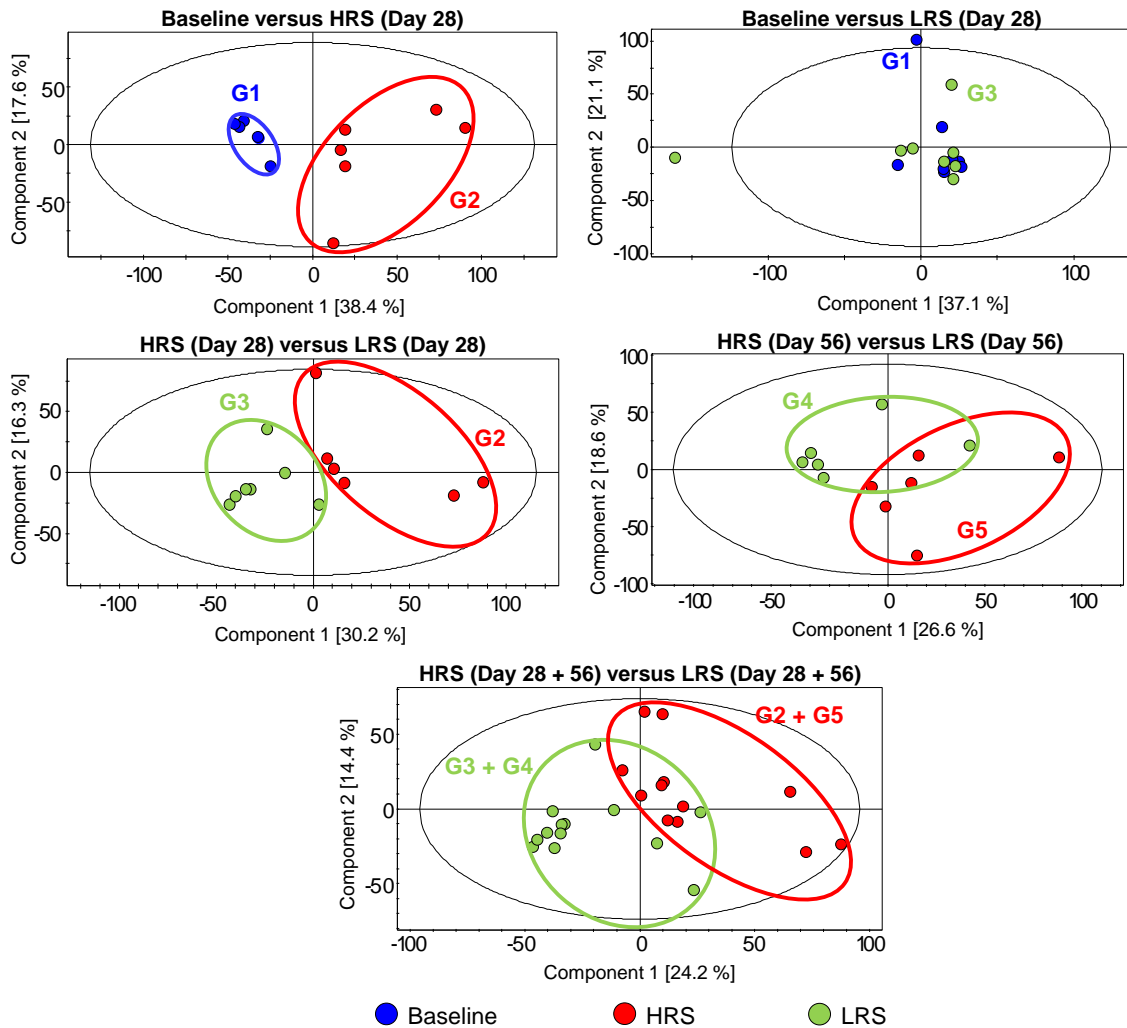


Figure 2.4-2: Unsupervised PCA scores scatter plots comparing the fecal metabolome

Comparison of different groups through PCA (UV scaling) of participants of the baseline (blue), HRS (red) and LRS (green) diet with respect to different time points, analyzed in (-) FT-ICR-MS mode. Top left: Baseline versus HRS (Day 28). Top right: Baseline versus LRS (Day 28). Middle left: HRS (Day 28) versus LRS (Day 28). Middle right: HRS (Day 56) versus LRS (Day 56). Bottom: HRS versus LRS, merged time points.

In (-) FT-ICR-MS mode, the metabolite profile through either high or low amount of RS compared to the baseline diet was changing extremely through the HRS diet, but relatively sparse through LRS diet, implying that the amount of RS played a crucial role on the response of the fecal metabolome. Therefore, the metabolite profile comparing the HRS and LRS diet – in both time points - was altered as well, whereas more significant features could be assigned to the HRS diet.

In general, the metabolite profile of the HRS diet at day 28 was comparable to the one of the HRS diet at day 56. However, it turned out that the metabolites significantly altered at day 28 of HRS diet were also present in the samples of the HRS diet at day 56, but showed comparably low intensity levels if LRS was consumed as diet 1 (day 28) followed by the HRS diet as diet 2 (day 56). This leads to the analysis, if the fecal metabolite profile changed between HRS at day 28 (G2) and LRS at day 56 (G4) of the same individuals, as well as between LRS at day 28 (G3) and HRS at day 56 (G5) of the same individuals. It was detected, that if HRS diet was consumed first, followed by the LRS diet, changes were more dominant (Figure 2.4-3 A), than when LRS diet was consumed first and followed by the HRS diet (Figure 2.4-3 B). Nevertheless, the significant metabolites between HRS and LRS at both time points were comparable, though with different intensity levels.

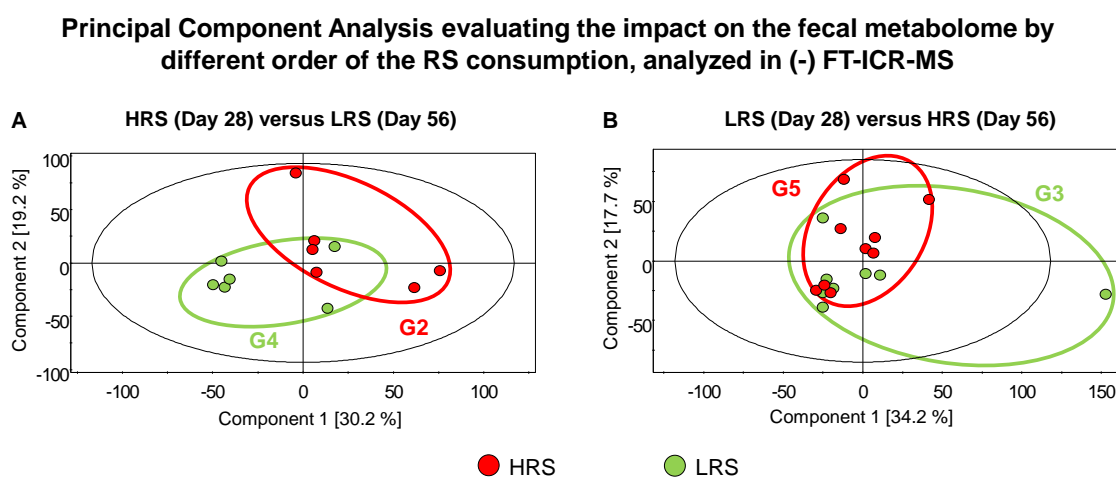


Figure 2.4-3: Unsupervised PCA scores scatter plots comparing the fecal metabolome due to different order.

Comparison of different groups through PCA (UV scaling) of participants of the HRS (red) and LRS (green) diet with respect to different order of low and high RS intake of the same individuals, analyzed in (-) FT-ICR-MS mode. A: HRS of Day 28 versus LRS (Day 56). B: LRS (Day 28) versus HRS (Day 56).

In (+) FT-ICR-MS mode, not only baseline diet and HRS, but also baseline and LRS diet showed a separation in the scores scatter plot (Figure 2.4-4). Here, it was remarkable that the separation was driven by baseline characteristic metabolites, wherefore the comparison between HRS and LRS diets showed no separation at all. In (+) FT-ICR-MS mode, the separations in the scores scatter plots of the PCA were predominantly driven by metabolites discriminative between the baseline diet and the RS diets. Differences in the metabolite profiles between the HRS or LRS diets at the same time points, and

between day 28 and day 56 of the HRS and LRS diets were rather sparse, compared to the significant changes between HRS and LRS observed in the (-) FT-ICR-MS analyses.

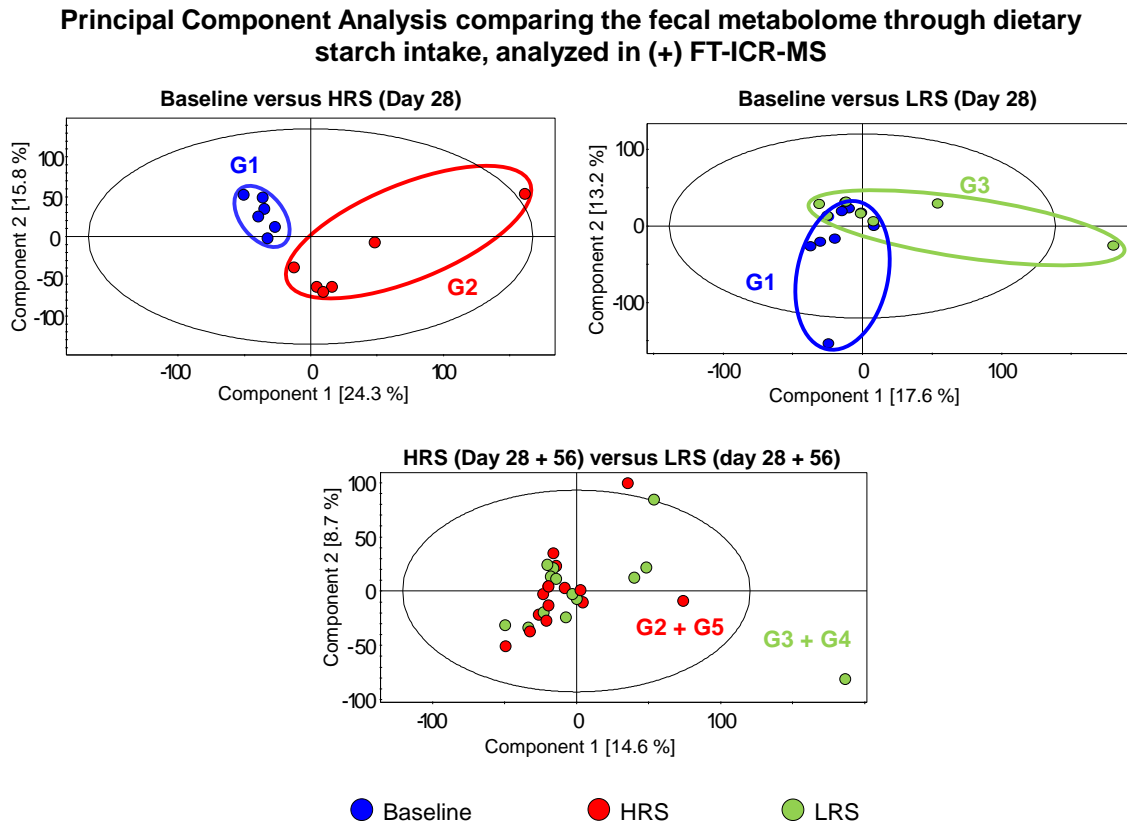


Figure 2.4-4: Unsupervised PCA scores scatter plots comparing the fecal metabolome.

Comparison of different groups through PCA (UV scaling) of participants of the baseline (blue), HRS (red) and LRS (green) diet with respect to different time points, analyzed in (+) FT-ICR-MS mode. Top left: Baseline versus HRS (DIET 1). Top right: Baseline versus LRS (DIET 1). Bottom: HRS versus LRS, merged time points.

There were no differences in the metabolite composition between both HRS diets at two different time points. Also, between both LRS diets at different time points no differences could be observed. Additionally, comparing the two RS groups by merging both HRS and both LRS diets, no changes could be observed. In 2015, Ordiz et al. investigated the impact of RS type 2 on the fecal metabolite profile of Malawi children suffering from intestinal inflammation (Ordiz et al. 2015). They did not see that RS reduced the inflammation, but they also detected different metabolite profiles between RS-rich diet and their habitual diet, predominantly caused by small organic metabolites increased by RS consumption. Also Lu et al. observed different metabolite profiles in fecal water samples of growing pigs after the consumption of a low or high RS diet (Lu et al. 2016). These findings agreed with our result that RS altered the metabolite profile differently than the baseline diet and a diet low in RS.

2.4.1.2 OPLS-DA for metabolite discrimination applied on different classification models

In order to classify the discriminant mass signals responsible for the separation, OPLS-DA classification models were applied of the (-) FT-ICR-MS (Maier et al. 2017) and the (+) FT-ICR-MS data. The PCA scores scatter plots already showed a separation between the different diets, especially between the baseline (G1) and HRS diet (G2), but also between HRS (G2, G5) and LRS (G3, G4) diets. Nevertheless, in order to detect mass signals responsible for the separation, several OPLS-DA classification models were performed of both, the (-) FT-ICR-MS and the (+) FT-ICR-MS data, as listed in Table 2.4-1. Each model was validated by cross validation analysis of variance (CV-ANOVA). Furthermore, the p-value, the goodness-of-fit $R^2Y(\text{cum})$ and the goodness-of prediction $Q^2(\text{cum})$ were reported. In negative mode, the classification models comparing the baseline diet (G1) to the LRS diet (G3), and comparing both diets at different time points (e.g. HRS (day 28) vs. HRS (day 56)) were not valid, as they did not pass the CV-ANOVA step. Nevertheless, seven valid OPLS-DA classification models could be achieved: 1. Baseline (G1) versus HRS diet (G2); 2. HRS (G2) versus LRS diet (G3); 3. HRS diet (G2, G5) versus LRS diet (G3, G4), merged time points; 4. HRS diet (G2) versus LRS diet (G3, G4); 5. Baseline diet (G1) versus all other diets at all time points; 6. HRS diet (G2, G5) versus all other diets and 7. LRS diet (G3, G4) versus all other diets.

On the contrary, in the positive mode there were no discriminant mass signals between the HRS and LRS diet at the same time point or at different time points. Also, here, the models comparing the same diet at different time points were not valid, wherefore no big differences in the metabolite profiles could be assumed. However, a classification model comparing the baseline diet (G1) and the HRS diet (G2), as well as a model comparing the baseline diet (G1) and the LRS diet (G3) could be achieved. Based on those models, another OPLS-DA classification model of the baseline diet (G1) and both RS diets at both time points (all other) was set up, which appeared to be highly valid, proved through CV-ANOVA. The previously described classification models indicated that the baseline diet displayed more discriminative mass signals in the positive ionization mode compared to the both RS diet and between both RS diets. Additionally, all mass signals detected as discriminant for each OPLS-DA classification model were subjected to another statistical test, the *post hoc* Kruskal-Nemenyi test for multiple comparisons of mean rank sums of the baseline diet, HRS and LRS diet.

Table 2.4-1: OPLS-DA models to compare different diet set-ups.

OPLS-DA models were created to compare different diet set-ups of fecal samples acquired through (-) FT-ICR-MS and (+) FT-ICR-MS. For (-) FT-ICR-MS OPLS-DA models: From Maier, T. V.; Lucio, M.; Lee, L. H.; VerBerkmoes, N. C.; Brislawn, C. J.; Bernhardt, J.; Lamendella, R.; McDermott, J. E.; Bergeron, N.; Heinzmann, S. S.; Morton, J. T.; González, A.; Ackermann, G.; Knight, R.; Riedel, K.; Krauss, R. M.; Schmitt-Kopplin, P.; Jansson, J. K.: Impact of Dietary Resistant Starch on the Human Gut Microbiome, Metaproteome, and Metabolome. *mBio* vol. 8 no. 5 e01343-17 (2017). Reprinted and modified from (Maier et al. 2017). Copyright (2017) Maier et al.

Description	Model	R ² Y(cum)	Q ² (cum)	p (CV-ANOVA)
(-) FT-ICR-MS				
Baseline vs. HRS (Day 28)	G1 vs. G2	0,68	0,52	0.037
Baseline vs. LRS (Day 28)	G1 vs. G3	-	-	n.s.
HRS (Day 28) vs. LRS (Day 28)	G2 vs. G3	0.99	0.67	< 0.001
HRS (Day 28) vs. LRS (Day 56)	G2 vs. G4	0,78	0,50	0.043
LRS (Day 28) vs. HRS (Day 56)	G3 vs. G5	-	-	n.s.
HRS (Day 28) vs. HRS (Day 56)	G2 vs. G5	-	-	n.s.
LRS (Day 28) vs. LRS (Day 56)	G3 vs. G4	-	-	n.s.
HRS vs. LRS	(G2, G5) vs. (G3, G4)	0,44	0,28	0.017
LRS vs. HRS (Day 28)	(G3, G4) vs. G2	0,92	0,56	0.016
Baseline vs. all other	G1 vs. all other	0,84	0,46	<0.001
HRS vs. all other	(G2,G5) vs. all other	0,43	0,32	<0.001
LRS vs. all other	(G3,G4) vs all other	0,83	0,39	0.014
(+) FT-ICR-MS				
Baseline vs. HRS (Day 28)	G1 vs G2	0.99	0.58	0.032
Baseline vs. LRS (Day 28)	G1 vs G3	0.87	0.40	0.055
Baseline vs. all other	G1 vs. all other	0.78	0.45	<0.001
HRS (Day 28) vs. LRS (Day 56)	G2 vs. G4	-	-	n.s.
LRS (Day 28) vs. HRS (Day 56)	G3 vs. G5	-	-	n.s.
HRS (Day 28) vs. HRS (Day 56)	G2 vs. G5	-	-	n.s.
LRS (Day 28) vs. LRS (Day 56)	G3 vs. G4	-	-	n.s.

The OPLS-DA scores scatter plots of the discrimination between both RS diets at the same time point, and the merged time points of the HRS and LRS diet is displayed in Figure 2.4-5 A and B, respectively. Here, a trend toward separation was observed between the HRS and LRS diets (Maier et al. 2017).

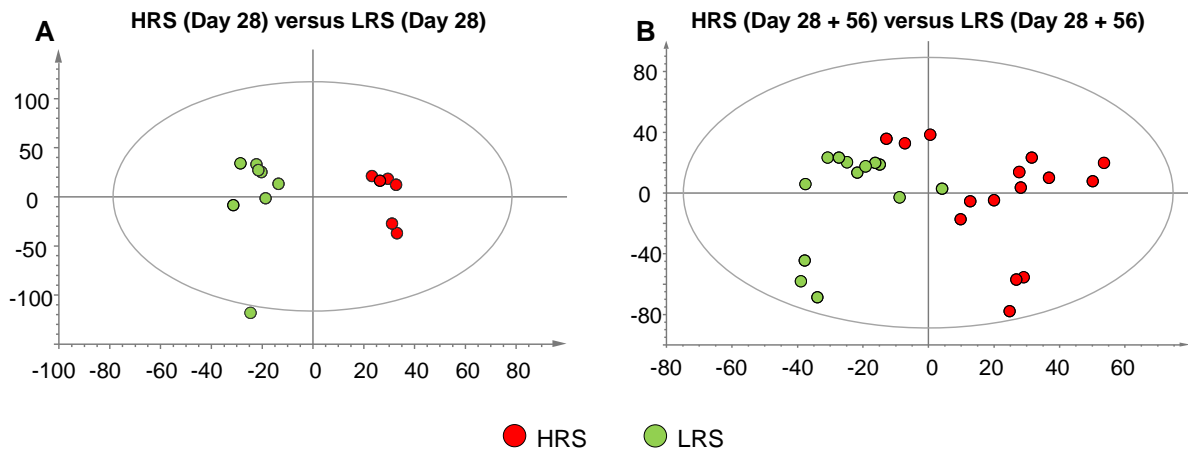


Figure 2.4-5: OPLS-DA scores scatter plot of fecal metabolome of HRS diet vs. LRS diet.

Comparison of different groups through OPLS-DA (UV scaling) of participants of the HRS (red) and LRS (green) diet with respect to different time points, analyzed in (-) FT-ICR-MS mode. A: HRS versus LRS diet, both at day 28. B: HRS versus LRS, merged time points. From Maier, T. V.; Lucio, M.; Lee, L. H.; VerBerkmoes, N. C.; Brislawn, C. J.; Bernhardt, J.; Lamendella, R.; McDermott, J. E.; Bergeron, N.; Heinzmann, S. S.; Morton, J. T.; González, A.; Ackermann, G.; Knight, R.; Riedel, K.; Krauss, R. M.; Schmitt-Kopplin, P.; Jansson, J. K.: Impact of Dietary Resistant Starch on the Human Gut Microbiome, Metaproteome, and Metabolome. *mBio* vol. 8 no. 5 e01343-17 (2017). Figure A reprinted and modified from (Maier et al. 2017). Copyright (2017) Maier et al.

Although the model comparing the HRS diets at different time points (G2 vs. G5) achieved through OPLS-DA analyses was not significant at all, the model comparing the baseline diet and the HRS diet at day 28 (G2) (Figure 2.4-6 A) revealed a few metabolites more strongly increased in HRS at day 28 (G2), than in HRS diet at day 56 (G5) compared to the baseline diet, but not significantly different from the HRS diet at day 56 (G5). Plotting the discriminative metabolites between baseline and HRS diet, the S-plot of the OPLS-DA analyses revealed several metabolites increased in the HRS diet on day 28. Those were heptadecenoic acid (C17:1), heptadecanoic acid (C17:0), octadecanoic acid (C18:0), icosanoic acid (C20:0), hexacosanedioic acid, cholesterol sulfate and an unknown metabolite (m/z 423.34797). In general, those metabolites showed consistently increased intensity levels through HRS diet intake at both time points compared to the baseline diet, but showed more diverse intensities levels in the respective HRS diet groups. One metabolite, namely pentadecanoic acid (C15:0, Figure 2.4-6 C) differed significantly between the HRS diet on day 28 and day 56 (p -value = 0.0105), being increased in day 28.

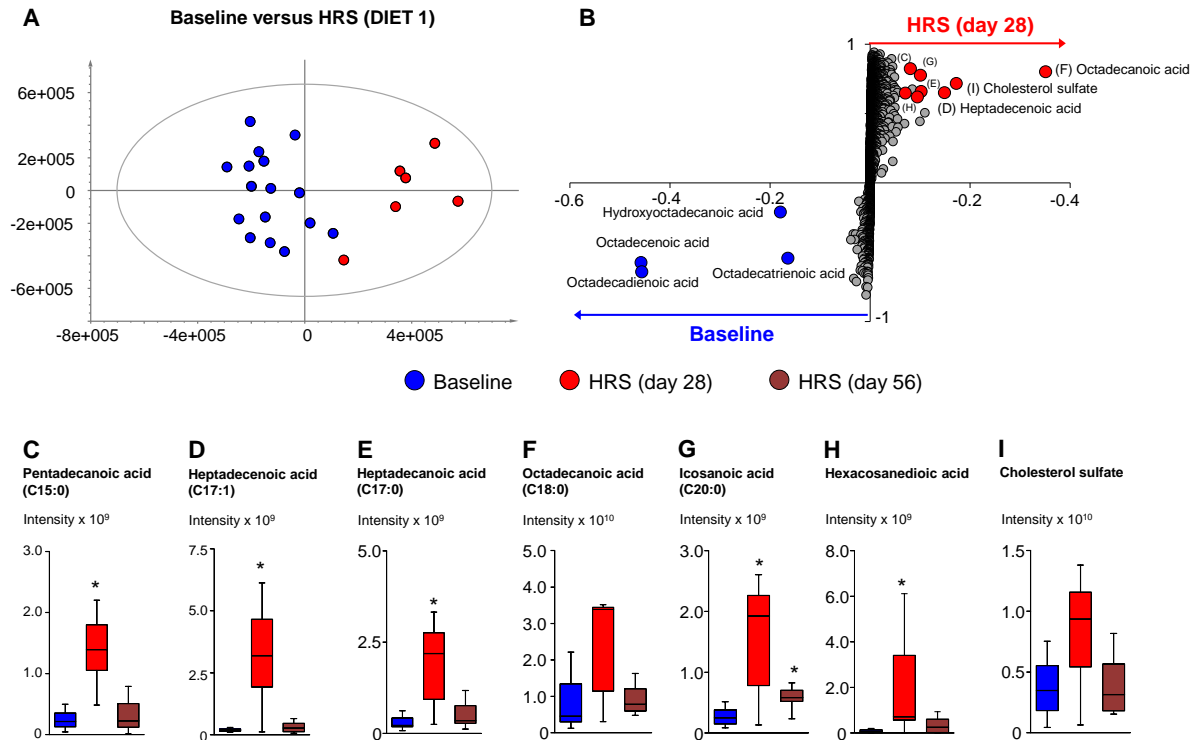


Figure 2.4-6: Differences between baseline and HRS diet at different time points

A: OPLS-DA scores scatter plot of fecal metabolome, measured in (-) FT-ICR-MS mode of baseline diet and HRS diet on day 28. B: S-Plot displaying mass signals highly discriminative between baseline and HRS diet on day 28, impacted differently in the HRS diet at day 56, such as (C) pentadecanoic acid, (D) heptadecenoic acid, (E) heptadecanoic acid, (F) octadecanoic acid, (G) icosanoic acid, (H) hexacosanedioic acid and (I) cholesterol sulfate. Further details are given in Table 6.1-7

Already the PCA revealed, if HRS diet was consumed first, followed by the LRS diet, changes were more dominant than the other way around. This was also confirmed by the OPLS-DA classification models comparing the impact of the order of RS (G2 vs. G4 or G3 vs. G5) consumption. Obviously, fatty acids were predominately altered by diet. Compared to the baseline diet, octadecanoic acid was highly increased through HRS consumption, whereas its related unsaturated species, including octadecenoic acid, octadecadienoic acid and octadecatrienoic acid were decreased. Its related unsaturated species, as well as a hydroxylated octadecanoic acid were high in participants consuming the baseline diet.

The model comparing the HRS diet at day 28 (G2) to the LRS diet at day 56 (G4) of the same individuals was slightly significant, whereas the other order was not. However, even despite some small differences, the two HRS diets had a similar impact on the global metabolite profile, independent of the time point or order of dietary starch intake. Since the OPLS-DA classification models comparing the

HRS diets at different time points and the LRS diet at different time points were not valid, the analyses were continued with considering both HRS diets as one group, as well as both LRS diets as one group.

In order to gain a first overview of the number of mass signals and metabolites discriminative for each diet class and for each OPLS-DA classification model, the loadings of each model-related S-plot ordinates were reported ($w[1]$ and $p(\text{corr})$). These values were calculated as percentages (% w and % p) of the highest discriminative metabolite of each group, averaged and logarithmized. Mass signals up to 60% of % w (equal to $\log > 1.78$) were counted as significant for each respective group, whereby double-listing in more than on model was possible. This resulted in several mass signals significantly altered by the HRS diet compared to the baseline diet and the LRS diet. In Figure 2.4-7 the significant mass signals for each OPLS-DA classification model and each diet are illustrated. As previously mentioned, a great number of mass signals were changed towards the HRS diet (17.6% - 26.4% of the metabolome ($n=5552$ mass signals)) in all classification models containing the HRS diet, and relatively few were significantly altered between the baseline (1.2% - 1.5%) and LRS diet (0.9% - 1.2%).

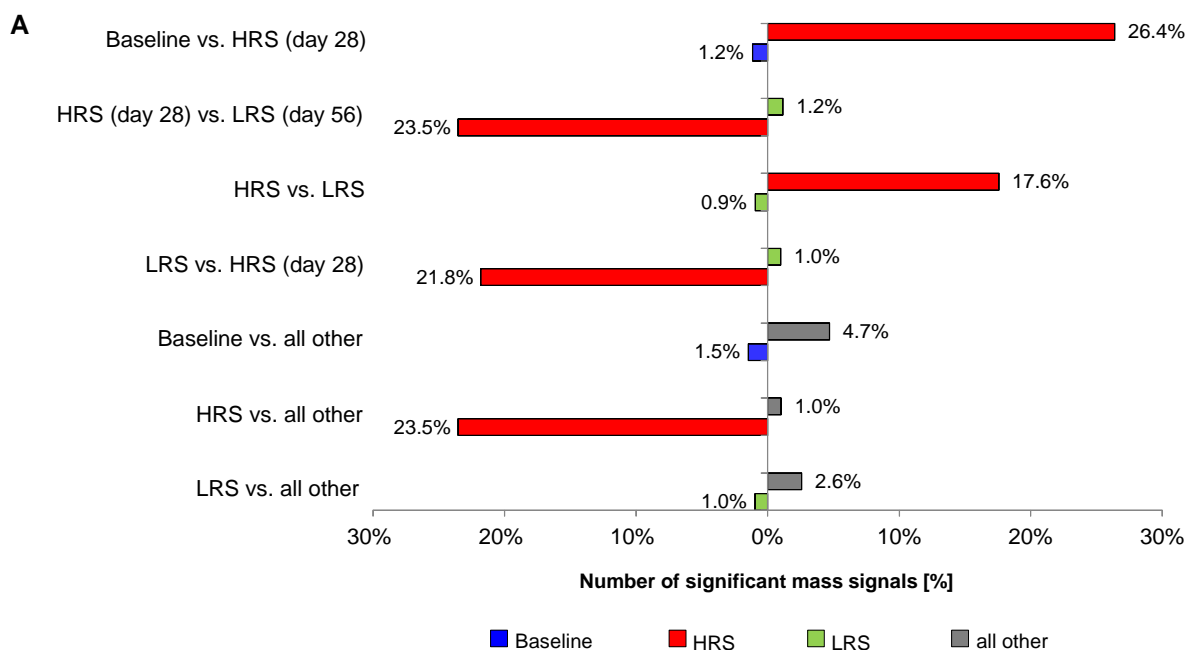


Figure 2.4-7: Overview of significant mass signals obtained through OPLS-DA.

Number of significant mass signals obtained through different OPLS-DA classification models of the (-) FT-ICR-MS mode comparing baseline (blue), HRS (red) and LRS (green) at different time points, as well as diet wise comparison to other groups.

Following this, the mass signals were assigned to metabolites using the MasSTRIX webserver (Wagele et al. 2012), which allowed classifying the significant mass signals to compound classes (Figure 2.4-8 A), and main pathways (Figure 2.4-8 B) of the KEGG pathway database. Only mass signals, which could be clearly assigned to a main compound classes or main pathways, respectively were taken into account for the calculations. Mass signals were excluded, if they were assigned to more than one main compound class, or more than one main pathway, or if the identification was unclear. Significantly increased mass signals in the HRS diet were predominately FAs (4.1% - 5.2%) and STs (4.7% - 7.7%). Through the pathway analysis, the lipid metabolism (1.8% - 2.8%), the metabolism of terpenoids and polyketides (1.8% - 2.2%), and the biosynthesis of other secondary metabolites (1.5% - 2.0%) could be detected to be affected through the consumption of a high amount of resistant starch. This analysis stated that RS consumption of either low or high in RS affected various compound classes differently and stressed the impact of RS on human metabolism.

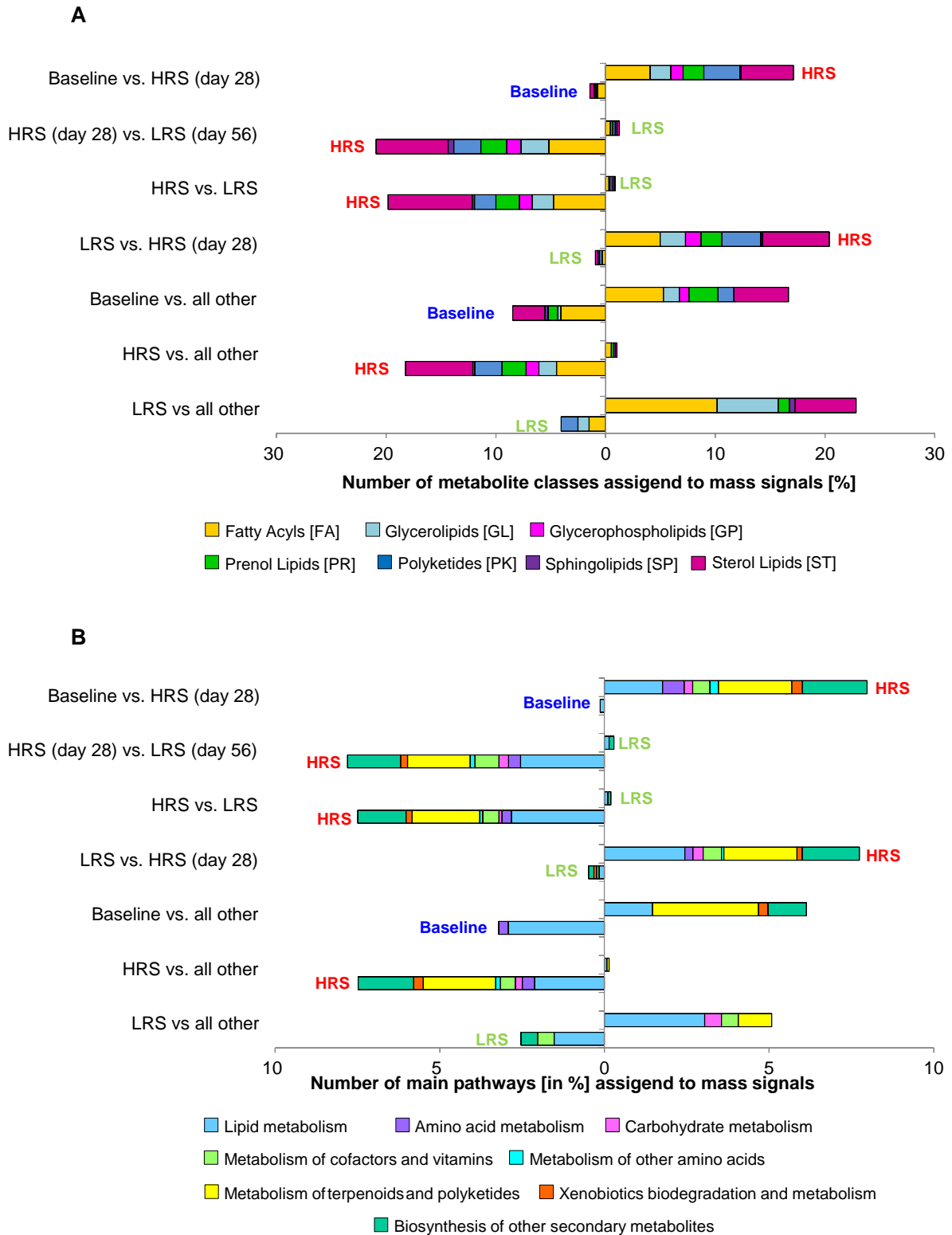


Figure 2.4-8: Mass signals classified into (A) number of compound classes and (B) main pathways.

Number of significant compound classes of the Lipid Maps database and main pathways of the KEGG pathway database assigned through the MassTRIX webserver, calculated based on the OPLS-DA classification models of the (-) FT-ICR-MS mode.

For the (+) FT-ICR-MS mode further classification models were applied. Here, baseline diet (G1) compared to the HRS diet at day 28 (G2) (Figure 2.4-9 A), and the comparison between baseline diet (G1) to the LRS diet (G3) (Figure 2.4-9 B) were significantly altered, which already was implied through the PCA. The most abundant and highly discriminative mass signals between the baseline diet and both RS diets, emerged as predominately metabolites of several lipid classes, especially phosphatidic acids (PA), which will be reviewed in detail in Chapter 2.4.1.5.1.

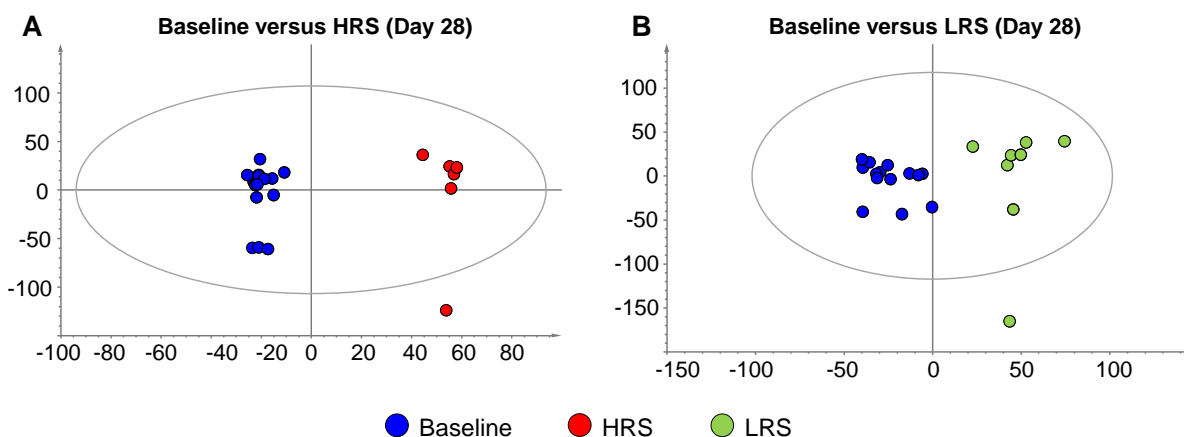


Figure 2.4-9: OPLS-DA scores scatter plot of fecal metabolome comparing baseline and RS diets.

Comparison of different groups through OPLS-DA (UV scaling) of participants of the baseline (blue), HRS (red) and LRS (green) diet, analyzed in (-) FT-ICR-MS mode. A: Baseline versus HRS diet at day 28. B: Baseline versus LRS, at day 28.

Additionally, the statistical models of the two HRS diets at different time points, as well as the LRS diet groups were not valid, since they did not pass the CV-ANOVA step. In contrast to the (-) FT-ICR-MS mode, both HRS diet groups compared to both LRS groups were not significant at all.

2.4.1.3 Correlation studies: metabolome and the amount of resistant starch

As next step, correlation studies between the amount of RS and all mass signals of the metabolome data were performed. Concerning this, metabolites which altered differently by baseline, high or low RS consumption or showed characteristic decreasing or increasing intensity patterns through varying amounts of RS were illustrated. Calculations were done with varying amounts of RS in grams (0 g : 38 g : 2 g). Several mass signals correlated positively with the amount of RS, which is displayed for (-) FT-ICR-MS ($p\text{-corr} < 1.09\text{E-}05$) in Figure 2.4-10 and for (+) FT-ICR-MS ($p\text{-corr} < 9.73\text{E-}04$) in Figure 2.4-11. For each ionization mode, the top 50 positively correlated mass signals to the HRS diet with a correlation value (R) ordered from high to low from $R = 0.77 - 0.60$ (-) or $R = 0.66 - 0.48$ (+) is illustrated.

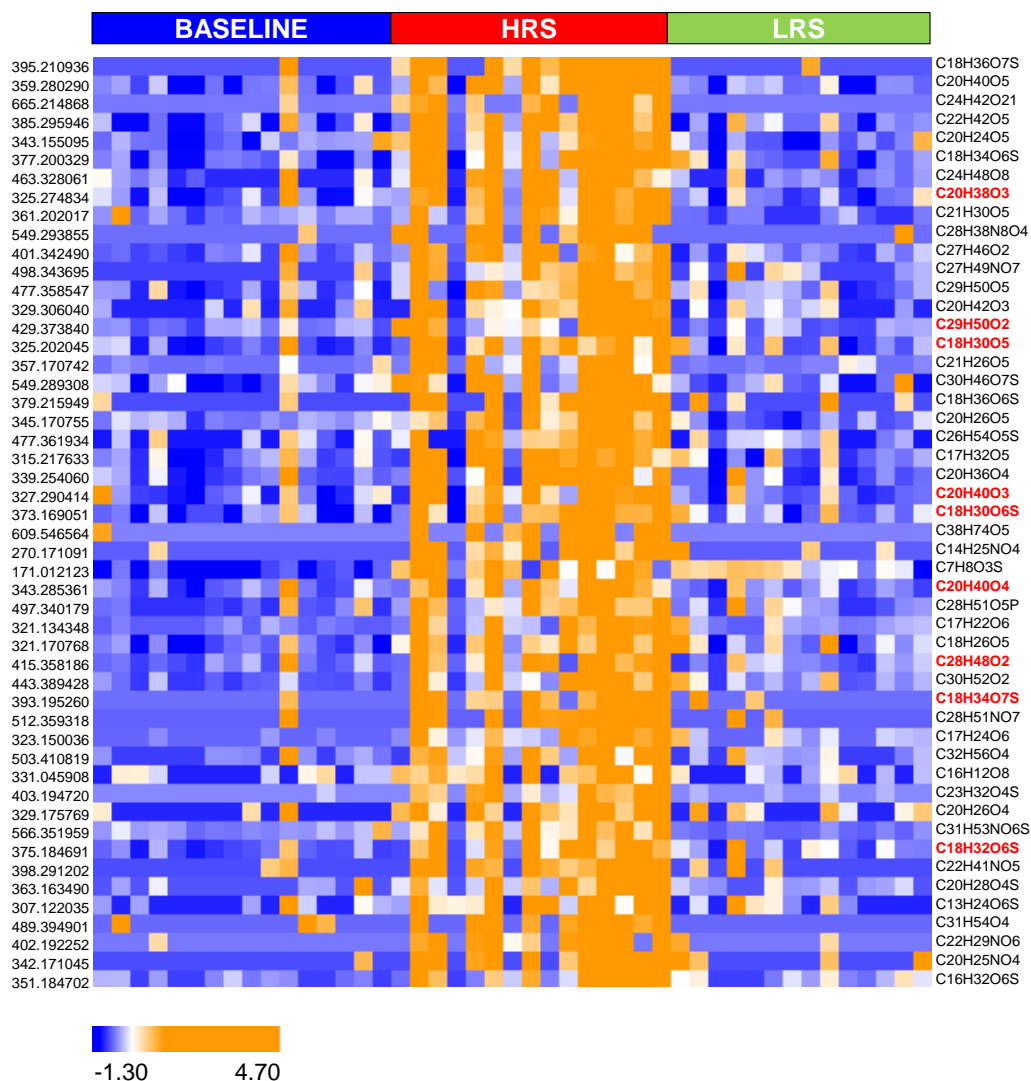


Figure 2.4-10: Top 50 metabolites positively correlated with HRS, analyzed in (-) FT-ICR-MS.

Heatmap of top 50 mass signals, presented as m/z and molecular formulas, which correlated positively with high amount of RS ranked from high to low correlation ($R = 0.77 - 0.60$) revealed trough Pearson correlation. Red labeled molecular formulas could be assigned to metabolites by database assignment. Further details are given in Table 6.1-8.

Most mass signals could be assigned to molecular formulas. Additionally, database comparison assigned some mass signals obtained through (-) FT-ICR-MS analyses to metabolites. The correlation revealed several metabolites, namely hydroxy fatty acids and oxylipins positively correlated with the HRS diet. These comprised the oxylipin dihydroxyoctadecadienoic acid ($C_{18}H_{30}O_5$) and the hydroxy fatty acids, such as hydroxyeicosanoic acid ($C_{20}H_{40}O_3$), hydroxyeicosenoic acid ($C_{20}H_{38}O_3$) and dihydroxyeicosanoic acid ($C_{20}H_{40}O_4$). Further sulfate conjugates of hydroxy fatty acids correlated highly with the amount of RS, namely hydroxyoctadecatrienoic acid sulfate ($C_{18}H_{30}O_6S$), dihydroxyoctadecenoic acid sulfate ($C_{18}H_{34}O_7S$) and hydroxyoctadecadienoic acid sulfate ($C_{18}H_{32}O_6S$),

whose molecular formula is labeled in red in Figure 2.4-10. Oxylipins are biosynthesized of polyunsaturated fatty acids (PUFAs), such as arachidonic acid and are involved in several processes and pathways, such as the arachidonic acid metabolism. These finding that oxylipins were correlated positively with RS consumption lead to further analyses in order reveal their contribution and biological importance in human lipid metabolism (Chapter 2.4.1.4) and to detect more oxylipin species in the fecal samples and evaluate the impact of RS on the oxylipin profile (Chapter 2.4.1.5.3). Additionally, mass signals assigned to intermediates in the tocopherol biosynthesis (α - β - γ -tocopherol, $C_{29}H_{50}O_2$ and $C_{28}H_{48}O_2$) were highly correlated with the amount of RS, whose molecular formula is labeled in red in Figure 2.4-10. On the contrary, none of the mass signals of the (+) FT-ICR-MS measurements positively correlated with RS could not be assigned to metabolites. The top 50 correlated mass signals are illustrated in Figure 2.4-11.

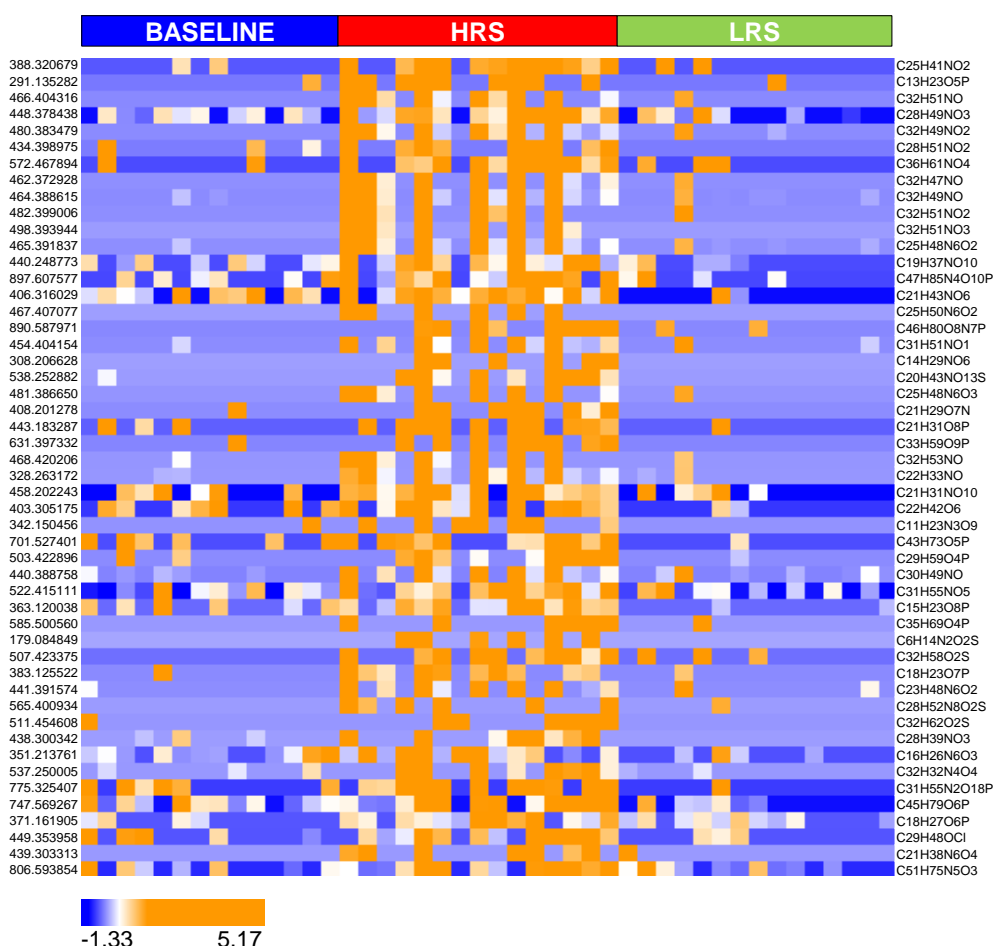


Figure 2.4-11: Top 50 highly correlated metabolites analyzed in (+) FT-ICR-MS.

Heatmap of the top 50 mass signals, presented as m/z and molecular formulas, which were correlated negatively with high amount of RS ranked from high to low correlation ($R = 0.66 - 0.48$) revealed trough Pearson correlation. Further details are given in Table 6.1-10.

2. Effect of resistant starch on the gut microbiome

Further information on correlation values and p-corr is given for (-) FT-ICR-MS in Table 6.1-8 and for (+) FT-ICR-MS in Table 6.1-10. In addition, mass signals were detected, which correlated negatively ($p\text{-corr} < 2.89\text{E-}02$) with the amount of RS. This led to several mass signals increased in the baseline diet and/or in the LRS diet. Further, it was observed, that mass signals being strongly increased in the baseline diet, showed lower intensity levels in the LRS diet and disappeared almost completely through the consumption of a high amount of RS. One of these mass signals was assigned as octadecadienoic acid (C18:2, C₁₈H₃₂O₂).

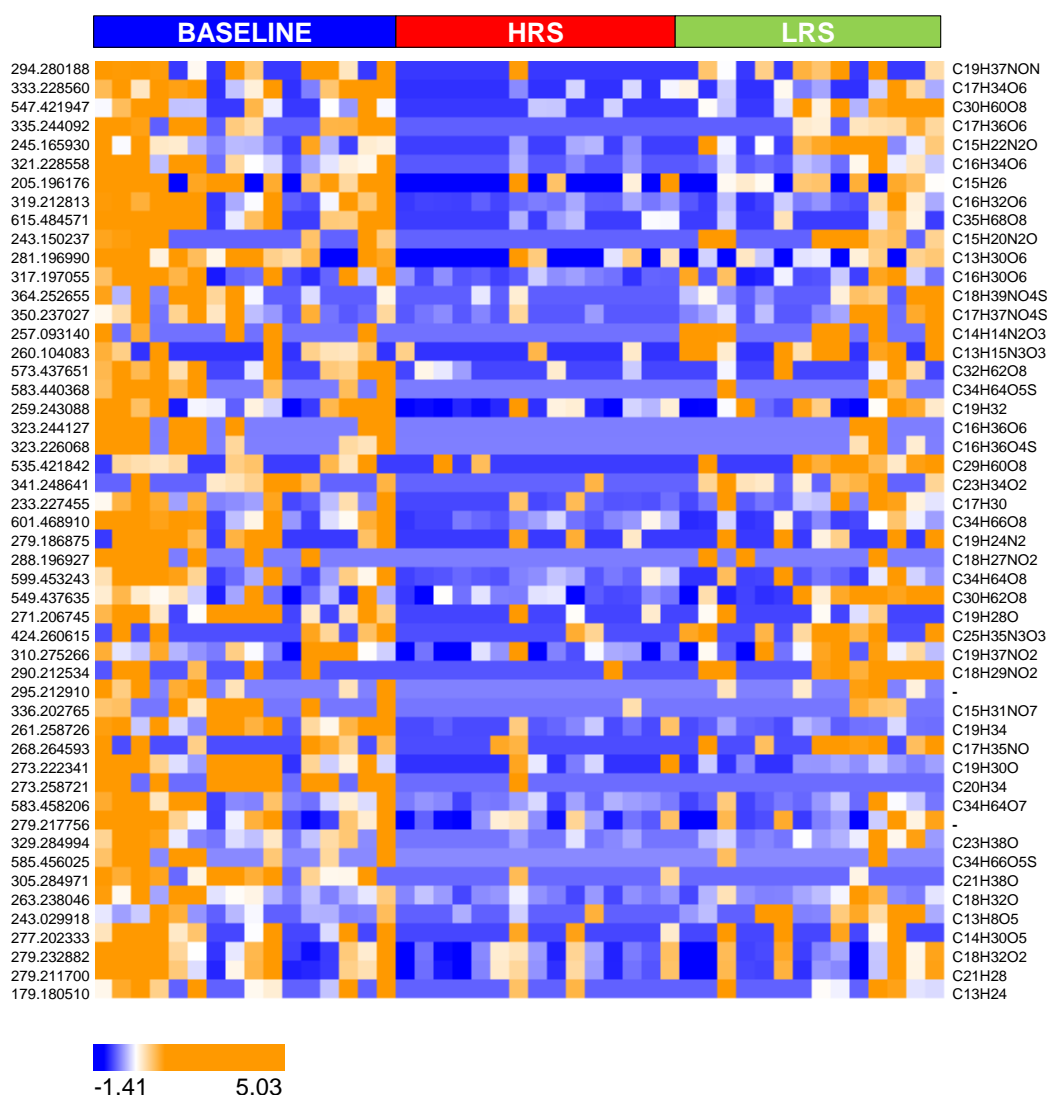


Figure 2.4-12: Top 50 metabolites negatively correlated with HRS, analyzed in (-) FT-ICR-MS.

Heatmap of the top 50 mass signals, presented as m/z and molecular formulas, which were correlated negatively with high amount of RS ranked from high to low correlation ($R = -0.49$ to -0.33) revealed by Pearson correlation. Further details are given in Table 6.1-9.

As previously shown, several mass signals significantly correlating with the amount of RS in both ionization modes were detected, where the high impact in the metabolite profile due to HRS dietary intake was demonstrated again. On the contrary, some mass signals even appeared to be negatively correlated to the amount of RS. Their level of correlation and significance was not as strong as detected in the positively correlated mass signals due to dietary starch intake. Most of the mass signals could be assigned to molecular formulas, whereas only a few metabolites could be assigned to compounds, which were mainly metabolites of the class of fatty acyls impacted through HRS diet. On the contrary, octadecadienoic acid (C18:2) was correlated negatively with the HRS diet and appeared to be increased in the baseline diet and suppressed through dietary starch intake in general. Metabolites observed in the correlation studies not only highlighted the enormous impact of HRS on the fecal metabolome, but also demonstrated how the differently affected metabolites were interrelated with varying amounts of RS.

2.4.1.4 Lipid metabolism affected by high resistant starch

Already in the correlation studies some metabolites of the lipid metabolism appeared to be altered by RS. For that reason, the lipid metabolism was considered in detail. In several studies, the lipid metabolism or lipid profiles of plasma and/or blood samples were detected to be impacted by dietary fiber, including mainly lipoproteins (e.g. VLDL, HDL, LDL, cholesterol and serum TG) and other lipid markers (Kabir et al. 1998, Hashizume et al. 2012) (Behall et al. 1989, Zhou et al. 2015). Additionally, several studies investigating the impact of dietary fiber on mammals is nicely reviewed by Lattimer and Haub in 2010 (Lattimer and Haub 2010). Furthermore, one study was conducted to investigate the impact of dietary fiber (resistant maltodextrin, RM) on fecal metabolic signatures of donor and recipient fecal microbiota transplanted mice, which appeared to be associated with RM-mediated improvement in mouse metabolic disease models (He et al. 2015). Here, they detected fecal metabolites of cholesterol metabolism, such as mevalonate and coprostanol significantly decreased levels in donor and recipient mice, which indicated an essential role of RM in cholesterol control (He et al. 2015).

However, the impact of dietary fiber on the lipid metabolism of fecal samples, including metabolites involved in several pathways of the human lipid metabolism is rather unknown. Thus, the effect of RS on lipid metabolism should be carefully examined in human studies (Higgins et al. 2004).

Here, the lipid metabolism will be reviewed in detail, focusing on specific pathways of the lipid metabolism, including alpha-linolenic acid metabolism, linoleic acid metabolism, biosynthesis of unsaturated fatty acids, fatty acid biosynthesis, steroid hormone biosynthesis, steroid biosynthesis, arachidonic acid metabolism, glycerolipids metabolism, primary bile acid biosynthesis, secondary bile acid biosynthesis and sphingolipid metabolism.

By running the MassTRIX webserver, the mass signals were not only assigned to compounds, but also to KEGG CIDs and specific pathway information. Therefore, the mass signals assigned to KEGG CIDs, including pathways information of the lipid metabolism, were selected for this analysis. This resulted in 66 metabolites of the lipid metabolism altered through diet. These changes were visualized in a heatmap, as shown in Figure 2.4-13.

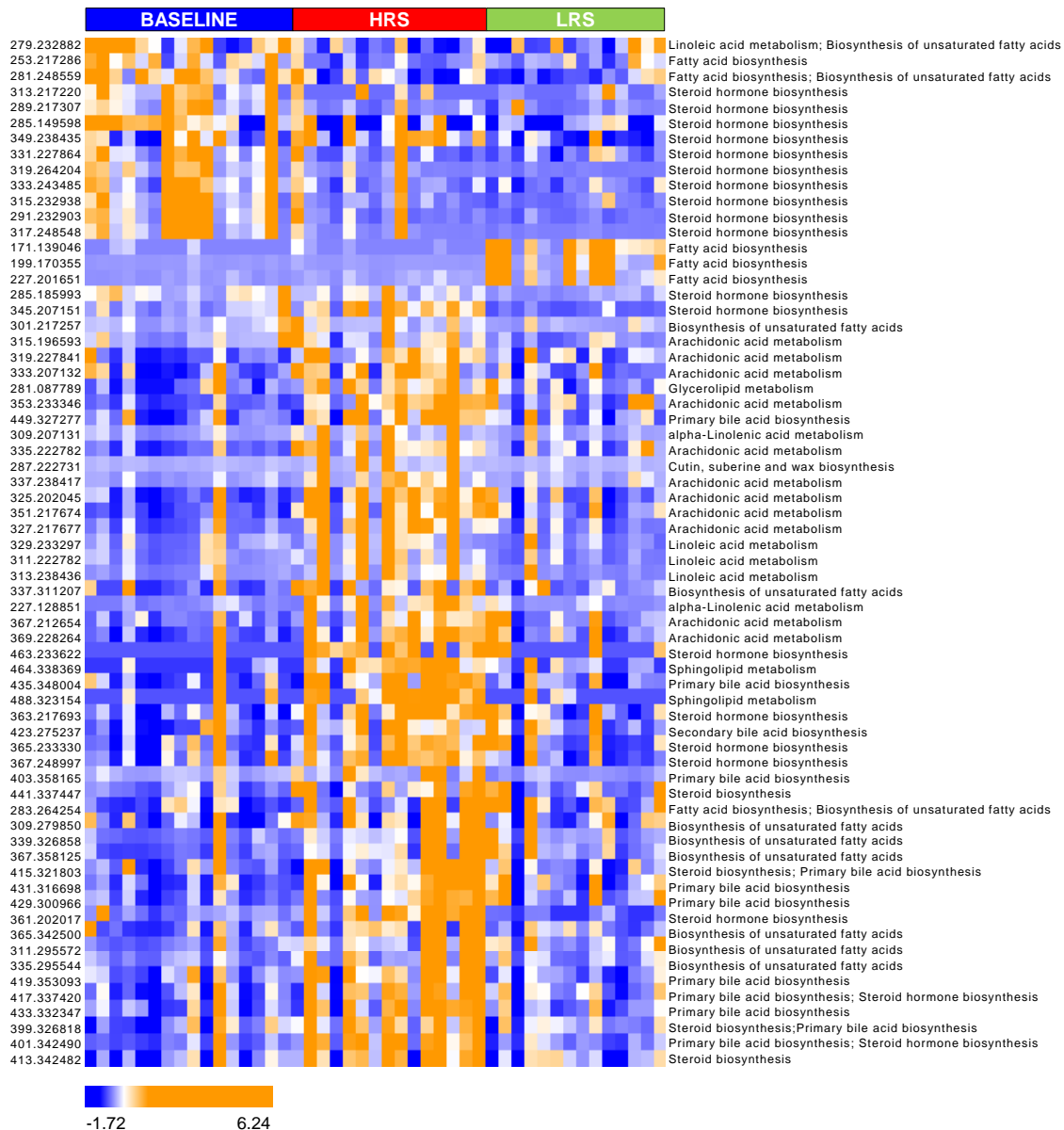


Figure 2.4-13: Metabolites of the lipid metabolism impacted through diet.

Heatmap of 66 significant metabolites, displayed in m/z of the lipid metabolism impacted through the baseline, HRS or LRS diet. Pathways of the lipid metabolism, such as alpha-linolenic acid metabolism, linoleic acid metabolism, biosynthesis of unsaturated fatty acids, fatty acid biosynthesis, steroid hormone biosynthesis, steroid biosynthesis, arachidonic acid metabolism, glycerolipids metabolism, primary bile acid biosynthesis, secondary bile acid biosynthesis and sphingolipid metabolism. Further details are listed in Table 6.1-11. From Maier, T. V.; Lucio, M.; Lee, L. H.; VerBerkmoes, N. C.; Brislawn, C. J.; Bernhardt, J.; Lamendella, R.; McDermott, J. E.; Bergeron, N.; Heinzmann, S. S.; Morton, J. T.; González, A.; Ackermann, G.; Knight, R.; Riedel, K.; Krauss, R. M.; Schmitt-Kopplin, P.; Jansson, J. K.: Impact of Dietary Resistant Starch on the Human Gut Microbiome, Metaproteome, and Metabolome. *mBio* vol. 8 no. 5 e01343-17 (2017). Reprinted and modified from (Maier et al. 2017). Copyright (2017) Maier et al.

The mass signals significantly changed were proven by the *post hoc* Kruskal-Nemenyi test, which is listed in the appendix in Table 6.1-11. Predominately three pathways seem to be highly impacted, which were the steroid hormone biosynthesis, arachidonic acid metabolism and primary bile acid biosynthesis (Maier et al. 2017). Thirteen metabolites of the lipid metabolism were significantly decreased in both

RS diets compared to the baseline diet. This comprises octadecadienoic acid (C18:2), hexadecenoic acid (C16:1), octadecenoic acid (C18:1) (Maier et al. 2017) and ten metabolites classified as sterol lipids and involved in steroid hormone biosynthesis.

Further, three fatty acids, namely decanoic acid (C10:0), dodecanoic acid (C12:0) and tetradecanoic acid (C14:0), all involved in the fatty acid biosynthesis, were solely increased in fecal samples of the LRS diet compared to the baseline and the HRS diet (Maier et al. 2017). Vastly more metabolites of the lipid metabolism, in fact 50, were significantly increased in the HRS diet, compared to the baseline diet and the LRS diet. It was noticeable that the arachidonic acid metabolism, primary bile acid metabolism, secondary bile acid metabolism and steroid biosynthesis primarily were highly impacted through the HRS diet (Maier et al. 2017). Metabolites involved in the arachidonic acid metabolism impacted through RS were several oxylipins, like hydroxyeicosatetraenoic acid, hydroxyxoeicosatetraenoic acid, hydroxyoctadecenoic acid, dihydroxyeicosatetraenoic acid, dihydroxyhexadecanoic acid, dihydroxyeicosatrienoic acid, dihydroxyoctadecadienoic acid, dihydroxyoctadecadienoic acid, dihydroxyoctadecenoic acid, trihydroxyeicosatrienoic acid, trihydroxyeicosatetraenoic acid, trihydroxyoctadecadienoic acid, trihydroxyoctadecenoic acid.

Additionally, several metabolites of the primary bile acid metabolism were found to be impacted through the HRS diet, such as trihydroxycholestanoic acid, tetrahydroxycholestane, dihydroxycholestenone, dihydroxycholestenoic acid, hydroxyoxocholestenoic acid, cholestanetriol, dihydroxycholesterol, trihydroxycholestanal, and hydroxycholesterol.

The secondary bile acid metabolism was not strongly affected to a lower extent, since only one metabolite involved was detected to be increased in the HRS diet samples, namely tetrahydroxycholanoic acid. Additionally, four metabolites of the steroid biosynthesis and eight ones of the steroid hormone biosynthesis, which were assigned as sterol lipids were found to be increased in the HRS diet. Further, several fatty acids, both saturated and unsaturated ones involved in the biosynthesis of unsaturated fatty acids were strongly increased in the fecal samples of the participants consuming the HRS diet. Those were octadecanoic acid (C18:0), icosanoic acid (C20:0), docosanoic acid (C22:0), tetracosanoic acid (C24:0), icosenoic acid (C20:1), icosapentanoic acid (C20:5), docosenoic acid (C22:1), docosadienoic acid (C22:2) and tetracosenoic acid (C24:1). Dodecenedioic acid, a metabolite of the alpha-linolenic acid metabolism was observed in the HRS diet.

To date, only little metabolomics research focusing on the impact of RS on a pathway-related level was found, especially in humans. To date, only one research group reported the effect of dietary RS intake in growing pigs (Lu et al. 2016). In accordance with our results, they also detected the lipid metabolism to be increased in pigs consuming a HRS diet (Lu et al. 2016). To conclude, metabolites of the lipid metabolism significantly affected by the baseline diet and by intake of RS were detected. This included a great number of metabolites that were highly impacted by the HRS diet. They were involved in e.g. arachidonic acid metabolism, primary bile acid metabolism and steroid biosynthesis. Within this study novel links between a RS diet and lipid metabolism were observed.

2.4.1.5 Different compound classes affected through baseline, HRS or LRS diet

2.4.1.5.1 Lipid patterns changed through baseline, HRS and LRS diet

The separation in the scores scatter plot of the PCA of the (+) FT-ICR-MS mode seems to be mainly driven by increased mass signals through baseline diet. Hereto, the multivariate data analyses reveal several mass signals significantly increased in the baseline diet, which were responsible for class discrimination between the baseline diet and both RS diets. Those mass signals could be assigned to various lipid classes, to main classes of the Lipid Maps database (Fahy et al. 2009). Lipids are important in intestinal biology (Gregory et al. 2013) and involved in several functional processes e.g. energy storage and acting as signaling molecules (Han and Gross 2005). Increased lipid abundancies are associated with several disorders caused by obesity (Mika and Sledzinski 2017). It is well known that different lipid species are altered in plasma of obese humans and that also diet has an impact on the plasma lipid composition of different lipid species (e.g. triacylglycerols (TAG), phospholipids and ceramides) (Mika and Sledzinski 2017). It was possible to study the lipid profiles through the investigation of the mass spectra generated through (+) FT-ICR-MS analyses. This revealed distinct patterns of several lipid classes predominantly increased in the fecal samples of the baseline diet, which means they were reduced through dietary starch intake (Table 2.4-2). Lipid classes, such as glycerolipids (GL), sphingolipids (SP) and glycerophospholipids (GP) were significantly changed, whereas mainly GP contributed to the discrimination between baseline and RS samples. However, the predominating lipid class significantly changed between the fecal samples of the baseline diet and dietary starch intake was several phosphatidic acids (PA) (Figure 2.4-14) ranging from chain length from C₁₆ to C₃₆. The majority of them was significantly decreased in both RS diets compared to the

2. Effect of resistant starch on the gut microbiome

baseline diet, namely PA(P-16:0), PA(O-16:0), PA(16:1), PA(P-18:0), PA(18:4), PA(18:3), PA(18:1), PA(20:4), PA(20:3), PA(20:2), PA(20:1), PA(20:0), PA(22:2), PA(32:0), PA(P-34:2)/PA(O-34:3), PA(P-34:0)/PA(O-34:1), PA(P-34:1)/PA(P-34:2), PA(O-34:0), PA(34:1), PA(34:0), PA(P-36:2)/PA(O-36:3), PA(P-36:1)/PA(O-36:2), PA(36:2), PA(36:1) and partially their “lyso” forms. Further details for PAs increased by baseline diet are given in the supplement in Table 6.1-12.

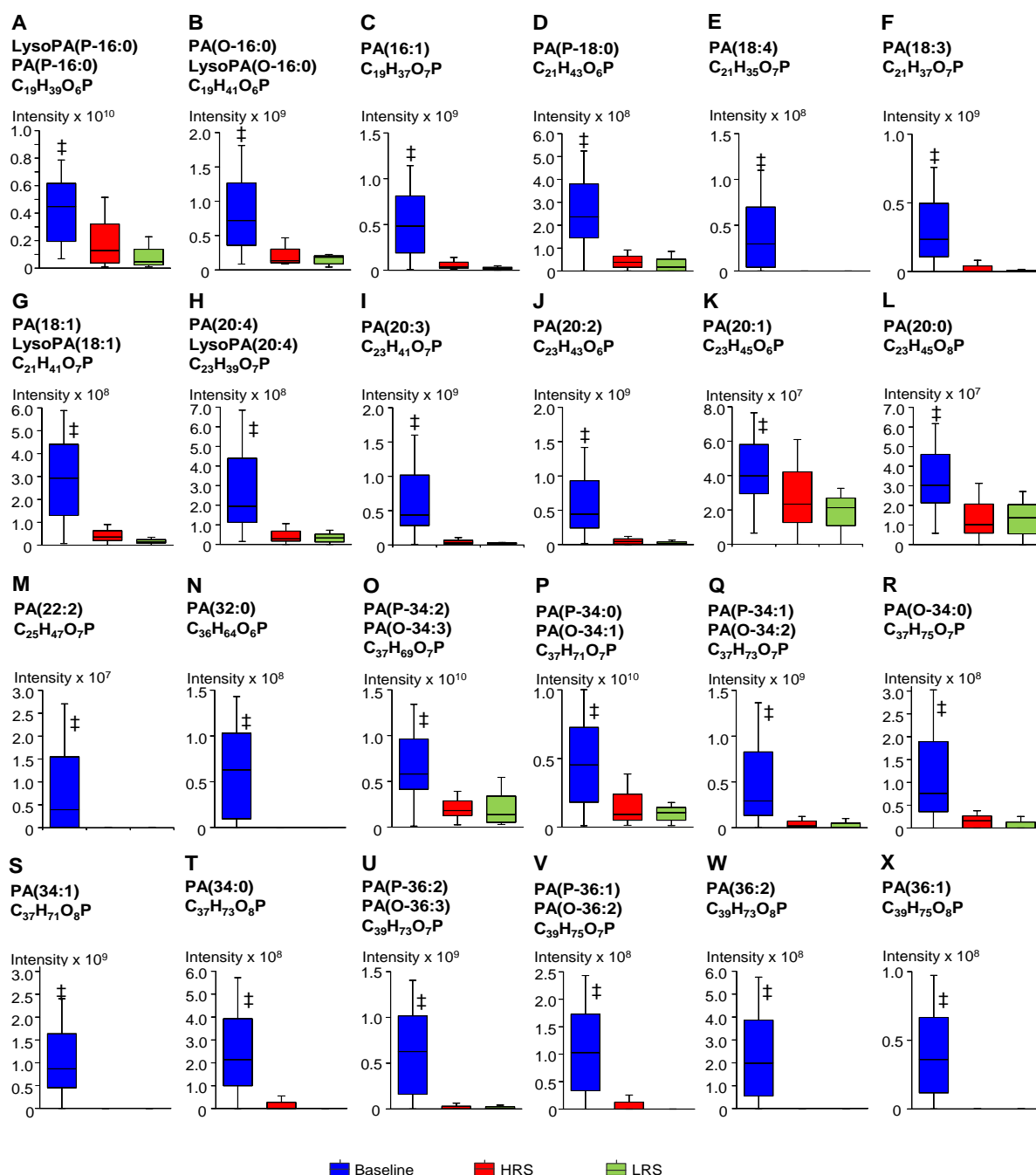


Figure 2.4-14: Phosphatidic acids significantly decreased through dietary starch intake.

Boxplots of 24 phosphatidic acids significantly changed in the baseline diet (blue) compared to the HRS (red) and LRS (green) diet, analyzed in (+) FT-ICR-MS mode. Molecular formulas calculated by NetCalc. p-values were calculated with the *post hoc* Kruskal-Nemenyi test. Further details are listed in Table 6.1-12.

Phosphatidic acids belong to the class of glycerophospholipids and play an essential role in the biosynthesis of triacylglycerols and phospholipids. Thus, they are key intermediates in the lipid metabolism and act as signaling molecules (Athenstaedt and Daum 1999). Further, they are involved in the production of phosphatidylcholines (PC), phosphatidylethanolamines (PE) and phosphatidylserines (PS) via diradylglycerols (DG) (Athenstaedt and Daum 1999), which thus might be a link to the increased levels of DGs, PCs, PEs and PSs, detected in the fecal samples of all participants consuming the baseline diet (Table 2.4-2).

However, a few PAs showed significantly (p -value < 0.014) increased levels through either the LRS diet (Figure 2.4-15 A-D) or RS intake in general (Figure 2.4-16 A-I).

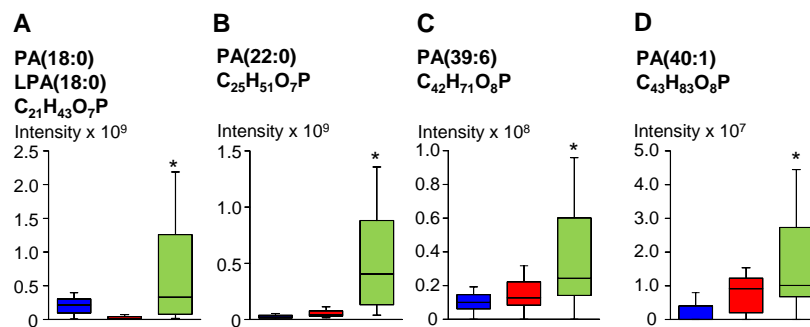


Figure 2.4-15: Phosphatidic acids altered through LRS diet.

Boxplots of 4 phosphatidic acids significantly increased in the LRS diet (green) compared to the baseline diet (blue) and the HRS (red), analyzed in (+) FT-ICR-MS mode. Molecular formulas calculated by NetCalc. p -values were calculated through the *post hoc* Kruskal-Nemenyi test. Further details are listed in Table 6.1-13.

2. Effect of resistant starch on the gut microbiome

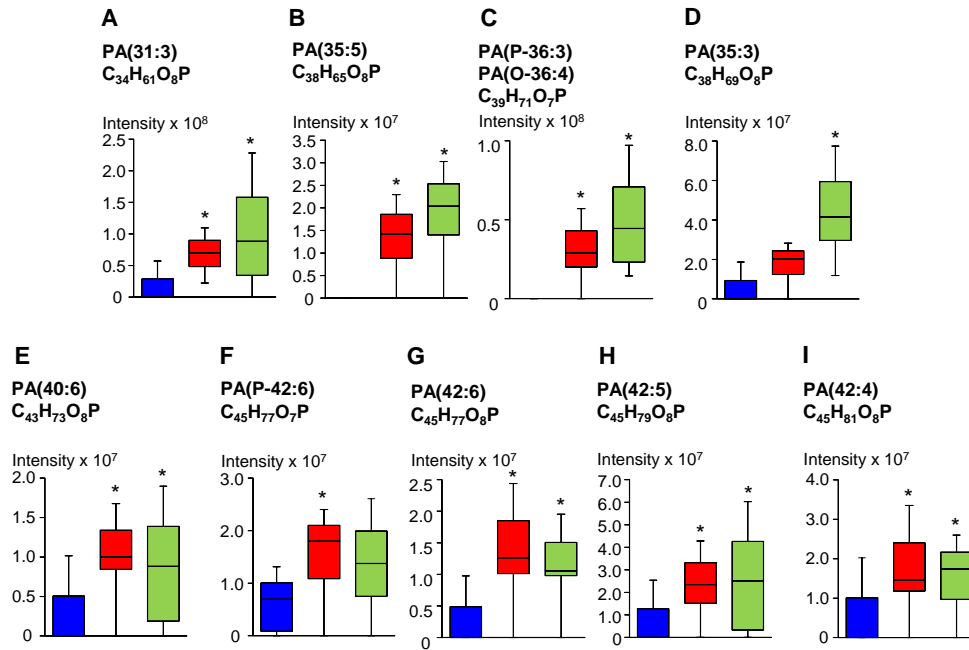


Figure 2.4-16: Phosphatidic acids increased through dietary starch intake.

Boxplots of 9 phosphatidic acids significantly increased in the HRS diet (red) compared to the baseline diet (blue) and the LRS (green), analyzed in (+) FT-ICR-MS mode. Molecular formulas calculated by NetCalc. p-values were calculated through the *post hoc* Kruskal-Nemenyi test. Further details are listed in Table 6.1-14

More details on the PA significantly changed through the LRS or both RS groups are listed for the LRS diet in Table 6.1-13 and for RS in general in Table 6.1-14. Though, phosphatidic acids significantly affected exclusively through the HRS diet could not be observed at all. A special class of PA, the cyclic phosphatidic acid (CPA), were the most abundant compounds detected in the baseline diet, namely CPA(16:0), CPA(18:2), CPA(18:1) and CPA(18:0). They were significantly decreased (p-value < 0.011) in both RS diets compared to the fecal samples of the baseline diet (Figure 2.4-17).

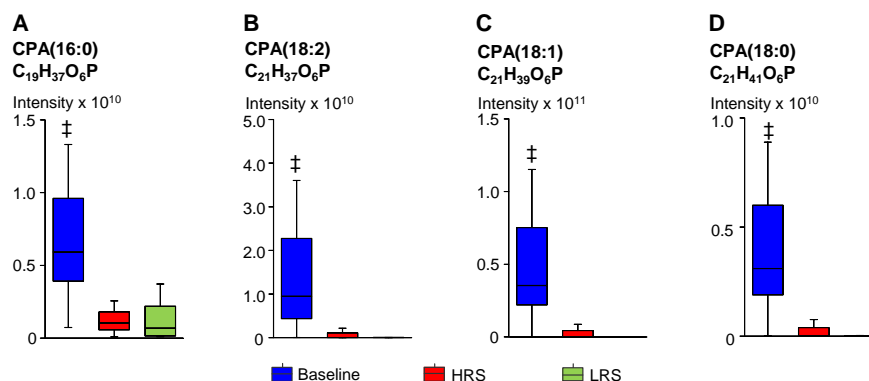


Figure 2.4-17: Cyclic phosphatidic acids significantly increased in baseline diet.

Boxplots of 4 cyclic phosphatidic acids significantly increased in the baseline diet (blue) compared to the HRS diet (red) and the LRS (green), analyzed in (+) FT-ICR-MS mode. Molecular formulas calculated by NetCalc. p-values were calculated through the *post hoc* Kruskal-Nemenyi test. Further details are listed in Table 6.1-15.

CPA can be generated from lysophosphatidylcholine (lysoPC) by the enzyme phospholipase D (PLD2) (Oishi-Tanaka and Glass 2010) and is an antagonist of the peroxisome proliferator-activated receptor-gamma (PPAR γ) (Tsukahara et al. 2010), a nuclear receptor, which regulates the expression of several genes. Further, insulin is a physiological activator of PLD2, i.e. induces higher levels of CPA (Tsukahara et al. 2010). CPA binds to and inhibits the nuclear hormone receptor PPAR γ . PPAR γ regulates several pathways of the carbohydrate- and lipid metabolism which are strongly associated with several human diseases, such as diabetes (Lehmann et al. 1995).

Participants suffering from insulin resistance are usually treated with synthetic agonists (e.g. insulin-sensitizer thiazolidinedione, TZD) and activators of PPAR γ . Through the activation of PPAR γ , the sensitivity of hepatocytes, muscle cells and adipose tissue for insulin is increased, which leads to improve insulin resistance in type 2 diabetes (Tsukahara et al. 2010). Further, the activation of the PPAR γ -receptor leads to an increased absorption and metabolization of free fatty acids.

Here, high levels of CPA were detected in the fecal samples of participants consuming the baseline diet, which does not contain RS. Since CPA inhibits the activation of PPAR γ , the reduction of insulin resistance is decreased. Through the intake of dietary starch, the levels of CPA were decreased. Therefore, it can be hypothesized that RS reduces the levels of CPA, relieves the inhibition of the PPAR γ -receptor and might increase the sensitivity for insulin of the cells.

Distinct patterns between the two diet classes concerning glycerophosphates (PA), glycerophosphocholines (PC), glycerophosphoethanolamines (PE), glycerophosphoglycerols (PG) and glycerophosphoserines (PS) were observed (Table 2.4-2).

2. Effect of resistant starch on the gut microbiome

Table 2.4-2: Lipids changed due to baseline and dietary starch diets.

Several lipid classes, such as diradylglycerols (DG), glycerophosphocholines (PC), glycerophosphoethanolamines (PE), glycerophosphoglycerols (PG), glycerophosphoserines (PS) and ceramides significantly impacted by the baseline or the RS diet, analyzed in (+) FT-ICR-MS mode. The table contains averaged experimental mass, compound name, monoisotopic mass, molecular formula calculated by NetCalc, arithmetic means of baseline, HRS and LRS, respectively, as well as p-values showing the significance according to diet comparison, calculated with the *post hoc* Kruskal-Nemenyi test.

Class	Mass (avg.)	Compound name	Monoisotopic mass	molecular formula	Mean B	Mean HRS	Mean LRS	p-value B vs. HRS	p-value B vs. LRS	Diet
Glycerolipids										
DG										
	593.514182	DG(34:2)	592.506675	C ₃₇ H ₆₈ O ₅	3.03E+07	1.04E+07	1.16E+07	1.20E-02	1.70E-02	B
	619.529873	DG(36:3)	618.522325	C ₃₉ H ₇₀ O ₅	1.36E+08	5.31E+07	3.92E+07	6.20E-03	5.60E-03	B
	621.545595	DG(36:2)	620.537975	C ₃₉ H ₇₂ O ₅	1.33E+08	4.97E+07	2.78E+07	2.62E-02	9.90E-03	B
Glycerophospholipids										
PC, PE, LysoPC										
	510.391609	PC(O-18:0)	509.384525	C ₂₆ H ₅₆ NO ₈ P	2.89E+07	0	0	1.40E-02	1.60E-02	B
	620.464465	PE(P-28:0)	619.457690	C ₃₃ H ₆₆ NO ₇ P	6.36E+07	1.57E+07	2.91E+07	1.90E-02	n.s.	B
	662.511832	PE(P-31:0) LysoPC(28:1)	661.504640	C ₃₆ H ₇₂ O ₇ NP	6.48E+07	2.13E+07	1.28E+07	5.50E-03	1.10E-03	B
	676.491434	PE(31:1), PC(38:1)	675.483905	C ₃₆ H ₇₀ NO ₈ P	2.57E+07	2.35E+06	1.82E+06	2.10E-02	1.20E-02	B
	686.511258	PE(P-33:2)	685.504640	C ₃₈ H ₇₂ NO ₈ P	2.83E+07	1.46E+06	0	1.14E-02	5.50E-03	B
	702.507079	PC(30:2); PE(33:2)	701.499555	C ₃₈ H ₇₂ NO ₈ P	1.83E+07	7.38E+05	1.55E+06	8.50E-03	1.22E-02	B
	706.537563	PC(30:0); PE(33:0)	705.530855	C ₃₈ H ₇₆ NO ₈ P	2.58E+07	1.30E+06	0	8.00E-04	1.30E-04	B
PG										
	469.256248	PG(15:1)	468.248820	C ₂₁ H ₄₁ O ₉ P	1.18E+08	2.38E+07	1.01E+07	4.00E-02	6.40E-04	B
	793.501957	PG(38:7)	792.494135	C ₄₄ H ₇₃ O ₁₀ P	1.02E+07	5.34E+06	5.39E+06	7.70E-02	2.20E-02	B
	565.350327	PG(22:2)	564.342719	C ₂₈ H ₅₃ O ₉ P	5.61E+07	1.08E+08	1.32E+08	4.80E-02	1.60E-02	RS
	719.522550	PG(O-33:2) PG(P-33:1)	718.514871	C ₃₉ H ₇₅ O ₉ P	1.68E+06	7.00E+06	2.38E+07	n.s.	2.90E-03	RS
	733.501478	PG(33:2)	732.494135	C ₃₉ H ₇₃ O ₁₀ P	1.44E+06	9.40E+06	5.82E+06	4.00E-03	5.30E-02	RS
	859.642752	PG(42:2)	858.634986	C ₄₈ H ₉₁ O ₁₀ P	7.01E+05	3.75E+06	3.65E+06	1.30E-02	1.60E-02	RS
	561.319223	PG(22:4)	560.311420	C ₂₈ H ₄₉ O ₉ P	7.88E+07	1.22E+08	1.61E+08	n.s.	1.50E-02	RS
PS										
	718.502437	PS(P-32:1)	717.494470	C ₃₈ H ₇₂ NO ₉ P	6.74E+06	0	0	9.90E-04	5.00E-04	B
Sphingolipids										
Ceramides										
	646.516576	CerP(36:1)	645.509692	C ₃₉ H ₇₂ NO ₈ P	1.37E+07	4.20E+06	3.99E+06	2.10E-02	4.30E-02	B

Glycerolipids, such as DG (DG(34:2), DG(36:3) and DG(36:2)) and SP (e.g. ceramides) were significantly increased in baseline diet samples. Diradylglycerols are well known for being intermediates in lipid synthesis (Robinson and Warne 1991). Additionally, glycerophosphocholines/ glycerophosphoethanolamines, such as PC(O-18:0), PE(P-28:0), PE(P-31:0) /LysoPC(28:1), PE(31:1)/PC(38:1), PE(P-33:2), PC(30:2)/PE(33:2) and PC(30:0)/PE(33:0) also were increased in the fecal samples of the participants consuming the baseline diet. Further, glycerophosphoserines, such as PS(P-32:1) and the sphingolipid CerP(36:1) were increased in the baseline diet. However, some lipids of the PGs appeared to be increased due to dietary starch intake in general compared to the baseline diet, namely PG(22:2), PG(O-33:2)/PG(P-33:1), PG(42:2) and PG(22:4).

Concerning this, Samuelsson et al. investigated the impact of on the serum lipid profile of different carbohydrate-rich diets, including inulin, resistant starch or kojak compared to a basal diet (Samuelsson et al. 2016). They detected several lipids, mainly lysophosphatidylcholines and phosphatidylcholines to be affected by diet, but only in the inulin, kojak and basal diet, whereas only two serum lipids were observed to be affected by RS.

On the contrary, within this study a great number of specific lipid species were detected in the fecal samples of participants consuming the baseline and the RS diet through (+) FT-ICR MS analyses, reflecting the changes in fecal metabolome due to diet. Most of the lipids appeared to be significantly increased in the baseline diet and suppressed by dietary starch intake in general. However, some PAs were also increased in the LRS diet and through dietary starch intake in general. Diet, especially the consumption of RS appeared to have an enormous impact on the fecal lipid profile, wherefore further future studies need to investigate the influence of RS on the fecal lipid composition.

2.4.1.5.2 Importance and differences of fatty acids in the human fecal metabolome

Several fatty acids were already detected to be significantly changed between the baseline, HRS or LRS diet (Maier et al. 2017) through the correlation studies or the pathways classification analysis. However, in this chapter, the overall fatty acid profile impacted through the different diets will be shown (Figure 2.4-18). In general, twenty-eight fatty acids, both, saturated and unsaturated were found to be significantly changed between fecal samples of the baseline diet and both RS samples.

2. Effect of resistant starch on the gut microbiome

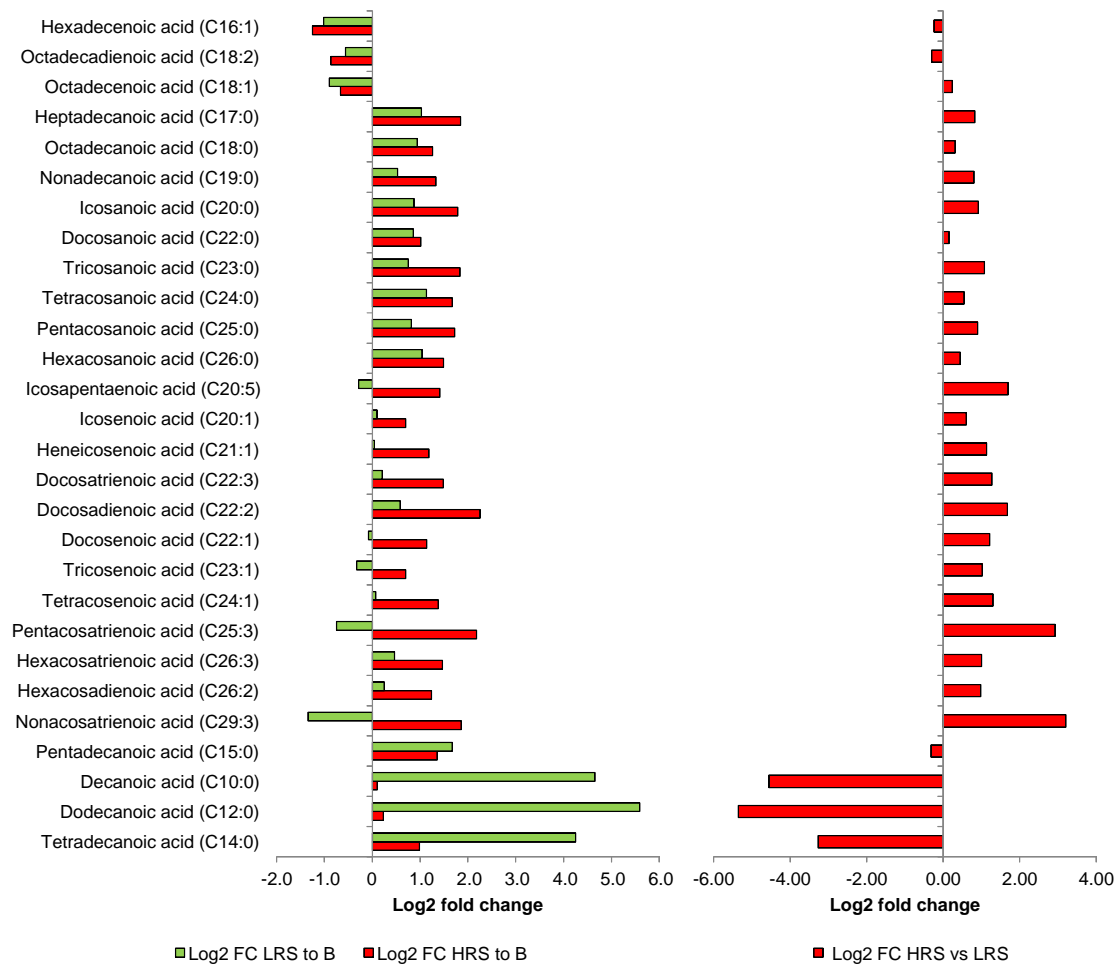


Figure 2.4-18: Fatty acids significantly changed through diet.

Fold change values for fatty acids significantly increased or decreased in HRS (red) or LRS diet (green), analyzed in (-) FT-ICR-MS mode. Left: Log2 fold change values of fatty acids significantly increased or decreased in HRS (red) or LRS (green) diet compared to baseline diet. Right: Log2 fold change values of fatty acids significantly increased or decreased in the HRS diet compared to the LRS diet. Further details are given in Table 6.1-16. From Maier, T. V.; Lucio, M.; Lee, L. H.; VerBerkmoes, N. C.; Brislawn, C. J.; Bernhardt, J.; Lamendella, R.; McDermott, J. E.; Bergeron, N.; Heinzmann, S. S.; Morton, J. T.; González, A.; Ackermann, G.; Knight, R.; Riedel, K.; Krauss, R. M.; Schmitt-Kopplin, P.; Jansson, J. K.: Impact of Dietary Resistant Starch on the Human Gut Microbiome, Metaproteome, and Metabolome. *mBio* vol. 8 no. 5 e01343-17 (2017). Illustration and data depiction modified from (Maier et al. 2017). Copyright (2017) Maier et al., Information about the creator and respective contributions, as well as the original material are available: <http://mbio.asm.org/content/8/5/e01343-17.full> with the original title: Classes of fatty acyls grouped according to their relative abundance following a specific diet category. Licence notice: <https://creativecommons.org/licenses/by/4.0/>.

The saturated fatty acids, heptadecanoic acid (C17:0), octadecanoic acid (C18:0), nonadecanoic acid (C19:0), icosanoic acid (C20:0), docosanoic acid (C22:0), tricosanoic acid (C23:0), tetracosanoic acid (C24:0), pentacosanoic acid (C25:0) and hexacosanoic acid (C26:0) were significantly increased to a similar extent by through dietary starch intake and showed a log2 fold change > 1 for the HRS compared to the baseline diet, and a log2 fold change > 0.53 for the comparison of the LRS diet and the baseline diet.

On the contrary, the fecal samples of the participants consuming the HRS diet were additionally characterized by increased levels of unsaturated fatty acids, namely icosapentanoic acid (C20:5), icosenoic acid (C20:1), heneicosenoic acid (C21:1), docosatrienoic acid (C22:3), docosadienoic acid (C22:2), docosenoic acid (C22:1), tricosenoic acid (C23:1), tetracosenoic acid (C24:1), pentacosatrienoic acid (C25:3), hexacosatrienoic acid (C26:3), hexacosadienoic acid (C26:2) and nonacosatrienoic acid (C29:3) with log₂ fold changes > 0.7. Thereof, nonacosatrienoic acid (C29:3) and pentacosatrienoic acid (C25:3) showed decreased levels in the LRS diet compared to the baseline diet. Comparing the fatty acid profiles between the HRS and LRS diet, almost all of the above mentioned fatty acids, except C18:0, C22:0, C24:0, C26:0 and C20:1, were strongly increased in the HRS diet (log₂ fold change from 0.8 – 3.2 HRS compared to LRS). Interestingly, pentadecanoic acid (C15:0) was increased in both RS diets. However, the increase observed in the LRS diet was slightly higher, compared to the HRS diet.

Additionally, octadecenoic acid (C18:1, Figure 2.4-19 C) and octadecadienoic acid (C18:2, Figure 2.4-19 B) were two of the most abundant metabolites (mean intensity >1x10¹¹) and significantly altered between the baseline diet and the two RS diets (Maier et al. 2017). Further, palmitoleic acid (C16:1, Figure 2.4-19 A) was increased in the baseline diet.

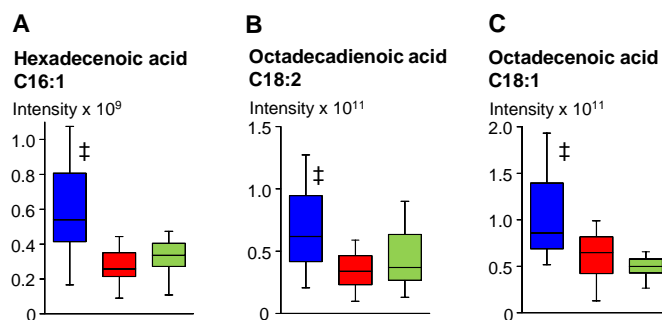


Figure 2.4-19: Unsaturated fatty acids increased in baseline diet.

Boxplots of 3 unsaturated fatty acids significantly increased in the baseline diet (blue) compared to the HRS diet (red) and the LRS (green), analyzed in (-) FT-ICR-MS mode. p-values were calculated through the Kruskal-Nemenyi Test. Further details are listed in Table 6.1-16.

In contrary, Sun et al. found octadecadienoic acid and octadecenoic acid to be enriched in samples of pigs consuming a raw potato starch diet, though in cecal samples of the pigs (Sun et al. 2016). They hypothesized that through raw potato starch, the significantly higher concentrations of unsaturated fatty acids in cecal samples may appear by a lower absorption of those fatty acids in the cecum (Sun et al. 2016). This might be an explanation, why in this study lower concentration levels of octadecadienoic

acid and octadecenoic acid were detected in the fecal samples after RS consumption. By contrast, already in 1974, Eyssen and Parmentier investigated the impact of starch diets, compared to lactose diets on the intestinal microflora of germfree and conventional rats (Eyssen and Parmentier 1974). They were interested in the fecal fatty acid profiles, which were analyzed by gas-liquid chromatography and revealed fatty acids, such as octadecanoic acid (C18:0) to be increased in conventional rats fed the starch diet and octadecenoic acid (C18:1) and octadecadienoic acid (C18:2) to be decreased in the conventional rats fed the starch diet. This was in agreement with our results on the profile of the above mentioned fatty acids in the human fecal samples through dietary starch intake. Remarkably, three fatty acids, which were decanoic acid (C10:0, Figure 2.4-20 A), dodecanoic acid (C12:0, Figure 2.4-20 B) and tetradecanoic acid (C14:0, Figure 2.4-20 C) showed increased levels in the fecal samples of participants receiving the LRS diet. In order to undoubtedly identify the significant fatty acids enriched solely in samples of participants consuming the LRS diet, this result was confirmed by applying a lipidomics-MS/MS approach in (-) ESI mode (method description in chapter 2.3.1.6) including respective standards (extracted ion chromatograms and MS/MS spectra are illustrated in Figure 5.1-1) (Maier et al. 2017).

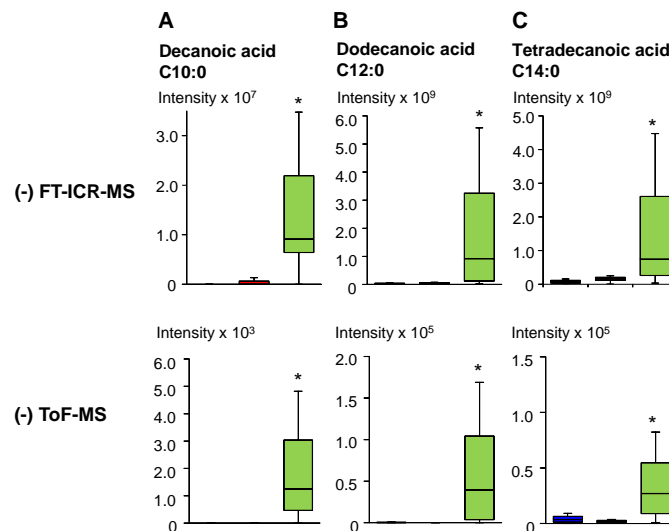


Figure 2.4-20: Saturated fatty acids significantly increased in samples of LRS diet.

Boxplots of 3 saturated fatty acids significantly increased in the LRS diet (green) compared to the baseline diet (blue) and HRS diet (red), analyzed in (-) FT-ICR-MS mode (top) and (-) ToF-MS (bottom) experiments. p-values were calculated through the *post hoc* Kruskal-Nemenyi Test. Further details are listed in Table 6.1-16. From Maier, T. V.; Lucio, M.; Lee, L. H.; VerBerkmoes, N. C.; Brislawn, C. J.; Bernhardt, J.; Lamendella, R.; McDermott, J. E.; Bergeron, N.; Heinzmann, S. S.; Morton, J. T.; González, A.; Ackermann, G.; Knight, R.; Riedel, K.; Krauss, R. M.; Schmitt-Kopplin, P.; Jansson, J. K.: Impact of Dietary Resistant Starch on the Human Gut Microbiome, Metaproteome, and Metabolome. *mBio* vol. 8 no. 5 e01343-17 (2017). Illustration of Figure B and C was modified from (Maier et al. 2017). Copyright (2017) Maier et al., Information about the creator and respective contributions, as well as the original material are available: <http://mbio.asm.org/content/8/5/e01343-17.full> with the original title: Identification of decanoic (C12:0) and tetradecanoic acid (C14:0). Licence notice: <https://creativecommons.org/licenses/by/4.0/>.

In order to find out where those differences originate from, the composition of both diets was considered. Certainly, diets were matched for protein, fat and total carbohydrate, and differed only with respect to the source of starch used (which was either high or low in resistant starch). It is therefore unlikely that the differences in decanoic acid, dodecanoic acid and tetradecanoic acid between the HRS and LRS diet occurred from differences in fat content between the diets. For this reason, those fatty acids appeared to be affected by the digestion of cornstarch low in resistant starch.

Further, several dicarboxylic acids, such as dodecenedioic acid, octadecanedioic acid, eicosanedioic acid and tricosanedioic acid were detected to be significantly increased in the HRS diet, compared to both, the baseline and the LRS diet (Figure 2.4-21).

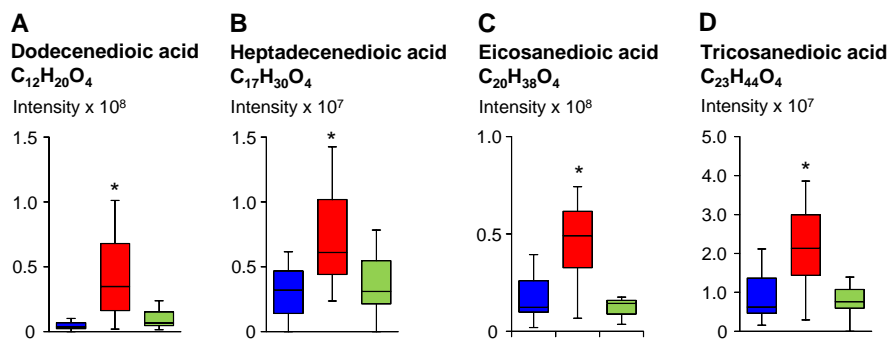


Figure 2.4-21: Dicarboxylic acids significantly increased in the HRS diet.

Boxplots of 4 dicarboxylic acids significantly increased in the HRS diet (red) compared to the baseline diet (blue) and the LRS diet (green), analyzed in (-) FT-ICR-MS mode. p-values were calculated with the Kruskal-Nemenyi Test. Further details are listed in Table 6.1-17.

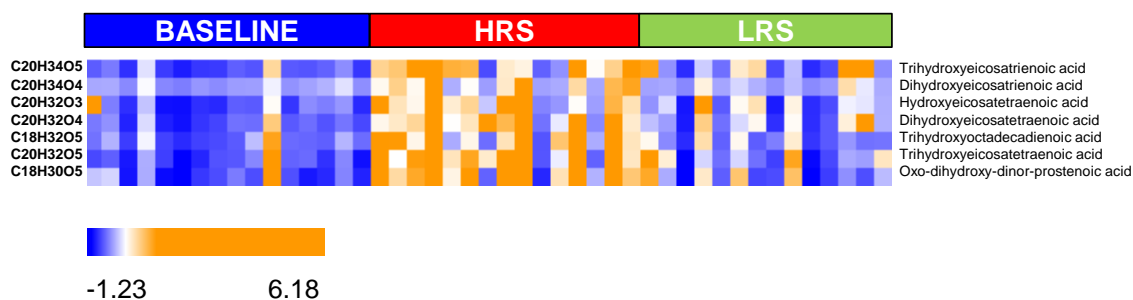
Through the conversion of monocarboxylic acids to their dicarboxylic acids in rat liver *in vitro*, Jin et al. wanted to investigate unsaturated dicarboxylic acids and their excretion in urine (Jin and Tserng 1990). They hypothesized dicarboxylic acids, especially dodecenedioic acid to be a metabolic precursor of octenedioic acids. In turn, octenedioic acids are derived from oleic and linoleic acids through several metabolic oxidation processes (Jin and Tserng 1990). However, they also concluded that the origin of dicarboxylic acids can be caused by multiple metabolic processes (Jin and Tserng 1990). In our study, increased levels of octadecadienoic acid (linoleic acid) and octadecenoic acid (oleic acid) were observed in the baseline diet. Accordingly, higher levels of dicarboxylic acids were detected through HRS consumption. Considering the results from Jin et al. in the 90's, our result lead to assume that through RS consumption the metabolic conversion to several dicarboxylic acids is affected.

2.4.1.5.3 Oxylipins, Hydroxy Fatty Acids and Octadecanoids

Since already the correlation studies revealed some hydroxy fatty acids and oxylipins to be altered by diet, the data was evaluated for other similar species in the fecal samples by considering related species listed in databases, such as Lipid Maps (Fahy et al. 2009), HMDB (Wishart et al. 2007, Wishart et al. 2013) and KEGG (Kanehisa and Goto 2000). This analysis revealed further oxylipins (Figure 2.4-22 A), hydroxy fatty acids (Figure 2.4-23 A) and octadecanoids (Figure 2.4-23 B) and some of their sulfate conjugated species to be important metabolites significantly increased in the HRS diet.

Oxylipins are bioactive fatty acids, derived from PUFAs, such as arachidonic and linoleic acid (Gouveia-Figueira et al. 2017, Mika and Sledzinski 2017). Enzymes, such as cyclooxygenase, lipoxygenase, hydroperoxydase and cytochrome P450 are involved in the formation of oxylipins (Nørskov et al. 2012, Gouveia-Figueira et al. 2017). Various classes of oxylipins exist, including many isomers (Nørskov et al. 2012). The eicosanoids represent one main class of the oxylipins and are formed from arachidonic acid, including prostaglandin, leukotriene and thromboxane (Noverr et al. 2003, Gabbs et al. 2015). Oxylipins are represented by mono-, di-, and tri-hydroxy fatty acids, as well as lipoxins, epoxy fatty acids or resolvins (Gabbs et al. 2015). Here, increased patterns of eicosanoids, namely hydroxyeicosatetraenoic acid, trihydroxyeicosatrienoic acid, dihydroxyeicosatrienoic acid, dihydroxyeicosatetraenoic acid, trihydroxyeicosatetraenoic acid, oxo-dihydroxy-dinor-prostenoic acid and trihydroxyoctadecadienoic acid were observed in the HRS diet samples. Also sulfated conjugates of several oxylipins were significantly increased on the HRS diet (Figure 2.4-22 B), namely trihydroxyoctadecadienoic acid sulfate, dihydroxyeicosatrienoic acid sulfate, dihydroxyeicosatetraenoic acid sulfate and hydroxyeicosatetraenoic acid sulfate.

A Eicosanoids



B Eicosanoid sulfates

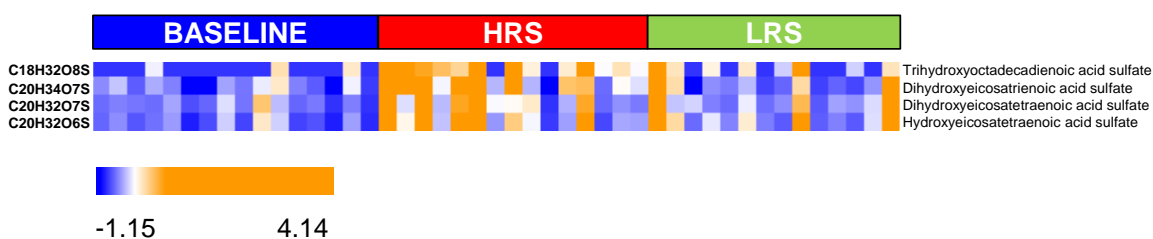


Figure 2.4-22: Oxylipins and their sulfated conjugates significantly increased in the HRS diet.

Heatmap of 7 oxylipins (A) and their respective sulfates (B), presented with molecular formulas and compound name, significantly increased in the HRS diet (red) compared to the baseline (blue) and LRS diet (green), analyzed in (-) FT-ICR-MS mode. Further details are given in (A) Table 6.1-18 and (B) Table 6.1-19.

Oxylipins were also observed to be excreted in feces of insects (Schulze et al. 2007), but can predominately found in several other materials, including plasma (Strassburg et al. 2012, Gouveia-Figueira et al. 2015), lung tissue (Gouveia-Figueira et al. 2017), tissue (Wong et al. 2014), urine, plants (Fauconnier et al. 2003, Glauser et al. 2008, Gobel and Feussner 2009, Vu et al. 2012, Geng et al. 2015) and cell cultures (Wolfer et al. 2015). Oxylipins are related to various activities. To mention a few: they influence insulin signaling and adipose tissue function (Grapov et al. 2012, Ingerslev et al. 2015) and they are said to induce several biological effects of the PUFAs, which comprises both, pro-inflammatory and anti-inflammatory effects (Mika and Sledzinski 2017).

Further, they are involved in several physiological processes, such as cell proliferation, apoptosis, blood pressure regulation, repairing tissue or blood clotting (Wolfer et al. 2015). In 2012, Nørskov et al. investigated the impact of whole grain wheat and wheat aleurone on plasma samples of pigs in contrast to refined flour (Nørskov et al. 2012). Through performing LC-MS analyses in negative electrospray ionization mode, they detected several oxylipins, namely two isomers of hydroxyoctadecadienoic acid, to be discriminant between both diet groups. These compounds were also detected in the flour and the

2. Effect of resistant starch on the gut microbiome

bread the pigs consumed. They hypothesized oxylipins as potential biomarkers for whole grain consumption ((Nørskov et al. 2012).

Additionally, another form of oxylipins, the mono-, di- and tri-hydroxy fatty acids (Figure 2.4-23 A), namely hydroxyeicosanoic acid, dihydroxydocosanoic acid, dihydroxyeicosanoic acid, dihydroxyhexadecanoic acid, tetrahydroxyoctadecanoic acid, hydroxyoctadecenoic acid, trihydroxyoctadecanoic acid and dihydroxyoctadecenoic acid were significantly increased in the fecal samples of participants consuming the HRS diet. Octadecanoids (Figure 2.4-23 B), such as trihydroxyoctadecenoic acid and dihydroxyoctadecadienoic acid react similar to the RS consumption as the hydroxy fatty acids.

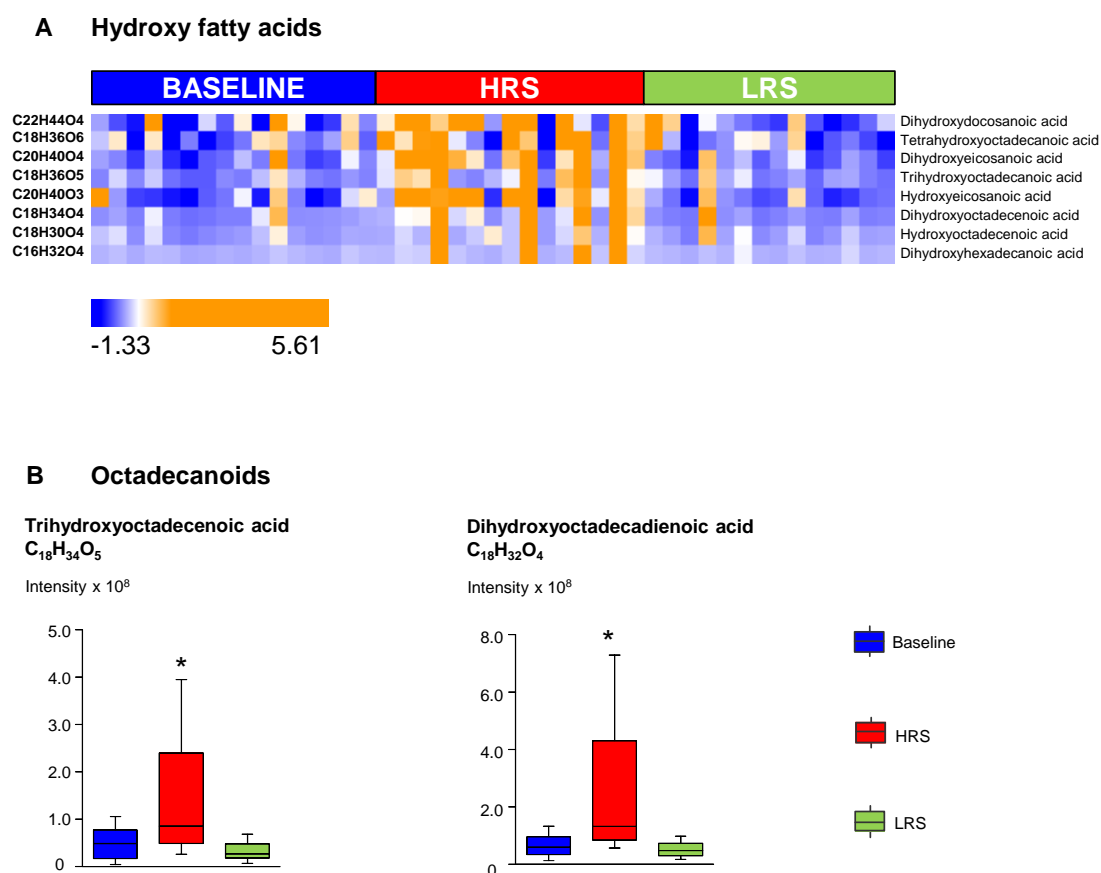


Figure 2.4-23: Hydroxy fatty acids and octadecanoids significantly increased in the HRS diet.

A: Heatmap of 8 hydroxy fatty acids and B: Boxplots of two octadecanoids, presented with molecular formulas and compound name, significantly increased in the HRS diet (red) compared to the baseline (blue) and LRS diet (green), analyzed in (-) FT-ICR-MS mode. Further details are given in Table 6.1-18.

Also sulfated conjugates of hydroxy fatty acids and octadecanoids were significantly increased on the HRS diet (Figure 2.4-24), namely dihydroxyoctadecenoic acid sulfate and hydroxyeicosanoic acid

sulfate. The sulfated conjugates of octadecanoids were dihydroxyoctadecadienoic acid sulfate and trihydroxyoctadecenoic acid sulfate.

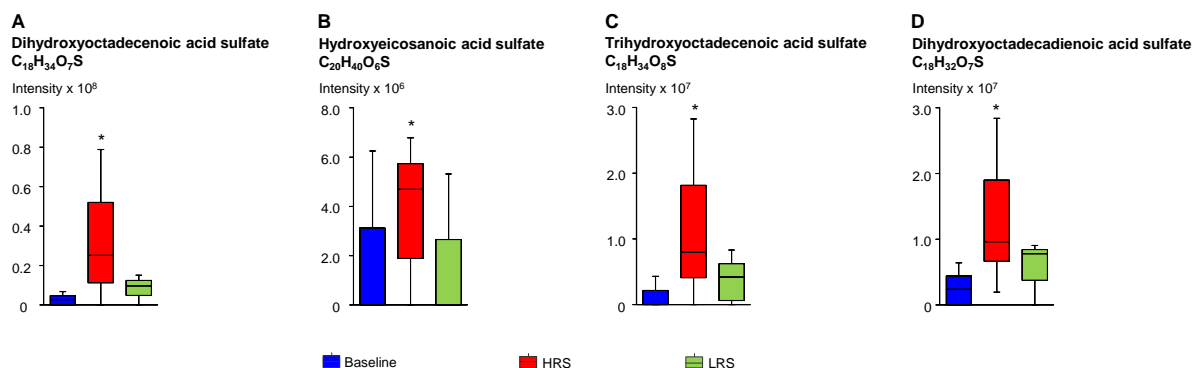


Figure 2.4-24: Sulfated hydroxy fatty acids and octadecanoids significantly increased in the HRS diet.

Boxplots of two hydroxy fatty acid sulfate conjugates (A, B) and octadecanoids sulfates (C, D), presented with molecular formulas and compound name, significantly increased in the HRS diet (red) compared to the baseline (blue) and LRS diet (green), analyzed in (-) FT-ICR-MS mode. Further details are given in Table 6.1-19.

It is well known, that oxylipins may either be formed from membrane-bound fatty acids, be derived from dietary fatty acids (Strassburg et al. 2014) or they could come directly from the consumed diet. However, the role of oxylipins is not clearly understood yet in mammals and humans (Fischer 1997, Shearer et al. 2010, Nørskov et al. 2012). Even if increased levels of several oxylipins due to HRS diet were detected, which were not ingredients of diet, their origin remains unclear. However, these results lead to the assumption that oxylipins may be characteristic for RS consumption as well.

2.4.1.5.4 Short-chain fatty acid profile through dietary starch intake

SCFAs are generated by the fermentation of carbohydrates in the gut by microbes. The SCFA have several health-promoting effects on the gut. Butyrate is known as major energy source for several colonocytes (Russell et al. 2013) and improves insulin sensitivity (Gao et al. 2009). Therefore, several studies were accomplished to investigate the impact of differently digestible carbohydrates on the animal and human SCFA profile in the cecum, ileum, colon or in feces (Fassler et al. 2006, Zhou et al. 2013, Fang et al. 2014, Fohse et al. 2015, Samuelsson et al. 2016), whereas generally significantly increased levels of SCFA, especially butyrate were observed through dietary starch intake.

In order to evaluate the impact of RS on the SCFA production, the SCFA profiles were assessed from the baseline, HRS and LRS diet in feces, using UHPLC-(+)-ToF-MS after the AMP+ derivatization

2. Effect of resistant starch on the gut microbiome

method. Propionic acid, butyric acid, and valeric and isovaleric acid did not significantly changed through the RS intake, though a tendency of increased levels of propionic acid and butyric acid were observed in the fecal samples of participants consuming the HRS diet (Figure 2.4-25) (Maier et al. 2017).

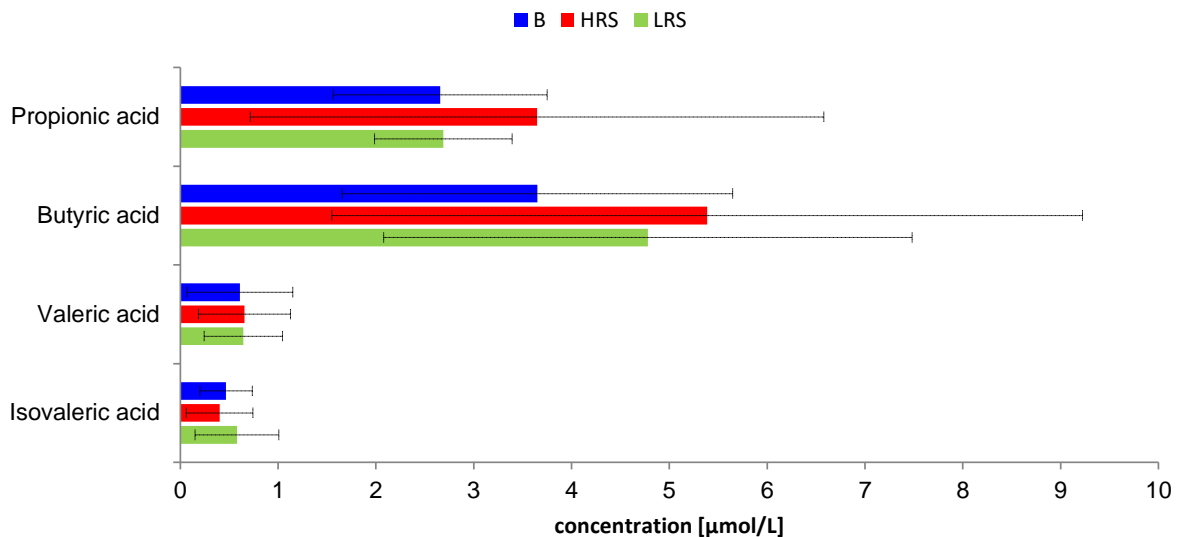


Figure 2.4-25: SCFA profiles altered in participants consumed the baseline, HRS or LRS diet.

Bar chart displaying the SCFA profile, including propionic acid, butyric acid, valeric acid and isovaleric acid detected in fecal samples of participants consuming the baseline (blue), the HRS diet (red) or the LRS diet (green). SCFA were detected as AMP⁺ derivatives in (+) ToF-MS mode. Further details are given in Table 6.1-20.

In contrast to many other studies investigating the SCFA production through dietary starch intake, tremendously increased level of the SCFA through either high or low RS intake could not be detected, especially not for butyric acid. A slight increase in intensity of butyric acid and propionic acid was observed (Maier et al. 2017). However, the individual differences were huge. The high inter-individual differences may in parts explain the contrasting results on SCFA production compared to existing literature. Since, metabolomics analysis did not reveal significant differences in the SCFA composition of the fecal samples of participants consuming the HRS diet, further proteome analysis might be able to gain a better insight into SCFA production and several pathways through the evaluation of responsible proteins affected through the baseline, HRS or LRS diet. Further, proteomics analyses were performed to confirm several findings observed through the metabolomics analyses (e.g. the lipid metabolism), to extend the view on the impact of RS on the human gut microbiome and find possible linkages between the metabolome and the microbiome.

2.4.2 Impact of resistant starch on the microbiome: genome and proteome level

RS is one of the biggest diet-derived energy sources for bacteria in the human intestine. Microbial fermentation of complex dietary carbohydrates has important consequences for health (Flint et al. 2012), since dietary starch intake can modify the microbial composition (Walker et al. 2011). It was already shown, that RS improves insulin sensitivity, initiated through colonic bacterial fermentation (Robertson et al. 2005) and may be of interest to prevent the risk for diabetes (Walker et al. 2011). Three of the most abundant bacteria in the gut, such as *Firmicutes*, *Bacteroidetes* and *Actinobacteria* are involved in starch fermentation (Birt et al. 2013). Macfarlane et al. detected two bacteria strains, *Bifidobacterium spp.* and *Clostridium butyricum*, which were able to utilize high-amylose starch and seemed to be important in the formation of high-amylose starch (Macfarlane and Englyst 1986), as present in RS type II used in our study.

2.4.2.1 Dynamics of the human microbiome in response to a resistant starch diet: genome level

In order to determine the gut microbiome compositions of participants consuming the baseline, HRS or LRS diets respectively; fecal samples of all participants were analyzed by 16S rRNA gene sequencing. Additionally, since nowadays tremendous amounts of genomic data can be produced, appropriate evaluation and visualization tools are required. One typical way visualizing genomic data are heatmaps (Bernhardt et al. 2009), displaying different taxonomic ranks of the genomic data, as performed in this study. In order to get a first overview of bacterial composition, the genomic data was displayed in different taxonomic levels, including phyla, order and genus level (Figure 2.4-26 left, from top to bottom). Correlations between OTUs and the amount of RS were displayed as well (Figure 2.4-26 right). It was revealed that diet had a significant impact on the microbiome composition, irrespective of the time of sampling during the crossover study. Through high resistant dietary starch intake, a significant increase of 16S rRNA OTUs of the *Firmicutes* phylum was observed (Figure 2.4-26). Increased relative amounts of species of the genera *Faecalibacterium*, *Roseburia* and *Ruminococcus* were observed (Maier et al. 2017), which were associated with butyrate production (Louis et al. 2010, Miquel et al. 2015), being an important metabolite for gut health. Further, they were found to be reduced in abundance in the gut microbiota of participants with type 2 diabetes mellitus (T2DM) compared to healthy individuals (Qin et al. 2012, Maier et al. 2017)

2. Effect of resistant starch on the gut microbiome

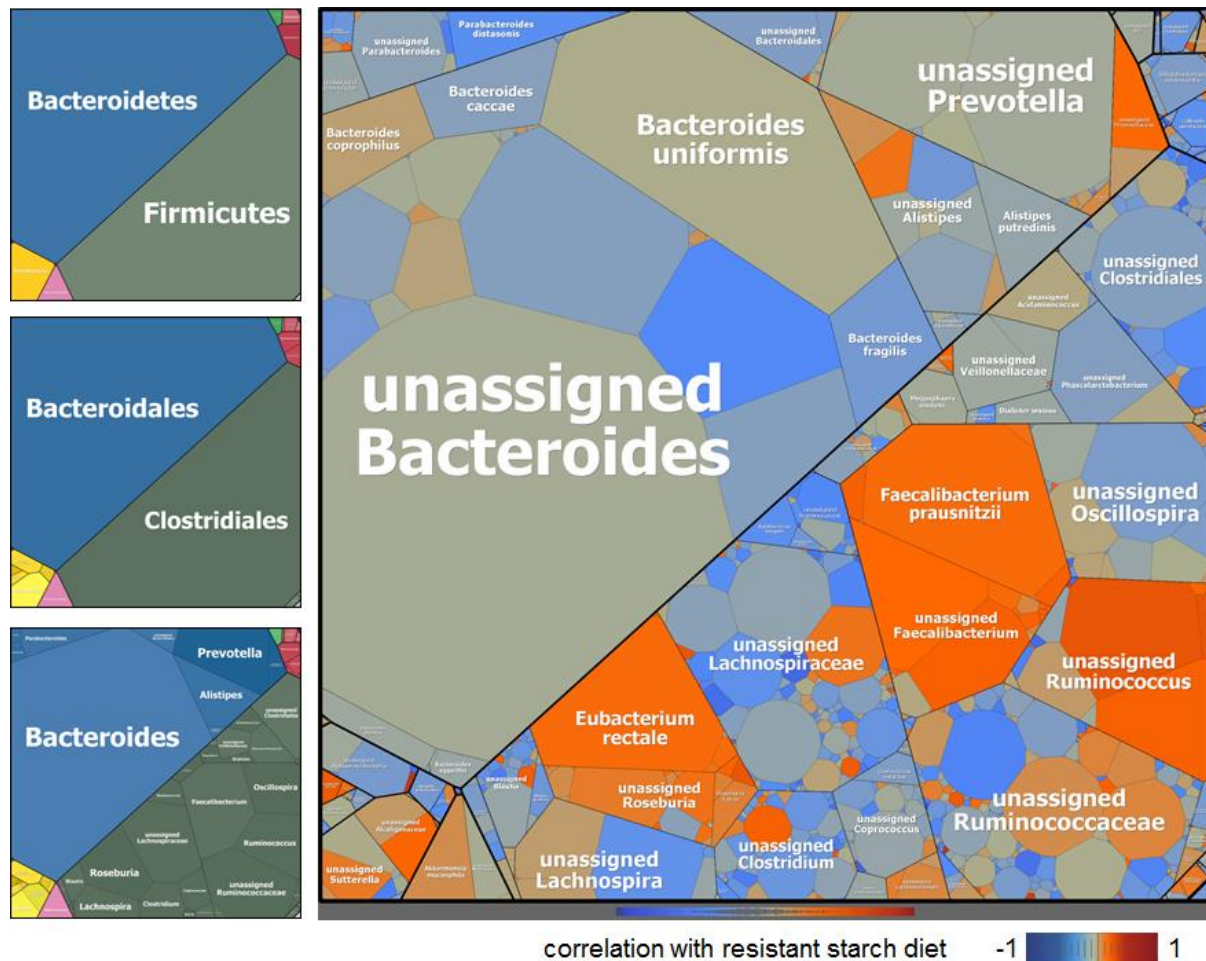


Figure 2.4-26: Taxonomic treemap of 16S rRNA OTUs.

Taxonomic treemaps of all participants from all experimental stages (baseline; LRS; HRS), as encoded by the cell sizes. Colors within the explanatory hierarchy treemaps in the top line (labels specify phylum, order, genus (from top to bottom)) specify bacteria on phylum level – Firmicutes (greenish grey); Actinobacteria (carmin red); *Bacteroidetes* (steel blue); *Proteobacteria* (yellow); *Fusobacteria* (plum); *Tenericutes* (antique pink); *Spirochaetes* (ocre); *Cyanobacteria* (green); *Verrucomicrobia* (pink). Cell colors of the large treemap show the correlation (Pearson correlation; -1 dark blue; -0.5 light blue; 0 medium grey; 0.5 orange; 1 dark red) of all participant specific 16S rRNA OTU counts with the resistant starch regime with 0; 0.05 and 1 for baseline; LRS and HRS respectively. From Maier, T. V.; Lucio, M.; Lee, L. H.; VerBerkmoes, N. C.; Brislawn, C. J.; Bernhardt, J.; Lamendella, R.; McDermott, J. E.; Bergeron, N.; Heinzmann, S. S.; Morton, J. T.; González, A.; Ackermann, G.; Knight, R.; Riedel, K.; Krauss, R. M.; Schmitt-Kopplin, P.; Jansson, J. K.: Impact of Dietary Resistant Starch on the Human Gut Microbiome, Metaproteome, and Metabolome. *mBio* vol. 8 no. 5 e01343-17 (2017). Reprinted and modified from (Maier et al. 2017). Copyright (2017) Maier et al., original material is available: <http://mbio.asm.org/content/8/5/e01343-17.full>.

Specific genera/species that increased and highly correlated with the HRS diet included *Faecalibacterium prausnitzii*, which is one of the most abundant bacteria in the human gut and previously was associated with a healthy gut status (Khan et al. 2012, Lin et al. 2014). Further genera/species increased in the HRS diet were unassigned *Prevotellaceae*, *Ruminococcus*, *Eubacterium rectale*, *Roseburia faecis* and *Akkermansia muciniphila* (Figure 2.4-26, right) (Maier et al.

2017), several of which have previously been reported to be increased in the colon following a HRS diet (Walker et al. 2011, Ze et al. 2012, Cockburn et al. 2015, Maier et al. 2017).

In conclusion, RS significantly altered the fecal microbial composition, which was shown as increased and positively correlating species of the Firmicutes phylum following the HRS diet, which were predominately species of *F. prausnitzii* and *E. rectale*. On the contrary, species of the *Bacteroides* phylum were correlated negatively and decreased in fecal samples of participants consuming the HRS diet. Additionally, we went beyond taxonomic characterization to also investigate the functional shifts and dynamics according to diet, evaluating proteomic data obtained through a shotgun metaproteomics approach as described in the following chapter (chapter 2.4.2.2).

2.4.2.2 Dynamics of the human microbiome in response to a resistant starch diet: proteome level

Individuals harbor their specific microbiomes, whose composition depends on a variety of factors, including the individual diet, health and physical fitness. Therefore, the proteome data sets of all 8 participants were clustered at the experimental stage „baseline“ by using TIGR multiple experiment viewer (TMEV / MEV) (Saeed et al. 2006) on species summarized protein counts. Then Voronoi treemaps of the participant specific microbiomes were built by using the taxonomic levels (from root via branches to leaves): kingdom, phylum, class, order, family, genus, species (Figure 2.4-27). Participant's microbiomes shown below are dominated by *Bacteroidetes* bacteria, especially *Bacteroidetes vulgatus* and *uniformis*, and those shown in the middle were less dominated by *B. vulgatus* or *uniformis*, but showed increased levels of species of the *Prevotellaceae*. The bottom microbiomes show a more Firmicutes dominated composition with *Eubacterium rectale*, *Ruminococcus bromii*, *Faecalibacterium prausnitzii* and *Roseburia* species as main constituents.

2. Effect of resistant starch on the gut microbiome

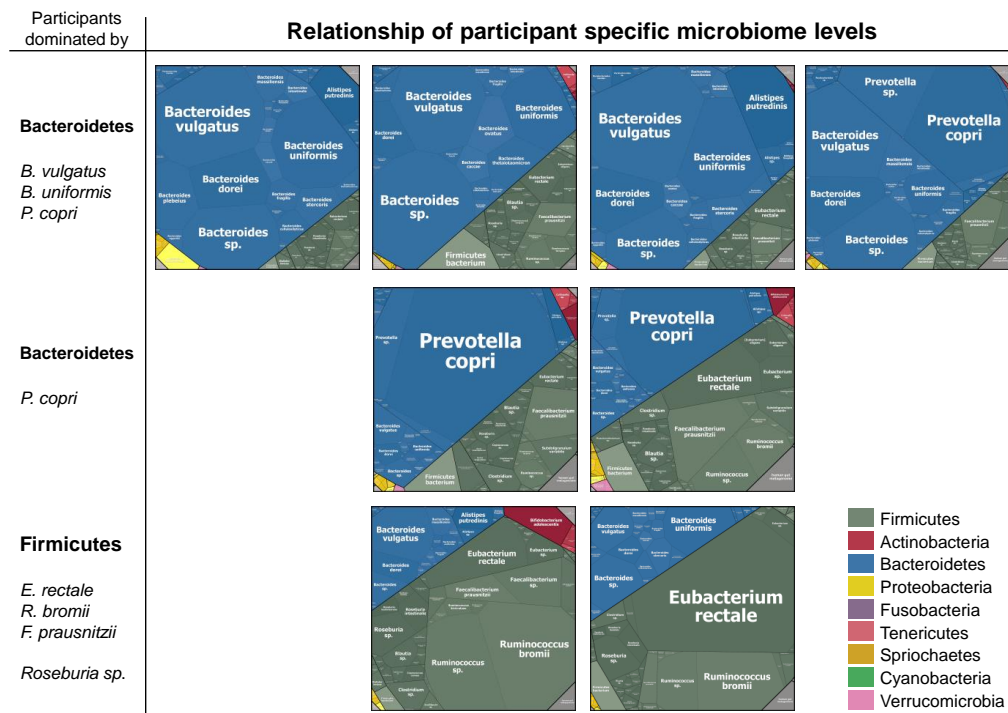


Figure 2.4-27: Voronoi Treemaps at experimental stage „baseline“ with their specific microbiomes.

Participants' microbiomes shown on top are dominated by Bacteroidetes bacteria, especially *Bacteroidetes vulgatus* and *uniformis*. The bottom left microbiomes show a more Firmicutes dominated composition with *Eubacterium rectale*, *Ruminococcus bromii* and *Roseburia species* as main constituents. Voronoi treemaps of the participant specific microbiomes were built by using the taxonomic levels (from root via branches to leaves): kingdom, phylum, class, order, family, genus, species. Cell sizes are proportionally sized according the species summarized protein counts. Colors specify bacteria on phylum level – Firmicutes (greenish grey); Actinobacteria (carmin red); Bacteroidetes (steel blue); Proteobacteria (yellow); Fusobacteria (plum); Tenericutes (antique pink); Spirochaetes (ocre); Cyanobacteria (green); Verrucomicrobia (pink). From Maier, T. V.; Lucio, M.; Lee, L. H.; VerBerkmoes, N. C.; Brislawn, C. J.; Bernhardt, J.; Lamendella, R.; McDermott, J. E.; Bergeron, N.; Heinzmann, S. S.; Morton, J. T.; González, A.; Ackermann, G.; Knight, R.; Riedel, K.; Krauss, R. M.; Schmitt-Kopplin, P.; Jansson, J. K.: Impact of Dietary Resistant Starch on the Human Gut Microbiome, Metaproteome, and Metabolome. mBio vol. 8 no. 5 e01343-17 (2017). Illustration modified from (Maier et al. 2017). Copyright (2017) Maier et al., Information about the creator and respective contributions, as well as the original material are available: <http://mbio.asm.org/content/8/5/e01343-17.full> with the original title: Individual response to resistant starch. Licence notice: <https://creativecommons.org/licenses/by/4.0/>.

This illustration emphasizes inter-individual differences in the gut microbiome and highlights different starting points of each individual in the RS dietary intervention. Next, we investigated common and mean changes in the individuals after RS intervention. Through high resistant dietary starch intake, a significant increase of species specific proteins in the Firmicutes phylum were observed (Figure 2.4-28), as already detected in the genome data. Here, the *butyrate-producing bacterium*, *Eubacterium sp.* (*E. rectale*, *E. eligens*), *Subdoligranulum sp.* (*S. variabile*), *Faecalibacterium sp.* (*F. prausnitzii*), *Blautia sp.*, *Coprococcus sp.* (*C. comes*), *Anaerostipes sp.* and *Clostridium sp.* were the most abundant species and correlated positively with a high amount of RS. On the contrary, most species of the Bacteroidetes phylum were negatively correlated to the HRS diet, except species of genera *Odoribacter* (*O. splanchnicus*) and *Parabacteroides* (*P. johnsonii*).

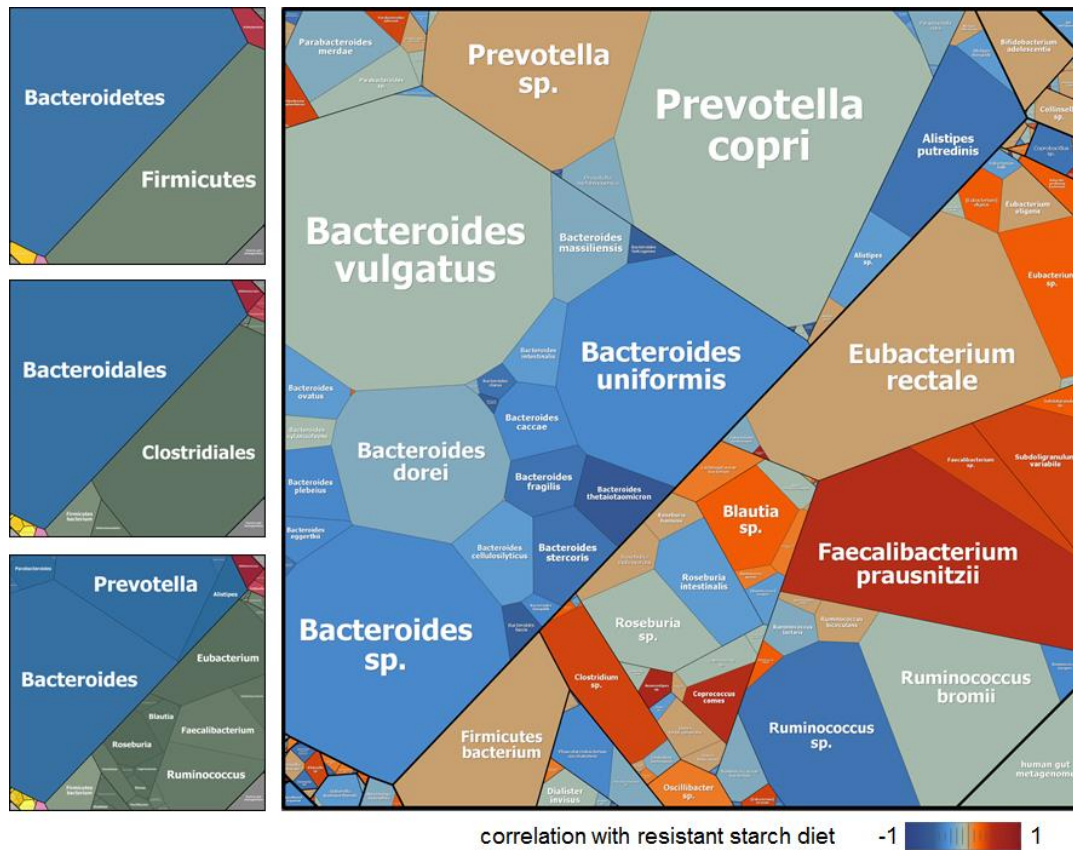


Figure 2.4-28: Taxonomic treemap of averaged species specific summarized protein counts.

Taxonomic treemaps from all experimental stages (baseline; LRS; HRS), as encoded by the cell sizes. Colors within the explanatory hierarchy treemaps in the top line (labels specify phylum, order, genus (from left to right)) specify bacteria on phylum level – *Firmicutes* (greenish grey); *Actinobacteria* (carmin red); *Bacteroidetes* (steel blue); *Proteobacteria* (yellow); *Fusobacteria* (plum); *Tenericutes* (antique pink); *Spirochaetes* (ocre); *Cyanobacteria* (green); *Verrucomicrobia* (pink). Cell colors of the large treemap show the correlation (Pearson correlation; -1 dark blue; -0.5 light blue; 0 medium grey; 0.5 orange; 1 dark red) of all participant specific z-scores (participant specific mean centering and standard deviation normalization) of the species summarized protein counts with the resistant starch regime with 0; 0.05 and 1 for baseline; LRS and HRS respectively. Z-scoring made sure that only changes of the bacterial amount in response to the resistant starch diet but not the different levels the bacteria occur in the individual gut floras were taken into account for the determination of the degree of correlation.

Further, the shotgun metaproteomics approach allowed to identify thousands of host and microbial proteins altered through RS. The Clusters of Orthologous Groups (COG) of proteins (Figure 2.4-29) (Tatusov et al. 2000) represented in the protein data are classified into functional groups, including among other those for energy production and conversion (C), amino acid metabolism and transport (E), nucleotide metabolism and transport (F), carbohydrate metabolism and transport (G), lipid metabolism (I) and translation (J). In addition, detected proteins of the COG main class (Figure 2.4-29 left top) and the COG sub class (Figure 2.4-29, left middle) were assigned to the bacterial phyla. This revealed proteins, predominantly assigned to phyla of *Firmicutes*, *Bacteroidetes*, *Actinobacteria* and *Proteobacteria*, the most abundant microbes in the human gut.

2. Effect of resistant starch on the gut microbiome

Further, bacterial proteins were correlated (Pearson correlation; -1: dark blue; -0.5: light blue; 0: grey; 0.5: orange; 1: dark red) with the RS regime with 0; 0.05 and 1 for baseline; LRS and HRS respectively (Figure 2.4-29, right).

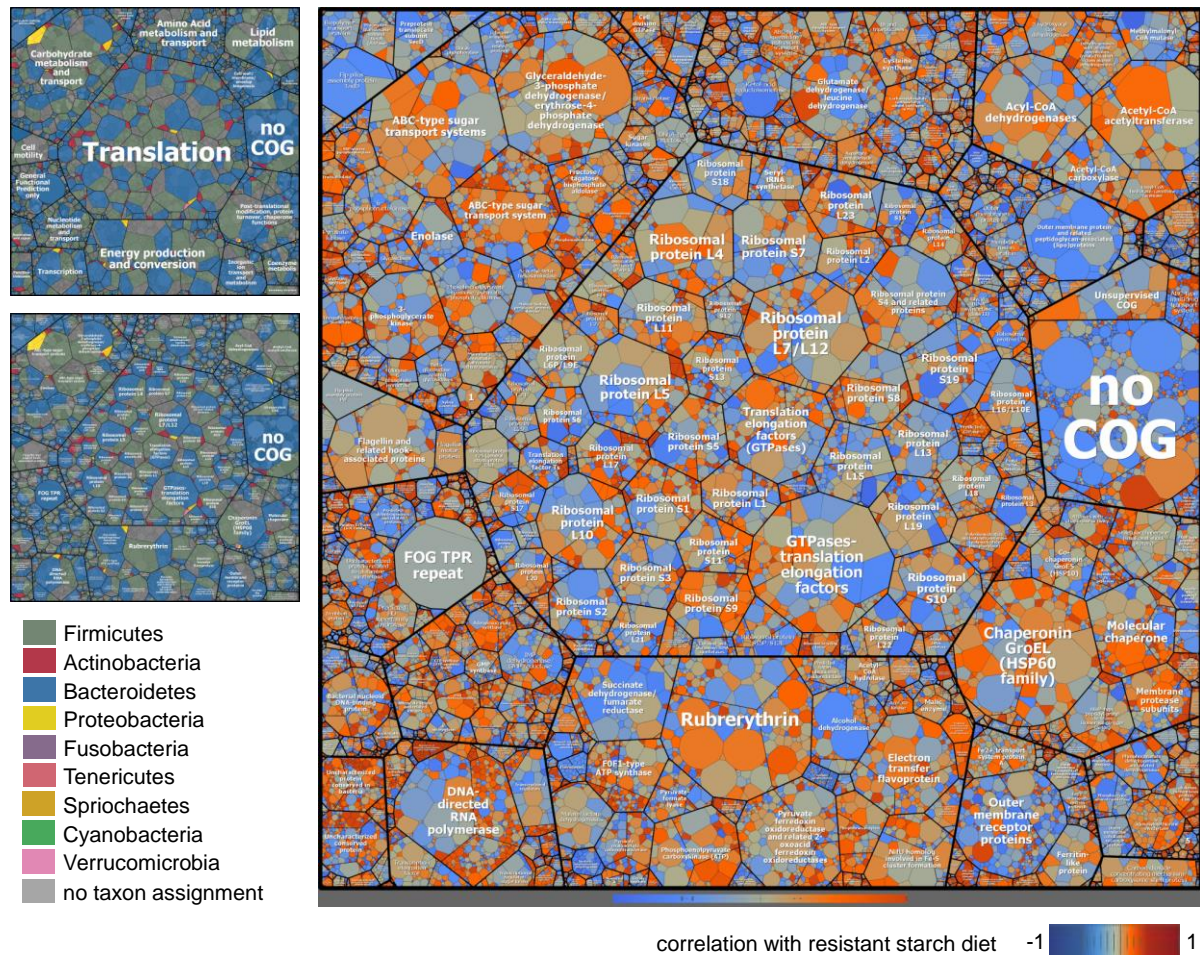


Figure 2.4-29: Treemap of averaged bacterial protein specific counts.

Treemap from all experimental stages (baseline; LRS; HRS), as encoded by the cell sizes. Colors within the explanatory hierarchy treemaps in the top line (COG main class; COG sub class; bacterial phylum (from top to bottom)). Cell colors of the large treemap show the correlation (Pearson correlation; -1 dark blue; -0.5 light blue; 0 medium grey; 0.5 orange; 1 dark red) of all participant specific z-scores (participant specific mean centering and standard deviation normalization) of the protein counts with the resistant starch regime with 0; 0.05 and 1 for baseline; LRS and HRS respectively. Z-scoring made sure that only changes of the protein amount in response to the resistant starch diet but not the different levels the proteins occur in the individual gut floras were taken into account for the determination of the degree of correlation. From Maier, T. V.; Lucio, M.; Lee, L. H.; VerBerkmoes, N. C.; Brislawn, C. J.; Bernhardt, J.; Lamendella, R.; McDermott, J. E.; Bergeron, N.; Heinzmann, S. S.; Morton, J. T.; González, A.; Ackermann, G.; Knight, R.; Riedel, K.; Krauss, R. M.; Schmitt-Kopplin, P.; Jansson, J. K.: Impact of Dietary Resistant Starch on the Human Gut Microbiome, Metaproteome, and Metabolome. *mBio* vol. 8 no. 5 e01343-17 (2017). In parts reprinted and modified from (Maier et al. 2017). Copyright (2017) Maier et al., original material is available: <http://mbio.asm.org/content/8/5/e01343-17.full>.

It turned out that a wide array of proteins was highly correlated to RS, but especially proteins of the GOG main classes. This included the carbohydrate metabolism and transport, as well as lipid metabolism, which showed highly correlated features to the HRS diet. The most abundant and highly

correlated proteins were the ABC-type sugar transport systems and glyceraldehyde-3-phosphate dehydrogenase of the carbohydrate metabolism and transport. Further, three enzymes involved in the lipid metabolism were increased in samples of the HRS diet, namely acyl-CoA dehydrogenase, acetyl-CoA acetyltransferase and enoyl-CoA hydratase. We observed, that proteins involved in the butyrate metabolism, such as enoyl-CoA hydratase (LRS vs. Baseline: p-value < 0.0001; LRS vs. HRS: p-value < 0.003) and butyrate kinase (Baseline vs. HRS: p-value < 0.001; HRS vs. LRS: p-value < 0.01) significantly changed with diet (Maier et al. 2017). A targeted quantification of butyrate in the samples revealed trends for increased butyrate accumulation in the HRS diet and to a lesser extent in the LRS diet, although highly variable between individuals (Chapter 2.4.1.5.4) (Maier et al. 2017). Cross-feeding effects between gut microbial populations were previously shown to increase variability between individuals because butyrate producers often take longer to establish after a dietary intervention (Belenguer et al. 2006, Maier et al. 2017).

Additionally, gut proteins were classified according to KEGG Digestion classes and correlated to the amount of RS, whereby alpha-amylase was found to be correlated negatively with the HRS diet. This appears, presumably because amylose-rich RS is not a substrate for α -amylase, the enzyme that hydrolyzes α -1,4 glycosidic linkages in starch (Rendleman 2000, Ramsay et al. 2006). Also, glucosidases, including beta-glucosidases (breaking complex carbohydrates into monomers) and alpha-glucosidases (breaking simple starches) were differently affected by HRS diet.

2.4.3 Multi-omics data integration

Nowadays, high-throughput technologies in genomics, proteomics and metabolomics allow to produce data on a massive scale (Meng et al. 2014), in which each of its omics-discipline is characterized by its complexity. Hereto, the human GIT and its microbiome is a complex ecosystem (Heintz-Buschart, et al. 2016), which is central in understanding the dynamics of health and disease. The integration of different omics-disciplines can provide a global picture of the microbial composition on a systems-level, understanding the host, microbial metabolism and protein expression, as well as the metabolic status of the human gut. The latter is of top priority to understand the impact of diet, especially of varying amounts of non-digestible carbohydrates, on the gut microbiome for health and disease.

2.4.3.1 Supervised ordination approach for multi-omics correlation

A supervised ordination approach (Figure 2.4-30) was applied, evaluating correlations among the genome, proteome and metabolome comparing baseline and the HRS diet (Figure 2.4-30 A). Also, a classification model was created for the comparison of the HRS diet and the LRS diet (Figure 2.4-30 B). This method was able to discriminate metabolites, proteins and OTUs that correlated with each other and with the different diets, gaining a first overview of possible connections (Maier et al. 2017). Therefore, a 25% limit (black line, shown dashed) of the highest discriminative feature of either the baseline diet or the HRS diet was set to detect highly correlated and highest discriminating features among the different diets. The same procedure was performed comparing the HRS to the LRS diet.

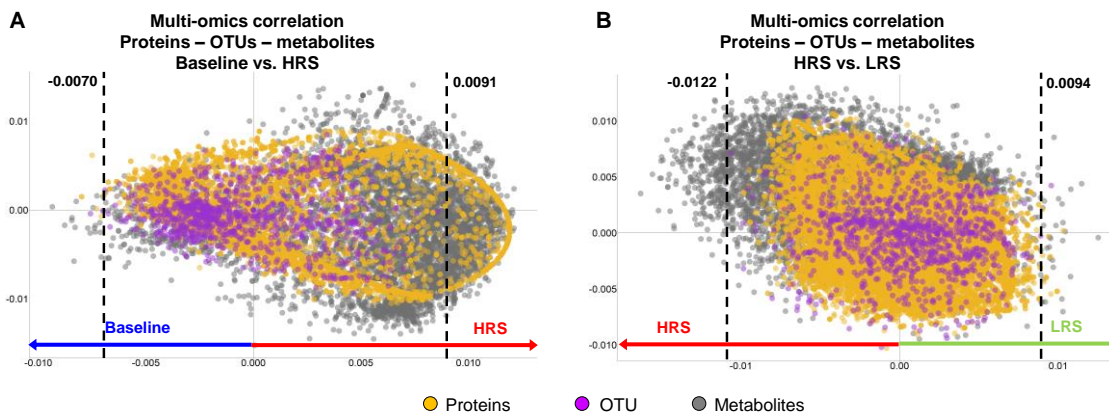


Figure 2.4-30: Multi-Omics integration through supervised ordination approach.

OPLS-DA plot of all data (Features: metabolites, 5552; Proteome, 57 397; OTUs, 1107) for A: baseline (blue, negative x-axis) versus HRS (red, positive x-axis); $p = 8.3 \cdot 10^{-6}$ (CV-ANOVA), $R^2Y(\text{cum}) = 0.96$, $Q^2(\text{cum}) = 0.88$. B: OPLS-DA plot for HRS (red, negative x-axis) versus LRS (green, positive x-axis); $p = 0.026$ (CV-ANOVA), $R^2Y(\text{cum}) = 0.883$, $Q^2(\text{cum}) = 0.534$. From Maier, T. V.; Lucio, M.; Lee, L. H.; VerBerkmoes, N. C.; Brislawn, C. J.; Bernhardt, J.; Lamendella, R.; McDermott, J. E.; Bergeron, N.; Heinzmann, S. S.; Morton, J. T.; González, A.; Ackermann, G.; Knight, R.; Riedel, K.; Krauss, R. M.; Schmitt-Kopplin, P.; Jansson, J. K.: Impact of Dietary Resistant Starch on the Human Gut Microbiome, Metaproteome, and Metabolome. *mBio* vol. 8 no. 5 e01343-17 (2017). Reprinted and modified from (Maier et al. 2017). Copyright (2017) Maier et al.

The metabolite profile was vastly changed by the HRS diet. Several features were highly correlated and significantly changed by the HRS diet. This included 17.83% of the total metabolome (990 metabolites) and 1.14% of the total proteome (649 proteins), but no OTUs significantly changed through the HRS diet. On the contrary, the baseline diet was characterized through 0.31% of the metabolome (17 metabolites), 0.008% of the total proteome (5 proteins) and 0.18% of the total genome (2 OTUs).

In general, metabolites, such as sterol lipids, fatty acyls, glycerolipids and polyketides correlated with ribosomal proteins (J), adenylosuccinate synthase (F), rubrerythrin (C), glyceraldehyde-3-phosphate

dehydrogenase (G) and fructose/tagatose bisphosphate aldolase (G) predominately in the HRS diet. In the baseline diet, correlations between genera of *Lachnospiraceae*, *Bacteroidetes*, ribosomal proteins, FAs and STs were detected. Further, the correlations between the HRS and LRS diet were investigated, which resulted in 0.34% of the metabolome (19 metabolites), 0.012% of the total proteome (7 proteins) and 0.09% of the total genome (1 OTUs) correlated through the LRS diet. In the HRS diet, only metabolites (1.87%) were found to be significantly changed, whereas no correlations between metabolites, proteins and OTUs were detected. The first OTU, detected as correlated with metabolites was a *Roseburia* sp. with some STs.

2.4.3.2 Mass-difference network analysis

The supervised ordination approach was complemented using a network-based CLR method (Faith et al. 2007) to display potential interactions of the genome, proteome and metabolome and to examine results across the different omics levels for an integrated systems picture (Maier et al. 2017). Differential expression was calculated as the fold change between mean abundance of each component (OTU, protein and metabolite) in the HRS participants versus baseline participants (Figure 2.4-31 A), as well as the LRS participants versus the baseline ones (Figure 2.4-31 B). Both were visualized in Cytoscape as a network. This allowed assigning various areas of the network to different metabolite compound classes (e.g. STs, GLs, GPs and FAs) and connected OTUs, and proteins. This result agreed with the supervised ordination approaches, that the discrimination in both models was mainly driven by metabolites.

A *F. prausnitzii* A2-165 strain, assigned as a species for a specific protein, namely phosphotransacetylase, involved in the energy production and conversion was found to be correlated with the HRS diet and showed connections to a glycerophospholipid (PG(15:0/0:0)). The CLR network comparing HRS to the baseline diet showed more features correlated or correlated negatively with the HRS diet compared to baseline than for the LRS diet compared to baseline, which again demonstrates that the HRS diet had a larger impact on the gut microbiome (Maier et al. 2017).

As previously described, genera of *Bacteroides* and *Lachnospiraceae* correlated negatively with RS and connected to unsaturated FAs and some STs (Maier et al. 2017). Thousands of metabolites were significantly more abundant or less abundant after the HRS diet, including sterol lipids, GPs, GLs, FAs,

2. Effect of resistant starch on the gut microbiome

PKs and lots of unknown metabolites, whereas only 3 more proteins (phosphoenolpyruvate carboxykinase (C), ribosomal protein L23 (J) and ABC-type sugar transport system (G) and 2 OTUs (*ruminococcaceae*) were revealed.

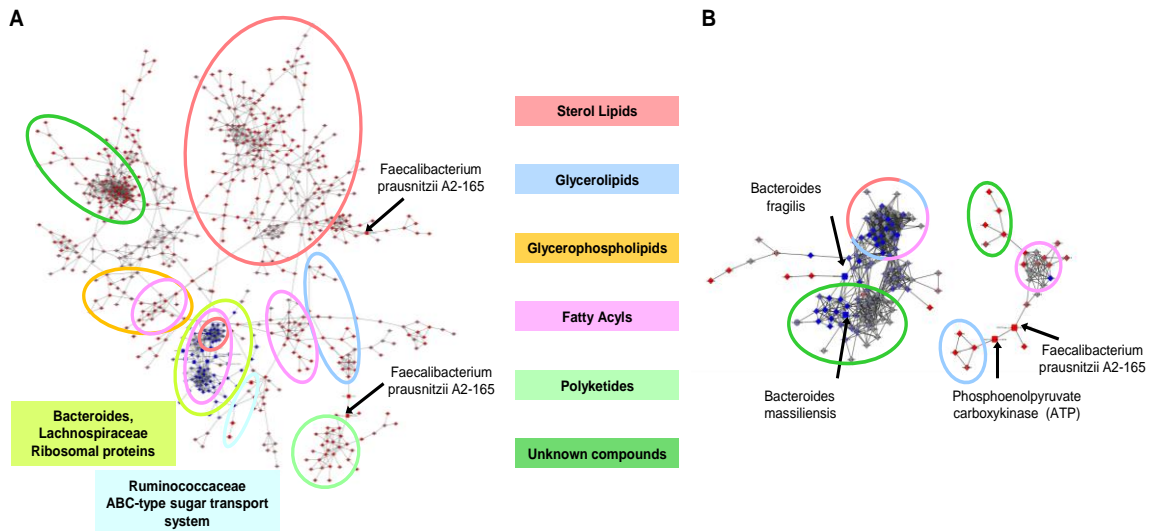


Figure 2.4-31: Multi-Omics integration displayed as CLR network.

A: CLR network displaying correlated features to the HRS diet (red) and negatively correlated to HRS diet (blue). B: CLR network displaying correlated features to the LRS diet (red) and negatively correlated to LRS diet (blue). Similarities (edges) within and between species, proteins, and metabolites (circles, squares, triangles, respectively) across participants and time points, including only nodes significantly higher (red) or lower (blue) in HRS or LRS respectively relative to baseline ($p < 0.05$). Areas of the network assigned to sterol lipids (red), glycerolipids (blue), glycerophospholipids (orange), fatty acyls (pink), polyketides (mint) and unknown metabolites (green). From Maier, T. V.; Lucio, M.; Lee, L. H.; VerBerkmoes, N. C.; Brislawn, C. J.; Bernhardt, J.; Lamendella, R.; McDermott, J. E.; Bergeron, N.; Heinzmann, S. S.; Morton, J. T.; González, A.; Ackermann, G.; Knight, R.; Riedel, K.; Krauss, R. M.; Schmitt-Kopplin, P.; Jansson, J. K.: Impact of Dietary Resistant Starch on the Human Gut Microbiome, Metaproteome, and Metabolome. *mBio* vol. 8 no. 5 e01343-17 (2017). Figure A was reprinted and modified from (Maier et al. 2017). Copyright (2017) Maier et al. Illustration of Figure B was reprinted and modified from (Maier et al. 2017). Copyright (2017) Maier et al., Information about the creator and respective contributions, as well as the original material are available: <http://mbio.asm.org/content/8/5/e01343-17.full> with the original title: Integrative association network of the microbiome under low resistant starch diet. Licence notice: <https://creativecommons.org/licenses/by/4.0/>.

When analyzing the combined CLR data, not only features that were associated with the different diets were observed, but also features that correlated with each other. This systems view of the metabolite composition and clustering confirms results from previous analyses of the influence of dietary RS on some members of the *Firmicutes*, such as *F. prausnitzii* (Haenen et al. 2013), and goes beyond them by also identifying correlations of specific species with single metabolites and proteins. For example, *F. prausnitzii* was correlated positively with the HRS diet and 14 novel metabolites with putative identifications as polyketides were found that correlated with this microorganism (Maier et al. 2017)

When analyzing the CLR network comparing the LRS diet to the baseline diet it was noticeable that comparatively fewer features correlated and a number of features were correlated negatively with the LRS diet. Comparing both networks, an accordance of one species specific protein of the *F. prausnitzii* A2-165, namely ribosomal protein L23, was observed to be correlated positively with the HRS diet, and to the LRS diet. These results also pointed towards key linkages between several members of the gut microbiome, metabolites and proteins produced in the gut (Maier et al. 2017).

These findings of the multi-omics analyses were summarized to evaluate the main effects of the RS diet on the gut microbiome and functions that they carry out and the multitude of processes that occur through HRS diet. Changes in the starch degradation and metabolism were detected. Glucosidases, proteins involved in sugar transport and in the glycolysis, could be observed. Proteins, such as beta-glucosidases, involved in breaking complex carbohydrates into monomers and proteins involved in transport systems for import of resultant free sugars into the cells were highly increased in the HRS diet.

On the contrary, alpha-glucosidases were in comparison less abundant in the HRS diet. Alpha-glucosidases break down simple starches, but the high amylose cornstarch in the HRS diet was not a substrate for alpha-glucosidase activity. Human alpha-amylase was also significantly less abundant in the HRS diet as expected due to the decrease in readily available starch. This study also reinforced the importance of *F. prausnitzii* for metabolism of non-dietary carbohydrates in the diet, including enzymes for butyrate production by this organism. In contrast, members of the *Bacteroides* were reduced in abundance following the HRS diet. A notable strength of the approach used here was that proteins and metabolites were collected from host and microbiome simultaneously, allowing a systems-level approach to observe their interplay. Taken together, our results emphasize the importance of longitudinal, multi-omics study designs for unraveling the effects of nutrition on the microbiome and health (Maier et al. 2017).

2.5 Summary and Conclusion

The aim of the study was to elucidate the impact of dietary starch (RS) on the human fecal metabolome and microbiome by applying an ultra-high resolution Fourier transform ion cyclotron resonance mass spectrometry based metabolomics approach, 16S rRNA sequencing and shotgun metaproteomics analyses in a controlled, randomized, within-subjects' crossover dietary intervention trial. Diet can influence the composition of the human microbiome, yet relatively few dietary ingredients were systematically investigated for their impact on the functional potential of the microbiome. However, the knowledge about the impact of HRS diets on the human metabolite profile is currently limited. Here, the fecal metabolome analyses revealed not only metabolites significantly correlated positively or negatively with the amount of RS, but also unveiled several pathways, especially the lipid metabolism to be highly impacted through the different diets. Among hundreds of unknown metabolites, several distinctive classes of metabolites such as fatty acids and oxylipins, changed between the baseline, HRS or LRS diet. Furthermore, several different lipid classes, namely glycerophosphocholines (PC), glycerophosphoethanolamines (PE), glycerophosphoglycerols (PG) and glycerophosphoserines (PS) showed distinct patterns between the two diet classes. Especially in the baseline diet, glycerophosphates (PA), including cyclic PAs, were significantly increased compared to both RS diet groups.

Further, 16S rRNA sequencing revealed consistent changes according to the three diet classes (Baseline, HRS and LRS). Consistent with previous reports (Walker et al. 2011), we found that the HRS diet induced a shift in the composition of the gut microbiome. There was a significant increase in the proportion of *Firmicutes* to *Bacteroides* following the HRS, compared to the baseline and LRS diets. These changes included increases in relative amounts of species in the genera *Faecalibacterium*, *Roseburia* and *Ruminococcus*, which were associated with butyrate production (Louis et al. 2010, Miquel et al. 2015) and found to be reduced in abundance in the gut microbiota of participants with type 2 diabetes mellitus (T2DM) compared to healthy individuals (Qin et al. 2012). To conclude, RS significantly altered the fecal microbial composition, which was represented by increased and positively correlated species of the *Firmicutes* phylum following the HRS diet, which were predominately species of *F. prausnitzii* and *E. rectale*. On the contrary, species of the *Bacteroides* phylum correlated negatively and decreased in fecal samples of participants consuming the HRS diet. Further, we went beyond

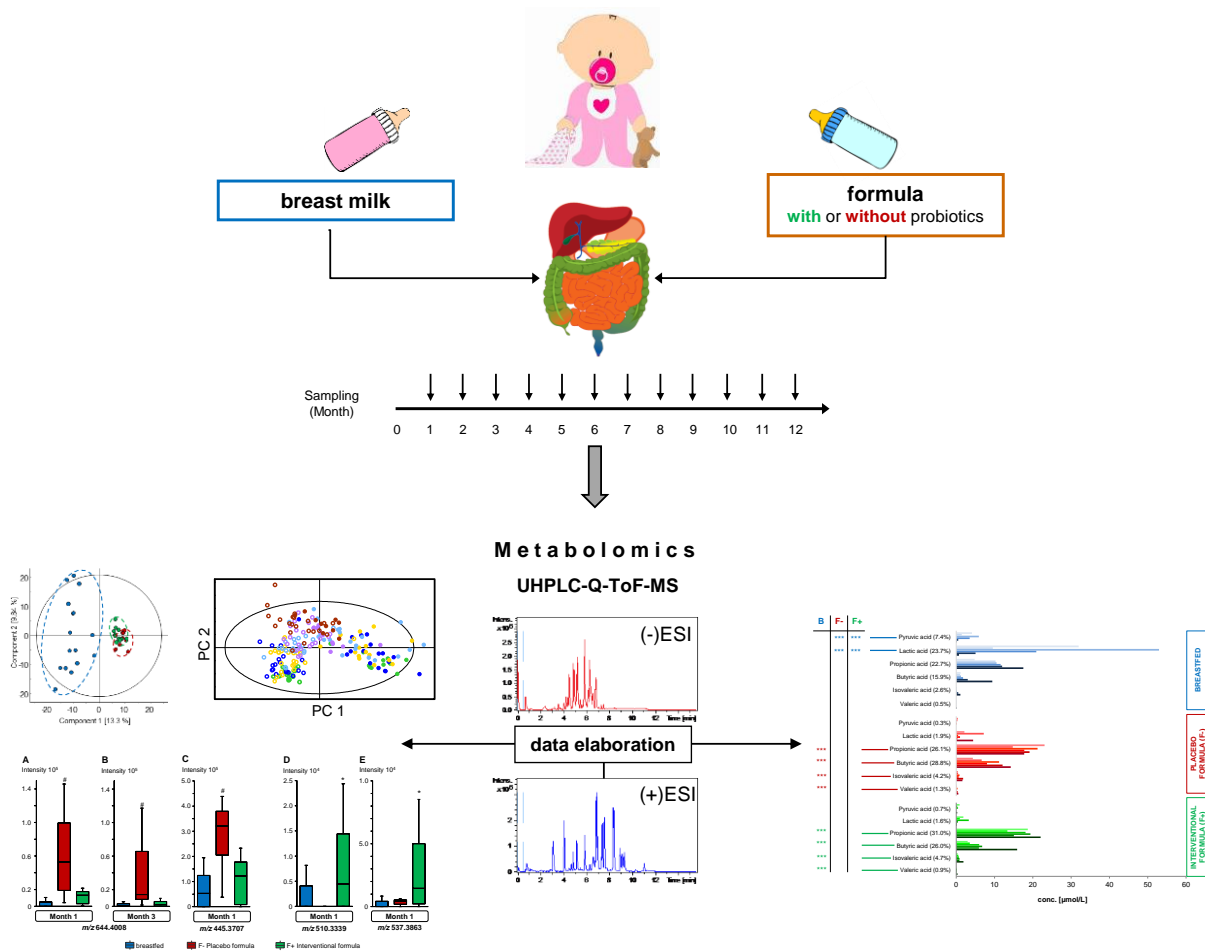
taxonomic characterization to also investigate the functional shifts in response to the diet. Therefore, a shotgun metaproteomics approach was conducted, which allowed to determine the identities of thousands of host and microbial proteins across the samples. This analysis revealed several proteins, involved in carbohydrate metabolism and transport, as well as in the lipid metabolism, especially the butyrate metabolism to be significantly increased in fecal samples of participants consuming the HRS diet.

Additionally, we were able to examine results across the different omics levels for an integrated systems picture. Therefore, a supervised ordination approach was applied in order to gain an overview about discriminating metabolites, proteins and OTUs that were correlated with each other and with the different diets, followed by CLR method network-based approach to detect linkages between specific OTUs, proteins and metabolites. Combining all analyses, it was possible to present the main effects of the RS diet on the gut microbiome and functions that they carry out.

These findings may help to understand the impacts of RS consumption. To conclude, future studies investigating the influence of RS on gut bacteria should consider the inclusion of tools such as metabolomics to understand the complexities of how this fermentable starch may influence bacterial and host metabolome (Chassard and Lacroix 2013) and biomarkers of bacterial activity, as well as focusing on bacterial community membership. There is good evidence that RS influences gut microbial communities involved in amylose breakdown and butyrate production, but there is a significant variability in responses. Advances in gut microbe profiling and metabolomics may help to understand the complexity of this variation (Lockyer and Nugent 2017).

Chapter III

Impact of breast feeding and bifidobacteria-supplemented formula on the infant fecal metabolite profile in the first year of life



Parts of this chapter (chapter III - Impact of breast feeding and bifidobacteria-supplemented formula on the infant fecal metabolite profile in the first year of life) are published in:

Bazanella, M., Maier, T. V., Clavel, T., Lagkouvardos, I., Lucio, M., Maldonado-Gómez, M. X., Autran, C., Walter, J., Bode, L., Schmitt-Kopplin, P., Haller, D.: Randomized controlled trial on the impact of early-life intervention with bifidobacteria on the healthy infant fecal microbiota and metabolome. *Am J Clin Nutr.* 106(5):1274-1286 (2017). (Bazanella et al. 2017)

Copyright (2017) American Society for Nutrition

3 Impact of breast feeding and bifidobacteria-supplemented formula on the infant fecal metabolite profile in the first year of life

3.1 Introduction

Colonization of the human intestinal tract commences during birth and is a complex process influenced by many factors. This comprises the gestational age at birth, maternal health and microbiota, antibiotic treatment, hospital hygiene, mode of delivery and type of feeding (Dominguez-Bello et al. 2010, Marques et al. 2010, Arrieta et al. 2014).

The intestinal microbiota and thus the metabolite profile of fecal samples of infants fed with breast milk differ significantly from the formula fed ones (Chow et al. 2014). This is predominantly influenced by a dominating amount of bifidobacteria species in the gut microbiota of breastfed infants (Chow et al. 2014), caused by HMOs in the breast milk (Arrieta et al. 2014). The HMOs enable the settlement and the survival of the bifidobacteria species in the gut. In contrast, feces of formula-fed infants harbor more diverse bacterial species (Chow et al. 2014), containing also *E. coli*, *Clostridium difficile*, *Bacteroides* and *Lactobacilli* (Harmsen et al. 2000, Penders et al. 2006).

From a nutritional point of view, breast milk is fundamental in early life development, since it contains the appropriate composition of nutrients, such as macro- and micronutrients. They are essential to support the development of the infants' immune system. Macronutrients are carbohydrates (e.g. lactose and oligosaccharides), fat (e.g. long-chain polyunsaturated fatty acids, LCPUFAs) and proteins (e.g. casein, α -lactalbumin, lactoferrin, secretory immunoglobulin IgA, lysozyme, and serum albumin, amino acids, and nucleotides) (Jenness 1979, Ballard and Morrow 2013). Micronutrients are especially vitamins, such as vitamin A, B1, B2, B6, B12 and D, the amount of which depends on the motherly diet and their body storages (Ballard and Morrow 2013).

Formula is an alternative nutrition for infants used as sole food or as supplementary food if the breast milk does not suffice. It is known, that infant formula with probiotic supplementation e.g. bifidobacteria (Conway 2001) is beneficially influencing the gut microbiota and the infants' health (Bergmann et al. 2014, Tanaka et al. 2015). However, it is not much known about the effect of probiotic formula on the development of the infants' intestinal gut microbiome. Therefore, it is a straightforward approach to

supplement infant formula with probiotic bifidobacteria in order to support infant's health and approach as closely as possible the gut microbiome of breastfed infants.

In recent years, research in the field of probiotics vastly increased. Even a greater focus sticks on revealing the impact of probiotics on the development of the infants' gut microbiome in early life stages, in contrast to breastfed ones. Effects of probiotics on the infant gut microbiome need to be investigated due to the decrease of willingness for weaning, wherefore the focus should be laid on the effect of probiotics on the healthy, developing gut microbiome of newborns. Already at birth, the gut microbiota of infants develops through maternal and environmental exposure and is colonized with several microorganisms. Further, compared to the adult gut microbiota, the infants' microbiota is more impressionable to environmental exposure, such as lifestyle, birth and nutrition (Arrieta et al. 2014).

Interestingly, several studies were published investigating the impact of diet on the infant fecal microbiota and health, though relatively few focused on the impact of diet and mode of delivery on the metabolome of the infants. Recently, Chow et al. investigated the fecal metabolite profiles of healthy, exclusively breast fed or formula-fed infants (without considering probiotics) before and during *in vitro* batch culture fermentation, analyzed by GC/MS and LC-MS/MS. An increase of human milk oligosaccharides (HMOs) and other metabolites (e.g. linoelaidate, hydroxyphenyllactate, lactate and taurocholate sulfate) was detected in the batch culture of breastfed infants. On the contrary, the metabolite profiles of cultures from formula-fed infants were shaped of around three times the number of significantly increased metabolites, including tocopherols, saturated fatty acids ranging from C5:0 up to C24:0, unsaturated fatty acids and bile acids (Chow et al. 2014).

Further, at birth, the infants' initial microbiota is influenced by either vaginal delivery (VD) or cesarean section (CS), which anon affects the microbes' composition in the gut (Dominguez-Bello et al. 2010). In general, the gut microbiota of vaginally born infants harbor bacteria such as *Prevotella*, *Lactobacillus*, and further bacteria from the maternal vagina and the ones present in the maternal gut (Mackie et al. 1999, Dominguez-Bello et al. 2010). On the contrary, *Proteobacteria*, *Propionibacterium* and *Streptococcus* predominately inhabit the gut microbiota of infants born by C-section (Backhed et al. 2015, Del Chierico et al. 2015, MacIntyre et al. 2015). Infants get used to solid food during their weaning period, where the infants are fed with a higher amount of carbohydrates, than those present in breast milk or formula. Also, the introduction of solid food alters the gut microbiota composition and plays a

significant role in the development. Especially the increasing amount in general, but also type of carbohydrates, such as complex carbohydrates play an important role in the microbial metabolic processing and SCFA production (Arrieta et al. 2014).

This aforementioned, established high-cohort study, including the metabolomics approach and the metabolite-OTU correlations enable not only to investigate the development of the gut microbiome over time with respect to the metabolic response due to the different feedings of either breastfed or formula-fed infants, but also to consider the impact of the mode of delivery on the infant gut microbiome at early life stages.

3.2 Objective and Goals

In order to support the infant's health equipping it with a beneficial gut microbiome, much effort has been undertaken to develop probiotic supplementation that increase e.g. health-promoting bifidobacteria in the intestinal microbiome. Relatively little research was done to investigate the impact of such probiotics with non-targeted meta-metabolome analyses. Therefore, a randomized, double-blinded, placebo-controlled trial with 106 healthy newborns was designed, to investigate the impact of bifidobacteria-supplemented formula on the infant gut microbiome and the metabolite pattern in the first year of life. The goals were to investigate and evaluate the metabolite profiles of fecal samples of the newborns over time, the impact of bifidobacteria-supplemented formula (F+) compared to the placebo group (F-) and in contrast to the breastfed (B) infants. Furthermore, metabolites differing between CS and VD were also investigated. To achieve this, an MS based metabolomics approach using UHPLC-ToF-MS in two different ionization modes was applied. Additionally, high-throughput 16S rRNA gene amplicon sequencing was performed to reveal relationships between metabolites and gut specific microbial species in relation to the type of feeding. Further, correlation techniques e.g. between metabolites and OTUs were applied. Fecal sample collection and coordination, as well as high-throughput 16S rRNA gene amplicon sequencing was performed and processed by Monika Bazanella (Chair of Nutrition and Immunology, Technische Universität München). Further information on fecal sample collection, on high-throughput 16S rRNA gene amplicon sequencing and data processing is given in (Bazanella et al. 2017).

3.2.1 Study design

The objective of the study was to describe the gut microbiota-mediated metabolic effects in infants after being fed with bifidobacteria-supplemented formula in contrast to breast feeding or the placebo formula. Therefore, 106 healthy infants were classified to two main groups, consisting of exclusively fed and mixed fed infants as shown in Figure 3.2-1. In the first group, the infants were fed exclusively with formula or were exclusively breastfed in the first year of life. The second main group was composed of infants, which were inconsistently fed with formula and/or breastfed over time. Both groups were differentiated into two formula-groups, receiving either the placebo or the bifidobacteria-supplemented formula with a mixture of four bifidobacteria species in equal shares of *Bifidobacterium longum*, *B. infantis*, *B. breve*, *B. bifidum* (108 cfu/g formula) (Bazanella et al. 2017).

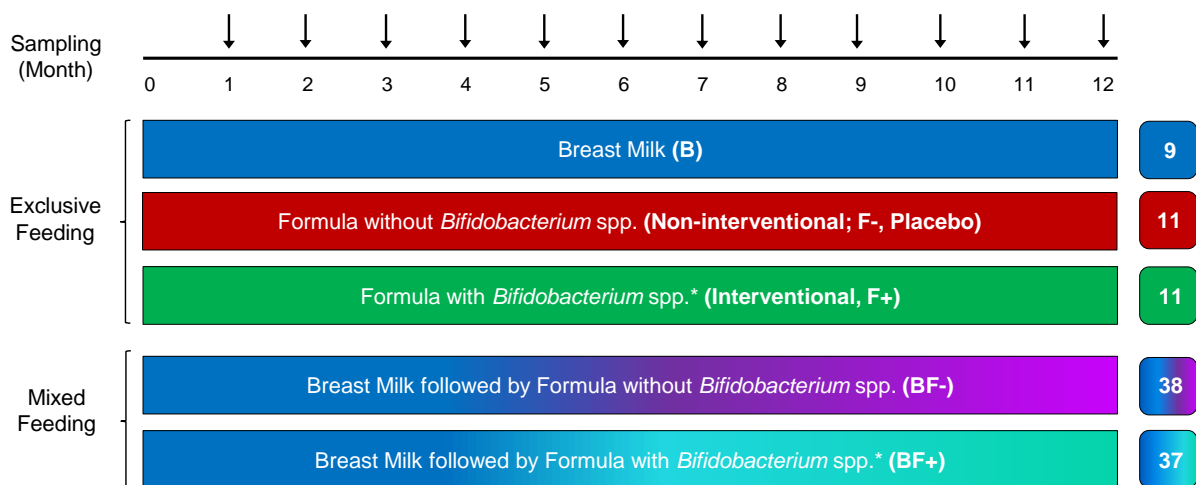


Figure 3.2-1: Study design of the InfantBio study.

Study design to evaluate the impact of bifidobacteria-supplemented formula in contrast to the placebo and the breastfed group in infants. Infants were assigned to either the exclusively or mixed fed group, differentiating in exclusively breast fed (blue), interventional formula-fed (green, with probiotics) or placebo formula-fed (red, without probiotics). *A mixture of four bifidobacteria was fed in equal shares of *Bifidobacterium longum*, *B. infantis*, *B. breve*, *B. bifidum* (108 cfu/g formula).

Another aspect was to investigate, if the mode of delivery (CS and VD) had influences on the metabolite profile in general. An overview of study population, the birth and feeding characteristics of the infants, which were studied in detail in the following chapters are given in Table 3.2-1.

Table 3.2-1: InfantBio study population characteristics.

Infant characteristics of exclusively and mixed fed infants, including gender (male or female), mode of delivery (vaginal delivery or cesarean section), birth weight and birth size of month 1, 3, 5, 7, 9 and 12. Data are shown as mean values, including standard deviations. Percentages are shown in brackets.

	Exclusive Feeding			Mixed Feeding	
	Breastfed (B) (n=9)	Placebo formula (F-) (n=11)	Interventional formula (F+) (n=11)	Breast milk + Placebo formula (BF-) (n=38)	Breast milk + Interventional formula (BF+) (n=37)
Birth characteristics					
Gender					
Male (%)	5 (4.7%)	6 (5.7%)	4 (3.8%)	13 (12.3%)	12 (11.3%)
Female (%)	4 (3.7%)	5 (4.7%)	7 (6.6%)	25 (23.6%)	25 (23.6%)
Distribution (Group)					
Male (%)	55%	55%	36%	34%	32%
Female (%)	45%	45%	64%	66%	68%
Mode of delivery					
Vaginal delivery (%)	3 (2.8%)	6 (5.7%)	6 (5.7%)	21 (19.8%)	22 (20.7%)
Cesarean section (%)	6 (5.7%)	5 (4.7%)	5 (4.7%)	17 (16.0%)	15 (14.2%)
Distribution (Group)					
Vaginal delivery (%)	33%	55%	55%	55%	60%
Cesarean section (%)	67%	45%	45%	45%	40%
Birth weight (g)					
	3515 ± 297	3246 ± 390	3327 ± 401	3175 ± 431	3421 ± 585
Month 1	4186 ± 333	4425 ± 480	4158 ± 667	4012 ± 514	4162 ± 721
Month 3	6116 ± 1066	6518 ± 994	6085 ± 607	5794 ± 1342	5838 ± 922
Month 5	6933 ± 839	7427 ± 1260	7236 ± 587	7106 ± 791	6960 ± 1090
Month 7	8095 ± 972	8505 ± 1218	8305 ± 832	8073 ± 1150	7879 ± 1163
Month 9	8700 ± 846	8685 ± 485	9166 ± 827	8535 ± 1247	8656 ± 1294
Month 12	9514 ± 1077	9350 ± 1196	10228 ± 905	9212 ± 1185	9093 ± 1262
Birth size (cm)					
	52.4 ± 1.7	50.7 ± 1.7	51.3 ± 2.9	51.0 ± 2.2	51.5 ± 2.7
Month 1	53.3 ± 3.4	54.4 ± 1.4	54.4 ± 2.9	54.1 ± 2.7	54.6 ± 2.9
Month 3	63.4 ± 2.7	63.0 ± 3.5	62.3 ± 3.0	61.7 ± 2.1	60.9 ± 3.1
Month 5	68.5 ± 3.5	66.9 ± 3.5	65.2 ± 2.3	66.0 ± 2.1	65.1 ± 3.2
Month 7	68.4 ± 4.5	80.0 ± 2.8	70.1 ± 2.8	69.6 ± 2.8	68.7 ± 3.1
Month 9	71.3 ± 2.5	72.3 ± 2.4	74.6 ± 4.0	72.9 ± 3.4	72.0 ± 4.2
Month 12	75.6 ± 4.1	78.2 ± 3.1	76.1 ± 4.4	75.3 ± 2.8	74.7 ± 3.5

Little research was done in the meta-metabolomics field. However, it is crucial to focus on the investigation of the metabolite profile due to different feeding types, since the metabolite profiles give a broad overview of functionality of the microbiome. Metabolomics allows to analyze and to identify thousands of metabolites and to gain a deeper insight into the complex interactions of gut microbes, feeding and the host. Investigating the metabolite profile is helpful to further assess the effect of bifidobacteria-supplemented formula on the healthy development of the infants' gut microbiome. Therefore, fecal samples of infants were collected monthly, whereas only samples every second month were taken into account for metabolome analysis. First, a non-targeted metabolomics approach was performed by UHPLC-(+)(-)-ToF-MS, followed by a subsequent series of targeted analyses, including SCFA analysis and MS/MS experiments for metabolite identification. Moreover, metabolites and OTUs - received from 16S rRNA gene sequence analyses (performed and processed by Monika Bazanella,

TU München, ZIEL) were correlated to detect significant microbial-metabolite relationships in the formula (probiotic and non-probiotic) and/or the breastfed group.

3.3 Materials and Methods

3.3.1 Metabolite extraction of fecal samples

The collected samples were extracted with MeOH (CHROMASOLV®, for HPLC, ≥99.9%, Sigma-Aldrich) as follows: First, all samples were centrifuged (4 °C, 12.000 rpm) for 60 minutes. Accrued fecal water was taken and transferred into a cryogenic vial and stored at -80 °C. The following steps were performed on ice. Approximately 50 mg of each fecal sample were weighed into NucleoSpin® Bead Tubes with ceramic beads, 1 mL of ice cold MeOH was added and homogenized in a TissueLyser II (Qiagen) for 5 minutes at a rate of 30 Hz in order to destroy the bacterial cells and extract the metabolites out of the fecal sample. Afterwards, the mixture was centrifuged (4 °C, 10.000 rpm; 5 minutes) and the supernatant was transferred into a 2 mL Eppendorf vial, stored at -80 °C until the analysis on a Waters ACQUITY UltraPerformance LC® system (Waters GmbH, Eschborn, Germany) coupled to a Bruker Daltonik (Bremen, Germany) maXis™ UHR-qToF-MS (Bazanella et al. 2017).

3.3.2 Non-targeted UHPLC-ToF-MS metabolite analysis of fecal methanol extracts

The MeOH extracts were measured with UHPLC-ToF-MS in positive and negative ESI mode. Measurements were conducted on a VisionHT C18 HL 1,5 µm (150mm x 2.0mm) (W. R. Grace & Co, Columbia, USA) in randomized order within ten batches. Gradient separation with a total runtime of 15.5 minutes (flow rate: 0.4 mL/min, column temperature: 40 °C, A: 5% ACN, 0.1% formic acid, B: 100% ACN, 0.1% formic acid) was performed of 5 µL of each sample injected in partial loop with 99.5% A and 0.5% B as starting condition. After 1.12 minutes B was increased to 99.5% within 5.3 minutes and hold for 3.6 minutes, followed by a rapid decrease to 0.5% B in 0.5 minutes and hold for 5 minutes. For quality control and for the after the measurement following normalization, a QC (mixture of all samples) was injected after each 10 samples. For the calibration of the MS data, a segment at the beginning of the chromatogram was added, while 1:4 diluted ESI-L Low Concentration Tuning Mix (G1969-85000, Agilent, Waldbronn, Germany) was injected. MS parameters are as follows: mass range: m/z 50 – 1000, dry gas: 8 L/min, dry temperature: 200 °C, nebulizer gas: 2 bar. During the analyses, samples were

kept at 4 °C in the sample manager (Bazanella et al. 2017). Further details on parameters are given in Table 6.2-4.

3.3.3 Automated data processing of high throughput samples

Data processing is challenging, because many factors and parameters must and/or need to be taken into account, depending on the type of data. Within this study, it was chosen to process the data for both ionization modes automatically as an end-to-end automation by using the Genedata Expressionist® Refiner MS for MS-based metabolomics data from the Genedata AG. With this method, thousands of samples – as in our study – can be processed. The automated processing and cleansing steps can be varied as needed. In this study, the LC-MS data underwent several steps including noise reduction, filtering, calibration, alignment, and peak clustering, as shown in detail in Figure 3.3-1. Here, the processing was divided into three main steps, consisting of stage 1, which included mainly noise reduction and the removal of artefacts, followed by stage 2. Within this step, the previously processed data from stage 1 was calibrated with the tune mix (Agilent Technologies, G1969-85000) injected at the beginning. Further, chromatogram retention time alignment was applied. In the last step, in stage 3, peaks in the chromatogram and isotope patterns were detected and merged in one big data matrix. The processed and obtained data matrix was further loaded to Genedata Analyst™ - a software tool for the integration and interpretation of the experimental data – for normalization of the data. Normalization is crucial due to enormous analysis time shifts. Therefore, the method of choice was a batch normalization, which corrects the data for batch and injection order effects in long-running MS experiments by using a linear regression between the quality control samples within the runs.

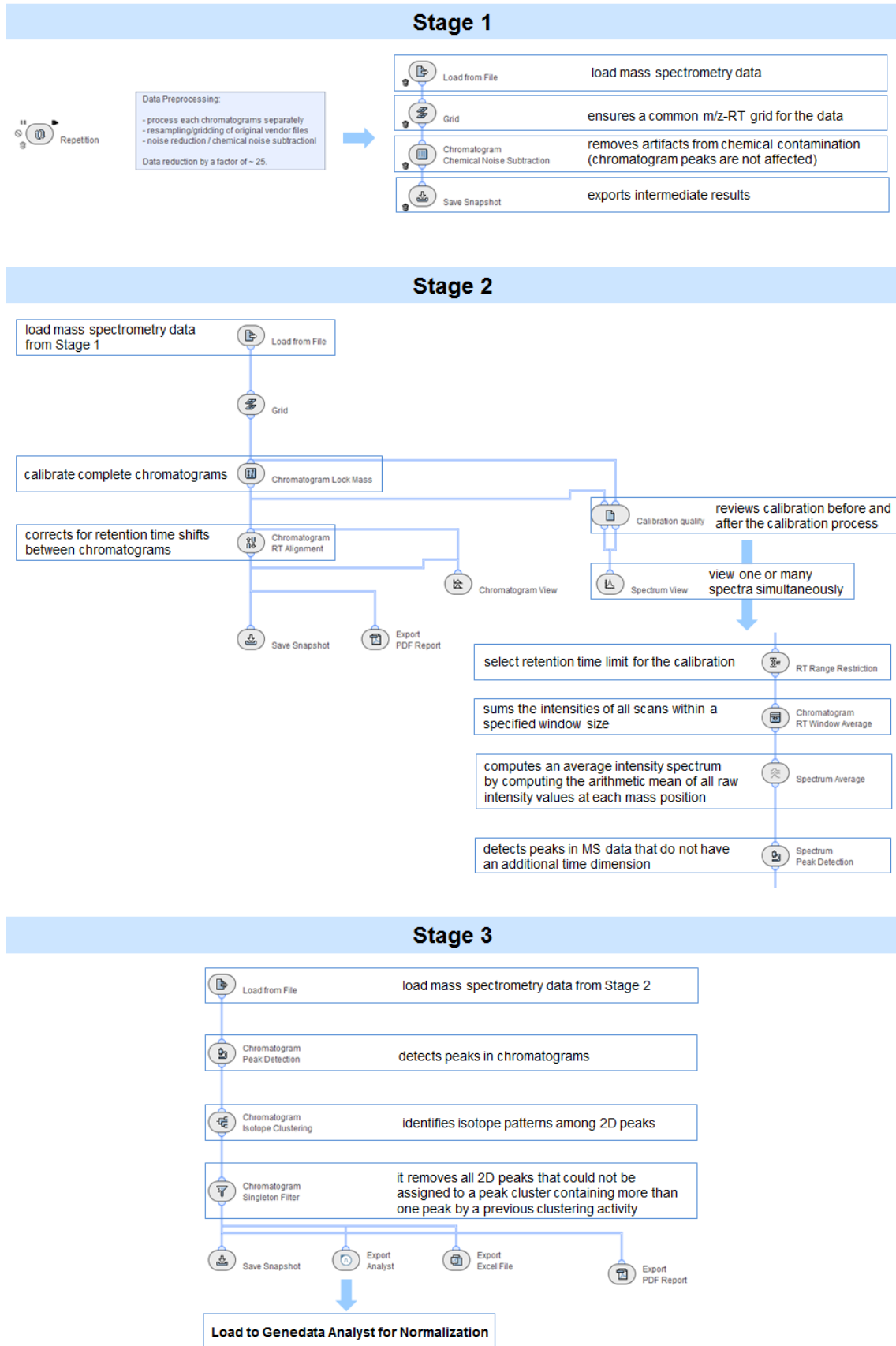


Figure 3.3-1: Genedata Expressionist® Refiner MS for Mass Spectrometry Workflow.

3.3.4 Data filtering, metabolite annotation and classification

For further data analysis the data matrices of the exclusively fed samples, the correlation studies and to investigate the monthly and feeding variances of the different groups (B, F, F- and F+) were processed similar. The data matrices for the correlation of metabolites and OTUs, the overall, and the monthly evaluation were filtered by mass defect above 0.9 and a cutoff for zero presence values was applied. This resulted in 710 ((-) ESI) and 2040 ((+) ESI) mass signals over time, considering month 1 up to month 12. Next, the mass signals were searched against the KEGG (Kanehisa and Goto 2000), HMDB (Wishart, Tzur et al. 2007, Wishart, Knox et al. 2009) and Lipid Maps (www.lipidmaps.org) (Fahy et al. 2009) databases as M+H, M+Na and M+K (positive) and M-H, M+FA-H, M+H₂O-H (negative) adducts using homo sapiens (hsa) as reference organism by the MassTRIX web server (Suhre and Schmitt-Kopplin 2008, Wagele, Witting et al. 2012) with a maximum error of 0.005 Da. In databases known metabolites were classified into compound classes by using the MassTRIX assigned compound IDs of the HMDB and Lipid Maps database and to related pathways using the information of KEGG (Bazanella et al. 2017).

3.3.5 Fatty acid analysis, focusing on SCFA and MCFA, lactic acid and pyruvic acid

For the analysis, the MeOH fecal extracts of the exclusively fed infants (month 1, 3, 5, 7, 9 and 12) and chemical standards (pyruvic acid, lactic acid, propionic acid, butyric acid, isobutyric acid, valeric acid, isovaleric acid, maleic acid, fumaric acid, succinic acid, hexanoic acid, heptanoic acid, nonanoic acid, octanoic acid and decanoic acid) (Chapter 6.2.1) were prepared and derivatized on ice as instructed in the AMP+ Mass Spectrometry Kit (Caymen Chemicals) product insert.

The fecal samples and chemical standards were prepared and measured as described in Chapter 2.3.1.7. The extractions of the mass signals, data processing, as well as statistical analyses were performed similarly as described in Chapter 2.3.1.7. Quantification was performed by external calibration (8 calibration points) based on the extracted peak areas of each standard concentration via the calculated calibration function (Table 3.3-1).

Table 3.3-1: SCFA results of the external calibration.

name	m/z (derivatized)	RT [min]	calibration function	coefficient of determination	method
Pyruvic acid	255,1134	4,1	$y = 17303x + 1473,3$	$R^2 = 0,9971$	MS
Lactic acid (conc. 0 – 5 µmol/L)	257,1290	3,6	$y = 19184x + 4630,4$	$R^2 = 0,9923$	MS
Lactic acid (conc. 5 – 52 µmol/L)	257,1290	3,6	$y = 7336,6x + 120551$	$R^2 = 0,995$	MS
Propionic acid	241,1341	4,0	$y = 1,2119x - 0,5784$	$R^2 = 0,999$	UV
Butyric acid	255,1497	4,6	$y = 59940x + 16956$	$R^2 = 0,9981$	MS
Isovaleric acid	269,1654	5,3	$y = 82730x + 6202,9$	$R^2 = 0,9993$	MS
Valeric acid	269,1654	5,5	$y = 92248x + 4883$	$R^2 = 0,9998$	MS

For PCA, the data was UV scaled. Scores scatter plots and loadings plot of correlations between SCFA to OTUs were illustrated as PCA, performed in SIMCA-P 9.0 (Umetrics, Umeå, Sweden). Correlation coefficients and p-corr were calculated in Microsoft Office Excel 2010 by applying the data analysis function "Regression". The EIC of mass signals, the MS/MS spectra and the MS/MS fragment mass lists for the comparison with several databases, as well as for in-silico platforms were created and extracted using Compass DataAnalysis Version 4.1 SR 1 (Bruker Daltonik GmbH, Bremen).

3.3.6 Standard operation procedure: metabolite profiling using RP- UHPLC-MS

Analyses were performed on a Waters ACQUITY UltraPerformance LC® system (Waters GmbH, Eschborn, Germany) coupled to a Bruker Daltonik (Bremen, Germany) maXis™ UHR-qToF-MS. Measurements were conducted on a BEH C18 (100 mm x 2.1 mm ID, 1.7 µm) (Waters, Milford, MA). Gradient separation with a total runtime of 10 minutes plus 5 minutes pre-run time (flow rate: 0.4 mL/min, column temperature: 40 °C, A: 100% MilliQ water, 0.1% formic acid, B: 100% ACN, 0.1% formic acid) was performed of 5 µL of each sample in partial loop with 95.0% A and 5% B as starting condition. After 1.12 minutes B was increased to 99.5% within 5.3 minutes and hold for 3.6 minutes until the end of the analysis. MS parameters were as follows: capillary voltage of 4500 V ((+)ESI) / 4000 V ((-)ESI) and end plate offset to -500 V, mass range: m/z 100 – 1500, spectra rate: 2.0 Hz, dry gas: 10 L/min, dry temperature: 200 °C, nebulizer gas: 2 bar, ion energy: 3 eV (ESI+) / -3 eV (ESI-). Further details are given in Table 6.2-5.

3.3.7 Tandem mass spectrometry (RP- UHPLC-(+/-)-ToF-MS/MS)

Selected fecal metabolite extracts represented for each group and all standards (chapter 6.2.1) were analyzed using the standard operation procedure (SOP) method previously described in chapter 3.3.6. All standards were prepared as 20 ppm standard solutions in 20% ACN out of an already existing fridge-stored 1000 ppm standard stock solution. MS parameters were as follows: capillary voltage of 4000 V

and end plate offset to -500 V, mass range: m/z 50 – 1500, dry gas: 10 L/min, dry temperature: 200 °C, nebulizer gas: 2 bar. Collision energies were 10 eV, 20 eV and 40 eV. Metabolites were identified by standards (fragmentation pattern and retention time). MS/MS spectra extraction and raw data processing was applied by using DataAnalysis Version 4.1 (Bruker Daltonik GmbH, Bremen, Germany).

3.3.8 Visualization, software and statistical evaluation

For PCA, the data was UV scaled and performed using SIMCA-P 9.0 (Umetrics, Umea, Sweden). For the heatmaps, the data was normalized by standardization. The heatmaps were created by using the Hierarchical Clustering Explorer 3.5 (Seo and Shneiderman 2002). Therefore, the data was normalized ($(X-m)/\sigma$) and clustered by rows (Euclidean distance). The significance was tested by applying the Kruskal-Nemenyi test for pairwise test of multiple comparisons of mean rank sums in R (Computing 2014) (package: 'PMCMR' version 4.1) (Pohlert 2014). The Mann-Whitney (or Wilcoxon rank sum test) test was performed in RStudio (Version 0.99.489). Boxplots were visualized by Excel (Microsoft Office Professional Plus 2010) and RStudio (Version 0.99.489). Two-sided t-test (heteroscedastic) was performed in Excel (Microsoft Office 2010). The log₂ fold change (log₂ FC) was calculated of the arithmetic mean sums in Microsoft Office Excel 2010.

For the correlations of metabolites and OTUs of month 1, 7 and 12, the data was UV scaled. Correlations were carried out through OPLS-DA in SIMCA-P 13.0.3 (Umetrics, Umeå, Sweden) and visualized as scores scatter plot and loadings plot of highly correlated features among the different datasets. The loadings of the complete dataset were extracted and visualized as loading plots using RStudio (Computing 2014) (Version 0.99.489) For each classification model, CV-ANOVA was applied in order to verify the robustness of each model. Indicators, such as the p-value, the goodness-of-fit $R^2Y(\text{cum})$ and the goodness-of prediction $Q^2(\text{cum})$ were reported.

The EIC of mass signals, the MS/MS spectra and the MS/MS fragment mass lists for the comparison with several databases, as well as for in-silico platforms were created and extracted using Compass DataAnalysis Version 4.1 SR 1 (Bruker Daltonik GmbH, Bremen).

3.4 Results and Discussion

3.4.1 Comparison of exclusively breastfed and formula-fed, respectively and mixed fed infants

In order to compare the metabolite profiles and to detect differences of the mixed feds to the two exclusively fed infant groups over time; a PCA of both ionization modes was performed. Additionally, the metabolite profiles of the mixed fed infants compared to both exclusively fed ones of month 1 and month 3 were considered as well. In the scores scatter plots a characteristic pattern between the three groups was observed over time (Figure 3.4-1, top), as well as in the monthly view (Figure 3.4-1, bottom). In both ionization modes, the scores scatter plots of the PCA revealed a separation between the two exclusively fed groups, whereas the mixed fed were in between and overlap with both exclusively feds.

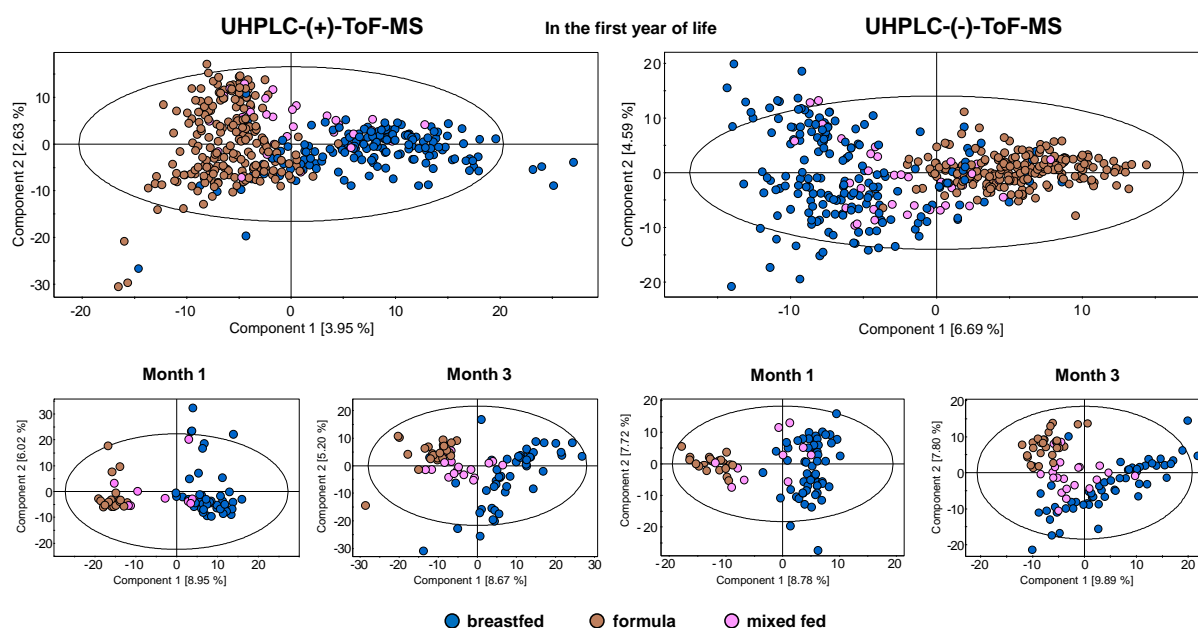


Figure 3.4-1: Unsupervised PCA scores scatter plots comparing exclusively and mixed fed infants.

Comparison of different groups through PCA (UV scaling) of infants exclusively breast fed (blue) or formula-fed (brown) compared to infants mixed fed (pink) over time (top), analyzed in UHPLC-(+)-ToF-MS (left) and UHPLC-(-)-ToF-MS (right). On the bottom PCA scores scatter plots of infants exclusively breast fed (blue) or formula-fed (brown) compared to infants mixed fed (pink) of month 1 (left) and month 3 (right) are displayed.

The loadings (=metabolites) responsible for the pattern in the scores scatter plot were extracted in order to evaluate the differences between the mixed fed infants compared to the two exclusively fed ones. Mostly, the metabolites showed inconsistent and different intensity levels, but no metabolites were found which invariably characterized the mixed fed infants compared to the two exclusively fed infants.

In addition, the infants' microbiota is rather impressionable to environmental exposure, especially to nutrition (Arrieta et al. 2014). Since the influences on the development of the fecal metabolome and microbiome should as low as possible, the mixed fed infants were excluded for all following analyses in this chapter. Doing so, it can be ensured that metabolites, which cannot be referred to either the breastfed group or the formula fed group, falsify the analyses. This allowed a more precise evaluation of the data, since the impact of breast and/or formula feeding with or without probiotics on the infants' fecal metabolome can be investigated more distinctively.

3.4.2 Differences in the fecal metabolome of exclusively fed (breastfed vs. formula-fed) infants

The focus here was laid on the metabolomics perspective of the development of the infant gut microbiome in relation to different feeding, as breast milk or probiotics. For a better evaluation of the data and the metabolite profiles, the exclusively breastfed or exclusively formula-fed will be looked at in detail. This perspective and the homogeneity of the groups were crucial and simplified the comparison between the groups to follow the progress over time, feeding differences and delivery effects.

3.4.2.1 In the first year of life

To get an overview of trends in the data and to evaluate the influence of feeding and the development of the fecal metabolome over time, an unsupervised multivariate data analysis technique (PCA) was performed on fecal samples including the months 1, 3, 5, 7, 9 and 12. The scores scatter plots with the first two generated components of the positive ionization (Figure 3.4-2 A) and the negative ionization mode (Figure 3.4-2 B) showed a clear separation of breastfed infants and formula-fed ones over time (Bazanella et al. 2017). Further, the metabolite dynamics show a convergence of feeding over time, which was more dominant in the (+) ESI-MS metabolite composition, than in (-) ESI-MS.

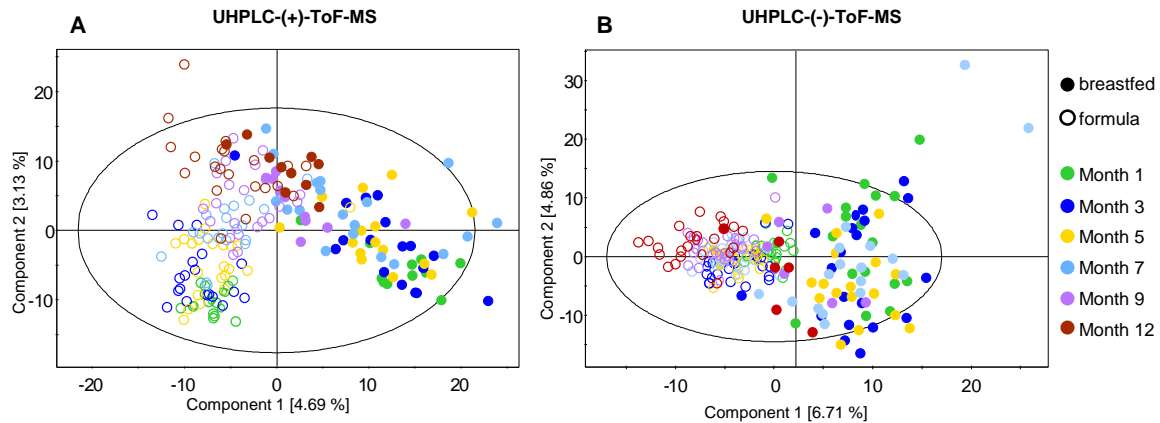


Figure 3.4-2: Unsupervised PCA scores plots of exclusively fed infants over time.

Comparison of fecal samples through PCA (UV scaling), displaying component 1 and 2, of infants either exclusively breast fed (filled circles) or exclusively formula-fed (blank circles) in month 1 (green), month 3 (blue), month 5 (yellow), month 7 (light blue), month 9 (purple) and month 12 (red), analyzed in (A) UHPLC-(+)-ToF-MS and (B) UHPLC-(-)-ToF-MS. Figure A from Bazanella, M., Maier, T. V., Clavel, T., Lagkouvardos, I., Lucio, M., Maldonado-Gómez, M. X., Autran, C., Walter, J., Bode, L., Schmitt-Kopplin, P., Haller, D.: Randomized controlled trial on the impact of early-life intervention with bifidobacteria on the healthy infant fecal microbiota and metabolome. *Am J Clin Nutr.* (2017), 106(5):1274-1286. Reprinted and adapted from (Bazanella et al. 2017) by permission of Oxford University Press. Copyright (2017) American Society for Nutrition.

In order to find metabolites, which were responsible for the feeding differences and the time trend in both ionization modes, a PLS-DA was applied. According to their variable important projection (VIP) values obtained by PLS-DA, the significant features among the different feeding types and months were extracted. The importance of the significant features is represented by a high VIP value. With a combination of the highest VIP values and results of further statistical tests, such as the two-sided Student's t-test, features were selected as changing significantly over time and through different feeding. They were visualized in a heatmap, illustrated in Figure 3.4-3. Detailed information on differences over time in both ionization modes are listed in Table 6.2-8 (breastfed, (+) ESI), Table 6.2-9 (formula-fed, (+) ESI), Table 6.2-10 (breastfed, (-) ESI) and Table 6.2-11 (formula-fed, (-) ESI). The tables include further information on retention time, compound name, if possible, VIP score of PLS-DA analysis and the respective p-values, obtained with Student's t-test (heteroscedastic)

In total, this analysis revealed 65 features in (-) ESI-MS and 85 features in (+) ESI-MS to be significantly different between breastfed and formula-fed infants. Compared to the breastfed group, several significantly increased features for the formula-fed group ((-) ESI: n=49, (+) ESI: n= 63) were observed in both ionization modes. The level of significantly altered metabolites in the breastfed group was comparably low ((-) ESI: n=17, (+) ESI: n=22). Chow et al. achieved similar results investigating the

impact of breast- and formula-feeding, before and during in vitro batch culture fermentation. They detected less metabolites significantly higher in breastfed infants, than in formula fed ones as well (Chow et al. 2014).

Further, the change of significant metabolites can be followed from month 1 to month 12, which showed the disappearance of these differences over time. The intensity decreased for all of them represented the change in feeding in detail and can be observed as well over time in the previously displayed PCA scores plot. Through the evaluation of the significant metabolites, many metabolites were found to be uniquely appeared in formula-fed infants. On the contrary, there were no metabolites, which exclusively appear only in breastfed infants.

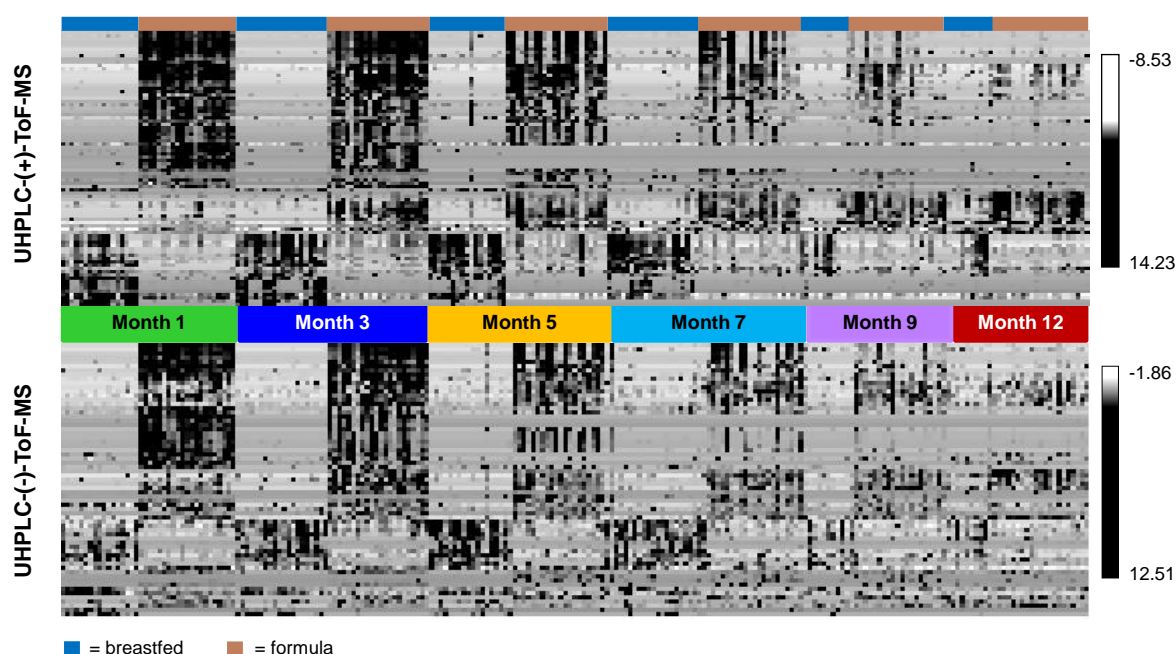


Figure 3.4-3: Heatmap of the most abundant and discriminating metabolites over time.

Heatmap of most abundant and highly discriminative mass signals (top: 85 variables, bottom: 65 variables) between exclusively breast fed (blue) and exclusively formula-fed (brown) infants (n=223), analyzed by UHPLC-(+)-ToF-MS (top) and UHPLC(-)-ToF-MS (bottom). For more details on the metabolites, which are responsible for the discrimination, the significant metabolites for the breastfed are listed in Table 6.2-8 (UHPLC-(+)-ToF-MS) and Table 6.2-10 (UHPLC(-)-ToF-MS) and the formula-fed (Table 6.2-9 (UHPLC-(+)-ToF-MS and Table 6.2-11 (UHPLC(-)-ToF-MS) group for both ionization modes are listed in the appendix.

The heatmap confirmed the results, which were already seen in the scores scatter plots of the PCA in Figure 3.4-2, namely a decrease in differentiating features between breastfed and formula-fed infants from month 1 to month 12. These differences were observed more clearly in the positive, than the negative ionization mode. In order to identify or even to classify the significant features, MS/MS

experiments were performed. The obtained MS/MS spectra were manually compared against spectral databases, such as Metlin and HMDB. Several mass signals were identified with the respective chemical standard and retention time matching as well. The information about the mass signals of which MS/MS experiments were performed are tagged in Table 6.2-8 (breastfed, (+) ESI), Table 6.2-9 (formula-fed, (+) ESI), Table 6.2-10 (breastfed, (-) ESI) and Table 6.2-11 (formula-fed, (-) ESI). The respective MS/MS spectra for both ionization modes of identified, as well as still unknown mass signals are shown in Chapter 5.2.1. In positive ionization mode, none of the mass signals, significantly altered in the breastfed or formula-fed group were identified. The respective mass spectra are illustrated in Figure 5.2-6 (formula-fed) and Figure 5.2-7 (breastfed). However, based on the MS/MS spectra and the comparison with similar fragmentation patterns listed in spectral databases, one mass signal was classified as prostaglandin (MS/MS spectrum in Figure 5.2-6 E).

In negative ionization mode, several mass signals increased in the breastfed infants over time were identified, including bile acids (e.g. cyprinolsulfate, sulfocholic acid; MS/MS spectra in Figure 5.2-1 A and B) and fatty acids (e.g. eicosatetraenoic acid; MS/MS spectrum in Figure 5.2-4 B), as well as hydroxyphenyllactic acid (MS/MS spectrum in Figure 5.2-4 C). In the formula-fed group, mass signals were identified as glucuronides of vitamin E intermediates (e.g. tocotrienol glucuronide, tocopherol glucuronide; MS/MS spectra in Figure 3.4-11 A and B), bile acids (e.g. glycochenodeoxycholic acid; MS/MS spectrum in Figure 5.2-3 B), oxylipins (e.g. dihydroxyoleic acid; MS/MS spectrum in Figure 5.2-5 A) and dicarboxylic acids, such as dodecenedioic acid (MS/MS spectrum in Figure 5.2-5 B). The importance of all identified metabolites is discussed in detail in the following chapters. The mass spectra of unidentified features increased in formula-fed infants are illustrated in Figure 5.2-8 and Figure 5.2-9.

Additionally, core metabolites that were present in 95% of all samples, independent of feeding or age were of interest. Therefore, metabolites were evaluated by applying a 5% filter to exclude all mass signals, which appear less than 11 times in $n = 224$ infants. This resulted in 67 of 710 (negative) and in 85 of 2040 (positive) mass signals, which further were filtered by constant intensity levels with a $\pm 15\%$ standard deviation over time. After filtration, 16 mass signals in the negative ionization mode and 15 mass signals in the positive ionization mode were detected with constant intensity levels over time as shown in Table 3.4-1. Molecular formula and compound annotation of the mass signals were assigned by running the MassTRIX webserver with an error of 0.005 Da. It was observed that

3. Impact of breast-feeding and bifidobacteria-supplemented formula

octadecenoic acid, hydroxyoctadecanoic acid and cholic acid were the most abundant and most consistent metabolites over time.

Table 3.4-1: Core metabolites over time in all infants independent from feeding.

Fifteen ((+) ESI) or sixteen ((-) ESI) core metabolites with constant intensity levels over time in all infants independent from feeding, calculated as arithmetic mean sums of month 1, 3, 5, 7, 9 and 12. Table contains averaged experimental mass, retention time (in minutes), compound name if possible, molecular formula from Genedata Refiner MS, as well as p-values showing the significance according to diet comparison, calculated with the two-sided heteroscedastic Student's t-test.

Mass (avg.)	Retention time [min]	Molecular Formula	Annotation	Mean Month 1	Mean Month 3	Mean Month 5	Mean Month 7	Mean Month 9	Mean Month 12
(+ ESI)									
283.2685	6.79	C18H34O2	Octadecenoic acid	3.97E+06	3.98E+06	4.58E+06	3.31E+06	3.57E+06	2.91E+06
425.2923	7.29	C23H40O4	no metabolite found	1.70E+05	1.86E+05	1.84E+05	1.94E+05	1.99E+05	1.96E+05
271.2760	7.52	C16H34	no metabolite found	5.25E+04	6.07E+04	4.95E+04	5.19E+04	4.89E+04	6.55E+04
420.3348	7.29	C20H34O8	no metabolite found	4.95E+04	5.37E+04	5.11E+04	5.42E+04	5.63E+04	6.43E+04
284.2991	8.23	C18H34O	no metabolite found	8.94E+05	1.26E+06	9.74E+05	1.38E+06	1.34E+06	1.44E+06
790.3831	5.23	C37H49N7O9S	no metabolite found	4.15E+04	4.21E+04	3.46E+04	4.28E+04	4.34E+04	3.46E+04
465.3778	7.29	C30H50O2	no metabolite found	4.65E+03	4.33E+03	6.13E+03	5.15E+03	5.16E+03	4.44E+03
171.1398	7.36	C9H18	no metabolite found	4.66E+04	4.80E+04	4.81E+04	4.70E+04	4.93E+04	4.81E+04
151.0366	0.65	C6H8O3	no metabolite found	3.81E+04	4.19E+04	4.66E+04	5.13E+04	5.56E+04	5.97E+04
251.0579	7.00	C2H8O7P2	no metabolite found	2.47E+04	2.49E+04	2.62E+04	3.46E+04	3.14E+04	3.13E+04
387.1846	5.23	C21H26O4	no metabolite found	1.32E+05	1.34E+05	1.19E+05	1.41E+05	1.39E+05	1.34E+05
540.4487	7.58	C35H54O3	no metabolite found	1.54E+04	1.31E+04	1.12E+04	1.12E+04	1.30E+04	1.04E+04
496.4204	7.59	C33H50O2	no metabolite found	1.46E+04	1.13E+04	9.50E+03	1.08E+04	1.29E+04	9.95E+03
128.0280	0.66	C2H6OS2	no metabolite found	4.69E+04	5.29E+04	6.03E+04	6.61E+04	7.13E+04	7.49E+04
526.4330	7.28	C31H56O5	no metabolite found	7.02E+03	7.17E+03	8.28E+03	9.67E+03	9.89E+03	8.04E+03
(-) ESI									
293.1783	6.81	C14H30O4S	no metabolite found	2.29E+04	2.44E+04	2.59E+04	2.87E+04	2.57E+04	3.09E+04
483.3287	5.08	C34H44O2	no metabolite found	8.04E+04	6.82E+04	7.60E+04	7.39E+04	6.31E+04	6.81E+04
299.2621	6.76	C18H36O3	Hydroxyoctadecanoic acid	3.84E+06	3.40E+06	3.75E+06	2.93E+06	3.27E+06	2.91E+06
297.1516	5.78	C19H22O3	no metabolite found	1.53E+04	1.20E+04	1.23E+04	1.31E+04	1.57E+04	1.81E+04
453.2477	5.10	C26H32O8	no metabolite found	1.16E+06	1.83E+06	1.93E+06	1.83E+06	1.67E+06	1.20E+06
337.2043	7.49	C20H26N4O	no metabolite found	1.88E+04	2.56E+04	1.92E+04	1.84E+04	1.59E+04	2.43E+04
405.2655	4.82	C24H38O5	no metabolite found	1.64E+05	2.24E+05	2.01E+05	2.62E+05	2.77E+05	2.33E+05
481.3132	4.74	C28H44N4O4	no metabolite found	1.07E+04	1.23E+04	1.29E+04	1.89E+04	1.45E+04	1.79E+04
399.1859	6.75	C23H28O6	no metabolite found	1.24E+05	1.04E+05	1.15E+05	1.00E+05	1.20E+05	1.17E+05
437.2926	5.83	C21H43O7P	no metabolite found	6.33E+05	6.33E+05	6.10E+05	5.95E+05	6.78E+05	8.11E+05
431.1719	5.22	C23H28O8	no metabolite found	1.97E+04	1.79E+04	1.34E+04	1.55E+04	1.84E+04	1.70E+04
478.2927	6.71	C23H46NO7P	no metabolite found	3.82E+04	3.76E+04	3.00E+04	3.56E+04	4.48E+04	2.99E+04
379.1581	7.39	C20H28O5S	no metabolite found	8.14E+03	7.18E+03	6.55E+03	5.69E+03	7.30E+03	9.41E+03
621.5046	6.76	C41H68O5	no metabolite found	4.29E+04	4.02E+04	4.23E+04	3.93E+04	4.38E+04	4.78E+04
481.3111	5.97	C28H44N4O4	no metabolite found	8.89E+04	1.21E+05	1.08E+05	1.09E+05	9.01E+04	7.49E+04
407.2818	5.16	C24H40O5	Cholic acid	6.91E+05	5.79E+05	6.31E+05	6.47E+05	6.18E+05	5.27E+05

Through this evaluation, differences in feeding over time and several core metabolites not to be affected by feeding were observed. Metabolites altered by either breast milk or formula were prevalent, wherefore possible metabolite changes due to probiotics might get lost. Therefore, monthly analysis of the fecal samples was required to detect metabolites which were influenced by probiotics in the infant formula. This could not be achieved by investigating the development of the metabolite profile over time. Thus, the fecal samples of exclusively breastfed and placebo and interventional formula-fed infants, respectively, were evaluated month by month in the next chapter.

3.4.2.2 Breastfed vs. interventional formula fed (F+) vs. placebo formula-fed (F-) by the month

In order to evaluate the impact of breast feeding and both formulas on the infant's fecal metabolome, the data was analyzed month by month. Here, month 1, 3, 5, 7, 9 and 12 of breastfed (B), interventional formula fed (F+) and placebo formula fed (F-) infants were considered for the analyses. Here, the focus was to detect monthly predominant and discriminant metabolites in fecal samples of breastfed and formula-fed infants in general. These findings then will be discussed in detail in the following chapters. To achieve this, a PCA of each single month of the (+) ESI (Figure 3.4-4) and (-) ESI (Figure 3.4-5) mode was applied to get an overview of the metabolite profile by month.

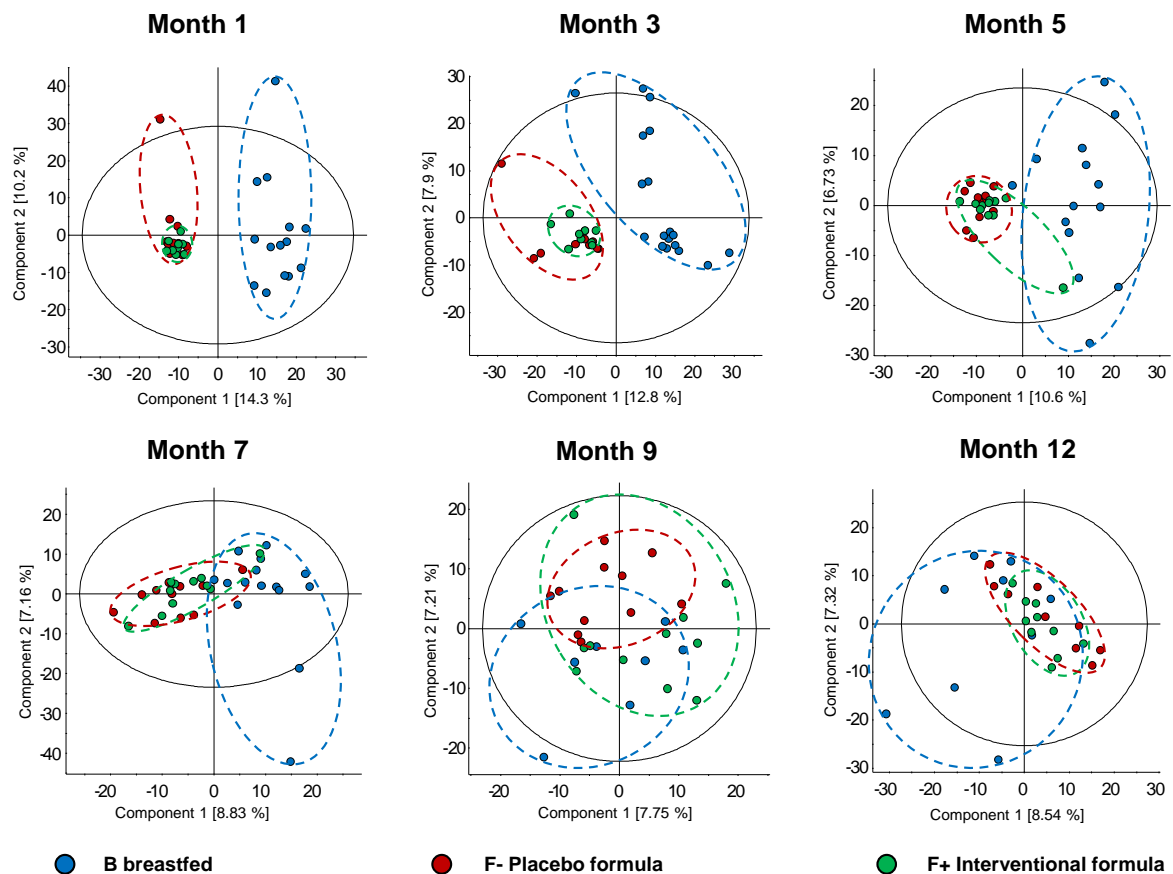


Figure 3.4-4: Unsupervised PCA scores plots of exclusively fed infants month by month.

Comparison of fecal samples of exclusively fed infants month by month (month 1, 3, 5, 7, 9 and 12) through PCA (UV scaling), displaying component 1 and 2, differentiating in exclusively breast fed (blue), interventional formula-fed (green, with probiotics) or placebo formula-fed (red, without probiotics), analyzed in UHPLC-(+)-ToF-MS.

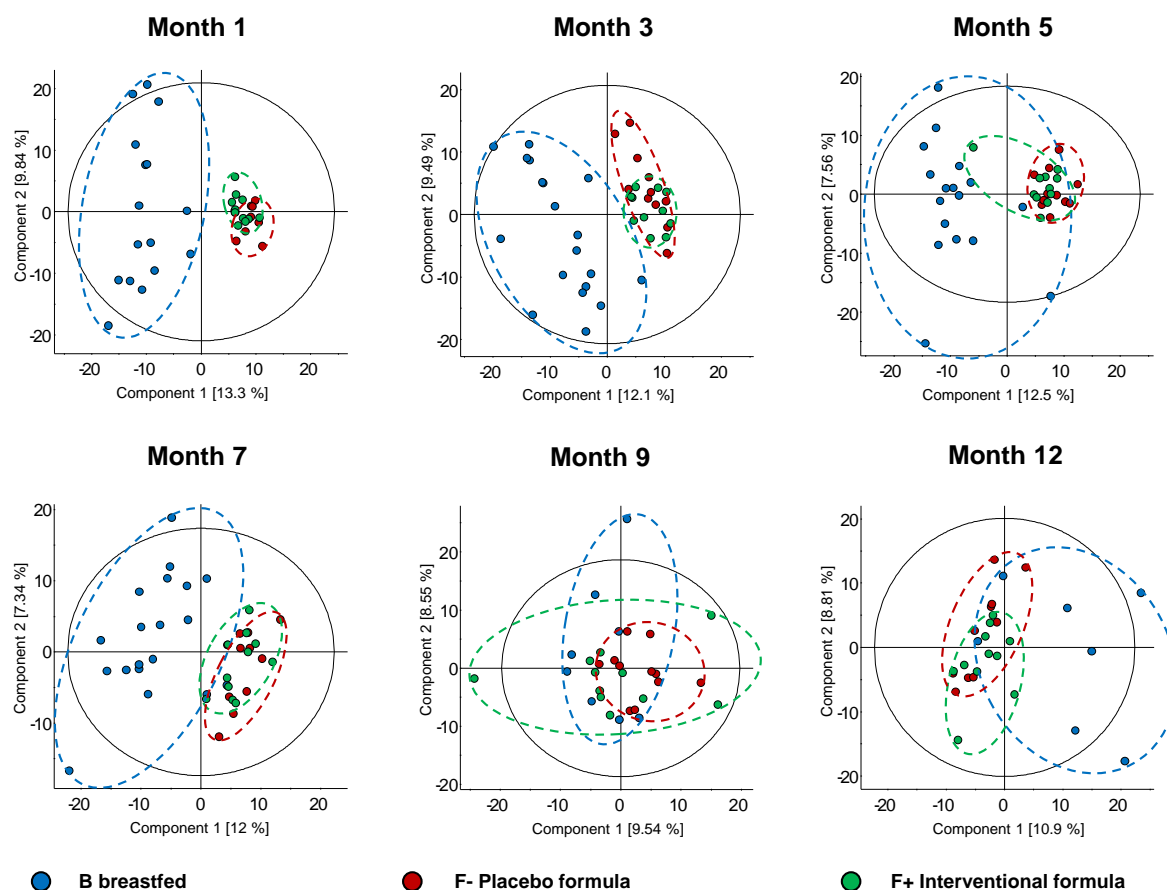


Figure 3.4-5: Unsupervised PCA scores plots of exclusively fed infants month by month.

Comparison of fecal samples of exclusively fed infants month by month (month 1, 3, 5, 7, 9 and 12) through PCA (UV scaling), displaying component 1 and 2, differentiating in exclusively breast fed (blue), interventional formula-fed (green, with probiotics) or placebo formula-fed (red, without probiotics), analyzed in UHPLC(-)-ToF-MS.

As already seen in the metabolite profile over time in Figure 3.4-2, a clear separation between breastfed and formula-fed infants was found for month 1 to month 7 in both ionization modes, which converged over time. Further, in month 1 a slight separation between the two formula-fed groups was observed. Additionally, the fecal samples of the breastfed infants in general showed more diverse individual profiles until month 12, than the formula-fed ones, whose individual metabolite profiles were similar and more clustered up to month 9. This indicated that the impact of formula was comparable within the formula groups and the inter-individual changes were not as high as effected through breast milk.

Within the overall and monthly analyses several metabolites emerged as strongly influenced by breastfeeding or formula-feeding. To identify the discriminating metabolites among the three groups (B, F+ and F-) for each month, a PLS-DA was applied. For each month, a model was created comparing always breastfed, interventional formula fed and the placebo formula fed infants. The obtained

significant mass signals given in VIP values were extracted and further evaluated as discussed in the following chapters. In month 1, a few mass signals were found to be increased by either interventional or placebo formula compared to breastfeeding, which among others showed the highest VIP values and will be examined in detail in chapter 3.4.3.

3.4.2.3 Pathway analysis - affected by nutrition - KEGG metabolic pathway analysis

The metabolism of infants is strongly influenced by nutrition, such as breastfeeding or formula. Chow et al. demonstrated the impact of breastfeeding and formula on the fecal metabolome of healthy infants through metabolic pathways classification. They illustrated not only super- and sub-pathways, including responsible metabolites for the discrimination of the metabolite profiles, but also that the same super-pathways (e.g. carbohydrate metabolism, lipid metabolism or the metabolism of cofactors and vitamins) are affected differently by formula and breastfeeding. Thus, they revealed metabolites of the bile acid metabolism, for instance 7-ketolithocholic acid and taurochenodeoxycholic acid sulfate, to be significantly higher in formula-fed infants, or the breastfed infants, respectively (Chow et al. 2014).

It is well known that a high amount of detected features obtained through metabolomics analyses remain unknown and even less are listed in databases (Bowen and Northen 2010). In order to get an overview of the metabolomics datasets, the mass signals were searched against the MassTRIX webserver with an error of 0.005 Da. Here, the data matrix showed 67%/50% ((+) ESI/(-) ESI) unknown features and 26%/33% annotated by MassTRIX, whereas 7%/14% are listed in the KEGG pathway database. Hereto, MassTRIX allowed assigning metabolites to KEGG IDs and the analogous sub-pathway, including e.g. the primary bile acid biosynthesis or the fatty acid biosynthesis. Accordingly, metabolites were classified to a super-pathway, based on the metabolite annotations obtained by MassTRIX. Taking into account that several annotated metabolites are involved in various sub-pathways of a super-pathway, the super-pathways were assigned and further considered for the pathway classification. In order to investigate the impact of exclusive breast-feeding and formula-feeding on a pathway-related level, the VIPs – responsible for the discrimination - obtained through the monthly PLS-DA analysis in chapter 3.4.2.2, were taken into account. Therefore, the metabolites of each month with a VIP > 1 were considered to calculate the amount of assigned metabolites classified to a super-pathway of the KEGG pathway database (e.g. lipid metabolism, carbohydrate metabolism or

the metabolism of cofactors and vitamins). It was revealed that breast- and formula feeding, strongly affect pathways of the lipid metabolism (Figure 3.4-6).

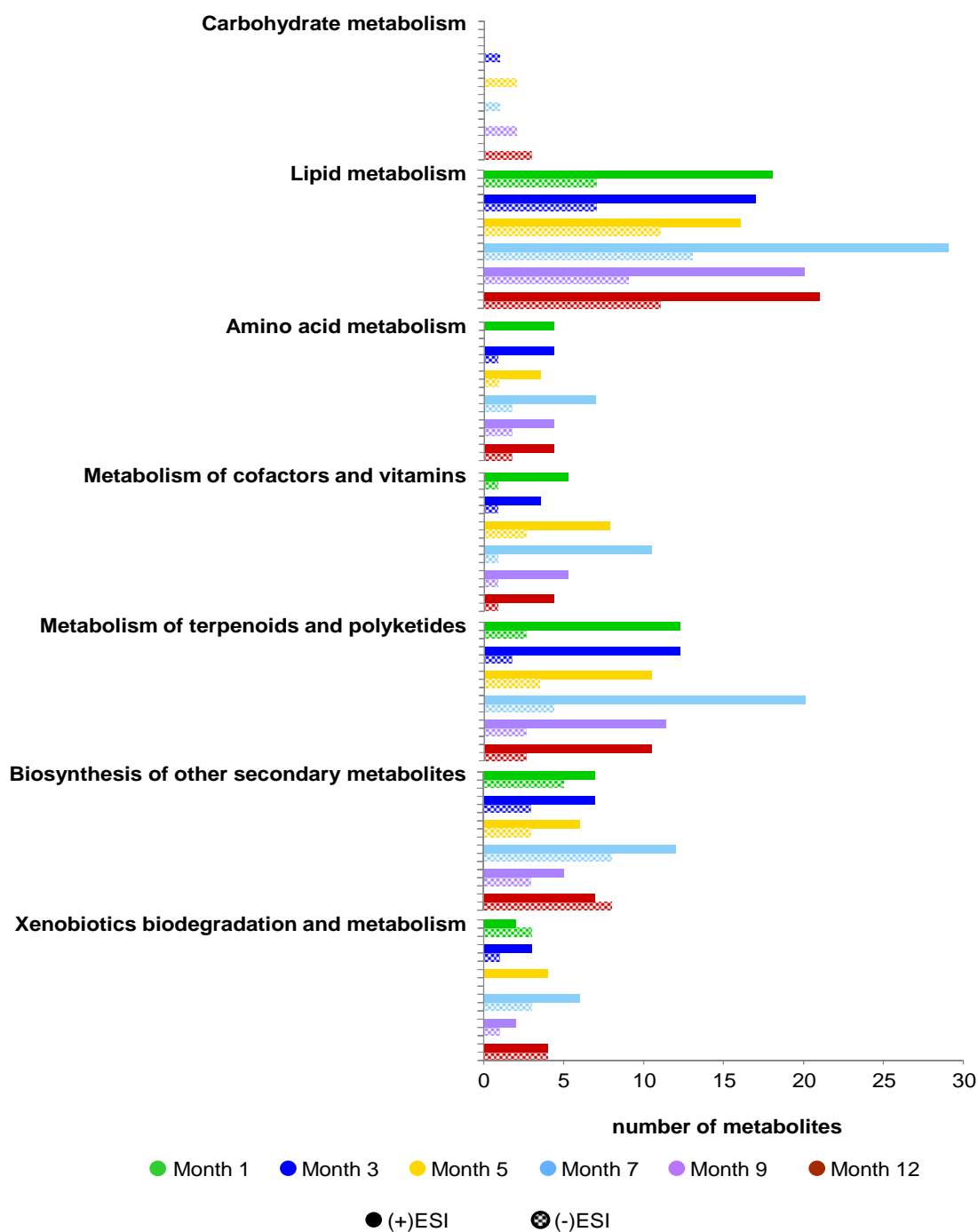


Figure 3.4-6: Significantly changed main pathways of KEGG metabolic pathways by month.

Number of significant main pathways of the KEGG pathway database assigned through the MassTRIX webserver, calculated based on the monthly PLS-DA classification models of the UHPLC-(+)-ToF-MS mode (filled) and UHPLC-(-)-ToF-MS mode (patterned), impacted through breastfeeding and formula in general.

Furthermore, it was of interest to evaluate which metabolites, in particular in the lipid metabolism, were affected differently through formula or breastfeeding, which is discussed in the next chapter.

3.4.2.4 Impact on the bile acid metabolism through breast- and formula feeding

Pathway classification analysis revealed different pathways to be altered by breast milk or formula. Especially, the lipid metabolism appeared to be highly impacted by breast- and formula feeding. Also, in the PLS-DA of the negative ionization mode (Chapter 3.4.2.1), a few bile acids were observed to be affected by breast milk or formula. Those bile acids turned out to be involved in the primary bile acid biosynthesis, a sub-pathway of the lipid metabolism. In order to find if further bile acids and sterol lipid-like compounds of the lipid metabolism were differently altered by feeding, metabolites were classified to their sub-pathway, they are involved in, using KEGG CIDs obtained by MasSTRIX. The obtained KEGG CIDs allowed assigning the metabolites to their sub-pathways. Accordingly, metabolites found in the data matrix were matched for mass signals, which appeared to be significantly changed by breast milk or formula, according to the PLS-DA analyses described in chapter 3.4.2.2.. Metabolites of the primary bile acid biosynthesis and bile acid structure related compounds were predominantly affected through the different feedings, which lead to a series of targeted bile acid analysis by UHPLC-ToF-MS in negative ionization mode, including MS/MS identification experiments

In general, bile acids are sterols, which are distinguished into primary (CA and CDCA) and secondary bile acids (deoxycholic acid and lithocholic acid). Microbes in the intestine are not only involved in the conversion of primary bile acids into secondary bile acids, but also influence the levels and types of bile acids produced and excreted in feces (Hammons et al. 1988). Primary bile acids originate from the conversion of cholesterol in the liver, followed by the conjugation by either taurine or glycine for the secretion into the bile (Gerard 2013, Aw and Fukuda 2015). The daily synthesis of bile acids in the liver is about 200 – 600 mg, of which almost the same amount is excreted in feces (Chiang 2013).

Bile acids undergo bacterial metabolism in the human gut and are converted (e.g. deconjugation, esterification and desulfatation). Through these processes, the secondary bile acids are formed, which result in more than 20 different secondary bile acids in adult human feces (Gérard, 2014). These bacterial conversions appear very early in life, wherefore secondary bile acids were already identified in meconium. Species, such as *Bacteroides*, *Eubacterium*, *Clostridium* and *Escherichia coli* are mainly

involved generating secondary bile acids (Xie et al. 2013, Aw and Fukuda 2015). Further bacteria involved in the bile acid metabolism are: *Bifidobacterium*, *Ruminococcus* and *Lactobacillus* (Gerard 2013).

Bile acids are important for digestion and nutrition. It was shown that diet impacts bile acid metabolism in infants (Hammons et al. 1988). Further, bile acids play an important role, especially in the modulation of lipids, glucose and the energy metabolism (Chiang 2013), whereas their main task entail to support the absorption of dietary lipids and lipid-soluble nutrients (Gerard 2013). Already in the 1980s and 1990s, several articles were published about the complexity of bile acids and the impact of nutrition on the bile acid metabolism, particularly infant nutrition (Hammons et al. 1988, Midtvedt and Midtvedt 1993, Jonsson et al. 1995).

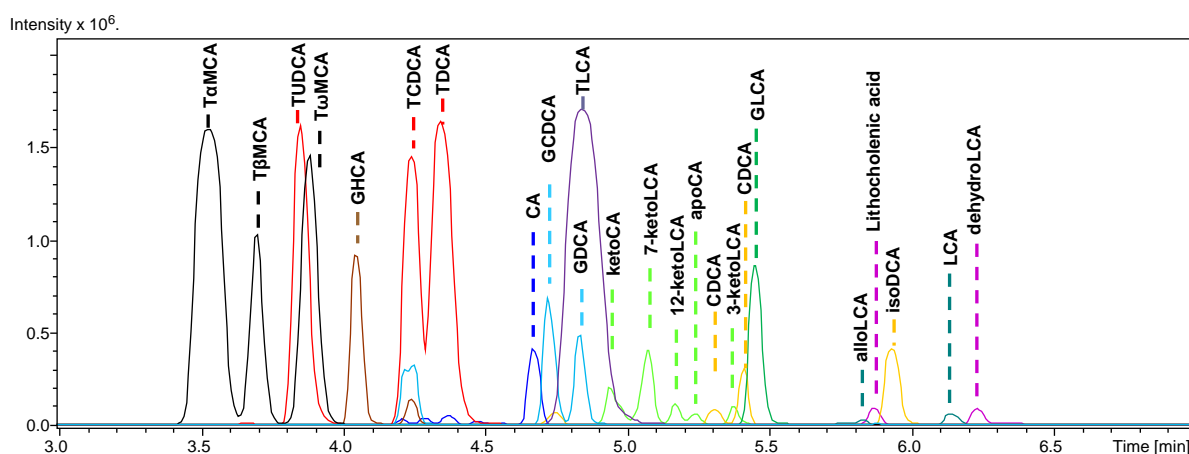
For targeted bile acid analysis, several representative samples of each feeding group and month were measured again using the SOP for RP-LC coupled to a ToF-MS (Chapter 3.3.6), were processed and evaluated as previously described. The mass signals of the bile acids were extracted and their patterns compared to previously obtained results. The bile acid patterns of both analyses were nearly identical, wherefore the SOP method was used for the MS/MS experiments (chapter 3.3.7) to identify affected bile acids due to breastfeeding or formula.

Some pre-selected bile acids detected in the data matrix of fecal samples of both, breastfed and formula-fed infant were analyzed by MS/MS experiments, varying in collision energies from 10 eV to 20 eV and 40 eV. A multitude of various isomeric bile acids exist, wherefore its identification can be difficult. In order to identify the bile acids more precise, a standard mixture of commercially available bile acids as listed in Table 3.4-2 was analyzed by the SOP method for UHPLC-ToF-MS in negative ionization mode (Figure 3.4-7), including MS/MS experiments of each single bile acid (Table 3.4-2) with collision energies of 10, 20 and 40 eV. Without prior chromatographic separation, the multitude of various isomeric bile acids would be indistinguishable. This method allowed identifying the bile acids not only by its fragmentation pattern, but also by retention time. Here, for the most part, the chromatographic separation was sufficient to separate isomeric bile acids as shown below in Figure 3.4-7.

Table 3.4-2: List of bile acid analyzed by UHPLC(-)-ToF-MS.

Table contains m/z [M-H], compound name, abbreviation and retention time in minutes [min]. Colors are according to the corresponding extracted ion chromatograms in Figure 3.4-7.

[M-H]	Compound name	Abbr.	retention time [min]	[M-H]	Compound name	Abbr.	retention time [min]
514.2844	α -Tauromuricholic acid	T α MCA	3.5	448.3069	Glycochenodeoxycholic acid	GCDCA	4.7
514.2844	β -Tauromuricholic acid	T β MCA	3.6	448.3069	Glycodeoxycholic acid	GDCA	4.8
514.2844	ω -Tauromuricholic acid	T ω MCA	3.7	482.2946	Taurolithocholic acid	TLCA	4.8
498.2895	Tauroursodeoxycholic acid	TUDCA	3.9	389.2697	5 α -Cholanolic Acid-3 α -ol-6-one	ketoCA	4.9
514.2844	Taurocholic acid	TCA	3.9	389.2697	3 α -Hydroxy-7 Ketolithocholic Acid	7-ketoLCA	5.0
464.3018	Glycohyocholic acid	GHCA	4.1	389.2697	3 α -Hydroxy-12 Ketolithocholic Acid	12-ketoLCA	5.1
407.2803	ω -Muricholic acid	ω MCA	4.2	389.2697	Apocholic acid	apoCA	5.2
448.3069	Glycohyodeoxycholic acid	GHDCa	4.2	391.2854	Chenodeoxycholic acid	CDCA	5.3
464.3018	Glycocholic acid	GCA	4.2	389.2697	3-Ketolithocholic acid	3-ketoLCA	5.4
498.2895	Taurochenodeoxycholic acid	TCDCa	4.2	391.2854	Deoxycholic acid	DCA	5.4
407.2803	α -Muricholic acid	α MCA	4.3	432.3119	Glycolithocholic acid	GLCA	5.4
407.2803	β -Muricholic acid	β MCA	4.3	375.2905	Allolithocholic acid	alloLCA	5.8
448.3069	Glycoursodeoxycholic acid	GUDCA	4.3	375.2905	Isolithocholic acid	isoLCA	5.8
498.2895	Taurodeoxycholic acid	TDCA	4.4	373.2748	Lithocholenic acid	-	5.9
391.2854	Hyodeoxycholic acid	HDCA	5.7	391.2854	Isodeoxycholic acid	isoDCA	5.9
391.2854	Ursodeoxycholic acid	UDCA	4.7	375.2905	Lithocholic acid	LCA	6.1
407.2803	Cholic acid	CA	4.7	373.2748	Dehydrolithocholic acid	dehydrLCA	6.2

**Figure 3.4-7: Extracted Ion Chromatogram of bile acids.**

EIC of 34 bile acids standard solution (25 ppm) analyzed by UHPLC(-)-ToF-MS analysis of 34 bile EIC were extracted with an error of ± 0.01 Da, Gaussian chromatogram smoothing, width: 0.5 [s], 1 cycle. List of all 34 bile acids with their corresponding [M-H] mass and retention time and the according color used in the EIC chromatogram are listed in Table 3.4-2.

The experimental chromatograms, the mass spectra and the retention time of the fecal bile acids in the samples were compared against the corresponding chromatograms and mass spectra obtained through the analysis of the chemical standard solutions under the same conditions. Thus, the mostly clear separation of isomeric bile acids allowed the conclusive identification of four bile acids to be affected by breast milk and/or formula, namely CA (MS/MS spectrum in Figure 5.2-2, A), CDCA (MS/MS spectrum in Figure 5.2-2, B), GCA (MS/MS spectrum in Figure 5.2-3, A) and GCDCA (MS/MS spectrum in Figure 5.2-3, B) from the primary and secondary bile acids biosynthesis, as schematically illustrated in Figure

3. Impact of breast-feeding and bifidobacteria-supplemented formula

3.4-8. Further, two more bile acids, cyprinolsulfate (MS/MS spectrum in Figure 5.2-1, A) and sulfocholic acid (MS/MS spectrum in Figure 5.2-1, B) were detected as significantly associated with the breastfed infants over time.

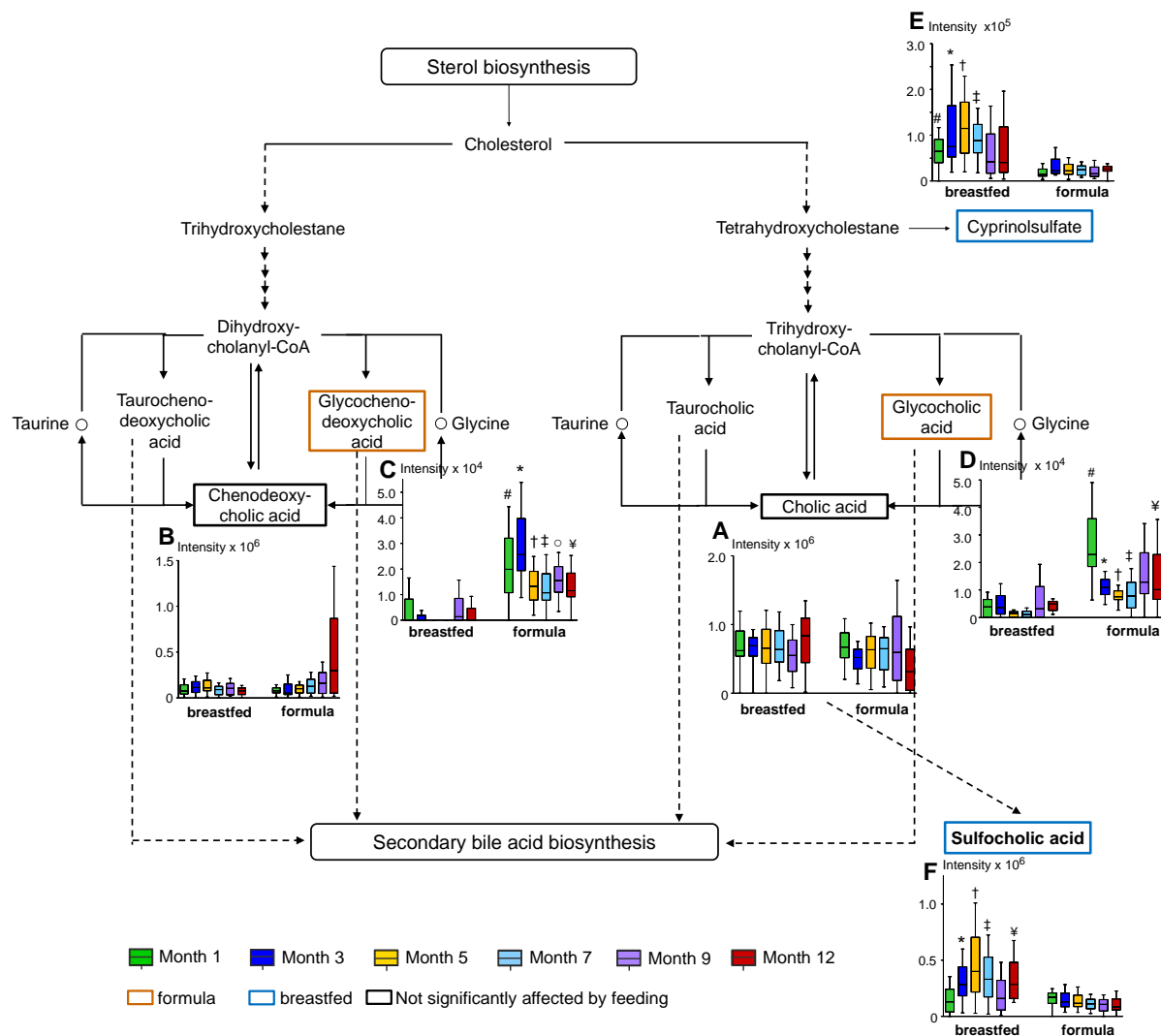


Figure 3.4-8: Schematic overview of the primary bile acid biosynthesis adapted from KEGG pathway (Kanehisa and Goto 2000).

Bile acid patterns of cholic acid and chenodeoxycholic acid, glycochenodeoxycholic acid and glycocholic acid, as well as Cyprinolsulfate and sulfocholic acid altered in breastfed (blue frame) and formula-fed (brown frame) infants, analyzed in (-)-ToF-MS mode. A: Cholic acid; B: Chenodeoxycholic acid. C26 glycine-conjugated bile acid patterns of (C) glycochenodeoxycholic acid and (D) glycocholic acid. C: # p-value = 8.766E-05; * p-value = 1.715E-07; † p-value = 2.481E-06; ‡ p-value = 2.374E-06; ○ p-value = 0.002756; ¥ p-value = 0.000983; D: # p-value = 7.258E-05; * p-value = 0.000201; † p-value = 5.164E-06; ‡ p-value = 0.0003769; ○ p-value = 0.05788; ¥ p-value = 0.02661. Sulfated bile acids in breastfed and formula-fed infants; E: Cyprinolsulfate; F: Sulfocholic acid. E: # p-value = 6.925E-05; * p-value = 1.277E-05; † p-value = 4.94E-06; ‡ p-value = 5.44E-07; ○ p-value = 0.06994; F: * p-value = 0.001851; † p-value = 0.0002354; ‡ p-value = 4.504E-05; ¥ p-value = 0.001508 (Mann-Whitney-Test - R Studio Version 0.98.1091). P-values are always in relation to the same month of the different feedings. Further details are given in Table 6.2-12.

In addition, CA and CDCA appeared as the most abundant bile acids detected over time. CA showed a more or less consistent level in both groups and CDCA showed consistent patterns in the breastfed infants over time. In the formula-fed ones, the intensity level of CDCA was increasing up to month 12. Additionally, the glycine-conjugated bile acids (GCDCA and GCA) were increased in the formula-fed infants over time, whereas the sulfated bile acids (cyprinolsulfate and sulfocholic acid) were erratically increased and widely spread in breastfed infants over time, while the pattern in the formula-fed ones was comparably low and rather consistent.

Cyprinolsulfate is an intermediate of the bile acid biosynthesis and has not yet been associated to infants fed with breast milk. It is known that the intestinal microflora is involved in the excretion of bile salts into feces. Through the sulfation, the solubility of bile acids increases. This ensures the decreased absorption in the intestine and promotes the excretion into feces (Eyssen et al. 1985, Alnouti 2009). In addition, sulfation is deemed to be an important step in detoxification of bile acids, whereas sulfated bile acids are less toxic than the unsulfated ones (Alnouti 2009). Concerning this, our results hinted that through breastfeeding the sulfation of bile acids is more stimulated, than through formula-feeding. This further lead to the assumption that breastfeeding had more impact of the detoxification of bile acids, than formula had and therefore showed higher levels in the fecal samples.

Other sulfated bile acids were already studied. In 1994, for example Wahlen et al. investigated the developmental pattern of urinary bile acid excretion in infants fed with different formula compared to breastfed ones. They observed that sulfated bile acids and the glycine-conjugates were not significantly different in the urine samples of all feeding groups (breast milk, cow's milk formula and soy formula) (Wahlen and Strandvik 1994).

Moreover, 5β -cholanolic acid- 7α -ol-3-one (also known as 3-Lithocholic acid) and 7-Ketolithocholic acid or 5α -Cholanolic acid- 3α -ol-6-one was partially significantly higher in formula fed infants, as presented in Figure 3.4-9. 7-Ketolithocholic acid or 5α -Cholanolic acid- 3α -ol-6-one could not be assigned clearly and even the experimental MS/MS spectra did not give any indication of one of these compounds. Currently, 7-ketolithocholic acid is predicted to be a major intermediate in the conversion of CDCA to UDCA in the intestine (Cao et al. 2011).

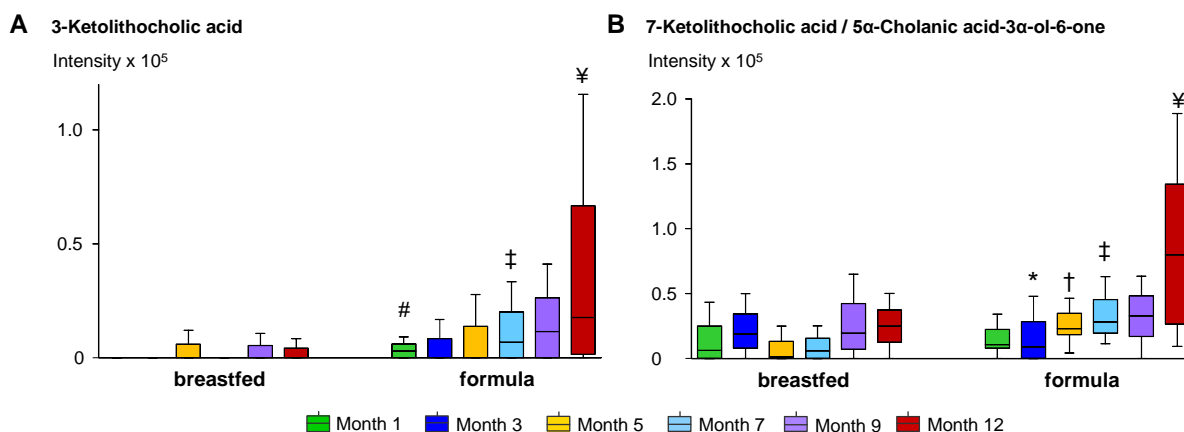


Figure 3.4-9: C24 bile acids changed over time in exclusively fed infants.

Bile acid profiles of C24 bile acids significantly increased in formula-fed infants over time, analyzed in (-)-ToF-MS mode. A: 3-Ketolithocholic acid; # p-value = 0.002784; ‡ p-value = 0.0007055; ¥ p-value = 0.02361; and B: 7-Ketolithocholic acid / 5 α -Cholanic acid-3 α -ol-6-one; B: * p-value = 0.02549; † p-value = 2.794E-05; ‡ p-value = 6.738E-06; ¥ p-value = 0.02787 (Mann-Whitney-Test). P-values are always in relation to the same month of the different feedings. Further details are listed in Table 6.2-13.

In 1995, Jönsson et al. accomplished a study on the intestinal microbial bile acid transformation in healthy breastfed infants up to 3-months (Jonsson et al. 1995). They revealed that already at first month of age, most of the fecal bile acids were deconjugated and that the bile acid pattern changes over time, but after 24 months the children had an almost adult bile acid pattern. Hammons et al. previously reported the analysis of CA and CDCA via GC-MS in solely breastfed and non-probiotic formula-fed infants and detected a lower concentration of CA in the breastfed infants than in the formula-fed ones up to the first 5 months. CDCA concentrations were not different in these two groups (Hammons et al. 1988). On the contrary, the relative level of the primary bile acid CA mostly remained mostly consistent over time and did not change due to different feeding. In contrast, the primary bile acid CDCA increased from month 1 to month 12 in the formula fed group, whereas the relative level in the breastfed group remained consistent over 12 months. To conclude, GCDCA and GCA were significantly increased in formula-fed infants over time and cyprinolsulfate and sulfocholic acid were increased in breastfed infants. On the contrary, CDCA showed similar patterns in the breastfed infants, but was significantly changed until month 12 in the formula-fed infants, whereas CA showed constant intensity levels over time in both groups. In general, significant differences in the type and intensity of several bile acids were observed between breastfed infants and formula-fed infants over time. Further details are given in Table 6.2-12.

In order to find differences in the levels of some of the identified bile acids in the fecal samples of the placebo formula-fed and the interventional formula-fed infants compared to the breastfed ones, the bile acids were evaluated by month including all three feeding groups, B, F- and F+. Subsequently, comparing the intensity levels between B vs. F-, B vs. F+ and F+ vs. F- of the corresponding infants, differences in CDCA, GCA, GCDCA and cyprinolsulfate were observed (Figure 3.4-10).

In month 1, CDCA (Figure 3.4-10 A) was significantly different between F- and F+ (p -value = 0.015) and showed increased intensity levels in the F+ group, which were comparable to the breastfed infants. In the following month the difference between the F+ and F- group disappeared. On the contrary, GCA (Figure 3.4-10 B) and GCDCA (Figure 3.4-10 C) were not significantly altered between the F- and the F+ group in month 1, but showed different intensity levels compared to the breastfed infants over time. It was remarkable that in month 1 the intensity levels of CDCA, GCA and GCDCA in the probiotics formula group leads to an approximation towards the breastfed infants, which pattern was not prevalent any more up to month 7 and almost disappeared. This finding leads to the assumption that probiotics may help to approximate breast milk.

Thereof, GCA (B vs. F-: p -value = 0.00034; B vs. F+: p -value = 0.014) and GCDCA (B vs F-: p -value = 6.7E-05, B vs. F+: p -value = 0.06) showed different significant changes compared to the breastfed group. On the contrary, the F- group was characterized by higher intensity levels than the F+ group compared to the breastfed infants. The difference in the level of significance between B vs. F- and B vs. F+ of GCA was also detected in month 3. Additionally, GCDCA was different between B. vs. F- and B vs. F+ up to month 5, as well. After month 7, the differences in the significance between B. vs. F- and B vs. F+ disappear, but the significance of the bile acids between the fecal samples of breastfed and formula-fed infants were still present up to month 12. Further details are given in Table 6.2-13.

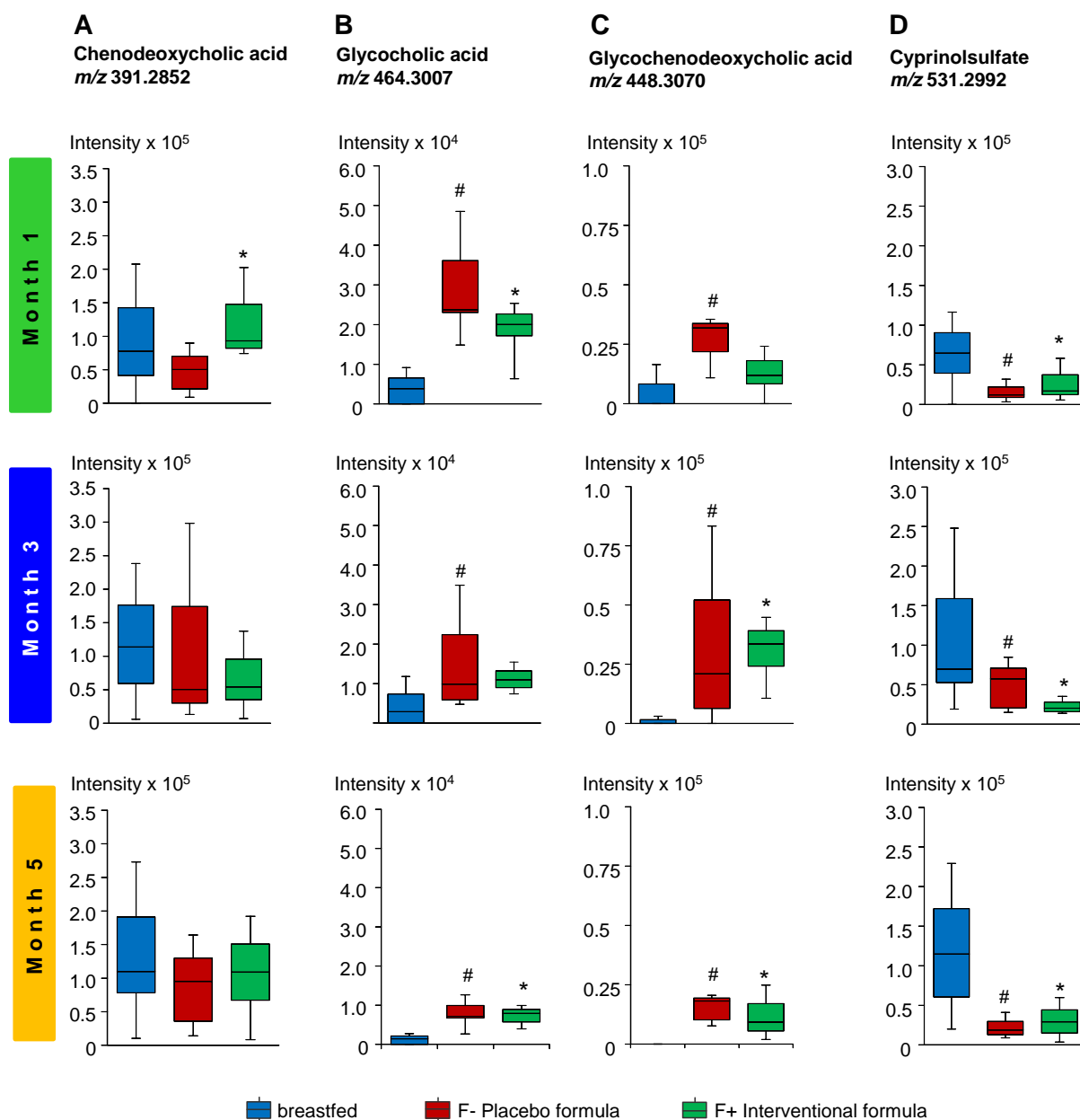


Figure 3.4-10: Differences in the bile acid profile between B, F- and F+ in month 1, 3 and 5.

Boxplots of bile acid profiles of CDCA, GCA and GCDCA significantly increased in formula-fed infants and cyprinolsulfate significantly increased in breast fed infants up to month 5, analyzed in (-)-ToF-MS mode A: Chenodeoxycholic acid: F+ vs. F-: *p-value = 0.015. B: Glycocholic acid: Month 1: B vs. F- : #p-value = 0.00034; B vs. F+: *p-value = 0.014. Month 3: B vs. F- : #p-value = 0.00035. Month 5: B vs. F- : #p-value = 3.00E-04; B vs. F+: *p-value = 6.30E-04. C: Glycochenodeoxycholic acid: Month 1: B vs. F-: #p-value = 6.7e-05. Month 3: B vs. F- : #p-value = 6.9e-06; B vs. F+: *p-value = 4.70E-04. Month 5: B vs. F-: #p-value = 5.2e-05; B vs. F+: *p-value = 0.0021. D: Cyprinolsulfate: Month 1: B vs. F-: #p-value = 0.00059; B vs. F+: *p-value = 0.02578. Month 3: B vs. F- : #p-value = 0.0030; B vs. F+: *p-value = 0.0015. Month 5: #p-value = 2.90E-04; B vs. F+: *p-value = 4.71E-03 (post hoc Kruskal-Nemenyi test). Further details are listed in Table 6.2-13.

The finding that secondary bile acids could be ambiguously neither detected nor identified in any of the three feeding groups was in contrast with previously published studies. Hammons et al. detected a higher concentration of lithocholic acid and deoxycholic acid in feces of formula fed infants (Hammons

et al. 1988). However, diet was observed to affect the bile acid metabolism in infants, widely differing between breastfed infants and formula-fed infants in sulfated and glycine-conjugated bile acids.

3.4.2.5 Intermediates of the tocopherol metabolism increased in formula fed infants

The statistical evaluation of the metabolite profiles of formula- and breastfed infants, revealed two highly significant mass signals, namely m/z 585.3432 and m/z 591.3879. In order to identify both, MS/MS experiments were performed. Through MS/MS experiments, similar fragmentation patterns were observed in both mass signals, with a characteristic loss of 176.03, which is distinctive for the loss of glucuronide fragments as shown in Figure 3.4-11. Therefore, the MS/MS spectra, as the unconjugated form were compared with the Metlin MS/MS database, which classified the two metabolites as γ -tocotrienol and γ -tocopherol.

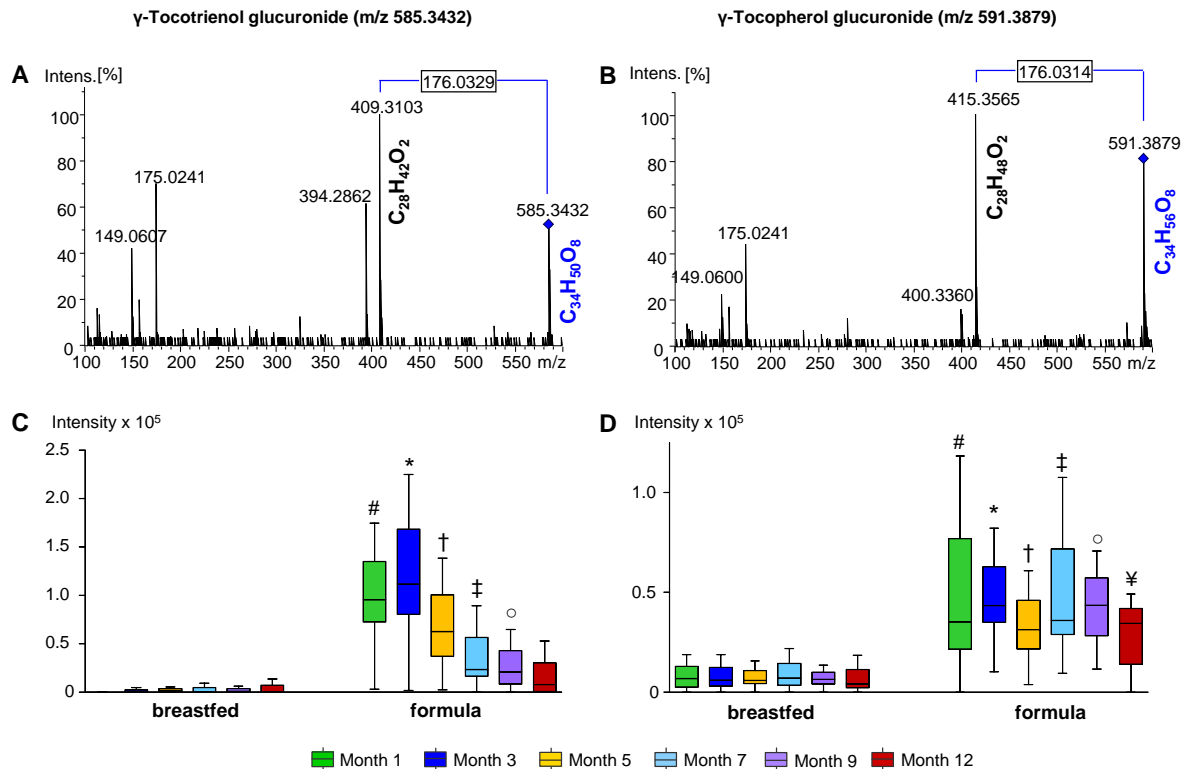


Figure 3.4-11: Vitamin E metabolite patterns in breastfed and formula-fed infants.

Experimental (-)-TOF-MS/MS spectra at 40 eV of A: γ -Tocotrienol glucuronide; B: γ -Tocopherol glucuronide and boxplots of the (C) γ -tocotrienol glucuronide and (D) γ -tocopherol glucuronide significantly increased in formula-fed infants over time. C: Month 1: # p-value = 9.78E-08; Month 3: * p-value = 6.14E-08; Month 5: † p-value = 6.32E-07; Month 7: ‡ p-value = 2.65E-06; Month 9: ○ p-value = 0.000554; D: Month 1: # p-value = 2.19E-05; Month 3: * p-value = 1.99E-07; Month 5: † p-value = 3.68E-08; Month 7: ‡ p-value = 6.56E-07; Month 9: ○ p-value = 9.30E-07; Month 12: ¥ p-value = 0.004312 (Mann-Whitney-Test). p-values are always in relation to the same month of the different feedings. Further details are listed in Table 6.2-14.

3. Impact of breast-feeding and bifidobacteria-supplemented formula

Differentiation between the β - and γ -tocopherol or tocotrienols respectively, having the same monoisotopic mass was enabled by different fragmentation patterns. Also Chow et al. detected higher levels (18.36-fold) of γ -tocopherol, an intermediate of the tocopherol metabolism, in exclusively formula-fed infants compared to breastfed infants. Assuming, that all vitamin E intermediates are glucuronidated and then excreted into feces, the monoisotopic masses of metabolites involved in the biosynthesis of tocopherol/tocotrienol were calculated as [M-H]- adducts and fictively conjugated with glucuronide. In this way, α -tocopherol glucuronide, α -tocotrienol glucuronide and δ -tocopherol glucuronide were also detected as significantly increased in the fecal samples of formula-fed infants.

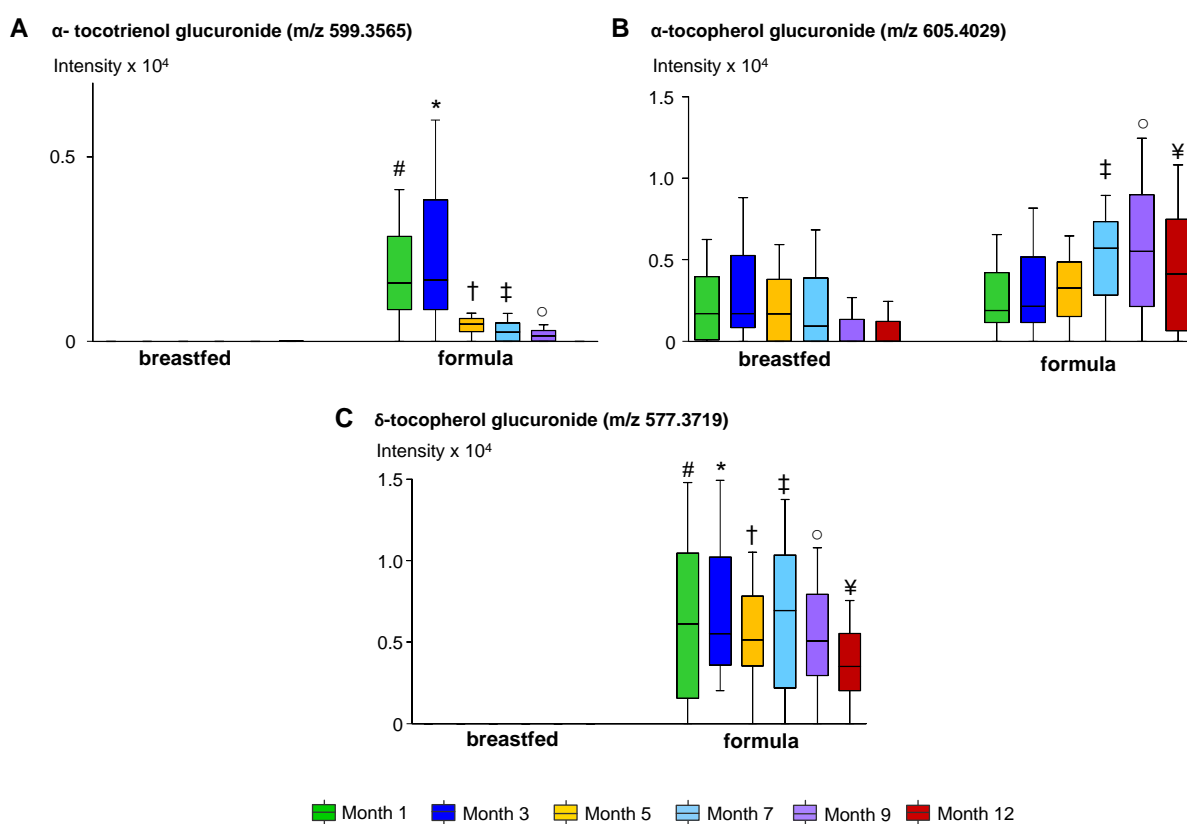


Figure 3.4-12: Over time patterns of intermediates of the biosynthesis of tocopherols.

Boxplots of potential metabolites involved in the biosynthesis of tocopherol differentiating between breastfed and formula-fed infants of month 1 (green), month 3 (blue), month 5 (yellow), month 7 (light blue), month 9 (purple) and month 12 (red). Significance was tested through the Mann-Whitney test; symbols #, *, †, ‡, °, ¥: p-value < 0.05. Further details are listed in Table 6.2-14.

Usually infants are born with relatively little amounts of vitamin E, as the placental transfer from the mother to the fetus is limited (Preedy and Watson 2007) and need to be supplied with it via their diet. Both are intermediates in the tocopherol/tocotorienol biosynthesis (vitamin E) and are essential nutrients, which cannot be synthesized endogenously (Chow et al. 2014) and need to be provided by

either breast milk or formula. In this study, the amount of vitamin E was 1.3 mg/100mL in each formula fed to the infants, whether it was pre-formula, follow-up or supplementary formula. As γ -tocotrienol and γ -tocopherol were distinctively classified through MS/MS experiments, their patterns in the formula-fed infants over time will be reviewed for possible relationships between the amount of formula the infants were fed and the intensity of tocotrienol and tocopherol detected in the fecal samples of the formula and the breastfed infants. Considering all months together, Pearson correlation ($\alpha = 0.05$) revealed a significantly positive relationship between the amount of formula fed and the intensity of tocotrienol ($r(221) = 0.64$, $p\text{-corr} < 0.001$) and tocopherol ($r(221) = 0.52$, $p\text{-corr} < 0.001$) detected in the fecal samples of formula-fed infants. Evaluating the correlations on a monthly view, a significant positive relationship between the amount of formula and the two metabolites was observed up to month 5. The positive relationship between the amount of formula and tocotrienol was further decreasing up to month 12, whereas for tocopherol the correlations are still present up to month 9, as shown in Table 3.4-3. The different correlation pattern leads to study the impact of tocotrienol on the tocopherol pattern and vice versa by applying the Pearson correlation, too.

Table 3.4-3: Correlations between tocopherol and tocotrienol and the amount of formula fed.

Correlations between the amount of formula and the metabolites, as well as the correlations among the different metabolites were obtained through Pearson correlation, recording the correlation coefficient (r), and the degrees of freedom (df), as well as $p\text{-corr}$ values calculated through regression analysis.

	Name	[M-H] ⁻	r	$p\text{-corr}$	df
Relationship between the amount of formula and the intensity levels	γ-tocotrienol glucuronide				
	Month 1	585.3419 $C_{34}H_{50}O_8$	0.79	3.32E-09	36
	Month 3		0.71	7.75E-08	40
	Month 5		0.65	3.94E-06	38
	Month 7		0.51	5.60E-04	30
	Month 9		0.53	0.0016	30
	Month 12		0.47	0.0105	27
	γ-tocopherol glucuronide				
	Month 1	591.3879 $C_{34}H_{56}O_8$	0.56	2.30E-04	36
	Month 3		0.55	1.41E-04	40
	Month 5		0.49	1.10E-03	38
	Month 7		0.61	1.64E-05	30
	Month 9		0.55	0.00094	30
	Month 12		0.33	0.08	27
Correlations between tocotrienol and tocopherol	Month 1		0.80	1.29E-09	36
	Month 3		0.77	1.98E-09	40
	Month 5		0.70	3.84E-07	38
	Month 7		0.75	1.52E-08	30
	Month 9		0.68	1.95E-05	30
	Month 12		0.26	0.17	27

It could be assumed that up to month 5, tocotrienol and tocopherol correlated predominantly positively with the amount of formula fed. After month 5 the predominating factor seems to be the coexistence of

the two vitamin intermediates and their significant positive relationship, as well as their dependency on one another, since the positive correlation persists up to month 9.

To further investigate, why formula-fed infants display higher intensities of tocotrienol and tocopherol compared to the relatively low amount in breastfed infant, the study of Haug et al in 1987 possibly provides some more insights (Haug et al. 1987). They analyzed the vitamin E content (α -, β - and γ -tocopherol) in breast milk samples of mothers of preterm and full-term infants. They observed that not only the vitamin E content of preterm and full-term breast milk showed similar concentration patterns, but also stage of lactation (colostrum, transitional and mature) of the breast milk samples played an important role on the vitamin E concentrations. Further, they showed that with the duration of lactation the concentration of vitamin E decreases.

Further studies confirm this finding (Kobayashi et al., Syvaaja et al and Boersma et al. (Kobayashi et al. 1975, Syvaaja et al. 1985, Boersma et al. 1991). The same result was obtained by Martysiak-Zurowska et al. (Martysiak-Zurowska et al. 2013), who analyzed α - and γ -tocopherol in breast milk samples of different stages of lactation (day 2, day 14, day 30 and day 90). They found concentration levels of γ -tocopherol in the breast milk samples from 0.022 mg/100mL – 0.060 mg/100mL and 0.207 mg/100mL – 0.999 mg/mL for α -tocopherol, depending on the stage of lactation. Compared to the vitamin E content in the formula within this study (1.3 mg/100 mL), the concentration levels are much higher than those detected in breast milk in previously performed studies. As previously postulated by Chow et al., this indicated either levels in the diet that are too excessive or that the tocopherols cannot be absorbed completely and are excreted into feces (Chow et al. 2014). It can be assumed that the amount of vitamin E in breast milk samples received by the infants is usually sufficient as the concentration levels in the breastfed infant were 1.65 – 7.65-fold lower than in the formula-fed infants (Table 6.2-14) and the formula-fed infants need to excrete this excess with feces.

3.4.2.6 Fatty acids and derivatives altered in breastfed and formula-fed infants

The fecal samples of the exclusively fed infants, which previously were evaluated by month revealed several mass signals assigned as FAs to be altered between breastfed and formula-fed infants over time. All detected FAs, including the saturated, medium-chain fatty acids (MCFAs) dodecanoic acid

(C12:0, Figure 3.4-13 A) and LCFA tetradecanoic acid (C14:0, Figure 3.4-13 B, MS/MS spectrum in Figure 5.2-4 A), were significantly increased in the breastfed infants (Bazanella et al. 2017). C12:0 and C14:0 were significantly increased in the breastfed infants up to month 5 (Figure 3.4-13 A, B). On the contrary, Chow et al. detected dodecanoic acid and tetradecanoic acid to be significantly higher in formula-fed infants (Chow et al. 2014).

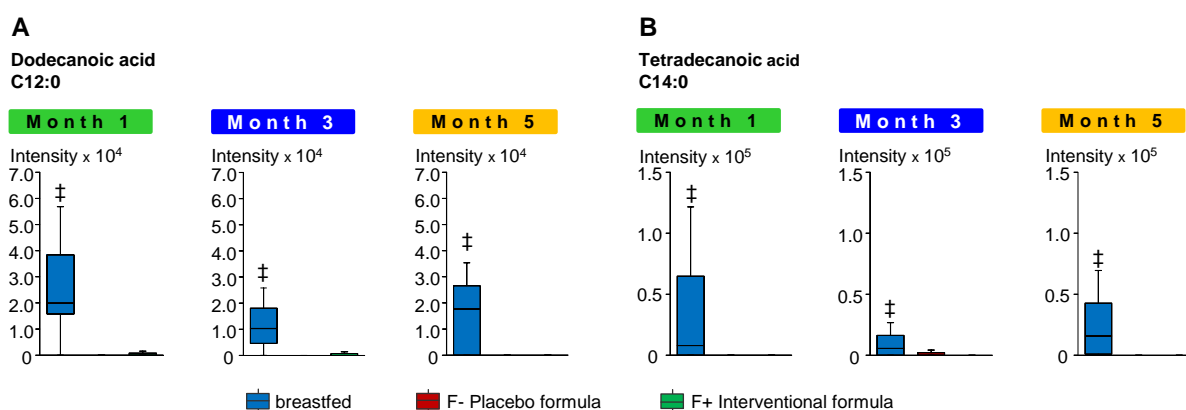


Figure 3.4-13: Saturated fatty acids increased in breast fed infants up to month 5.

Boxplots of saturated fatty acids significantly increased in breast fed infants (blue) in month 1 (green), month 3 (blue) and month 5 (yellow). Significance was tested by *post hoc* Kruskal-Nemenyi test; A: Dodecanoic acid, B: Tetradecanoic acid, A: Month 1 ‡ p-value = 2.00E-03 (B vs. F-) and p-value = 1.40E-03 (B vs. F+); Month 3 ‡ p-value = 9.20E-04 (B vs. F-) and p-value = 1.92E-03 (B vs. F+); Month 5 ‡ p-value = 1.20E-02 (B vs. F-). B: Month 1 ‡ p-value = 2.95E-02 (B vs. F-) and p-value = 9.40E-03 (B vs. F+); Month 3 ‡ p-value = 5.60E-03 (B vs. F+); Month 5 ‡ p-value = 7.00E-03 (B vs. F-) and p-value = 2.90E-02 (B vs. F+). Further details are listed in Table 6.2-15

The unsaturated LCFA hexadecenoic acid (C16:1, Figure 3.4-14 A), and LCPUFAs, such as eicosatetraenoic acid (ETA, C20:4, Figure 3.4-14 B, MS/MS spectrum in Figure 5.2-4 B) and icosapentaenoic acid (EPA, C20:5, Figure 3.4-14 C) were significantly higher in breastfed infants. Further details are given in Table 6.2-15. The experimental MS/MS spectra were compared manually against the METLIN database within an error of 0.05 Da (Smith et al. 2005). Further, experimental (-)-ToF-MS/MS spectra were compared against mass spectra acquired by Walker et al. (Walker et al. 2014).

It was revealed that C16:1, C20:4 and C20:5 were significantly higher up to month 7. On the contrary, in month 7 only C20:4 appeared to be significantly higher by breastfeeding. Eicosatetraenoic acid (C20:4) was another ingredient in the different formula feds; however, the intensity of eicosatetraenoic acid was higher in the breastfed infants than in those fed with formula. It was observed that in month 1 until month 5 the intensity level of hexadecenoic acid in the probiotics formula group leads to an

approximation towards the breastfed infants, which pattern was not prevalent any more in month 7 and almost disappeared.

Additionally, it was remarkable that inter-individual differences in the breastfed group were much higher than in both formula groups. Concerning this, it is well known, that the fatty acids in human milk are strongly influenced by maternal diet, which has consequences to the fecal metabolome of infants. Especially, LCPUFAs are said to be strongly related to maternal diet (Ballard and Morrow 2013). The high inter-individual changes in the breastfed might imply this message by Ballard et al.. However, the metabolic processes for biosynthesis, metabolism of the variety of fatty acids and their excretion are multiple, whereas about their presence in the fecal samples of breastfed and formula-fed infants no distinct conclusions can be drawn.

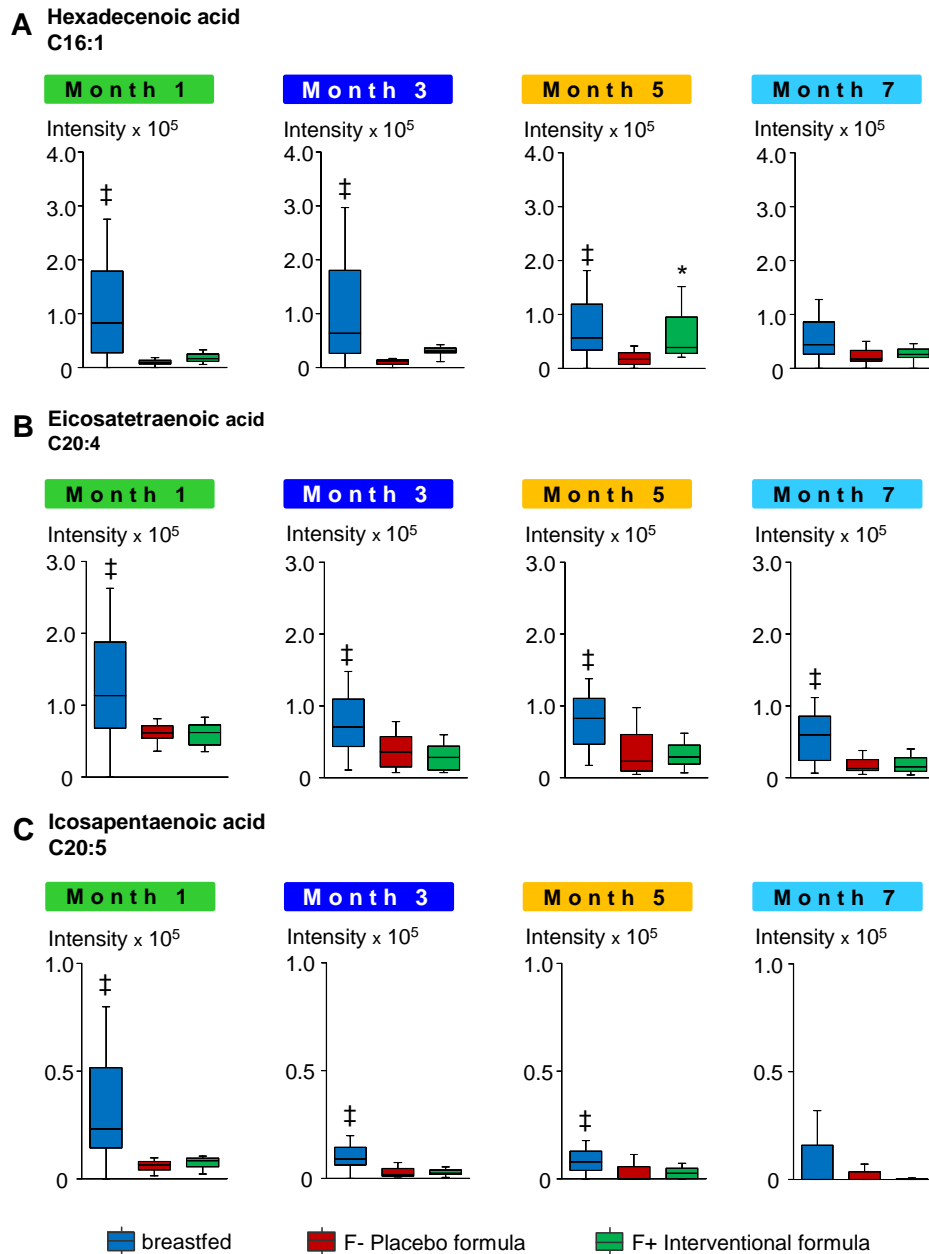


Figure 3.4-14: Unsaturated long-chain fatty acids significantly increased in breastfed infants.

Boxplots of monounsaturated fatty acids, such as (A) hexadecenoic acid and long-chain polyunsaturated fatty acids, such as (B) eicosatetraenoic acid and (C) icosapentaenoic acid significantly increased in breast fed infants (blue) compared to interventional formula-fed (green) and placebo formula-fed infants (red) in month 1 (green), month 3 (blue), month 5 (yellow) and month 7 (light blue). A: Month 1 ‡ p-value = 1.50E-03 (B vs. F-) and p-value = 5.28E-02 (B vs. F+); Month 3 ‡ p-value = 1.30E-03 (B vs. F-); Month 5 ‡ p-value = 1.20E-02 (B vs. F-) and * p-value = 2.30E-02 (F- vs. F+). B: Month 1 ‡ p-value = 5.10E-02 (B vs. F-) and p-value = 2.10E-02 (B vs. F+); Month 3 ‡ p-value = 3.10E-03 (B vs. F+); Month 5 ‡ p-value = 9.60E-03 (B vs. F-) and p-value = 2.66E-02 (B vs. F+); Month 7 ‡ p-value = 2.30E-02 (B vs. F-) and p-value = 2.30E-02 (B vs. F+). C: Month 1 ‡ p-value = 5.90E-03 (B vs. F-) and p-value = 3.08E-02 (B vs. F+); Month 3 ‡ p-value = 8.90E-03 (B vs. F-) and p-value = 2.70E-03 (B vs. F+); Month 5 ‡ p-value = 1.30E-02 (B vs. F-). Level of significance was tested by *post hoc* Kruskal-Nemenyi test. Further details are listed in Table 6.2-15.

Additionally, the medium-chain dicarboxylic dodecanedioic acid (Figure 3.4-15 A, MS/MS spectrum in Figure 5.2-5 B), also known as traumatic acid, as well as dihydroxyoleic acid (Figure 3.4-15 B, MS/MS

spectrum in Figure 5.2-5 A) were significantly increased in the formula-fed infants. It was noteworthy that in 99% of the breastfed infants, dodecanedioic acid was not present at all in the first year of life. Dodecanedioic acid and dihydroxyoleic acid were not significantly changed between infants fed with placebo formula or interventional formula, but also responded differently in the two formulas as seen in varying intensity levels of the respective feeding group. However, probiotics in formula did not bring the patterns of dodecanedioic acid and dihydroxyoleic acid closer to the breastfed one, as seen in fatty acid profiles of hexadecenoic acid and LCPUFA.

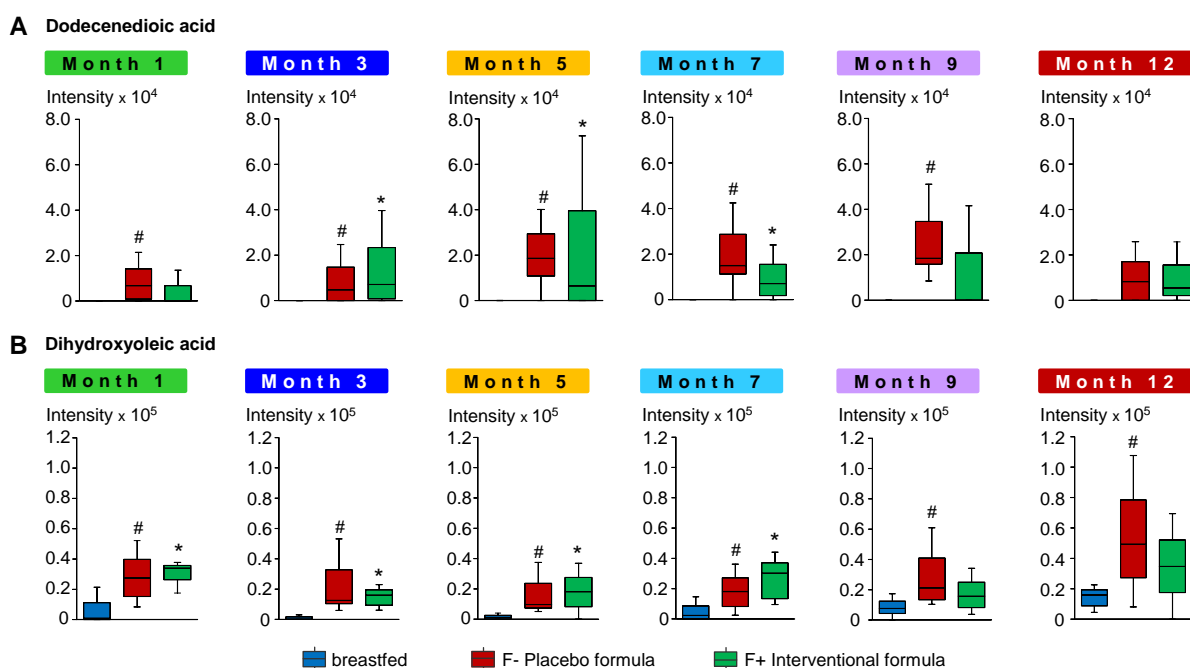


Figure 3.4-15: Dodecanedioic acid (A) and dihydroxyoleic acid (B) increased in formula-fed infants.

Boxplots of dodecanedioic acid (A) and dihydroxyoleic acid (B) significantly increased in breast fed infants (blue) compared to placebo formula-fed (red) and interventional formula-fed (green) in month 1 (green), month 3 (blue), month 5 (yellow), month 7 (light blue), month 9 (purple) and month 12 (red). A: Month 1 # p-value = 7.00E-03 (B vs. F-); Month 3 # p-value = 1.30E-02 (B vs. F-) and * p-value = 2.00E-03 (B vs. F+); Month 5 # p-value = 3.10E-04 (B vs. F-) and * p-value = 6.96E-03 (B vs. F+); Month 7 # p-value = 2.90E-04 (B vs. F-) and * p-value = 1.42E-02 (B vs. F+); Month 9 # p-value = 3.50E-04 (B vs. F-). B: Month 1 # p-value = 1.30E-03 (B vs. F-) and * p-value = 6.50E-05 (B vs. F+); Month 3 # p-value = 1.20E-05 (B vs. F-) and * p-value = 4.10E-05 (B vs. F+); Month 5 # p-value = 7.20E-04 (B vs. F-) and * p-value = 1.79E-03 (B vs. F+); Month 7 # p-value = 4.07E-02 (B vs. F-) and * p-value = 8.30E-04 (B vs. F+); Month 9 # p-value = 7.00E-03 (B vs. F-); Month 12 # p-value = 1.70E-02 (B vs. F-). Significance was tested with the *post hoc* Kruskal-Nemenyi test; further details are listed in Table 6.2-16.

Further, hydroxyphenyllactic acid (Figure 3.4-16, MS/MS spectrum in Figure 5.2-4 C) was increased in the fecal samples of breastfed infants over time. Although the fecal hydroxyphenyllactic acid was not significantly changed between infants fed with the placebo formula or the interventional formula, here, either, different intensity levels were observed between the two formula-fed infants (Figure 3.4-16).

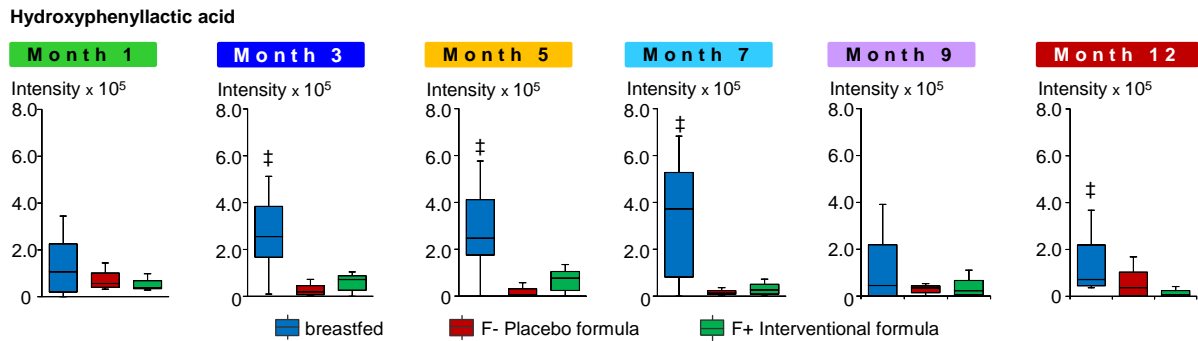


Figure 3.4-16: Hydroxyphenyllactic acid increased in breastfed infants over time.

Boxplots of hydroxyphenyllactic acid significantly increased in breast fed infants (blue) compared to placebo formula-fed (red) and interventional formula-fed (green) in month 1 (green), month 3 (blue), month 5 (yellow), month 7 (light blue), month 9 (purple) and month 12 (red). Month 3 # p-value = 5.80E-05 (B vs. F-) and * p-value = 5.40E-03 (B vs. F+); Month 5 # p-value = 2.10E-04 (B vs. F-) and * p-value = 2.42E-02 (B vs. F+); Month 7 # p-value = 2.50E-03 (B vs. F-) and * p-value = 2.26E-02 (B vs. F+); Month 12 # p-value = 1.70E-03 (B vs. F+). Significance was tested with the *post hoc* Kruskal-Nemenyi test; further details are listed in Table 6.2-16.

Hydroxyphenyllactic acid belongs to the class of phenylpropanoic acids and is a tyrosine metabolite that derives from microbial breakdown of undigested proteins. (Chow et al. 2014). Beloborodova et al. detected that phenyllactic and p-hydroxyphenyllactic acids are produced by bifidobacteria and lactobacilli *in vitro* (Beloborodova et al. 2012). Breast milk is a source of bifidobacteria and lactobacilli species, which are known to be transferred to the infants by breastfeeding (Martin et al. 2003, Martin et al. 2012, Soto et al. 2014). Including the findings from Beloborodova et al., higher levels of hydroxyphenyllactic acid in breastfed infants were reasonable. Concerning this, in the formula-fed infants the intensity of hydroxyphenyllactic acid was comparatively small, even though the interventional formula was substituted with bifidobacteria strains. Although hydroxyphenyllactic acid did not show differences between probiotic formula and the placebo one in month 1, the differences developed over time and got more dominant in the following months. It was observed, that the patterns of hydroxyphenyllactic acid in the probiotics group showed a little approximation towards the breastfed group until month 9. Breastfeeding is supposed to improve infants' health and lowers the development of several diseases, such as otitis media, necrotizing enterocolitis, inflammatory bowel disease, diabetes or allergic diseases (Soto et al. 2014). Our results indicated similar effects of breast milk and probiotic formula and strengthened the use of probiotics to improve infants' health.

3.4.2.7 Impact of different feeding types on the SCFA profile (breastfed vs. formula-fed)

In humans, 95% of synthesized SCFAs are absorbed in the colon, whereas 5% are secreted in feces (den Besten et al. 2013). Further, they contribute to *de novo* production of lipids by serving as energy substrate or signaling molecules. The production of SCFA strongly correlates with and is influenced by food intake and dietary changes in the human gut microbiome. SCFA are microbial fermentation products derived from dietary substrates, especially from carbohydrates obtained from breast milk and formula. Therefore, the SCFA profiles, and the concentration levels of lactic acid and pyruvic acid in feces were further assessed from the exclusively breastfed and exclusively formula-fed cohorts using UHPLC-ToF-MS, illustrated as EIC view in Figure 3.4-17.

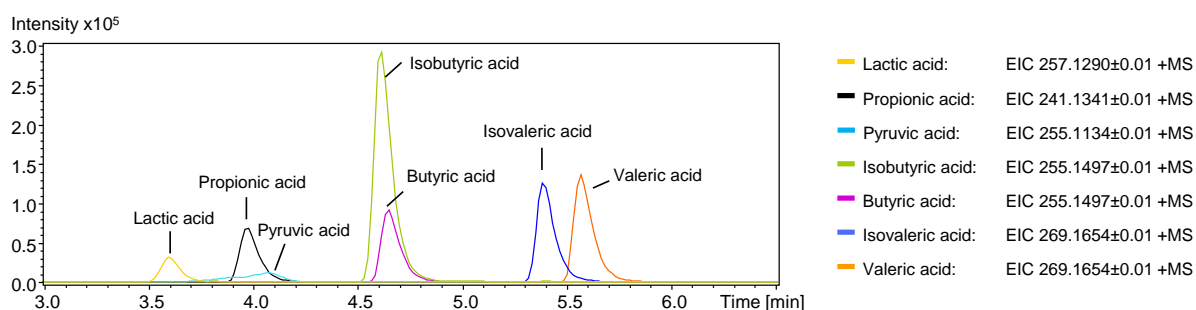


Figure 3.4-17: Extracted ion chromatogram of SCFA, lactic and pyruvic acid.

Extracted ion chromatogram with an error of ± 0.05 Da of pyruvic acid, lactic acid (yellow), propionic acid (black), butyric acid (purple) and isobutyric acid (green), as well as valeric (orange) and isovaleric acid (blue), analyzed in UHPLC-(+)-ToF-MS.

In order to assess the impact of different feedings on the fatty acid profile, especially the SCFA profile of infants over time, propionic acid, butyric and isobutyric acid, and valeric and isovaleric acid were analyzed. Further, the MCFA hexanoic acid, heptanoic acid, octanoic acid, nonanoic acid and decanoic acid were derivatized. The carboxylic acids of the carbohydrate metabolism, such as lactic acid, pyruvic acid, fumaric acid, maleic acid, and succinic acid were considered as well. The MCFA C6:0 up to C10:0 did not show to be affected by feeding, neither were maleic, fumaric and succinic acid. Evaluating the total fecal SCFA concentrations, slight differences among breastfed and the two formula-fed infants were observed, mainly because of higher concentration levels of butyric and propionic acid in the formula-fed infants, which accounted for 90% of the total SCFA profile. Fecal samples of formula-fed infants showed 2.5-fold increased total SCFA concentration levels in average over time. For further analyses, pyruvic acid, lactic acid, propionic acid, butyric acid, isovaleric acid and valeric acid were considered. With respect to the SCFA and carboxylic acid production, the individual response of each

infant was observed to be immense and their concentrations were marked by wide variations. Table 3.4-4 lists the concentrations of each fatty and carboxylic acid by month as mean value and individual range concentration.

Table 3.4-4: Mean and individual range of SCFA, pyruvic and lactic acid concentrations (in $\mu\text{mol/L}$)

Arithmetic mean sums of lactic and pyruvic acid, as well as total SCFA concentration, including propionic acid, butyric acid, valeric acid and isovaleric acid changed in breastfed (blue) and both formula-fed groups (F+/F-), differentiating in the concentration levels by month and fatty acid. The mean value, as well as the individual range is displayed of month 1, 3, 5, 7, 9, and 12 of each fatty acid, separated in feeding.

	Breast-fed infants		Formula-fed infants (F-)		Formula-fed infants (F+)	
	Mean	Individual range	Mean	Individual range	Mean	Individual range
<i>Pyruvic acid</i>						
Month 1	4.0	0.0 - 17.0	0.5	0.0 - 2.7	0.9	0.0 - 3.3
Month 3	1.4	0.0 - 3.8	0.3	0.0 - 1.8	0.3	0.0 - 2.4
Month 5	5.8	0.0 - 19.0	< 0.1	0.0 - 0.4	0.5	0.0 - 5.2
Month 7	3.4	0.0 - 14.2	0.1	0.0 - 0.6	0.0	0
Month 9	0.5	0.0 - 2.4	0.0	0	< 0.1	0.0 - 0.2
Month 12	0.1	0.0 - 0.7	0.0	0	0.3	0.0 - 2.3
<i>Lactic acid</i>						
Month 1	31.4	0.0 - 101.4	2.1	0.0 - 15.3	1.9	0.0 - 11.4
Month 3	9.4	0.0 - 60.1	7.0	0.0 - 40.8	0.9	0.0 - 5.2
Month 5	52.0	0.0 - 192.1	0.5	0.0 - 3.2	3.3	0.0 - 13.3
Month 7	20.5	0.0 - 133.5	1.0	0.0 - 6.9	0.4	0.0 - 4.0
Month 9	5.0	0.0 - 37.5	0.2	0.0 - 2.0	0.1	0.0 - 1.4
Month 12	0.7	0.0 - 3.8	4.3	0.0 - 41.5	0.1	0.0 - 0.5
<i>Total SCFA</i>						
Month 1	1.5	0.0 - 11.8	6.9	0.0 - 35.4	5.5	0.0 - 44.7
Month 3	2.8	0.0 - 23.4	5.4	0.0 - 26.4	4.4	0.0 - 44.5
Month 5	2.9	0.0 - 30.8	8.2	0.0 - 35.7	6.2	0.0 - 25.0
Month 7	3.3	0.0 - 21.8	6.5	0.0 - 50.1	6.8	0.0 - 41.5
Month 9	3.8	0.0 - 24.5	8.2	0.0 - 29.2	5.5	0.0 - 49.1
Month 12	6.9	0.0 - 25.5	8.3	0.0 - 54.1	10.1	0.0 - 52.4
<i>Propionic acid</i>						
Month 1	4.7	0.0 - 8.5	22.7	0.0 - 35.4	18.7	7.8 - 44.8
Month 3	10.1	0.0 - 23.4	14.5	0.0 - 26.4	13.4	0.0 - 44.5
Month 5	10.3	3.2 - 30.8	20.9	0.0 - 35.7	18.1	11.7 - 25.0
Month 7	11.3	0.0 - 21.8	17.5	0.0 - 50.2	19.4	0.0 - 41.5
Month 9	11.8	0.0 - 24.5	18.8	0.0 - 29.2	15.0	0.0 - 49.1
Month 12	17.2	11.8 - 25.5	17.4	0.0 - 54.1	22.0	8.2 - 52.4
<i>Butyric acid</i>						
Month 1	1.1	0.0 - 11.8	4.3	0.0 - 11.8	2.9	0.0 - 12.3
Month 3	1.0	0.0 - 7.5	6.5	0.0 - 14.3	3.5	0.0 - 7.6
Month 5	1.2	0.0 - 9.9	10.9	0.0 - 25.8	6.0	0.7 - 12.5
Month 7	1.8	0.0 - 10.9	7.9	0.0 - 15.9	6.8	0.0 - 17.5
Month 9	3.0	0.0 - 7.5	11.9	0.0 - 27.0	5.9	0.0 - 19.1
Month 12	9.3	1.5 - 20.5	14.0	0.0 - 28.3	15.9	2.9 - 31.0
<i>Isovaleric acid</i>						
Month 1	< 0.1	0.0 - 8.7E-5	0.4	0.0 - 1.4	0.4	0.0 - 1.0
Month 3	0.2	0.0 - 1.4	0.5	0.0 - 1.7	0.6	0.0 - 1.5
Month 5	< 0.1	0.0 - 0.8	0.8	0.0 - 2.5	0.7	0.04 - 1.3
Month 7	0.2	0.0 - 0.7	0.6	0.0 - 1.9	0.8	0.0 - 2.3
Month 9	0.5	0.0 - 2.2	1.8	0.0 - 3.1	0.8	0.0 - 2.9
Month 12	1.1	0.1 - 3.1	1.6	0.0 - 4.1	1.9	0.3 - 6.1
<i>Valeric acid</i>						
Month 1	0.0	0	0.1	0.0 - 0.4	0.0	0
Month 3	0.1	0.0 - 1.0	0.1	0.0 - 0.5	< 0.1	0.0 - 0.2
Month 5	< 0.1	0.0 - 0.2	0.3	0.0 - 1.1	0.2	0.0 - 0.8
Month 7	< 0.1	0.0 - 0.2	0.1	0.0 - 0.3	0.2	0.0 - 0.7
Month 9	0.0	0.0 - 0.04	0.4	0.0 - 1.7	0.1	0.0 - 0.4
Month 12	0.2	0.0 - 0.7	0.5	0.0 - 3.0	0.4	0.0 - 1.1

3. Impact of breast-feeding and bifidobacteria-supplemented formula

Even if the infants' individual concentration levels were present, the overall evaluation revealed significant changes in SCFA, pyruvic acid and lactic acid concentration levels among breastfed and formula-fed infants. The four most abundant SCFA, lactic and pyruvic acid are listed above and most significant changes were calculated on the basis of the entirety of all detected fatty acids. Herewith, the predominating carboxylic acid in breastfed infants was lactic acid (23.7%), followed by the SCFA propionic acid (22.7%), butyric acid (15.9%), pyruvic acid (7.4%), isovaleric acid (2.6%) and finally valeric acid (0.5%). In contrast, the fecal samples of the formula-fed infants (F+/F-) were dominated by propionic acid (31.0%/26.1%) and butyric acid (26.0%/28.8%), followed by isovaleric acid (4.7%/4.2%), lactic acid (1.6%/1.9%), valeric acid (0.9%/1.3%) and pyruvic acid (0.7%/0.3%). Even though the fatty acid profiles were not different between the bifidobacteria supplemented and placebo group, it was demonstrated that formula-feeding compared to breast-feeding generally leads to significantly higher concentrations of propionic, butyric, valeric and isovaleric acid. In contrast, pyruvic and lactic acid were detected at significantly higher concentrations in breastfed infants than in formula-fed ones (Bazanella et al. 2017) as illustrated in Figure 3.4-18.

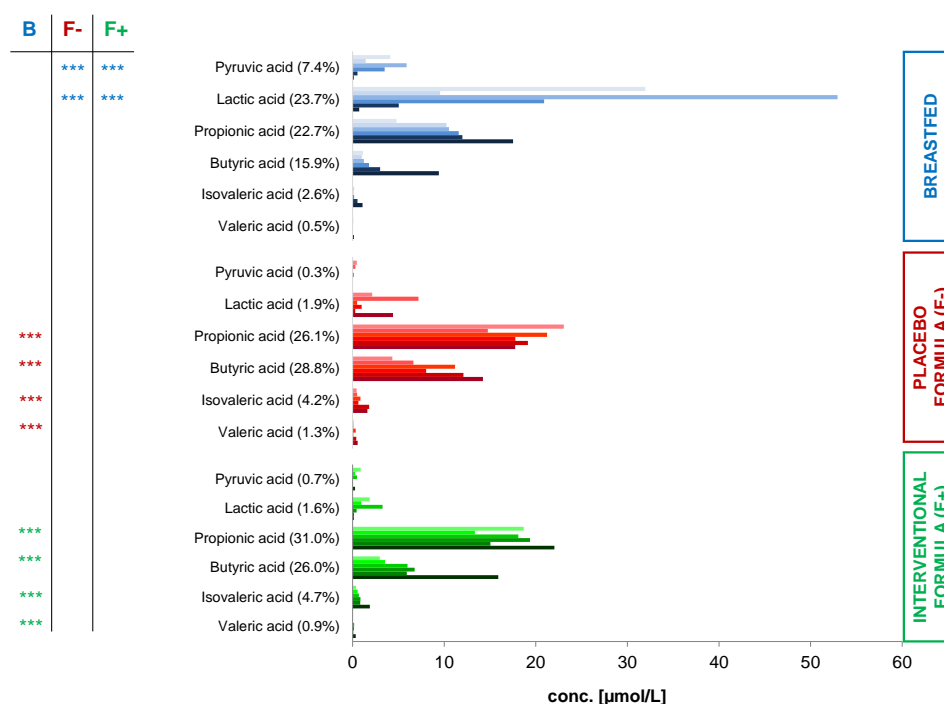


Figure 3.4-18: Pyruvic acid, lactic acid and SCFA impacted through diet.

Impact of breast milk (blue), bifidobacteria-supplemented formula (green) or the placebo group (red) on the fatty acid profile of infants over time, analyzed in UHPLC-(+)-ToF-MS. Colors are encoded by month from light to dark color, where the light color represents month 1 and as darker the color up to month 12. p-value: 0 **** 0.001 *** 0.01 ** 0.05 as listed in detail in Table 3.4-5. From Bazanella, M., Maier, T. V., Clavel, T., Lagkouvardos, I., Lucio, M., Maldonado-Gómez, M. X., Autran, C., Walter, J., Bode, L., Schmitt-Kopplin, P., Haller, D.: Randomized controlled trial on the impact of early-life intervention with bifidobacteria on the healthy infant fecal microbiota and metabolome. *Am J Clin Nutr.* (2017), 106(5):1274-1286. Reprinted and adapted from (Bazanella et al. 2017) by permission of Oxford University Press. Copyright (2017) American Society for Nutrition.

Their significance was calculated with the *post hoc* Kruskal-Nemenyi test (Table 3.4-5), considering the fatty acid mean values of each feeding group (all months included).

Table 3.4-5: Pyruvic acid, lactic acid and SCFA significantly changed through diet.

Results of the significance between pyruvic acid, lactic acid and SCFA obtained with *post hoc* Kruskal-Nemenyi test calculated of arithmetic mean values of each group (all month included).

Pyruvic acid	B	F+
F+	2.00E-06	-
F-	7.00E-07	0,96

Lactic acid	B	F+
F+	1.30E-05	-
F-	7.50E-06	0,98

Propionic acid	B	F+
F+	1.70E-04	-
F-	3.00E-06	0,64

Butyric acid	B	F+
F+	2.00E-06	-
F-	1.60E-09	0,41

Isovaleric acid	B	F+
F+	1.80E-07	-
F-	6.80E-07	0,98

Valeric acid	B	F+
F+	3.70E-03	-
F-	1.10E-05	0,33

In general, the SCFA profile in infants is distinguished from the profile in fecal samples of adults. The earliest feces (meconium) of infants contain only low SCFA concentrations, which are increasing after some days due to the colonization of microbes in the microbiota (Edwards and Parrett 2002). Previously, it was reported that the dominating fatty acids in adults are acetic, propionic and n-butyric acid (57:22:21) (Szyliet and Andrieux 1993), whereas in the breastfed infants acetic acid and lactic acid are the predominating ones and the levels of propionic and butyric acid are rather low (Edwards et al. 1994). In contrast, fecal samples of formula-fed infants are characterized by acetic acid, propionic acid and higher concentration levels of butyric acid compared to breastfed ones.

In breastfed infants, the SCFA patterns of propionic acid and butyric acid were detected to increase constantly from month 1 up to month 12, whereas in the formula groups, propionic acid showed the highest and most constant concentration levels over time. Additionally, in the formula-fed infants, butyric acid concentration levels were increased over time and generally ~ a 5-fold higher concentration level than in breastfed infants. Butyric acid preferably serves as energy substrate for the colonocytes in the intestine and is beside acetic and propionic acid one of the most abundant representing SCFA in the colon. Further, butyric acid is discussed to be essential for the health of the colon in adults (Edwards and Parrett 2002), the suppression of inflammations and cancer (Hamer et al. 2008). Furthermore, in the late 1980, Bullen et al. among others investigated the impact of formula and breast feeding on the fecal flora of infants over a period of 6 weeks and also detected higher concentration levels of both, valeric and isovaleric acid, in fecal samples of infants fed with formula (Bullen et al. 1977), which was in accordance with our over time results for breast- or formula-feeding.

Reports from previous studies also suggested lactic acid to be the dominant carboxylic acid in feces from breastfed infants (Ogawa et al. 1992), while formula-fed infants have higher abundances of propionic and butyric acids (Edwards et al. 1994). Hereto, adult feces usually contains no lactic acid (Edwards and Parrett 2002). It was suggested that lactic acid plays a fundamental and controlling role in the colonization of the intestine. Also, lactic acid (23.7%) was observed as the predominate fatty acid in breastfed infants, reaching its maximum at month 5, and again decreasing until month 12. The formula-fed infants presented with a 13-fold lower concentration and abundance of lactic acid on average (1.6 – 1.9%) in all months.

Breast milk is a source of bifidobacteria and lactic acid-producing bacteria (LAB), such as lactobacillus, lactococcus, or streptococcus, which produce the major end product lactic acid from the fermentation of carbohydrates involving the glycogenesis, gluconeogenesis or pyruvate metabolism (Pokusaeva et al. 2011, Chow et al. 2014), which potentially explains the high amount of lactic acid in breastfed infants through breast feeding. In contrast to the formula-fed infants, pyruvic acid concentration levels were also significantly increased in the breastfed ones, but showed – as lactic acid - inconstant concentration levels over time. In general, it was noticeable that the over time pattern was identical to the lactic acid one, whose relation to each other was confirmed by monthly correlations of the pyruvic and lactic acid concentration levels in the breastfed infants (Month 1: $r(11) = 0.54$, $p\text{-corr} = 0.055$; Month 3: $r(12) = 0.41$, $p\text{-corr} = 0.1$; Month 5: $r(11) = 0.82$, $p\text{-corr} = 0.00055$; Month 7: $r(12) = 0.85$, $p\text{-corr} = 8.35941E-05$).

Already in 1942, Stotz et al. revealed the relation between pyruvic acid and lactic acid in blood samples of humans, pigeons, and rats, which can serve as a measure for excitement, exercise, and different degrees of fasting. It was claimed, that a deviation of those relationship to be evidence of a more fundamental disturbance in pyruvate metabolism (Stotz and Bessey 1942). A deviation of the relationship between pyruvic and lactic acid could not be observed in the fecal samples of infants fed with breast milk. Moreover, pyruvic acid is an immediate precursor of lactic acid and both are intermediate compounds in the metabolism of carbohydrates, proteins, and fat, wherefore their presence – although in less concentrations than lactic acid - in fecal samples of breast fed infants, due to the microbial composition of breast milk and the colonization in the infants' gut, is reasonable.

In order to see relationships between the abundance of SCFA and the microbial species in the fecal microbiome, SCFA and OTUs were correlated, which revealed several correlations of SCFA, pyruvic and lactic acid and the OTUs. First, the abundance matrix was filtered, excluding OTUs with an abundance of $n \leq 3$ (10%). The data matrices of the SCFA and the OTUs of month 1, month 7 and month 12, respectively were merged and analyzed by PCA (scores scatter plots in Figure 3.4-19 A) and their corresponding loading plots (Figure 3.4-19 B) in order to visualize the relationship between the variables of the metabolites (yellow) and OTUs (grey) including their distribution among the three feeding groups along a two dimensional space. Here - as previously shown in Figure 3.4-18 - lactic and pyruvic acid were the significantly different metabolites in the breastfed infants, whereas propionic, butyric, valeric and isovaleric acid could be associated with the formula-fed infants as they are significantly changed compared to the breastfed infants.

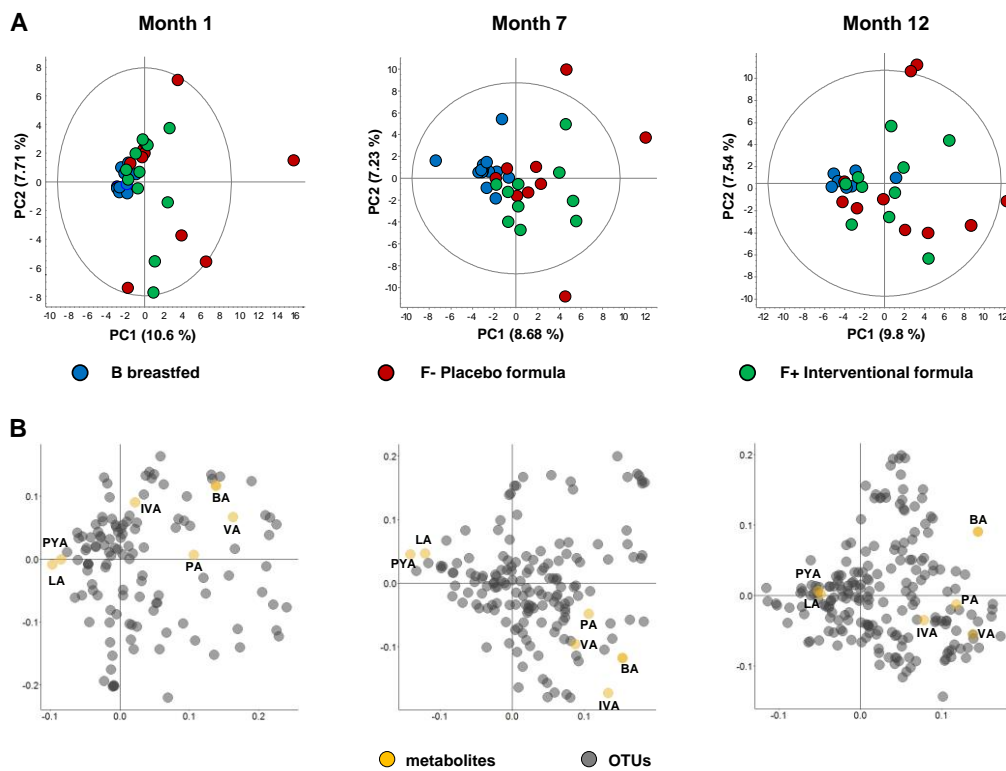


Figure 3.4-19: Correlation between SCFA and OTUs of month 1, month 7 and month 12.

Correlations between SCFA (yellow), lactic acid (yellow), pyruvic acid (yellow) and OTUs (grey). A: Scores scatter plot of PCA analysis (UV scaling). B: PCA loading plot with the variables responsible for the profile in the scores scatter plot in A; LA = lactic acid, PYA = pyruvic acid, IVA = isovaleric acid, PA = propionic acid, BA = butyric acid, VA = valeric acid.

Further, this analysis revealed a relationship between lactic acid and the genera of *Bifidobacterium sp.*, *Streptococcus sp.* in month 1 and *Lactobacillus sp.* in month 7, which are all known to be the major producer of lactic acid from the fermentation of carbohydrates (Chow et al. 2014). Anon, pyruvic acid is not only highly correlated to lactic acid, but also shows correlations with *Bifidobacterium sp.* in month 1 and *lactobacillus sp.* in month 7, as well. In month 1, butyric acid was predominately correlated to *Clostridium (sensu stricto)*, *Clostridium (sensu stricto) 1* and *Lachnospira sp.* in month 7. Valeric acid was observed to be highly correlated with *Flavonifractor* in month 7, *Ruminococcus2 sp.* and *Ruminococcus sp.* in month 12. In addition, propionic acid was related to *Ruminococcaceae sp.* in month 12. Further details are given in Table 3.4-6.

Table 3.4-6: Correlation between SCFA and OTUs of month 1, 7 and 12 in the different feeding groups.

Correlations between the SCFA and OTUs of month 1, 7 and 12 were obtained through Pearson correlation, recording the correlation coefficient (r), and the degrees of freedom (df), as well as p-corr values calculated through regression analysis.

Name	OTU	ID	r	p-corr	df
Pyruvic acid [AMP+]					
Month 1	<i>Bifidobacterium sp.</i>	OTU 2	0.45	7.00E-03	32
Month 7	<i>Lactobacillus sp.</i>	OTU 62	0.70	1.81E-06	34
Lactic acid [AMP+]					
Month 1	<i>Bifidobacterium sp.</i>	OTU 2	0.53	1.00E-03	32
	<i>Streptococcus sp.</i>	OTU 48	0.60	2.00E-04	32
Month 7	<i>Lactobacillus sp.</i>	OTU 62	0.90	1.29E-13	34
Propionic acid [AMP+]					
Month 12	<i>Ruminococcaceae sp.</i>	OTU 127	0.54	3.00E-03	26
Butyric acid [AMP+]					
Month 1	<i>Clostridium (sensu stricto)</i>	OTU 416	0.61	< 0.05	32
	<i>Clostridium (sensu stricto) 1</i>	OTU 182	0.52	1.60E-03	32
Month 7	<i>Lachnospira sp.</i>	OTU 36	0.45	5.00E-03	34
Valeric acid [AMP+]					
Month 7	<i>Flavonifractor</i>	OTU 29	0.46	4.70E-03	34
Month 12	<i>Ruminococcus2 sp.</i>	OTU 448	0.83	4.29E-08	26
	<i>Ruminococcus sp.</i>	OTU 43	0.65	2.00E-04	26

In consequence of different SCFA, lactic and pyruvic acid profiles, it could be concluded that the colonization of microbes and the relationship with metabolic activity of the infant gut microbiome of breastfed infants differ markedly from the one of formula-fed infants, irrespective of whether or not the infants are fed with or without probiotics. In addition to the distinct pattern of fatty acids between breastfed and formula-fed infants, the individual variance was co-dominant.

3.4.3 Differences in non-probiotic fed and probiotic fed infants

One of the main goals of this study was to reveal marked differences in the fecal metabolome between the infants, consuming the interventional formula or the placebo formula, which might be indicators for similar effects between breast milk and probiotic formula. Therefore, in this chapter the focus was to evaluate and to find differences of the two formula-fed groups, including the breastfed group. The breastfed group was considered as well to be able to compare the two formula diets to breastfeeding and to find possible similarities between the breastfed and interventional formula-fed group. This may lead to an approximation of the fecal metabolome due to probiotics towards the breastfed infants. Nevertheless, mass signals similarly impacted through the interventional formula and breast milk or the placebo formula and breast milk were taken into account as well.

Already the previously performed month by month PLS-DA (Chapter 3.4.2.2) revealed some mass signals to be affected by either interventional formula or placebo formula. In order to detect further mass signals to be affected by the two formulas differently, both groups were evaluated by month taking the matrix of each month separately of the PCA plots in Figure 3.4-4 and Figure 3.4-5 respectively. Several mass signals were observed to be altered differently in the placebo or the probiotics group. For identification (+) TOF MS/MS experiments of all F+ and F- discriminating metabolites were performed, whereas only one could be identified. This comprised one mass signal, which was increased in the placebo formula group (F-) and was detected in both ionization modes. Namely the mass signal at retention time 6.1 minutes with m/z 440.2844 in (+) ESI mode and m/z 438.2606 in (-) ESI mode. Through the annotation and following MS/MS experiments, it could be constrained to a lysophosphatidylethanolamines (LysoPE) 15:0/0:0 (Bazanella et al. 2017), a glycerophospholipid derived from phosphatidylethanolamines through partial hydrolysis of one fatty acid group (Gregory et al. 2013). The experimental MS/MS spectrum is shown in Figure 3.4-20 and was compared manually against the METLIN database with an error of 0.01 Da. The function of LysoPE (15:0/0:0) in the human gut microbiome of infants and the role in exclusively formula fed without probiotics in comparison to probiotic formula fed infants remains unclear.

However, it was observed that the intensity level in the F+ group was more similar to the breastfed one than the F- group. LysoPE 15:0/0:0 (Bazanella et al. 2017) was only significantly changed in month 1 and in no other months between F+ and F- up to month 12.

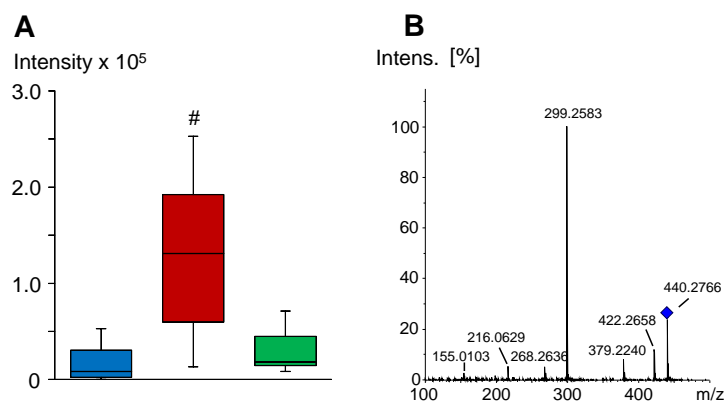


Figure 3.4-20: Lysophosphatidylethanolamine LysoPE(15:0) significantly increased in F- infants.

Boxplot of (A) Lysophosphatidylethanolamine LysoPE(15:0) significantly increased (B vs. F-: p-value = 0.00033, F- vs. F+: p-value = 0.09) in infants fed with the placebo formula (red) compared to breast fed (blue) and interventional formula-fed (green) infants, analyzed in (+) ToF-MS. B: The experimental (+) TOF MS/MS spectra of m/z 440.2844, collision energy 20 eV.

Another two unknown metabolites could be observed, whereas the mass signal m/z 644.4008 was significantly increased in month 1 and month 3 in the F- group, as well as m/z 445.3707 in month 1 (Figure 3.4-21 A/B/C). The mass signal with m/z 445.3707 showed an increase over time in both formula-fed groups, but was not significantly different anymore between those two groups after month 1. Again, it was remarkable that the intensity levels of all three mass signals in the probiotics group were similar to the breastfed group, whereas the intensities in the placebo group were rather high.

The mass signal m/z 510.3339 was discriminative for the F+ group (Figure 3.4-21 D, MS/MS spectra in Figure 5.2-10). Also, m/z 537.3863 showed increased intensities in the F+ group, even if the changes are not significant. However, these two mass signals, changed in the F+ group showed similar fragmentation patterns (MS/MS spectra in Figure 5.2-10), assuming they are structure-related compounds.

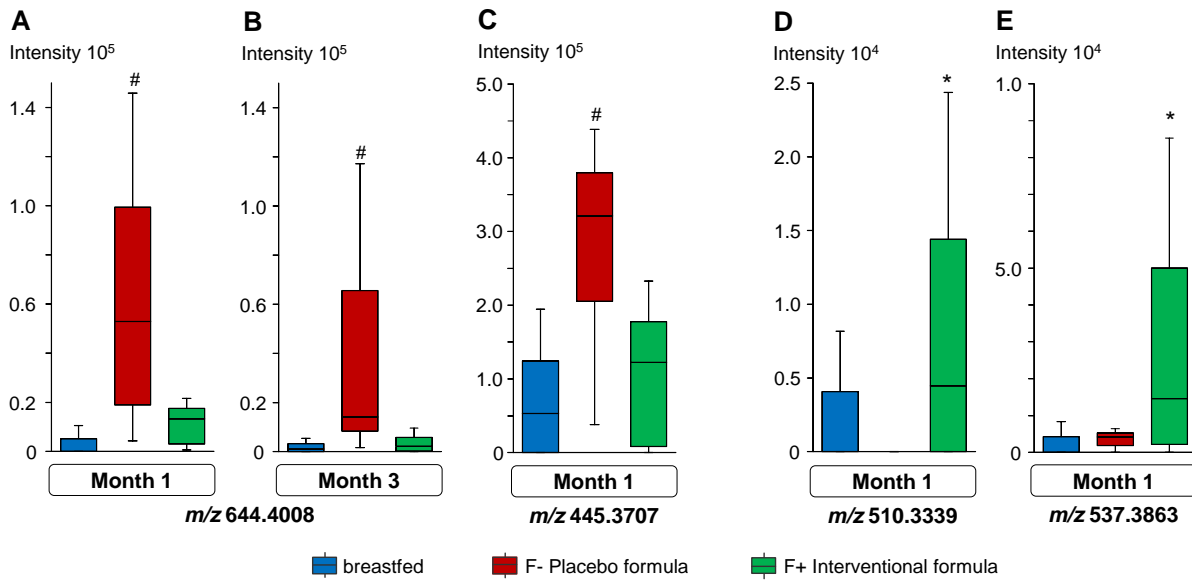


Figure 3.4-21: Mass signals at early life significantly changed through placebo or interventional formula.

Boxplots of mass signals significantly increased in placebo formula-fed (A, B, C, red) infants or interventional fed ones (D, E, green) compared to breast fed infants (blue), analyzed in UHPLC-(+)-ToF-MS mode. A/B: m/z 644.4008 significantly increased in F- fed infants (# p-value < 0.027) in month 1 and 3. C: m/z 445.3707 significantly increased in F- fed infants (# p-value < 0.05). D: m/z 510.3339 significantly increased in F+ fed infants (* p-value < 0.042) and E: m/z 537.3863 (*p-value < 0.022). Significance was tested through the *post hoc* Kruskal-Nemenyi test; further details are listed in Table 6.2-18.

Further mass signals differing between the probiotics group and the placebo group were observed in the negative ionization mode. This comprises LysoPE (15:0/0:0), which already was identified in the positive ionization mode and increased in infants fed with the placebo formula. Further unknown metabolites with m/z 516.3156, m/z 573.3827 were significantly changed in the F- group. One mass signal with m/z 541.3335 was increased in the F+ group. All significant metabolites for either the F+ or the F- group were only increased in month 1 – except m/z 644.4008 ((+) ESI). All shown metabolites revealed a clear distinction between the two formula-fed groups, and as time passed, those metabolites decrease in the groups or level with the breastfed and/or probiotics group. Additionally, it could be observed that some of those metabolites showed similar patterns in the breastfed and the interventional formula-fed group. This observation could lead to assume that the probiotic formula had the same impact on specific fecal metabolites as breast milk.

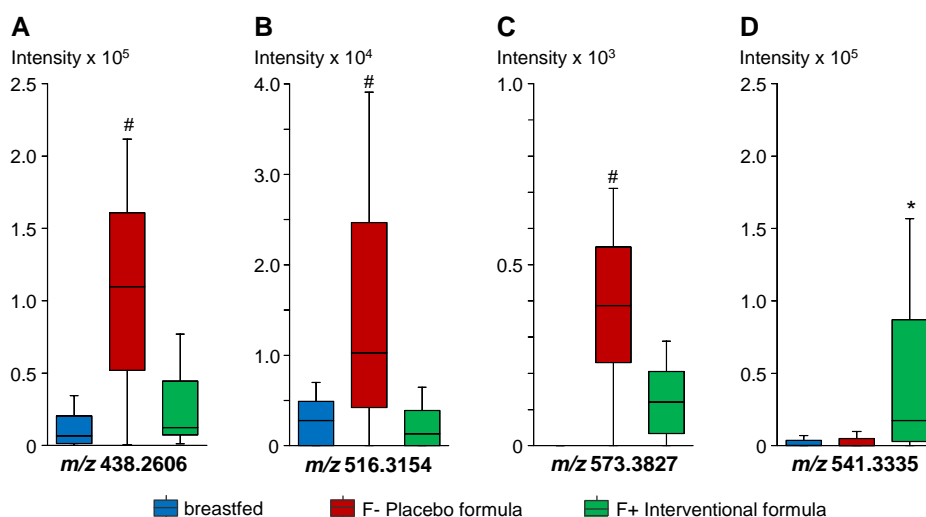


Figure 3.4-22: Mass signals at month 1 significantly changed through placebo or interventional formula.

Boxplots of mass signals significantly increased in placebo formula-fed (A, B, C, red) infants or interventional fed ones (D, green) compared to breast fed infants (blue), analyzed in UHPLC(-)-ToF-MS mode. A: m/z 438.2606 significantly increased in F- fed infants (# p -value < 0.005) in month 1. B: m/z 516.3154 significantly increased in F- fed infants (# p -value < 0.029). C: m/z 573.3827 significantly increased in F- fed infants (# p -value < 0.024) and D: m/z 541.3335 significantly increased in F+ fed infants (* p -value < 0.061). Significance was tested through the *post hoc* Kruskal-Nemenyi test; further details are listed in Table 6.2-18.

Unfortunately, it was not possible to identify the other unknown metabolites or to compare the experimental MS/MS spectra with any database. All mass spectra were compared against METLIN, HMDB and in-silico MS/MS platforms (e.g. MetFrag (Ruttkies et al. 2016)), but did not provide sufficient information for classification or either identification. The applicable experimental MS/MS spectra are displayed in the supplement in chapter 5.2.1.4.

Several changes significantly differed in the F+ and the F- groups were also observed later on in life. This included the mass signals with m/z 378.2958 (month 5) significantly increased in the interventional group (Figure 3.4-23 C). On the contrary, mass signals with m/z 403.2689 (month 9) and m/z 298.1122 (month 12) were significantly increased in the placebo group (Figure 3.4-23 A, B), but their identity remains unclear.

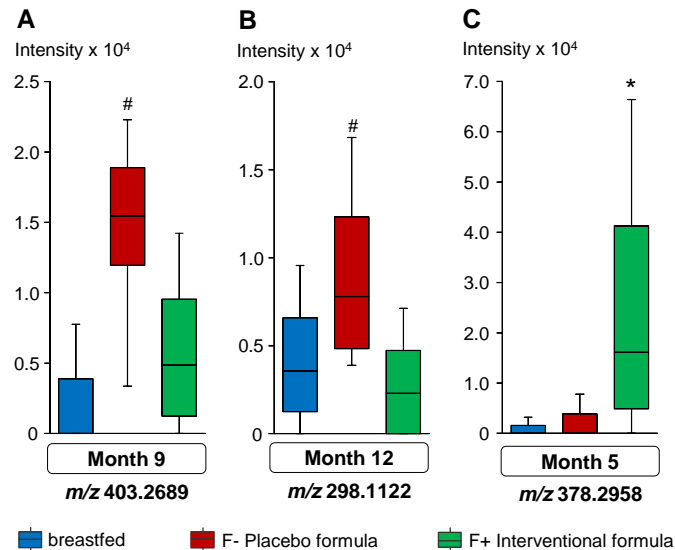


Figure 3.4-23: Mass signals significantly changed through placebo or interventional formula later in life.

Boxplots of mass signals significantly increased in placebo formula-fed (A, B, red) infants or interventional fed ones (C, green) compared to breast fed infants (blue), analyzed in UHPLC(-)-ToF-MS mode. A: m/z 403.2689 significantly increased in F- fed infants (# p-value < 0.038) in month 1. B: m/z 298.1122 significantly increased in F- fed infants (# p-value < 0.032). C: m/z 378.2958 significantly increased in F+ fed infants (# p-value < 0.033). Significance was tested through the *post hoc* Kruskal-Nemenyi test; further details are listed in Table 6.2-18.

To conclude, in the first year of life, differences in the fecal samples of infants either fed with the placebo formula or the interventional formula could be observed, displaying a few mass signals, which were significantly altered through different formula. It was remarkable that the intensity levels of almost all mass signals in the probiotics formula group leads to an approximation towards the breastfed infants. All those mass signals emerged as very important, wherefore not only the identification of those metabolites has top priority, but also further research and long-time studies are needed to evaluate the possible health promoting effect of probiotics on the development of the infant's fecal metabolome.

3.4.4 Correlation studies between OTUs and fecal metabolites of breast- and formula-fed infants

In order to determine microbiome-metabolome characteristics of breastfeeding and formula-feeding, metabolite and microbiota data were combined to search for correlations of metabolites and OTUs at an early (month 1), mid (month 7) and late (month 12) time point. For the correlation, metabolites of the positive or negative ionization mode, respectively and the 16S data of the exclusively fed infants of month 1, 7 and 12 separately were merged and analyzed by OPLS-DA. In order to extrapolate the mass signals and correlated OTUs of month 1, 7 and 12 respectively, which are responsible for the discrimination of the investigated groups (B, F+ and F-), the loadings of each month of the OPLS-DA analysis were extracted. The loadings plots are illustrated in Figure 3.4-24 for UHPLC-(+)-ToF-MS mode (top) and UHPLC-(-)-ToF-MS mode (bottom). Further, CV-ANOVA was applied in order to verify the robustness of each model. Indicators, such as the p-value, the goodness-of-fit $R^2Y(\text{cum})$ and the goodness-of prediction $Q^2(\text{cum})$ were reported (Bazanella et al. 2017) and read as shown in Table 3.4-7.

Table 3.4-7: Orthogonal signal corrected OPLS/O2PLS-DA results from different model comparison.

Mode	Models	$R^2Y(\text{cum})$	$Q^2(\text{cum})$	p-value (CV-ANOVA)
(+) ESI	Month 1	0.94	0.48	$6.72 \cdot 10^{-7}$
	Month 7	0.53	0.38	$1.84 \cdot 10^{-8}$
	Month 12	0.4	0.18	0.0194
(-) ESI	Month 1	0.94	0.53	$1.28 \cdot 10^{-9}$
	Month 7	0.54	0.42	$1.43 \cdot 10^{-9}$
	Month 12	0.34	0.21	0.003

In order to reveal if both of the formula fed groups of month 12 can be separated, an additional orthogonal component was added to the model. It was possible to confirm that no further separation among the Y-axis could be obtained.

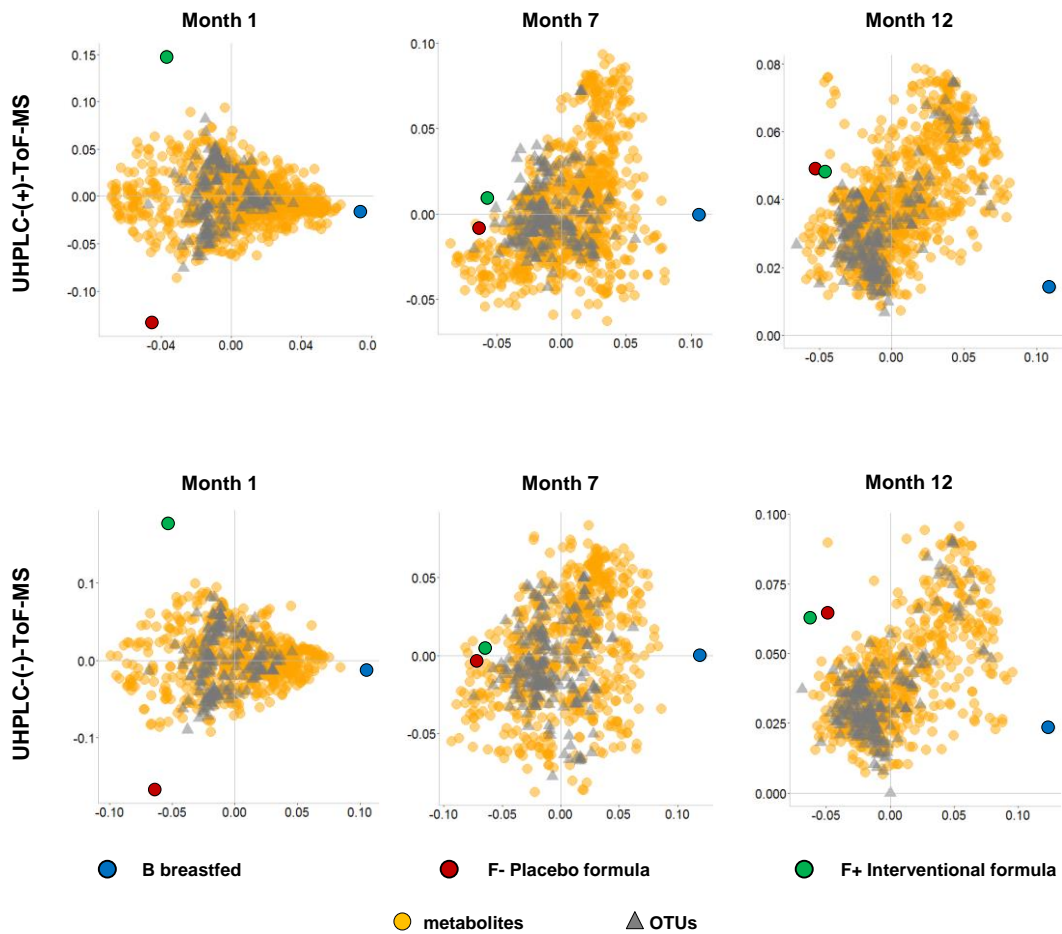


Figure 3.4-24: Correlation studies between metabolites and OTUs at month 1, 7, and 12

Correlations between metabolites and OTUs of month 1, 7 and 12, analyzed in UHPLC-(+)-ToF-MS (top) and UHPLC-(-)-ToF-MS (bottom), obtained through OPLS-DA analyzed and illustrated as loadings plot of all metabolites (yellow) and OTUs (grey) (circles=metabolites, triangle=OTU) Top: month 1, $R^2(\text{cum})=0.94$, $Q^2(\text{cum})=0.48$; $p=6.72 \times 10^{-7}$ (CV-ANOVA); month 7, $R^2(\text{cum})=0.53$, $Q^2(\text{cum})=0.38$; $p=1.84 \times 10^{-8}$ (CV-ANOVA) and month 12, $R^2(\text{cum})=0.47$, $Q^2(\text{cum})=0.106$; $p=0.305$ (CV-ANOVA, orthogonal component). Bottom: month 1, $R^2(\text{cum})=0.94$, $Q^2(\text{cum})=0.53$; $p=1.28 \times 10^{-9}$ (CV-ANOVA); month 7, $R^2(\text{cum})=0.54$, $Q^2(\text{cum})=0.42$; $p=1.43 \times 10^{-9}$ (CV-ANOVA) and month 12, $R^2(\text{cum})=0.34$, $Q^2(\text{cum})=0.21$; $p=0.003$ (CV-ANOVA, orthogonal component)

Relatively less information about specific metabolites, which differ in fecal samples of healthy breast fed or formula fed infants – except bile acids and SCFA – is available. Therefore, the non-targeted metabolomics approach enabled to evaluate a broader range of discriminating metabolites, containing known and unknown features and their correlated OTUs in fecal samples of the exclusively breast milk, interventional and placebo group.

Moreover, through correlation experiments of all metabolites and OTUs, 6 OTUs were detected, which are involved in the separation of the different feeding groups and contribute in the feeding-specific shaping of the fecal ecosystem at month 1 (Bazanella et al. 2017). Furthermore, the correlation revealed a relation between F+ specific metabolites and two species (OTU 4, *Bifidobacterium bifidum*; OTU 142,

Lactococcus sp.) in month 1. In contrast, some F- specific metabolites were related with *Bacteroides* sp. (OTU 10, OTU 18) (Bazanella et al. 2017).

In month 7, a relation between *Bifidobacterium* sp. (OTU 1) and specific metabolites was detected in month 7. On the contrary, through formula feeding, a correlation with *Flavonifractor* sp. (OTU 29) showed up. Also, in month 12, several correlations among metabolites and OTUs were observed in the formula-fed infants, including *Flavonifractor* sp. (OTU 29) and *Coprobacillus* sp. (OTU 125). Further details are given in Table 3.4-8. The most important mass signals and correlated OTUs for each month and within each feeding group (B, F, F+ and F+) were illustrated in Figure 3.4-25 and listed by rank from high to low importance for month 1 in Table 6.2-19, for month 7 in Table 6.2-20 and for month 12 in Table 6.2-21.

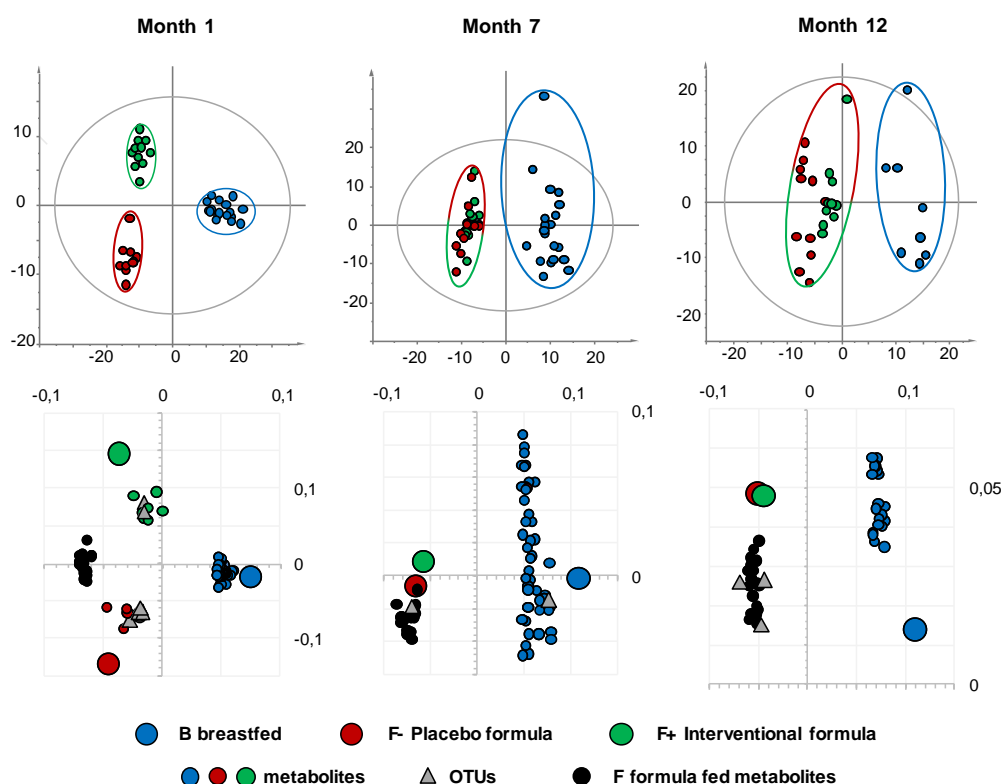


Figure 3.4-25: Correlation studies between metabolites and OTUs at month 1, 7, and 12.

Correlations between metabolites and OTUs of month 1, 7 and 12, analyzed in UHPLC-(+)-ToF-MS, obtained through OPLS-DA analyzed and illustrated as scores plot (top) and loadings plot of main discriminating and correlating features (circles=metabolites, triangle=OTU; bottom) of month 1, $R^2(\text{cum})=0.94$, $Q^2(\text{cum})=0.48$; $p=6.72 \times 10^{-7}$ (CV-ANOVA); month 7, $R^2(\text{cum})=0.53$, $Q^2(\text{cum})=0.38$; $p=1.84 \times 10^{-8}$ (CV-ANOVA) and month 12, $R^2(\text{cum})=0.47$, $Q^2(\text{cum})=0.106$; $p=0.305$ (CV-ANOVA, orthogonal component). Further details are listed in Table 6.2-19 (month 1), Table 6.2-20 (month 7) and Table 6.2-21 (month 12). From Bazanella, M., Maier, T. V., Clavel, T., Lagkouvardos, I., Lucio, M., Maldonado-Gómez, M. X., Autran, C., Walter, J., Bode, L., Schmitt-Kopplin, P., Haller, D.: Randomized controlled trial on the impact of early-life intervention with bifidobacteria on the healthy infant fecal microbiota and metabolome. *Am J Clin Nutr.* (2017), 106(5):1274-1286. Reprinted and adapted from (Bazanella et al. 2017) by permission of Oxford University Press. Copyright (2017) American Society for Nutrition.

Table 3.4-8: Correlation between feeding cohort specific metabolites and OTUs.

Correlations between the feeding cohort specific metabolites and OTUs of month 1, 7 and 12 were obtained through Pearson correlation, recording the correlation coefficient (r), and the degrees of freedom (df), as well as p -corr values calculated through regression analysis. Table contains m/z of mass signals obtained through UHPLC-(+)-ToF-MS analysis, compound name, if possible and month, the correlation was observed at. From Bazanella, M., Maier, T. V., Clavel, T., Lagkouvardos, I., Lucio, M., Maldonado-Gómez, M. X., Autran, C., Walter, J., Bode, L., Schmitt-Kopplin, P., Haller, D.: Randomized controlled trial on the impact of early-life intervention with bifidobacteria on the healthy infant fecal microbiota and metabolome. *Am J Clin Nutr.* (2017), 106(5):1274-1286. Reprinted and adapted from (Bazanella et al. 2017) by permission of Oxford University Press. Copyright (2017) American Society for Nutrition.

Feed	m/z	retention time [min]	Compound	Month	OTU	ID	r	p -corr	df
F-	440.2844	6.12	LysoPE(15:0/0:0)	Month 1	<i>Bacteroides sp.</i>	OTU 10	0.75	7.21E-08	36
F-	616.3490	6.36	no metabolite found	Month 1	<i>Bacteroides sp.</i>	OTU 18	0.57	2.14E-04	36
F+	813.5680	4.79	no metabolite found	Month 1	<i>Bifidobacterium sp.</i>	OTU 4	0.49	2.00E-03	36
F+	417.3345	6.72	no metabolite found	Month 1	<i>Lactococcus sp.</i>	OTU 142	0.45	4.16E-03	36
B	206.0830	3.62	no metabolite found	Month 7	<i>Bifidobacterium sp.</i>	OTU 1	0.52	3.94E-04	40
B	261.1469	2.80	no metabolite found	Month 7	<i>Bifidobacterium sp.</i>	OTU 1	0.54	1.89E-04	40
F	417.3371	9.53	no metabolite found	Month 7	<i>Flavonifractor sp.</i>	OTU 29	0.42	5.60E-03	40
F	407.2455	3.05	no metabolite found	Month 7	<i>Flavonifractor sp.</i>	OTU 29	0.54	1.78E-04	40
F	427.3608	7.53	no metabolite found	Month 12	<i>Flavonifractor sp.</i>	OTU 29	0.64	2.90E-04	25
F	303.1916	3.16	no metabolite found	Month 12	<i>Flavonifractor sp.</i>	OTU 29	0.58	1.37E-03	25
F	447.3480	7.64	no metabolite found	Month 12	<i>Coprobacillus sp.</i>	OTU 125	0.54	3.58E-03	25

Through correlations of metabolites of the negative ionization mode and OTUs, also no correlations up to the top 50 highest ranked metabolites and OTUs affected through breastfeeding were observed in month 1. The most important mass signals and correlated OTUs for each month and within each feeding group (B, F, F+ and F+) were illustrated in Figure 3.4-26.

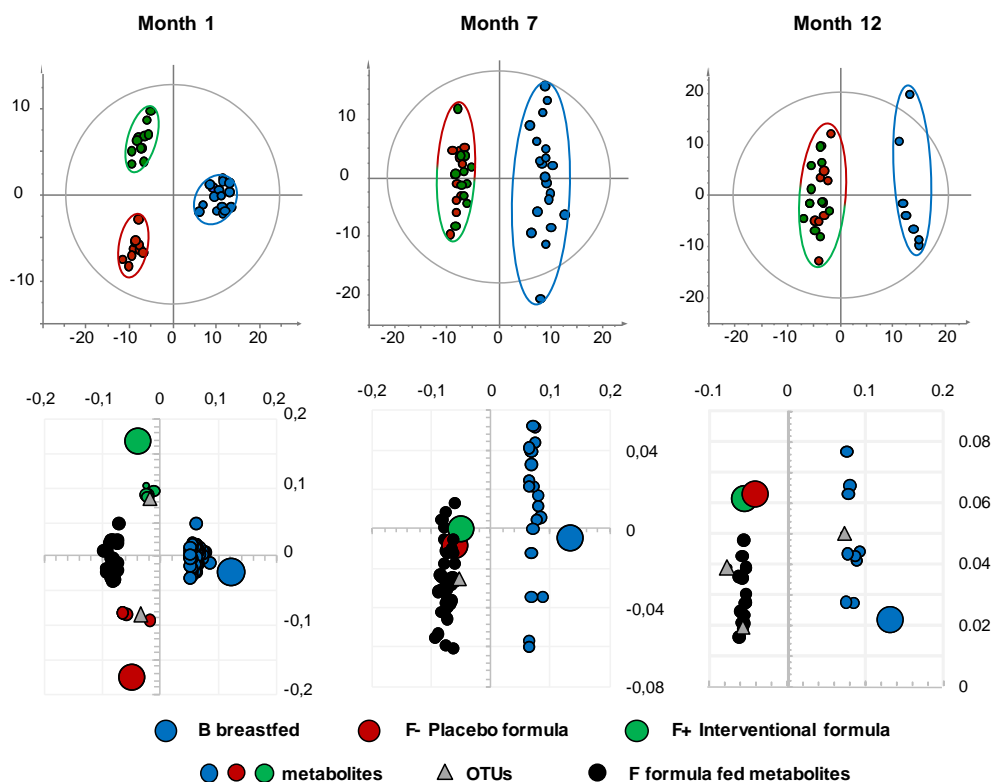


Figure 3.4-26: Correlation studies between metabolites and OTUs at month 1, 7, and 12.

Correlations between metabolites and OTUs of month 1, 7 and 12, analyzed in UHPLC(-)-ToF-MS, obtained through OPLS-DA, analyzed and illustrated scores plot (top) and loadings plot of main discriminating and correlating features (circles=metabolites, triangle=OTU; bottom) of month 1, $R^2(\text{cum})=0.94$, $Q^2(\text{cum})=0.53$; $p=1.28 \times 10^{-9}$ (CV-ANOVA); month 7, $R^2(\text{cum})=0.54$, $Q^2(\text{cum})=0.42$; $p=1.43 \times 10^{-9}$ (CV-ANOVA) and month 12, $R^2(\text{cum})=0.34$, $Q^2(\text{cum})=0.21$; $p=0.003$ (CV-ANOVA, orthogonal component). Further details are listed in Table 6.2-22 (month 1), Table 6.2-23 (month 7), and Table 6.2-24 (month 12).

On the contrary, a correlation between F+ specific metabolites, especially the unknown m/z 541.3335 and *Bifidobacterium* sp. (OTU 4) could be revealed. In the placebo formula group, a relationship between metabolites of the F- metabolites and *Bacteroides* sp. (OTU 10), especially with m/z 438.2606, which was already correlated to OTU 10 evaluating the data of the positive ionization. Through (+) ToF MS/MS experiments and the comparison of the experimental MS/MS spectra with the METLIN database, it was previously classified as LysoPE (15:0/0:0). LysoPE (15:0) recently was detected by Faith et al., who claimed metabolite-microbial community interactions among lysophosphatidylethanolamine (LysoPE15) and *Bacteroides* species in cecum samples. They observed increased concentrations of LysoPE15 if *B. ovatus* or *B. vulgatus* are present and reach its highest concentration levels if both species are present (Faith et al. 2014). Main correlated features are listed by rank from high to low importance for month 1 in Table 6.2-22, for month 7 in Table 6.2-23 and for month 12 in Table 6.2-24.

In month 7, *flavonifractor sp.* (OTU 29) showed up as correlated to traumatic acid in the formula-fed group, whereas no correlation was observed between metabolites and OTUs impacted through breastfeeding. Here, in month 12 also a correlation of *enterococcus sp.* (OTU 14) and metabolites significant for the breastfed infants was detected. In the formula-fed group *flavonifractor sp.* (OTU 29) and the bile acid 6-lithocholic acid were highly correlated. Further details are listed in Table 3.4-9.

Table 3.4-9: Correlation between feeding cohort specific metabolites and OTUs.

Correlations between the feeding cohort specific metabolites and OTUs of month 1, 7 and 12 were obtained through Pearson correlation, recording the correlation coefficient (r), and the degrees of freedom (df), as well as p -corr values calculated through regression analysis. Table contains m/z of mass signals obtained through UHPLC(-)-ToF-MS analysis, compound name, if possible and month, the correlation was observed at.

Feed	m/z	retention time [min]	Compound	Month	OTU	ID	r	p -corr	df
F-	438.2606	6.10	no metabolite found	Month 1	<i>Bacteroides sp.</i>	OTU 10	36	8.39E-05	0.59
F+	541.3335	5.47	no metabolite found	Month 1	<i>Bifidobacterium sp.</i>	OTU 4	36	4.00E-03	0.45
F	227.1281	5.16	Traumatic acid	Month 7	<i>Flavonifractor sp.</i>	OTU 29	40	4.00E-03	0.43
F	435.2754	5.46	no metabolite found	Month 7	<i>Flavonifractor sp.</i>	OTU 29	40	2.41E-05	0.60
B	583.2704	4.87	no metabolite found	Month 12	<i>Enterococcus sp.</i>	OTU 14	26	3.21E-05	0.70
B	546.1973	0.93	no metabolite found	Month 12	<i>Enterococcus sp.</i>	OTU 14	26	4.55E-03	0.52
F	389.2686	5.89	6-Lithocholic acid	Month 12	<i>Flavonifractor sp.</i>	OTU 29	26	4.00E-03	0.61
F	389.2685	6.74	no metabolite found	Month 12	<i>Flavonifractor sp.</i>	OTU 29	26	9.58E-05	0.67

As in month 1 no correlations among highly significant metabolites impacted through breastfeeding and OTUs were observed. It encourages the assumption that the metabolites are a major driver for the discrimination of breast- from formula-fed groups. It was already observed that the differences between breast and formula groups were maintained until the end of intervention at 1 year, but it's remarkable that the correlations of metabolites and OTUs were highly present in the formula-fed group, and the OTUs play an important part in contributing to the discrimination of F+ and F-, as seen in month 1. On the contrary, considering the highly significant discriminative features impacted through breastfeeding in month 1, 7 and 12, it appeared predominantly driven by metabolites, rather than through OTUs, even if the metabolites are gaining lesser influence on the discrimination of those two groups in later life. Abdulkadir et al. evaluated the use of probiotics in preterm infants and their impact on the microbiome and metabolome (Abdulkadir et al. 2016). They concluded that metabolite profiles are different between probiotic and control groups. This result strengthens our results on the discrimination of breast fed and formula fed infants over time.

3.4.5 Delivery effects on the infant fecal metabolome

It is already known, that the infant microbiota is impacted by the mode of delivery (Gronlund et al. 1999, Mackie et al. 1999, Penders et al. 2006, Dominguez-Bello et al. 2010). During vaginal birth, the neonate is mainly exposed to maternal bacteria through the birth canal, and the birth canal is occupied by a characteristic set of bacteria (Dominguez-Bello et al. 2010), which pass over and forms the infants microbiota. Further, after birth the GIT of infants get colonized immediately through environmental and skin exposure of the mother (Biasucci et al. 2008). The GIT shows distinct patterns of the microbial composition in infants born by C-section or by vaginal birth.

Knight et al. showed that the infants gut microbiota born by C-section is similar to the mother's skin microbiota. The infants born vaginally showed similar patterns to the mother's vaginal microbiota (Dominguez-Bello et al. 2010). It was observed, that the bacterial composition in infants born by C-section was less diverse, than those born vaginally with predominating groups of Bifidobacteria species (Biasucci et al. 2008). Those altered microbial compositions in either infant born by C-section or by vaginal birth may also result to a differently impacted fecal metabolome. Hereof, relatively few studies were available evaluating the possible relationship between the mode of delivery and the metabolome (Fanos et al. 2012).

However, in 2009, Hyde et al. detected a modified metabolomics profiles in liver samples of piglets due to the mode of delivery, mentioning higher levels of oxaloacetate, aspartate, α -ketoglutarate and glutamate and lower levels of glucose and succinate in the cesarean born piglets (Hyde et al. 2009). Also Diaz et al. observed distinct urinary NMR metabolite signatures significantly ($p < 0.05$) changed through the different mode of delivery, such as trigonelline and indoxyl sulfate (in vaginal delivery) or acetone and dimethylamine (in cesarean section) (Diaz et al. 2016). Nevertheless, studies investigating the mode of delivery into relation to the metabolome, especially considering human individuals and the fecal metabolome are rare.

In order to evaluate the impact of the mode of delivery on the metabolite profile, the fecal samples of either VD or CS were analyzed by month, without considering the type of feeding. In order to detect only mass signals significant for the different modes of delivery, mass signals impacted though feeding were eliminated. Through the application of the Mann-Whitney test (p -value > 0.01) and log₂ fold change calculations, five metabolites were detected as significantly impacted by the mode of delivery

(Bazanella et al. 2017) in month 1, but which could not persist in the following months, namely metabolites with the nominal mass 344 (positive ionization mode) and 328, 280, 890 and 288 (negative ionization mode).

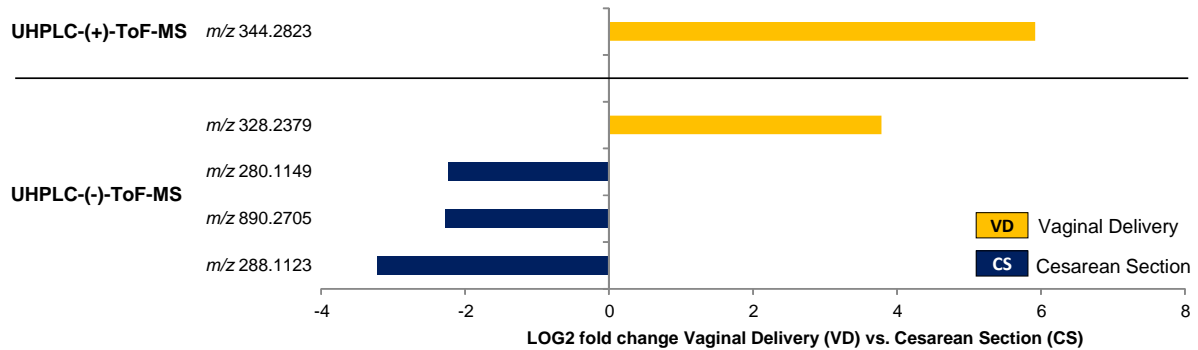


Figure 3.4-27: Differences in the metabolite profile due to cesarean or vaginal delivery in month 1.

Log₂ fold change values for metabolites increased or decreased through vaginal delivery (yellow) or cesarean section (blue), analyzed in HPLC-(+)-ToF-MS (top) and UHPLC-(-)-ToF-MS (bottom) mode.

The mass signals were assigned to metabolites listed in databases but did not reveal useful information. Nevertheless, this study showed that the fecal metabolome was impacted by the mode of delivery in early life stages, even if no further information was given on the origin and the classification of the metabolites. In respect thereof, MS/MS experiments may be helpful to characterize the metabolome or possibly identify those metabolites impacted by mode of delivery in early life stages. This may further lead to a better understanding of the impact of the mode of delivery, in relation to health-promoting effects and the developing microbiota and their corresponding metabolome.

3.5 Summary and Conclusion

The aim of the study was to elucidate the impact of breast feeding and two different formulas, one without, the other with bifidobacteria-supplementation (probiotics) on the fecal metabolome of healthy infants by applying ultra-high performance liquid chromatography-mass spectrometry based metabolomics approach, in a double-blinded, randomized and placebo controlled intervention trial. Additional 16S rRNA sequencing complemented the analysis in order to investigate the complex interplay between organisms and metabolites.

Probiotic supplementation of infant formula became popular, aiming at beneficially influencing the gut microbiome and infant well-being. However, only little is known about the effects of probiotic-supplemented formula on the development of the intestinal ecosystem. Therefore, during the first year of life, infants were fed a bifidobacteria-supplemented (intervention) or non-supplemented (placebo) formula, either from birth on or after weaning. The infants were divided into two main groups, including exclusively fed infants and mixed fed infants, whereas analyses were performed concentrating on the exclusively fed infants. This allowed a more precise evaluation of the impact of breast feeding and formula feeding with or without probiotics on the infants' gut microbiome. Monthly fecal samples up to one year of age were collected, in order to evaluate the overall fecal metabolite and microbiota profile impacted through breast feeding, interventional formula and the placebo formula.

The metabolite profile showed a clear separation between breastfed infants and formula-fed ones in early life stages, which converged over time. The monthly evaluation of the data revealed slightly differences in the metabolite profiles between the interventional and placebo formula group in month 1, which identity remains unclear. However, one metabolite discriminative between both formula and increased in the placebo formula-fed infants could be identified as a lysophosphatidylethanolamines (LysoPE) 15:0/0:0. It was remarkable that several metabolites of the probiotics formula group leads to an approximation towards the breastfed infants. This finding leads to the assumption that probiotic supplementation may help to approximate breast milk and strengthened the use of probiotics. However, the occurrence of these similar effects remains still unknown and for the moment was suggestively an initial sign for the effects of probiotics. To investigate the impact of probiotics in contrast to breast milk, further research is strongly needed.

Additionally, the metabolomics approach revealed that through breast- and formula feeding, pathways of the lipid metabolism showed to be highly impacted, especially metabolites of the primary bile acid biosynthesis. The glycine-conjugated bile acids (GCDCA and GCA) were increased in the formula-fed infants over time. Several bile acids were affected differently in the two formula groups. While some bile acids in the probiotics group lead to an approximation towards the breastfed infants, they were increased in the non-probiotic group. Further, the sulfated bile acids (cyprinolsulfate and sulfocholic acid) were erratically increased and widely spread in breastfed infants over time, whereat the pattern in the formula-fed ones was quite lower and rather consistent. The fecal samples of the infants fed with formula showed increased levels of intermediates of the vitamin E biosynthesis, which were not only correlated with each other, but also highly correlated with the amount of formula the infants were fed with.

It was observed that different fatty acid classes, such as saturated, unsaturated and hydroxylated fatty acids were significantly different between the breast fed infants and the formula-fed ones. Further, SCFA were analyzed which revealed increased levels of lactic acid and pyruvic acid in the breast fed infants, whereas propionic acid, butyric acid, valeric acid and isovaleric acid were significantly different in the formula-fed infants. However, SCFA profiles were not different between the interventional and the placebo formula fed infants. The correlation between SCFA and OTUs revealed positive correlations between lactic acid and species of the *Bifidobacterium*, *Streptococcus* and *Lactobacillus*, all LAB bacteria in the gut. Moreover, the correlation of all metabolites and OTUs revealed 6 OTUs being involved in the feeding-specific shaping of the fecal ecosystem at month 1. Both, metabolomic and the 16S data revealed that the differences in bacterial and metabolite profiles between interventional and placebo groups disappeared over time. Further, the fecal samples of the infants were evaluated to detect differences in the metabolite profile due to cesarean section or vaginal delivery, which revealed some metabolites to be discriminating between both modes of delivery. In conclusion, this placebo-controlled intervention study clearly showed that bifidobacteria-supplemented formula modulates the infant fecal metabolome and microbiome at very early stages in life, with no detectable long-term consequences for gut microbiome assembly or function. The impact of sequentially changing bacterial and metabolite profiles on human health remained completely unclear and requires additional studies.

Chapter IV

4 Thesis summary and concluding remarks

The presented thesis illustrates two mass spectrometry based metabolomics studies to evaluate the nutritional impact of prebiotics (chapter II) and probiotics (chapter III) on the human gut microbiome and its related effects on host and gut metabolism. Non-targeted metabolite analyses were performed in negative and positive ionization mode and results were used to guide a subsequent series of targeted metabolite analyses. Additional 16S rRNA sequencing and shotgun proteomics complemented the analysis in order to investigate the complex interplay between organisms, metabolites and functional processes in the adult and infant gut microbiome.

Dietary starch affected the adult fecal metabolome differently, while the time point of starch consumption is negligible. Characteristic differences in the fecal metabolome between differently digestible carbohydrates (resistant starch type 2) were observed in a controlled, randomized, within-subjects' crossover dietary intervention trial of participants suffering from insulin resistance. Diet with high resistant starch affected the fecal metabolome immensely. Thereto, the ultra-high resolution FT-ICR-MS based metabolomics approach was highly suitable for investigating the function of the gut microbiome and host metabolism and helped to evaluate the effect of different diets. Additionally, it made a comprehensive overview of metabolites from different chemical classes and pathways available. Specific fatty acids, bile acids, oxylipins and several compounds of the lipid metabolism were strongly affected by digestion of different prebiotics, compared to the non-dietary starch diet. These also include finding novel links between a RS diet and lipid metabolism by the host and microbiome. Especially lipids, namely phosphatidic acids showed differently altered patterns by the consumption of carbohydrates varying in the amount of dietary starch. However, cyclic phosphatidic acids showed decreased intensity levels through dietary starch intake.

The high amount of resistant starch altered the fecal microbial composition arising with a high abundance of *Firmicutes*, especially *Faecalibacterium prausnitzii* and *Eubacterium rectale*, whereas the abundance of *Bacteroides* was low. The applied shotgun proteomics approach allowed classifying thousands of host and microbial proteins impacted by resistant starch and confirmed several results already observed through the metabolomics analyses, such as the impact of RS on the lipid metabolism.

Understanding the complexity arising in the human gut, including its microbial composition, host and/or microbial metabolism, protein expression, as well as the metabolic status is of top priority to understand the impact of diet, especially of varying amounts of non-digestible carbohydrates. Therefore, the applied multi-omics integration enabled to gain a deeper insight into main effects of the resistant starch diet on the gut microbiome and functions that they carry out. These results emphasize the importance of further multi-omics study designs, to clarify the effects of nutrition on the microbiome and health.

Long-term effects of probiotic baby food on gut physiology are widely unknown, wherefore research is still needed. Additionally, long-term effects of probiotics on the gut microbiota need to be investigated due to the decrease of willingness for weaning. The focus should be laid on the effect of probiotics on the healthy, developing gut microbiota of newborns. Thus, the second part of the thesis discussed the impact of diet on the infant gut microbiome. This study wanted to investigate the impact of probiotics on the gut microbiota and fecal metabolome within the first year of life. By means of metabolomics, detailed information of the fecal metabolome and differences within feeding types was achieved.

Metabolite profiles were clearly distinct between breast- and formula-fed infants, and they converged overtime. The metabolite profiles were altered differently through breastfeeding and formula, independent of type of formula. However, in the probiotics group several metabolites occurred that showed similar patterns as the breastfed infants. Several distinct metabolic effects were seen that made the use of probiotic formula feeding more similar to breast milk. Probiotic supplementation may help to approximate breast milk. However, these similar effects cannot yet be explained and their occurrence remains still unknown and these results were suggestively initial signs for the effects of probiotics. Accordingly, the overall metabolite pattern was still more similar between the two formulas than between probiotics supplementation and breast milk. Therefore, further research is needed in order to optimize probiotics in terms of selection of strains, route of administration and dose.

Pathways analysis revealed the lipid metabolism, especially the bile acid biosynthesis to be differently impacted by breast- and formula-feeding. While breastfeeding seemed to influence sulfated bile acids, formula revealed high levels of glycine conjugated bile acids. Further metabolites altered by breastfeeding were identified as carboxylic acids and numerous fatty acids, varying in chain length and saturation degree. On the contrary, fecal sample of the formula-fed infants were dominated by several metabolites of the tocopherol biosynthesis, carboxylic acids and oxylipins.

Generally, formula-feeding lead to significantly higher proportions of propionic, butyric, valeric and isovaleric acid, whereas the fecal samples of breastfed infants were dominated by pyruvic and lactic acid. Correlations studies revealed lactic acid and pyruvic acid to be highly associated with species, such as *Bifidobacterium sp.*, *Streptococcus sp.* and/or *Lactobacillus sp.* Additional correlation studies of the whole metabolomics and microbiome set revealed several relationships between metabolites and OTUs over time involved in the feeding-specific groups, which were shaping the fecal ecosystem and therefore contribute to the separation of the feeding groups. Of particular interest was the relation between F+ specific metabolites and two species, namely *Bifidobacterium bifidum* and *Lactococcus sp.*, in contrast to the correlation of F- specific metabolites and *Bacteroides spp.* Breastfed specific metabolites seem not to be set into relation with characteristic species. Nevertheless, metabolites were the driving force behind the class discrimination of breastfed and formula-fed infants over time. In conclusion, the study demonstrated that the infant microbiome and metabolome can be altered by bifidobacteria-supplemented formula in early life. These results support the assumption that probiotics partially alter the infant microbiome and metabolome towards a similar impact owing to breastfeeding. Accordingly, consideration should also be which metabolic effects are of interest through probiotic supplementation to approximate breast milk, e.g. the bile acid metabolism to improve fat digestion, customize SCFA profile or to improve protein digestion to enable the settlement of phenyl lactate- or p-cresol sulfate-producer. Depending on this, specific strains should be selected for supplementation.

It was demonstrated that fecal samples were highly suitable to evaluate the impact of diet on the human gut microbiome. Many mass signals were observed to be altered with diet as well, whose identity remains still unknown. Dealing with the unknown and identifying metabolites was difficult and demanding and is still a major drawback in metabolomics, which poses many challenges of experimental and analytical nature. This harbors several difficulties in data evaluation and interpretation. Nevertheless, fecal non-targeted metabolomics came out as a powerful discipline to discover the impact of diet on the human microbiome. A series of targeted analyses revealed in both studies, that especially the metabolite classes of fatty acids, carboxylic acids and steroids, such as bile acids were affected by diet, as well as metabolites of the lipid metabolism. In both studies a comprehensive overview of metabolites from different chemical classes and pathways were detected to be highly impacted by pre- and probiotics.

Chapter V

5 Supplementary data

5.1 Dietary study

5.1.1 MS/MS identification experiments

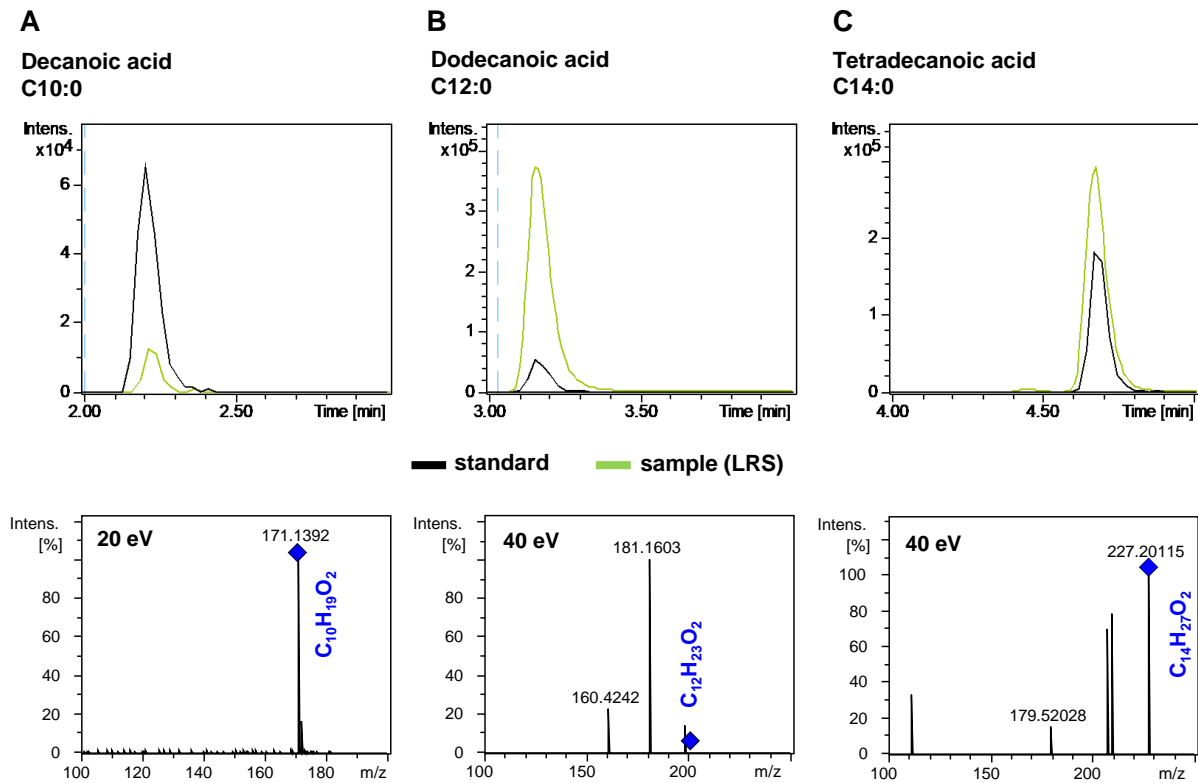


Figure 5.1-1: Identification of (A) decanoic acid, (B) dodecanoic acid, and (C) tetradecanoic acid.

Extracted ion chromatograms (EICs) (top) and MS/MS spectra (bottom) acquired in (-)-ToF-MS mode of decanoic acid (20 eV), dodecanoic acid (40 eV) and tetradecanoic acid (40 eV) of samples (green) and respective standards (black). From Maier, T. V.; Lucio, M.; Lee, L. H.; VerBerkmoes, N. C.; Brislawn, C. J.; Bernhardt, J.; Lamendella, R.; McDermott, J. E.; Bergeron, N.; Heinzmann, S. S.; Morton, J. T.; González, A.; Ackermann, G.; Knight, R.; Riedel, K.; Krauss, R. M.; Schmitt-Kopplin, P.; Jansson, J. K.: Impact of Dietary Resistant Starch on the Human Gut Microbiome, Metaproteome, and Metabolome. *mBio* vol. 8 no. 5 e01343-17 (2017). Illustration of Figure B and C was modified from (Maier et al. 2017). Copyright (2017) Maier et al., Information about the creator and respective contributions, as well as the original material are available: <http://mbio.asm.org/content/8/5/e01343-17.full> with the original title: Identification of decanoic (C12:0) and tetradecanoic acid (C14:0). Licence notice: <https://creativecommons.org/licenses/by/4.0/>.

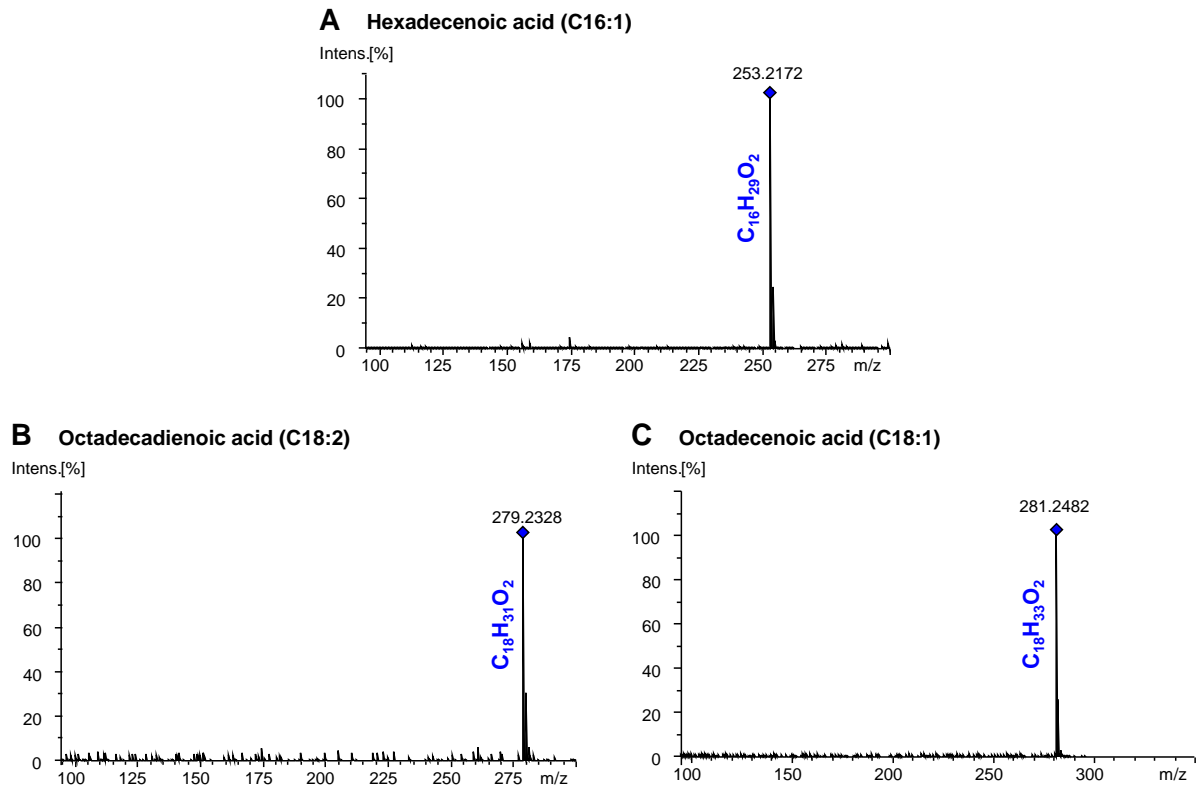


Figure 5.1-2: Fatty acids in the human fecal metabolome significantly increased in the baseline diet.

Experimental (-)-ToF-MS/MS spectra of (A) hexadecenoic acid (C16:1), (B) octadecadienoic acid (C18:2) and (C) octadecenoic acid (C18:1) increased in the fecal samples of the baseline diet. A: Hexadecenoic acid (C16:1) m/z 253.2172, at retention time 5.5 minutes. B: Octadecadienoic acid (C18:2) (m/z 279.2328) at retention time 6.05 minutes. C: Octadecenoic acid (C18:1) (m/z 281.2485) at retention time 7.58 minutes. Analyses were performed by UHPLC-ToF-MS

5.2 InfantBio-study

5.2.1 MS/MS identification experiments

Identification of the metabolites was carried out through (+) and (-) TOF-MS/MS experiments as described in chapter 3.3.7. Experimental MS/MS spectra were compared manually with METLIN database (Smith et al. 2005) and mostly against the experimental MS/MS spectra obtained from standards, measured under the same conditions.

5.2.1.1 Bile acids

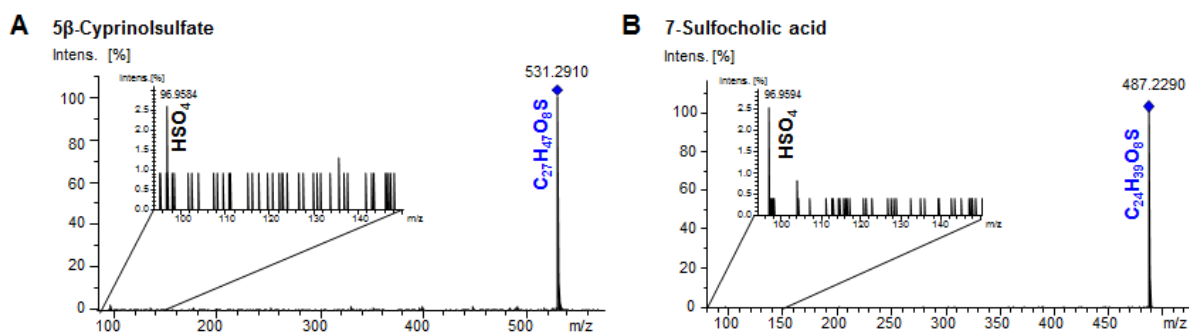


Figure 5.2-1: Experimental (-)-ToF-MS/MS spectra of bile acid sulfate conjugates.

Experimental (-)-ToF-MS/MS spectra of (A) cyprinolsulfate and (B) Sulfocholic acid increased in breastfed infants. A: Cyprinolsulfate (m/z 531.2910) at retention time 4.71 minutes. B: Sulfocholic acid (m/z 487.2290) at retention time 4.48 minutes. Analyses were performed by UHPLC-ToF-MS.

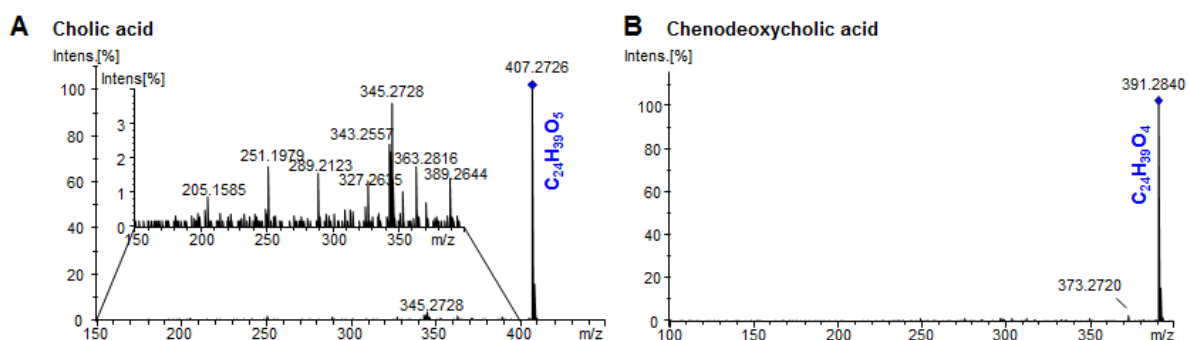


Figure 5.2-2: Experimental (-)-ToF-MS/MS spectra of primary bile acids.

Experimental (-)-ToF-MS/MS spectra of (A) cholic acid and (B) chenodeoxycholic acid, identified in breast fed and formula-fed infants. A: Cholic acid (m/z 407.2818) at retention time 5.15 minutes. B: Chenodeoxycholic acid (m/z 391.2852) at retention time 5.85 minutes. Analyses were performed by UHPLC-ToF-MS.

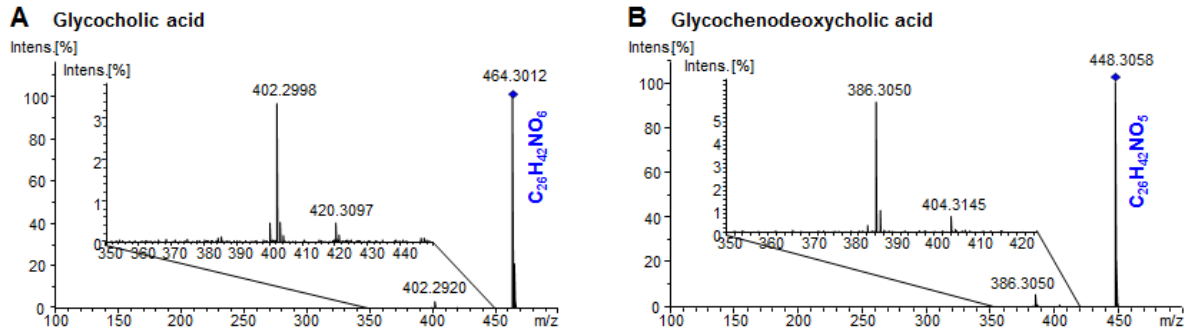


Figure 5.2-3: Experimental (-) ToF-MS/MS spectra of bile acid glycine conjugates.

Experimental (-)ToF-MS/MS spectra of (A) glycocholic acid and (B) glychenodeoxycholic acid, acid increased in formula-fed infants. A: Glycocholic acid (m/z 464.3007) at retention time 4.69 minutes. B: Glychenodeoxycholic acid (m/z 448.3070) at retention time 5.22 minutes. Analyses were performed by UHPLC-ToF-MS.

5.2.1.2 Fatty acids altered in either breastfed or formula-fed infants

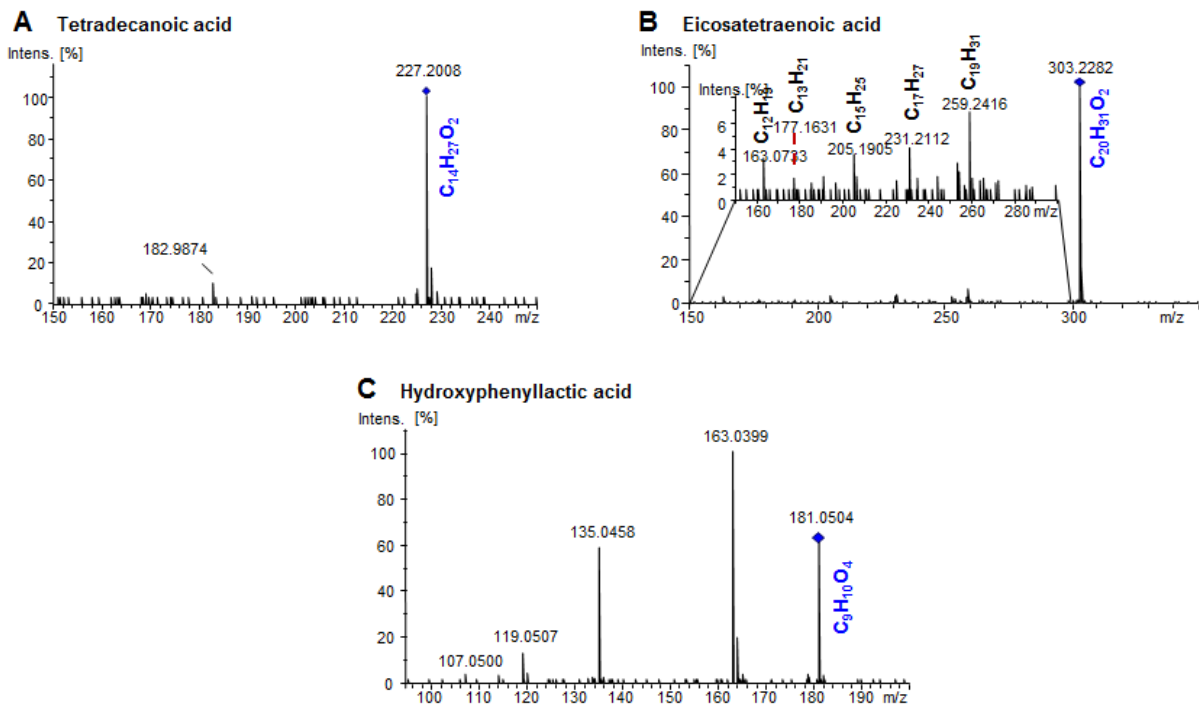


Figure 5.2-4: Experimental (-)ToF-MS/MS spectra of metabolites increased in breastfed infants.

A: Tetradecanoic acid (m/z 227.2007) at retention time 7.22 minutes. B: Eicosatetraenoic acid (m/z 303.2316) at retention time 7.25 minutes. C: Hydroxyphenyllactic acid (m/z 181.0504) at retention time 2.81 minutes. Analyses were performed by UHPLC-ToF-MS.

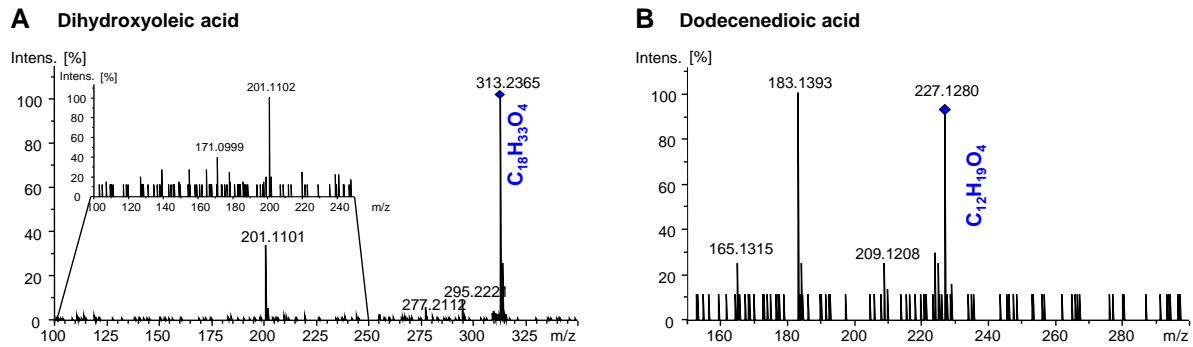


Figure 5.2-5: Experimental (-)-ToF-MS/MS spectra of fatty acids increased in formula-fed infants.

A: Dihydroxyoleic acid (m/z 313.2336) at retention time 5.64 minutes. B: Dodecenedioic acid (m/z 227.1280) at retention time 5.16 minutes. Analyses were performed by UHPLC-ToF-MS.

5.2.1.3 Unknowns, but highly significant affected by either breast milk or formula

Through the statistical evaluation several metabolites were detected impacted through either breastfeeding or formula and were significantly changed in those two groups over time. MS/MS experiments were applied in (+) ESI (Chapter 5.2.1.3.1) and (-) ESI (Chapter 5.2.1.3.2) mode and different collision energies in order to identify or even classify these important metabolites, responsible for the discrimination. However, the performed MS/MS experiments did not provide sufficient information about the identity or the classification of the metabolites.

5.2.1.3.1 (+) ToF-MS

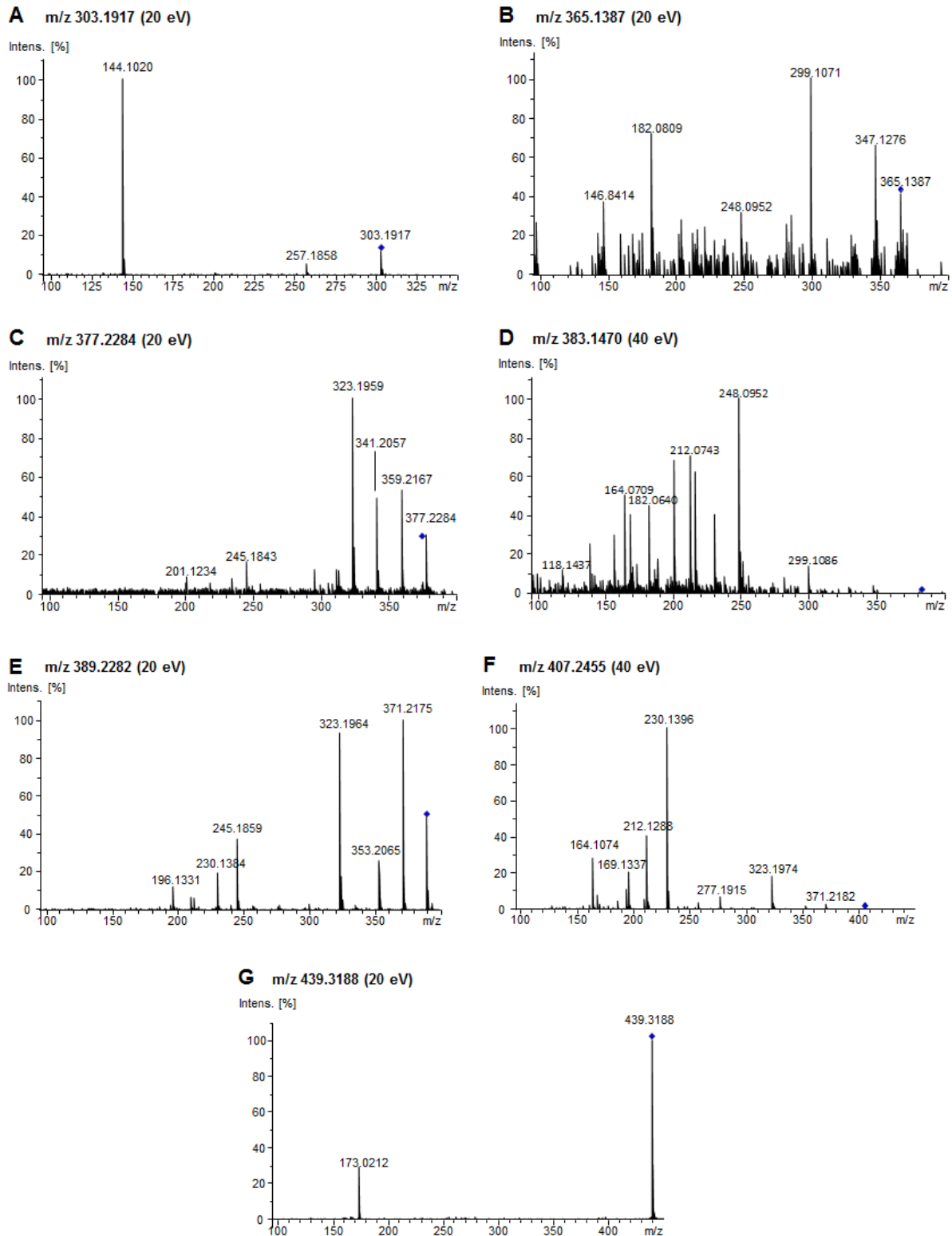


Figure 5.2-6: Experimental (+) ToF-MS/MS spectra of unknown features increased in formula-fed infants.

A: m/z 303.1917, RT 3.16 min. B: m/z 365.1387, RT 1.20 min. C: m/z 377.2284, RT 3.10 min. D: m/z 383.1470, RT 1.21 min. E: m/z 389.2282, RT 3.04 min. F: m/z 407.2455, RT 3.05 min. G: m/z 439.3188, RT 8.51 min. Analyses were performed by UHPLC-ToF-MS.

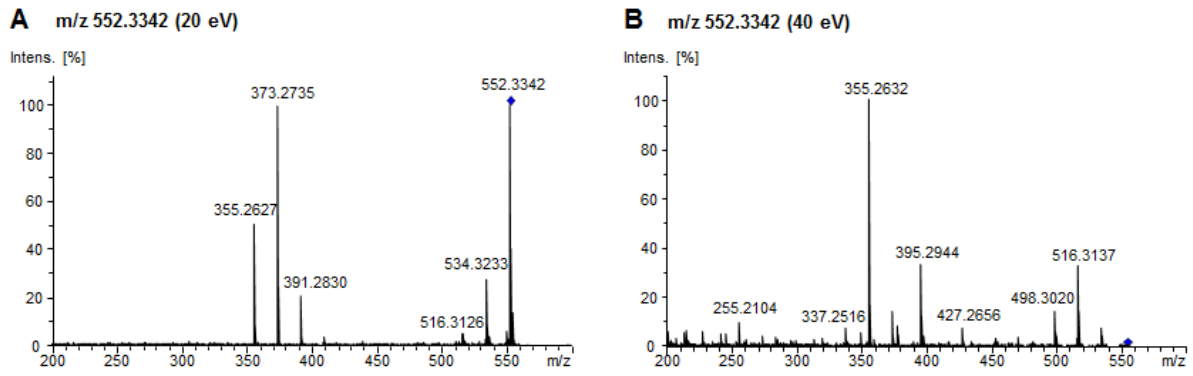


Figure 5.2-7: Experimental (+) ToF-MS/MS spectra of unknown features increased in breastfed infants.

A: m/z 552.3342, RT 4.99 min, collision energy 20 eV. B: m/z 552.3342, RT 4.99 min, collision energy 40 eV. Analyses were performed by UHPLC-ToF-MS.

5.2.1.3.2 (-) ToF-MS

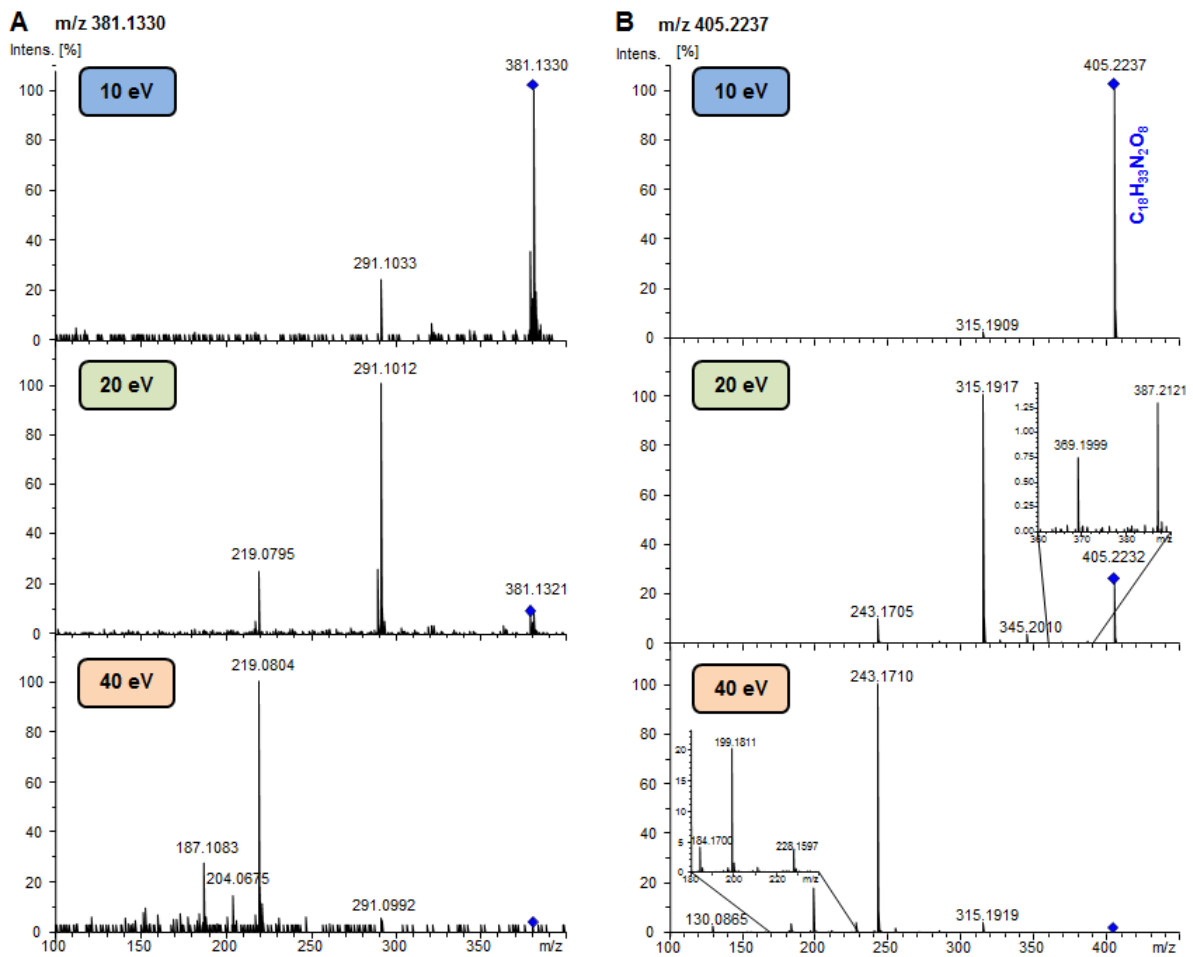


Figure 5.2-8: Experimental (-) ToF-MS/MS spectra of unknown features increased in formula-fed infants.

A: m/z 381.1330, RT 1.23 min, collision energy 10 eV (top), 20 eV (middle), 40 eV (bottom). B: m/z 405.2237, RT 3.11 min, collision energy 10 eV (top), 20 eV (middle), 40 eV (bottom). Analyses were performed by UHPLC-ToF-MS.

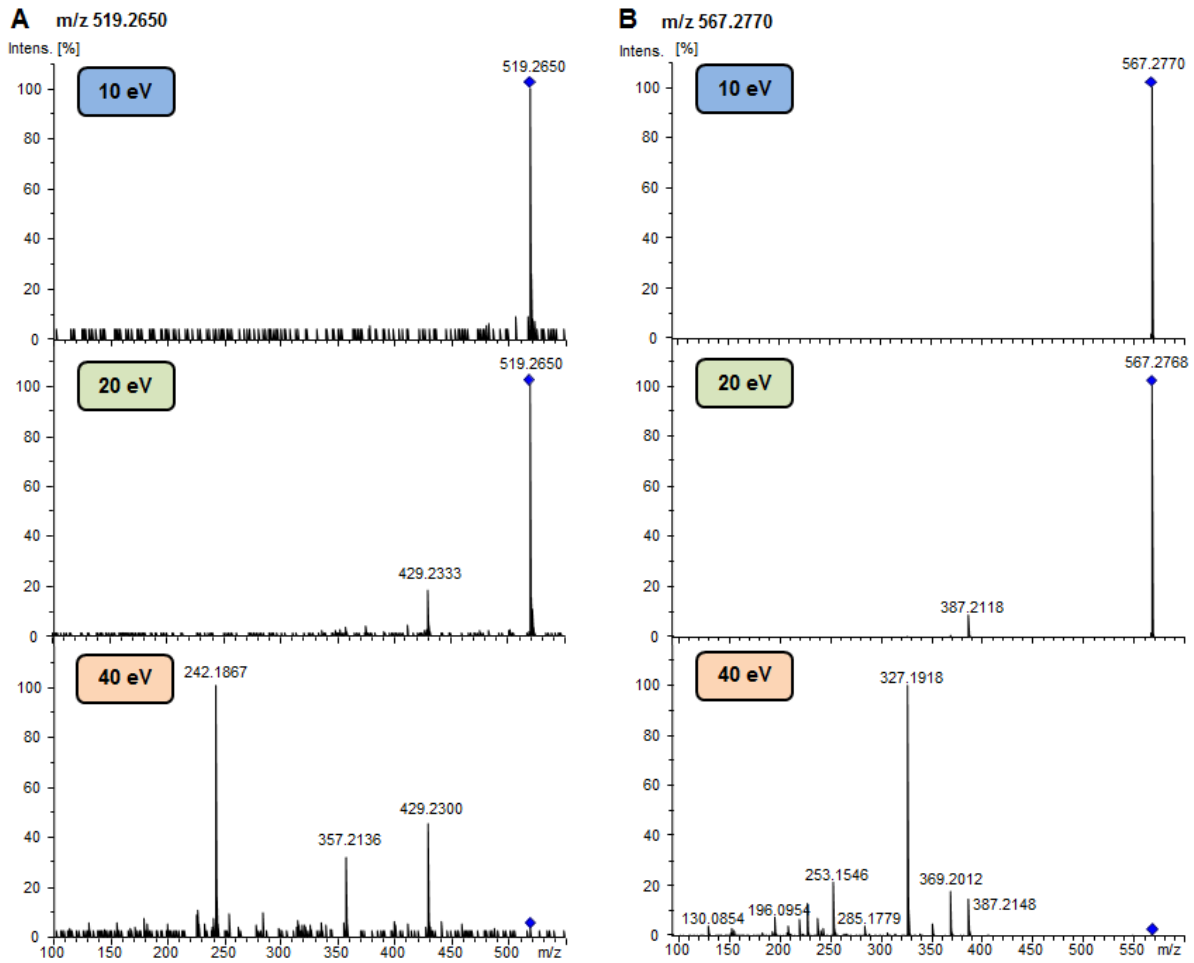


Figure 5.2-9: Experimental (-) ToF-MS/MS spectra of unknown features increased in formula-fed infants.

A: m/z 381.1330, RT 1.23 min, collision energy 10 eV (top), 20 eV (middle), 40 eV (bottom). B: m/z 405.2237, RT 3.11 min, collision energy 10 eV (top), 20 eV (middle), 40 eV (bottom). Analyses were performed by UHPLC-ToF-MS.

5.2.1.4 Differences in $F+$ and $F-$, MS/MS spectra of discriminating features

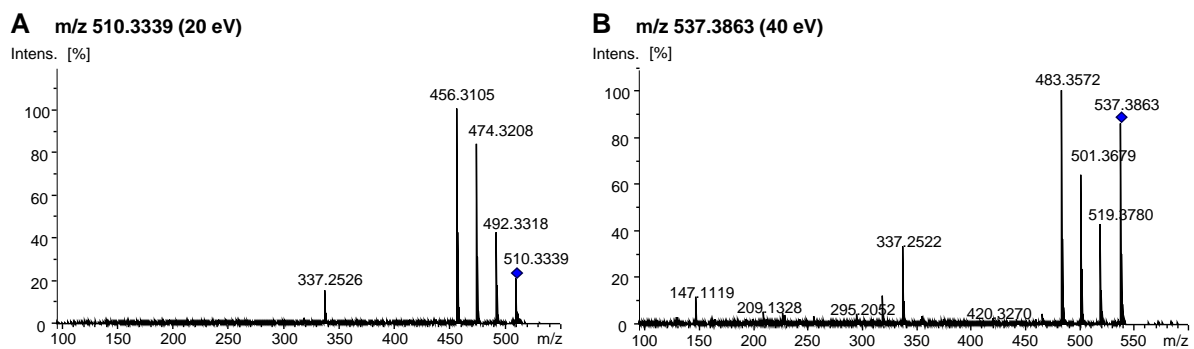


Figure 5.2-10: Experimental (+) ToF-MS/MS spectra of unknown features increased in $F+$.

A: m/z 510.3339, RT 4.49 min, collision energy 20 eV. B: m/z 537.3863, RT 4.14 min, collision energy 20 eV. Analyses were performed by UHPLC-ToF-MS.

Chapter VI

6 Appendix

6.1 Tables of the dietary study

6.1.1 Chemicals and other consumable material

Table 6.1-1: Chemicals

Name	Manufacturer	Details
MilliQ water	-	Merck Millipore Integral water purification system (18 M Ω , TOC < 5 ppb)
methanol	Sigma-Aldrich, St.Louis, USA	CHROMASOLV® for LC-MS, \geq 99.9%
acetonitrile	Sigma-Aldrich, St.Louis, USA	CHROMASOLV® for LC-MS, \geq 99.9%
isopropanol	Sigma-Aldrich, St.Louis, USA	CHROMASOLV® for LC-MS, \geq 99.9%
formic acid	Fluka	for mass spectrometry
L-Arginine	Sigma-Aldrich, St.Louis, USA	>98%
ammonium acetate	Biosolve BV, Valkenswaard, Netherlands	ULC/MS
ammonium formiate	Sigma-Aldrich, St.Louis, USA	10 M in Water
acetic acid	Biosolve BV, Valkenswaard, Netherlands	-
propionic acid	Sigma-Aldrich, St.Louis, USA	\geq 99.5%
butyric acid	Sigma-Aldrich, St.Louis, USA	\geq 99%
valeric acid	Sigma-Aldrich, St.Louis, USA	\geq 99%
isovaleric acid	Sigma-Aldrich, St.Louis, USA	99%
decanoic acid	Sigma-Aldrich, St.Louis, USA	\geq 99.5%
dodecanoic acid	Sigma-Aldrich, St.Louis, USA	\geq 98%
ESI Tune Mix	Agilent	G1969-85000

Table 6.1-2: Columns

Name	Manufacturer	Details
BEH C8	Waters GmbH, Eschborn, Germany	1.7 μ m, 2.1mmx150mm
Cortecs C18 column	Waters GmbH, Eschborn, Germany	1.6 μ m, 2.1mmx150mm

6.1.2 Instrument Setup

6.1.2.1 FT-ICR-MS

Table 6.1-3: FT-ICR-MS: solariX™ Bruker Daltonik GmbH.

Parameter	(-) FT-ICR-MS	(+) FT-ICR-MS
Mass range in Da	122.9 – 1000.0	147.4 – 2000.0
Acquired scans	500	500
Capillary [V]	3600	3700
Drying Gas Flow rate [L/min]	4.0	4.0
Dry Gas Temperature [°C]	180.0	180.0
Ion Accumulation Time [s]	0.300	0.100
Nebulizer Gas Flow Rate [bar]	2.0	2.0
Spray Shield [V]	500	500
Flow rate [μ L/min]	2.0	2.2 bar

6.1.2.2 UHPLC-ToF-MS conditions

For SCFA analyses and the lipidomics approach a Waters ACQUITY-UPLC® system (Waters GmbH, Eschborn, Germany) was used, including following devices: binary solvent manager, sample manager, column manager and a PDA detector, coupled to an Bruker UHR-qToF-MS (maXis™, Bruker Daltonik GmbH, Bremen, Germany). The used parameters are given in Table 6.1-4 (SCFA) and Table 6.1-5 (Lipidomics).

Table 6.1-4: SCFA Analysis

Parameter	(+) ToF-MS
LC	
Run time [min]	22
Flow rate [mL/min]	0.3
Injection volume [µL]	1
Injection	Partial loop
Column temperature [°C]	40
ToF-MS	
Mass range in Da	50.0 – 1200
Spectrum rate in Hz	1
Ion cooler RF	50 Vpp
Ion cooler transfer time	75 µs
Threshold Signal to Noise	500
Quadrupole [eV]	3
Capillary [V]	4500
End plate offset [V]	-500
Nebulizer Gas Flow Rate [bar]	2.0
Drying Gas Flow rate [L/min]	8.0
Dry Gas Temperature [°C]	200

Table 6.1-5: Lipidomics Approach

Parameter	(-) ToF-MS	(+) ToF-MS
LC		
Run time [min]	30	30
Flow rate [mL/min]	0.25	0.25
Injection volume [µL]	5	5
Injection	partial loop	Partial loop
Column temperature [°C]	40	40
ToF-MS		
Mass range in Da	100 - 1500	100 - 1500
Spectrum rate in Hz	2	2
Ion cooler RF	50 Vpp	50 Vpp
Ion cooler transfer time	75 µs	75 µs
Threshold Signal to Noise	500	500
Quadrupole [eV]	3	3
Capillary [V]	4000 V	-4500 V
End plate offset [V]	-500	-500
Nebulizer Gas Flow Rate [bar]	2.0	2.0
Drying Gas Flow rate [L/min]	8.0	8.0
Dry Gas Temperature [°C]	200	200
MS/MS	DDA	DDA

6.1.2.3 Other Instruments

Table 6.1-6: Other Instruments

Parameter	Manufacturer	Details
refrigerated Centrifuge	Eppendorf	5804R
ultrasonic bath	Bandelin Sonorex	RK100H
Vortex	Scientific Industry	Vortex Genie 2

6.1.3 OPLS-DA for metabolite discrimination applied on different classification models

Table 6.1-7: Mass signals differed between the HRS diet at day 28 and day 56.

Mass signals differed between HRS diets at different time points, including averaged experimental mass, compound name, monoisotopic mass, molecular formula, obtained with NetCalc, arithmetic mean of the compared feeding groups and p-values of the respective group comparisons, obtained with *post hoc* Kruskal-Nemenyi test.

Mass (avg.)	Compound name	Monoisotopic mass	molecular formula	Mean B	Mean HRS (day 28)	Mean HRS (day 56)	p-value B vs. HRS (day 28)	p-value B vs. HRS (day 56)	p-value HRS (day 28) vs. HRS (day 56)
241.217282	Pentadecanoic acid	242.224032	C15H30O2	2.99E+08	1.39E+09	3.45E+08	3.30E-03	n.s.	1.05E-02
267.232910	Heptadecenoic acid	268.239682	C17H32O2	2.16E+08	4.76E+09	3.11E+08	2.20E-02	n.s.	n.s.
269.248611	Heptadecanoic acid	270.255332	C17H34O2	4.02E+08	2.50E+09	7.42E+08	1.30E-02	n.s.	n.s.
283.264254	Octadecanoic acid	284.270982	C18H36O2	7.47E+09	2.48E+10	1.32E+10	n.s.	n.s.	n.s.
311.295572	Icosanoic acid	312.302282	C20H40O2	3.28E+08	1.90E+09	6.20E+08	1.10E-02	2.00E-02	n.s.
425.363670	Hexacosanedioic acid	426.370362	C26H50O4	2.08E+08	2.05E+09	7.02E+08	4.90E-02	n.s.	n.s.
465.304411	Cholesterol sulfate	466.311132	C27H46O4S	3.98E+09	8.11E+09	3.87E+09	n.s.	n.s.	n.s.

6.1.4 Correlation studies: impact of the amount of RS on the metabolite profile.

Table 6.1-8: Top 50 metabolites highly correlated with resistant starch.

List of top 50 highest correlated metabolites with the amount of resistant starch, analyzed in (-) FT-ICR-MS; ranked from high to low correlation ($R = 0.77 - 0.60$) with degrees of freedom $df(43)$. Table contains averaged experimental mass, compound name, monoisotopic mass, molecular formula, obtained with NetCalc, arithmetic mean of the compared feeding groups and correlation coefficients obtained through Pearson correlation with their respective p -values, obtained with regression analysis.

Mass (avg.)	Compound name	Monoisotopic mass	molecular formula	Mean B	Mean HRS	Mean LRS	Pearson R	p-corr
395.210936	no metabolite found	396.217626	C18H36O7S	2.36E+05	3.23E+06	1.97E+05	0.77132683	5.63E-10
359.280290	no metabolite found	360.287026	C20H40O5	2.86E+06	1.20E+07	2.94E+06	0.73250929	1.07E-08
665.214868	no classification possible	666.222144	-	1.41E+05	3.66E+06	0.00E+00	0.7013282	8.05E-08
385.295946	no classification possible	386.302676	C22H42O5	2.31E+06	1.07E+07	3.21E+06	0.69973083	8.87E-08
343.155095	no classification possible	344.162374	C20H24O5	3.03E+06	1.08E+07	2.84E+06	0.69810954	9.78E-08
377.200329	no metabolite found	378.207610	C18H34O6S	2.17E+06	1.19E+07	4.11E+06	0.69579389	1.12E-07
463.328061	no metabolite found	464.335337	C24H48O8	2.71E+06	1.42E+07	2.92E+06	0.69125046	1.47E-07
325.274834	Hydroxyeicosenoic acid	326.282110	C20H38O3	3.01E+07	7.70E+07	3.02E+07	0.68034232	2.73E-07
361.202017	no classification possible	362.209293	C21H30O5	5.61E+06	2.07E+07	2.11E+06	0.66984831	2.73E-07
549.293855	no metabolite found	550.301131	-	1.45E+05	3.18E+06	2.95E+05	0.66842993	4.85E-07
401.342490	Hydroxycholesterol	402.349766	C27H46O2	1.86E+07	7.74E+07	1.87E+07	0.6539574	5.23E-07
498.343695	no metabolite found	499.350971	C27H49O7N	1.05E+06	1.01E+07	2.59E+06	0.65263132	1.11E-06
477.358547	no classification possible	478.365823	C29H50O5	6.50E+07	2.09E+08	7.63E+07	0.65174755	1.18E-06
329.306040	no metabolite found	330.313316	C20H42O3	1.48E+06	7.16E+06	1.84E+06	0.6510479	1.24E-06
429.373840	α -Tocopherol	430.381116	C29H50O2	4.27E+07	2.05E+08	3.81E+07	0.65036125	1.28E-06
325.202045	Dihydroxyoctadecadienoic acid	326.209321	C18H30O5	1.17E+07	3.82E+07	1.62E+07	0.64718015	1.33E-06
357.170742	no classification possible	358.178018	C21H26O5	3.65E+06	4.66E+07	3.71E+06	0.64359006	1.55E-06
549.289308	no metabolite found	550.296584	C30H46O7S	2.11E+07	5.54E+07	2.22E+07	0.64321989	1.85E-06
379.215949	no metabolite found	380.223225	C18H36O6S	3.67E+05	4.07E+06	9.88E+05	0.64153437	1.89E-06
345.170755	Gibberellin	346.178031	C20H26O5	7.73E+06	2.47E+07	5.71E+06	0.64107917	2.05E-06
477.361934	no metabolite found	478.369210	C26H54O5S	3.18E+06	1.39E+07	4.17E+06	0.63904662	2.09E-06
315.217633	no metabolite found	316.224909	C17H32O5	3.45E+06	9.47E+06	3.90E+06	0.63878174	2.31E-06
339.254060	no classification possible	340.261336	C20H36O4	9.71E+06	2.91E+07	1.02E+07	0.63826894	2.34E-06
327.290414	Hydroxyeicosanoic acid	328.297690	C20H40O3	7.28E+07	1.84E+08	6.84E+07	0.63555912	2.39E-06
373.169051	Hydroxyoctadecatrienoic acid sulfate	374.176327	C18H30O6S	2.27E+06	1.00E+07	3.97E+06	0.63340471	3.01E-06
609.546564	DG(25:0)	610.553840	C38H74O5	1.26E+05	2.03E+06	0.00E+00	0.63216567	3.19E-06
270.171091	no metabolite found	271.178367	C14H25O4N	1.37E+05	3.24E+06	7.35E+05	0.63200944	3.22E-06
171.012123	no classification possible	172.019399	C7H8O3S	7.95E+05	7.71E+06	4.67E+06	0.63024247	3.49E-06
343.285361	Dihydroxyeicosanoic acid	344.292637	C20H40O4	9.50E+06	2.82E+07	9.37E+06	0.6288236	3.73E-06
497.340179	no metabolite found	498.347455	C28H51O5P	5.02E+06	3.05E+07	8.99E+06	0.62624877	4.20E-06
321.134348	no classification possible	322.141624	C17H22O6	1.71E+06	3.40E+07	7.76E+06	0.62246539	4.99E-06
321.170768	no classification possible	322.178044	C18H26O5	2.49E+06	8.89E+06	4.61E+06	0.62148717	5.21E-06
415.358186	β - γ -Tocopherol	416.365462	C28H48O2	5.36E+07	2.53E+08	6.47E+07	0.61926492	5.76E-06
393.195260	Dihydroxyoctadecenoic acid sulfate	394.202536	C18H34O7S	3.62E+06	3.19E+07	1.07E+07	0.6179283	6.11E-06
443.389428	no metabolite found	444.396704	C30H52O2	1.66E+05	3.09E+06	4.28E+05	0.61770636	6.17E-06
512.359318	no metabolite found	513.366594	C28H51O7N	3.16E+05	3.40E+06	5.58E+05	0.61719973	6.31E-06
323.150036	no classification possible	324.157312	C17H24O6	4.31E+05	2.13E+07	4.84E+06	0.61572926	6.73E-06
503.410819	no metabolite found	504.418095	C32H56O4	2.27E+06	1.32E+07	3.19E+06	0.61522577	6.89E-06
331.045908	no classification possible	332.053184	C16H12O8	1.55E+06	6.03E+06	1.62E+06	0.61274598	7.68E-06
403.194720	no classification possible	404.201996	C23H32O4S	2.20E+05	1.63E+07	7.60E+05	0.61066595	8.40E-06
566.351959	no metabolite found	567.359235	C31H53O6NS	6.15E+05	3.98E+06	1.50E+06	0.60893158	9.06E-06
329.175769	no metabolite found	330.183045	C20H26O4	3.36E+07	1.45E+08	1.16E+07	0.60885327	9.09E-06
375.184691	Hydroxyoctadecadienoic acid sulfate	376.191967	C18H32O6S	5.72E+06	2.83E+07	1.07E+07	0.60871325	9.14E-06
398.291202	no metabolite found	399.298478	C22H41O5N	2.71E+05	2.56E+06	6.81E+05	0.60743195	9.66E-06
307.122035	no metabolite found	308.129311	C13H24O6S	1.43E+06	1.02E+07	1.88E+06	0.60575575	1.04E-05
489.394901	no metabolite found	490.402177	C31H54O4	1.77E+06	7.63E+06	2.23E+06	0.60559898	1.04E-05
363.163490	no metabolite found	364.170766	C20H28O4S	4.54E+05	2.20E+06	0.00E+00	0.60554261	1.05E-05
402.192252	no metabolite found	403.199528	C22H29O6N	1.64E+05	4.12E+06	4.78E+05	0.60544948	1.05E-05
342.171045	no classification possible	343.178321	C20H25O4N	1.39E+05	2.49E+06	8.18E+05	0.60508416	1.07E-05
351.184702	no metabolite found	352.191978	C16H32O6S	2.16E+06	1.56E+07	4.53E+06	0.60462505	1.09E-05

Table 6.1-9: Top 50 metabolites negatively correlated with resistant starch.

List of top 50 highest correlated metabolites with the amount of resistant starch, analyzed in (-) FT-ICR-MS; ranked from high to low correlation ($R = -0.49 - -0.33$) with degrees of freedom $df(43)$. Table contains averaged experimental mass, compound name, monoisotopic mass, molecular formula, obtained with NetCalc, arithmetic mean of the compared feeding groups and correlation coefficients obtained through Pearson correlation with their respective p-values, obtained with regression analysis.

Mass (avg.)	Compound name	Monoisotopic mass	molecular formula	Mean B	Mean HRS	Mean LRS	Pearson R	p-corr
294.280188	no metabolite found	295.287464	C19H37ON	2.74E+06	2.35E+05	1.81E+06	-0.48973931	6.32E-04
333.228560	no classification possible	334.235836	C17H34O6	1.07E+07	1.09E+06	3.67E+06	-0.48680938	6.76E-04
547.421947	no metabolite found	548.429223	C30H60O8	4.36E+06	6.02E+05	7.16E+06	-0.46710337	1.24E-03
335.244092	no metabolite found	336.251368	C17H36O6	2.96E+06	0.00E+00	1.09E+06	-0.46598275	1.23E-03
245.165930	no classification possible	246.173206	C15H22ON2	6.33E+06	7.38E+05	8.18E+06	-0.46102219	1.45E-03
321.228558	no metabolite found	322.235834	C16H34O6	3.26E+07	1.28E+06	1.08E+07	-0.44904872	1.93E-03
205.196176	no classification possible	206.203452	C15H26	2.40E+06	6.53E+05	1.31E+06	-0.44617556	2.09E-03
319.212813	no classification possible	320.220089	C16H32O6	1.30E+08	2.17E+07	4.33E+07	-0.44546042	2.11E-03
615.484571	no metabolite found	616.491847	C35H68O8	9.07E+06	1.04E+06	1.78E+06	-0.43557107	2.70E-03
243.150237	no classification possible	244.157513	C15H20ON2	1.27E+06	0.00E+00	2.15E+06	-0.43360576	2.96E-03
281.196990	no metabolite found	282.204266	C13H30O6	3.80E+06	1.08E+06	1.62E+06	-0.41776084	4.20E-03
317.197055	Prenol Lipids [PR]	318.204331	C16H30O6	5.33E+07	1.47E+07	2.73E+07	-0.41189929	4.85E-03
364.252655	no metabolite found	365.259931	C18H39O4NS	1.41E+07	1.23E+06	9.74E+06	-0.39247556	7.61E-03
350.237027	Sphingolipids [SP]	351.244303	C17H37O4NS	2.50E+07	2.84E+06	1.75E+07	-0.38866253	8.28E-03
257.093140	no metabolite found	258.100416	C14H14O3N2	7.23E+05	0.00E+00	1.66E+06	-0.38500087	9.15E-03
260.104083	no classification possible	261.111359	C13H15O3N3	1.19E+06	4.06E+05	2.38E+06	-0.38466223	9.23E-03
573.437651	no classification possible	574.444927	C32H62O8	1.01E+07	1.59E+06	3.58E+06	-0.38213039	9.41E-03
583.440368	no metabolite found	584.447644	C34H64O5S	3.56E+06	0.00E+00	1.29E+06	-0.37985271	9.92E-03
259.243088	Sterol Lipids [ST]	260.250364	C19H32	3.90E+07	1.92E+07	2.93E+07	-0.37510598	1.10E-02
323.244127	no metabolite found	324.251403	C16H36O6	1.77E+06	0.00E+00	5.16E+05	-0.37434371	1.11E-02
323.226068	no metabolite found	324.233344	C16H36O4S	3.98E+06	0.00E+00	8.97E+05	-0.37345317	1.13E-02
535.421842	no metabolite found	536.429118	C29H60O8	1.67E+06	5.00E+05	2.82E+06	-0.37238793	1.19E-02
341.248641	Fatty Acyls [FA]	342.255917	C23H34O2	1.93E+06	2.21E+05	2.49E+06	-0.37070542	1.22E-02
233.227455	no classification possible	234.234731	C17H30	5.67E+07	1.16E+07	4.98E+07	-0.37042369	1.22E-02
601.468910	Fatty Acyls [FA]	602.476186	C34H66O8	1.94E+08	4.22E+07	5.12E+07	-0.37028382	1.20E-02
279.186875	no classification possible	280.194151	C19H24N2	2.37E+06	5.18E+05	1.37E+06	-0.36940342	1.24E-02
288.196927	no classification possible	289.204203	C18H27O2N	1.06E+06	0.00E+00	6.24E+05	-0.36893456	1.25E-02
599.453243	no metabolite found	600.460519	C34H64O8	7.46E+07	1.65E+07	3.07E+07	-0.36497438	1.35E-02
549.437635	no metabolite found	550.444911	C30H62O8	9.65E+06	5.10E+06	1.45E+07	-0.36423447	1.41E-02
271.206745	Sterol Lipid	272.214021	C19H28O1	3.82E+06	6.96E+05	1.49E+06	-0.36392954	1.38E-02
424.260615	no metabolite found	425.267891	C25H35O3N3	1.25E+06	3.39E+05	2.61E+06	-0.36357053	1.43E-02
310.275266	Sphingolipids [SP]	311.282542	C19H37O2N	7.45E+06	2.76E+06	5.72E+06	-0.36270886	1.43E-02
290.212534	no classification possible	291.219810	C18H29O2N	6.44E+05	1.67E+05	1.64E+06	-0.36249078	1.47E-02
295.212910	no metabolite found	296.220186	-	2.86E+06	0.00E+00	1.10E+06	-0.36248338	1.42E-02
336.202765	no metabolite found	337.210041	C15H31O7N	2.62E+06	1.21E+05	5.26E+05	-0.3610839	1.45E-02
261.258726	no classification possible	262.266002	C19H34	6.96E+07	1.06E+07	8.40E+06	-0.36047574	1.46E-02
268.264593	no classification possible	269.271869	C17H35O1N	1.24E+06	3.10E+05	1.82E+06	-0.35741567	1.61E-02
273.222341	no classification possible	274.229617	C19H30O	9.67E+06	2.03E+06	1.84E+06	-0.35535737	1.62E-02
273.258721	no classification possible	274.265997	C20H34	1.69E+06	1.38E+05	0.00E+00	-0.35175663	1.73E-02
583.458206	no metabolite found	584.465482	C34H64O7	2.34E+07	4.57E+06	7.33E+06	-0.35151916	1.76E-02
279.217756	no metabolite found	280.225032	-	2.76E+07	1.49E+07	1.87E+07	-0.34623722	1.96E-02
329.284994	no classification possible	330.292270	C23H38O	2.48E+07	1.79E+06	2.09E+07	-0.34512162	2.02E-02
585.456025	no metabolite found	586.463301	C34H66O5S	2.66E+06	0.00E+00	5.38E+05	-0.34309745	2.07E-02
305.284971	no classification possible	306.292247	C21H38O	4.27E+06	4.33E+05	1.47E+05	-0.33880207	2.22E-02
263.238046	no classification possible	264.245322	C18H32O	1.20E+07	2.61E+06	5.82E+06	-0.33815254	2.28E-02
243.029918	no classification possible	244.037194	C13H8O5	1.01E+07	2.17E+06	1.66E+07	-0.33588389	2.43E-02
277.202333	no metabolite found	278.209609	C14H30O5	3.46E+06	7.91E+05	1.96E+06	-0.33557151	2.40E-02
279.232882	Octadecadienoic acid (C18:2)	280.240158	C18H32O2	6.49E+10	3.56E+10	4.39E+10	-0.33433519	2.45E-02
279.211700	no metabolite found	280.218976	C21H28	1.43E+07	7.83E+06	9.46E+06	-0.33146917	2.58E-02
179.180510	no classification possible	180.187786	C13H24	3.04E+06	5.40E+05	2.28E+06	-0.32578466	2.89E-02

Table 6.1-10: Top 50 metabolites highly correlated with resistant starch analyzed in (+) FT-ICR-MS.

List of top 50 highest correlated metabolites with the amount of resistant starch, analyzed in (+) FT-ICR-MS; ranked from high to low correlation ($R = 0.66 - 0.48$) with degrees of freedom $df(42)$. Table contains averaged experimental mass, compound name, monoisotopic mass, molecular formula, obtained with NetCalc, arithmetic mean of the compared feeding groups and correlation coefficients obtained through Pearson correlation with their respective p -values, obtained with regression analysis.

Mass (avg.)	Compound name	Monoisotopic mass	molecular formula	Mean B	Mean HRS	Mean LRS	Pearson R	p-corr
388.320679	no metabolite found	387.313403	C25H41O2N	5.99E+05	3.79E+06	3.67E+05	0.65783914	1.22E-06
291.135282	no metabolite found	290.128006	C13H23O5P	1.04E+05	1.41E+06	9.52E+04	0.61356018	9.48E-06
466.404316	no metabolite found	465.397040	C32H51ON	9.08E+05	1.34E+07	0.00E+00	0.59002116	2.50E-05
448.378438	no metabolite found	447.371162	C28H49O3N	4.47E+06	1.55E+07	5.83E+06	0.57055207	5.26E-05
480.383479	no metabolite found	479.376203	C32H49O2N	5.19E+06	6.37E+07	0.00E+00	0.56970331	5.43E-05
434.398975	no metabolite found	433.391699	C28H51O2N	0.00E+00	5.80E+06	1.14E+06	0.56259152	7.04E-05
572.467894	no metabolite found	571.460618	C36H61O4N	2.27E+06	8.74E+06	1.41E+06	0.56183382	7.24E-05
462.372928	no metabolite found	461.365652	C32H47ON	1.06E+06	1.57E+07	0.00E+00	0.55822314	8.24E-05
464.388615	no metabolite found	463.381339	C32H49ON	4.21E+07	5.53E+08	8.90E+06	0.55784291	8.35E-05
482.399006	no metabolite found	481.391730	C32H51O2N	5.46E+05	6.75E+06	0.00E+00	0.55493596	9.25E-05
498.393944	no metabolite found	497.386668	C32H51O3N	0.00E+00	9.48E+06	0.00E+00	0.5515672	1.04E-04
465.391837	no metabolite found	464.384561	C25H48O2N6	1.22E+07	1.61E+08	2.25E+06	0.54901667	1.14E-04
440.248773	no metabolite found	439.241497	C19H37O10N	2.52E+06	1.70E+07	5.25E+06	0.5486816	1.15E-04
897.607577	no metabolite found	896.600301	C47H85O10N4P	1.58E+06	8.56E+06	2.58E+06	0.54085388	1.50E-04
406.316029	no metabolite found	405.308753	C21H43O6N	1.06E+06	8.17E+06	5.03E+06	0.5350666	1.83E-04
467.407077	no metabolite found	466.399801	C25H50O2N6	0.00E+00	3.86E+06	0.00E+00	0.53333561	1.93E-04
890.587971	no metabolite found	889.580695	C46H80O8N7P	5.44E+05	3.89E+06	0.00E+00	0.53326831	1.94E-04
454.404154	no metabolite found	453.396878	C31H51ON	2.35E+06	2.33E+07	4.29E+05	0.53316549	1.94E-04
308.206628	no metabolite found	307.199352	C14H29O6N	0.00E+00	7.50E+05	0.00E+00	0.53235023	2.00E-04
538.252882	no metabolite found	537.245606	C20H43O13NS	0.00E+00	2.78E+07	6.63E+05	0.5315267	2.05E-04
481.386650	no metabolite found	480.379374	C25H48O3N6	1.33E+06	1.80E+07	0.00E+00	0.52741493	2.34E-04
408.201278	no metabolite found	407.194002	C21H29O7N	0.00E+00	7.55E+06	1.10E+06	0.52435974	2.59E-04
443.183287	no metabolite found	442.176011	C21H31O8P	4.03E+05	4.11E+06	1.28E+06	0.52210447	2.78E-04
631.397332	no metabolite found	630.390056	C33H59O9P	0.00E+00	5.88E+06	1.19E+06	0.51936626	3.03E-04
468.420206	no metabolite found	467.412930	C32H53ON	6.38E+05	1.13E+07	3.17E+05	0.51788048	3.18E-04
328.263172	no metabolite found	327.255896	C22H33ON	1.52E+06	2.42E+07	3.67E+05	0.51388547	3.60E-04
458.202243	no metabolite found	457.194967	C21H31O10N	2.07E+06	6.23E+06	2.71E+06	0.51018534	4.03E-04
403.305175	no metabolite found	402.297899	C22H42O6	4.74E+05	5.91E+06	3.24E+06	0.50689457	4.46E-04
342.150456	no metabolite found	341.143180	C11H23O9N3	0.00E+00	2.13E+06	2.73E+05	0.50653697	4.51E-04
701.527401	no metabolite found	700.520125	C43H73O5P	7.98E+05	1.71E+07	8.31E+06	0.50548864	4.65E-04
503.422896	no metabolite found	502.415620	C29H59O4P	4.89E+05	3.46E+07	5.73E+06	0.50496877	4.73E-04
440.388758	no metabolite found	439.381482	C30H49O1N	9.27E+06	5.84E+07	3.47E+06	0.50366207	4.92E-04
522.415111	no metabolite found	521.407835	C31H55O5N	1.16E+07	2.44E+07	1.17E+07	0.50125046	5.28E-04
363.120038	no metabolite found	362.112762	C15H23O8P	2.41E+05	6.49E+06	2.35E+06	0.49866966	5.71E-04
585.500560	no metabolite found	584.493284	C35H69O4P	5.07E+05	5.89E+06	0.00E+00	0.49617119	6.14E-04
179.084849	no metabolite found	178.077573	C6H14O2N2S	0.00E+00	9.80E+05	0.00E+00	0.49415831	6.51E-04
507.423375	no metabolite found	506.416099	C32H58O2S	1.54E+06	4.69E+06	0.00E+00	0.49355726	6.63E-04
383.125522	no metabolite found	382.118246	C18H23O7P	2.44E+05	4.14E+06	5.93E+05	0.4933104	6.68E-04
441.391574	no metabolite found	440.384298	C23H48O2N6	2.77E+06	2.01E+07	5.87E+05	0.49199175	6.94E-04
565.400934	no metabolite found	564.393658	C28H52O2N8S	4.23E+05	5.75E+06	0.00E+00	0.49003064	7.34E-04
511.454608	no metabolite found	510.447332	C32H62O2S	0.00E+00	2.44E+06	3.08E+05	0.4895417	7.45E-04
438.300342	no metabolite found	437.293066	C28H39O3N	0.00E+00	3.50E+07	2.94E+06	0.48889718	7.59E-04
351.213761	no metabolite found	350.206485	C16H26O3N6	1.73E+06	1.20E+07	4.74E+06	0.48544596	8.37E-04
537.250005	no metabolite found	536.242729	C32H32O4N4	2.30E+06	8.75E+07	7.65E+06	0.48501901	8.48E-04
775.325407	no metabolite found	774.318131	C31H55O18N2P	3.46E+05	3.17E+06	1.69E+06	0.4836444	8.81E-04
747.569267	no metabolite found	746.561991	C45H79O6P	5.15E+06	2.37E+07	1.38E+07	0.48204707	9.22E-04
371.161905	no metabolite found	370.154629	C18H27O6P	2.93E+06	8.88E+06	1.43E+06	0.48166558	9.32E-04
449.353958	no metabolite found	448.346682	C29H48OiCl	7.76E+06	5.20E+07	1.95E+07	0.48156999	9.34E-04
439.303313	no metabolite found	438.296037	C21H38O4N6	1.28E+06	1.23E+07	0.00E+00	0.48079739	9.55E-04
806.593854	no metabolite found	805.586578	C51H75O3N5	6.67E+06	2.03E+07	7.30E+06	0.48013356	9.73E-04

6.1.5 Lipid metabolism affected by high resistant starch

Table 6.1-11: Metabolites of the lipid metabolism altered through baseline, HRS or LRS diet.

List of significantly changed metabolites of the lipid metabolism through baseline, HRS or LRS diet, analyzed in (-) FT-ICR-MS; Table contains averaged experimental mass, compound name, monoisotopic mass, molecular formula, obtained with NetCalc, arithmetic mean of the compared feeding groups and their respective p-values, obtained with *post hoc* Kruskal-Nemenyi test and their corresponding sub-pathway. From Maier, T. V.; Lucio, M.; Lee, L. H.; VerBerkmoes, N. C.; Brislawn, C. J.; Bernhardt, J.; Lamendella, R.; McDermott, J. E.; Bergeron, N.; Heinzmann, S. S.; Morton, J. T.; González, A.; Ackermann, G.; Knight, R.; Riedel, K.; Krauss, R. M.; Schmitt-Kopplin, P.; Jansson, J. K.: Impact of Dietary Resistant Starch on the Human Gut Microbiome, Metaproteome, and Metabolome. *mBio* vol. 8 no. 5 e01343-17 (2017). Data from Figure 2.4-13, reprinted and modified figure from (Maier et al. 2017). Copyright (2017) Maier et al.

Mass (avg.)	Compound name	Monoisotopic mass	molecular formula	Mean B	Mean HRS	Mean LRS	p-value B vs. HRS	p-value B vs. LRS	p-value HRS vs. LRS	Pathway
279.232882	Octadecadienoic acid (C18:2)	280.240158	C18H32O2	6.49E+10	3.56E+10	4.39E+10	3.10E-02	n.s.	n.s.	Linoleic acid metabolism; Biosynthesis of unsaturated fatty acids
253.217286	Hexadecenoic acid (C16:1)	254.224562	C16H30O2	7.31E+08	3.07E+08	3.62E+08	4.30E-03	n.s.	n.s.	Fatty acid biosynthesis
281.248559	Octadecenoic acid (C18:1)	282.255835	C18H34O2	9.91E+10	6.25E+10	5.31E+10	1.54E-02	1.10E-03	n.s.	Fatty acid biosynthesis; Biosynthesis of unsaturated fatty acids
313.217220	no classification possible	314.224496	C21H30O2	1.15E+07	4.40E+06	7.05E+06	1.10E-02	2.70E-02	n.s.	Steroid hormone biosynthesis
289.217307	no classification possible	290.224583	C19H30O2	1.72E+07	7.34E+06	1.01E+07	1.53E-02	1.50E-03	n.s.	Steroid hormone biosynthesis
285.149598	no classification possible	286.156874	C18H22O3	3.79E+06	2.21E+06	1.30E+06	n.s.	4.40E-03	n.s.	Steroid hormone biosynthesis
349.238435	no classification possible	350.245711	C21H34O4	1.07E+07	1.32E+07	6.67E+06	n.s.	n.s.	2.00E-02	Steroid hormone biosynthesis
331.227864	no classification possible	332.235140	C21H32O3	1.77E+07	8.64E+06	6.61E+06	1.88E-02	9.70E-03	n.s.	Steroid hormone biosynthesis
319.264204	no classification possible	320.271480	C21H36O2	7.46E+07	2.97E+07	4.12E+06	3.00E-02	2.90E-06	4.70E-02	Steroid hormone biosynthesis
333.243485	no classification possible	334.250761	C21H34O3	3.43E+07	1.83E+07	1.29E+07	n.s.	3.70E-03	n.s.	Steroid hormone biosynthesis
315.232938	no classification possible	316.240214	C21H32O2	4.03E+07	1.26E+07	7.39E+06	2.35E-02	2.20E-04	n.s.	Steroid hormone biosynthesis
291.232903	no classification possible	292.240179	C19H32O2	4.55E+07	1.59E+07	6.82E+06	6.30E-03	3.40E-05	n.s.	Steroid hormone biosynthesis
317.248548	no classification possible	318.255824	C21H34O2	1.28E+08	2.98E+07	4.70E+06	2.60E-02	4.00E-06	n.s.	Steroid hormone biosynthesis
171.139046	Decanoic acid (C10:0)	172.146322	C10H20O2	5.84E+05	6.27E+05	1.47E+07	n.s.	3.40E-04	8.20E-04	Fatty acid biosynthesis
199.170355	Dodecanoic acid (C12:0)	200.177631	C12H24O2	4.16E+07	4.88E+07	2.00E+09	n.s.	6.40E-05	2.00E-03	Fatty acid biosynthesis
227.201651	Tetradecanoic acid (C14:0)	228.208927	C14H28O2	9.44E+07	1.87E+08	1.80E+09	n.s.	9.20E-05	n.s.	Fatty acid biosynthesis
285.185993	no classification possible	286.193269	C19H26O2	6.79E+07	3.70E+07	1.27E+07	n.s.	6.40E-04	8.48E-03	Steroid hormone biosynthesis
345.207151	no classification possible	346.214427	C21H30O4	2.44E+07	6.08E+07	5.77E+06	n.s.	1.10E-02	5.30E-06	Steroid hormone biosynthesis
301.217257	Icosapentanoic acid (C20:5)	302.224533	C20H30O2	3.66E+07	9.74E+07	3.01E+07	n.s.	n.s.	2.00E-02	Biosynthesis of unsaturated fatty acids
315.196593	15-Deoxy-delta-12,14-PGJ2	316.203869	C20H28O3	1.19E+07	2.14E+07	7.63E+06	n.s.	n.s.	8.60E-03	Arachidonic acid metabolism
319.227841	Hydroxyeicosatetraenoic acid	320.235117	C20H32O3	2.49E+07	7.63E+07	3.64E+07	1.70E-04	n.s.	3.78E-02	Arachidonic acid metabolism
333.207132	Hydroxyoxoicosatetraenoic acid	334.214408	C20H30O4	1.13E+07	2.25E+07	1.21E+07	1.20E-02	n.s.	n.s.	Arachidonic acid metabolism
281.087789	no classification possible	282.095065	C10H18O9	3.70E+06	1.11E+07	5.92E+06	1.00E-03	n.s.	4.20E-02	Glycerolipid metabolism
353.233346	Trihydroxyeicosatrienoic acid	354.240622	C20H34O5	1.16E+07	5.77E+07	3.09E+07	2.20E-04	n.s.	n.s.	Arachidonic acid metabolism
449.327277	Trihydroxycholestanic acid	450.334553	C27H46O5	1.08E+08	2.47E+08	1.25E+08	8.70E-03	n.s.	n.s.	Primary bile acid biosynthesis
309.207131	Hydroxyoctadecenoic acid	310.214407	C18H30O4	1.95E+07	8.62E+07	2.42E+07	5.00E-03	n.s.	2.20E-02	alpha-Linolenic acid metabolism
335.222782	Dihydroxyeicosatetraenoic acid	336.230058	C20H32O4	9.07E+06	3.47E+07	1.59E+07	3.90E-05	n.s.	2.50E-02	Arachidonic acid metabolism
287.222731	Dihydroxyhexadecanoic acid	288.230007	C16H32O4	1.68E+07	1.91E+08	2.27E+07	5.20E-03	n.s.	n.s.	Cutin, suberine and wax biosynthesis

337.238417	Dihydroxyeicosatrienoic acid	338.245693	C20H34O4	1.69E+07	1.02E+08	2.57E+07	7.20E-04	n.s.	4.30E-02	Arachidonic acid metabolism
325.202045	Dihydroxyoctadecadienoic acid	326.209321	C18H30O5	1.17E+07	3.82E+07	1.62E+07	3.00E-04	n.s.	1.36E-02	Arachidonic acid metabolism
351.217674	Trihydroxyeicosatetraenoic acid	352.224950	C20H32O5	6.85E+06	2.35E+07	1.26E+07	1.10E-04	n.s.	4.18E-02	Arachidonic acid metabolism
327.217677	Trihydroxyoctadecadienoic acid	328.224953	C18H32O5	2.56E+07	1.02E+08	3.04E+07	6.60E-04	n.s.	1.18E-02	Arachidonic acid metabolism
329.233297	Trihydroxyoctadecenoic acid	330.240573	C18H34O5	5.81E+07	1.90E+08	5.35E+07	n.s.	n.s.	1.10E-02	Linoleic acid metabolism
311.222782	Dihydroxyoctadecadienoic acid	312.230058	C18H32O4	7.47E+07	2.63E+08	6.36E+07	9.10E-03	n.s.	1.10E-03	Linoleic acid metabolism
313.238436	Dihydroxyoctadecenoic acid	314.245712	C18H34O4	2.09E+08	1.04E+09	1.97E+08	4.05E-03	n.s.	5.90E-04	Linoleic acid metabolism
337.311207	Docosenoic acid (C22:1)	338.318483	C22H42O2	1.40E+08	3.07E+08	1.33E+08	6.30E-03	n.s.	n.s.	Biosynthesis of unsaturated fatty acids
227.128851	Dodecenedioic acid	228.136127	C12H20O4	5.99E+06	5.53E+07	1.10E+07	5.10E-04	n.s.	n.s.	alpha-Linolenic acid metabolism
367.212654	6-Keto-PGE1	368.219930	C20H32O6	9.60E+06	2.53E+07	1.85E+07	9.40E-03	n.s.	n.s.	Arachidonic acid metabolism
369.228264	6-Keto-PGF1alpha	370.235540	C20H34O6	7.68E+06	2.49E+07	1.62E+07	5.20E-04	n.s.	n.s.	Arachidonic acid metabolism
463.233622	no classification possible	464.240898	C25H36O8	2.49E+05	2.68E+06	1.31E+06	6.60E-03	n.s.	n.s.	Steroid hormone biosynthesis
464.338369	no metabolite found	465.345645	C27H47O5N 1	1.61E+06	7.18E+06	2.90E+06	6.20E-04	n.s.	4.31E-02	Sphingolipid metabolism
435.348004	Tetrahydrocholestane	436.355280	C27H48O4	3.08E+07	6.37E+07	2.90E+07	1.20E-02	n.s.	1.90E-02	Primary bile acid biosynthesis
488.323154	Carboprost Tromethamine	489.330430	C25H47O8N 1	9.04E+05	5.03E+06	7.54E+05	4.20E-03	n.s.	6.00E-03	Sphingolipid metabolism
363.217693	Urocortisone	364.224969	C21H32O5	2.71E+06	6.44E+06	3.59E+06	2.60E-03	n.s.	3.62E-02	Steroid hormone biosynthesis
423.275237	Tetrahydroxycholanoic acid	424.282513	C24H40O6	1.37E+07	2.43E+07	1.91E+07	8.30E-03	n.s.	n.s.	Secondary bile acid biosynthesis
365.233330	Urocortisol	366.240606	C21H34O5	5.73E+06	9.76E+06	6.48E+06	1.50E-02	n.s.	n.s.	Steroid hormone biosynthesis
367.248997	no classification possible	368.256273	C21H36O5	5.85E+06	1.08E+07	4.45E+06	1.41E-02	n.s.	4.20E-03	Steroid hormone biosynthesis
403.358165	no classification possible	404.365441	C27H48O2	1.19E+07	5.19E+07	4.77E+06	n.s.	2.91E-02	2.60E-03	Primary bile acid biosynthesis
441.337447	no classification possible	442.344723	C29H46O3	5.38E+06	1.40E+07	8.16E+06	4.40E-02	n.s.	n.s.	Steroid biosynthesis
283.264254	Stearic acid (C18:0)	284.271530	C18H36O2	7.47E+09	1.78E+10	1.44E+10	3.40E-02	n.s.	n.s.	Fatty acid biosynthesis; Biosynthesis of unsaturated fatty acids
309.279850	Icosenoic acid (C20:1)	310.287126	C20H38O2	1.15E+09	1.87E+09	1.23E+09	4.00E-02	n.s.	n.s.	Biosynthesis of unsaturated fatty acids
339.326858	Docosanoic acid (C22:0)	340.334134	C22H44O2	2.00E+08	4.04E+08	3.64E+08	4.60E-03	n.s.	n.s.	Biosynthesis of unsaturated fatty acids
367.358125	Tetracosanoic acid (C24:0)	368.365401	C24H48O2	6.11E+07	1.95E+08	1.34E+08	5.40E-03	n.s.	n.s.	Biosynthesis of unsaturated fatty acids
415.321803	Dihydroxycholestenone	416.329079	C27H44O3	2.85E+07	5.59E+07	2.79E+07	3.60E-02	n.s.	n.s.	Steroid biosynthesis; Primary bile acid biosynthesis
431.316698	Dihydroxycholestenoic acid	432.323974	C27H44O4	4.08E+07	9.38E+07	5.81E+07	6.70E-03	n.s.	n.s.	Primary bile acid biosynthesis
429.300966	Hydroxyoxocholestenoic acid	430.308242	C27H42O4	8.45E+06	2.20E+07	1.67E+07	2.50E-03	n.s.	n.s.	Primary bile acid biosynthesis
361.202017	no classification possible	362.209293	C21H30O5	5.61E+06	2.07E+07	2.11E+06	9.60E-03	n.s.	5.90E-06	Steroid hormone biosynthesis
365.342500	Tetracosenoic acid (C24:1)	366.349776	C24H46O2	1.19E+08	3.08E+08	1.25E+08	3.60E-02	n.s.	n.s.	Biosynthesis of unsaturated fatty acids
311.295572	Icosanoic acid (C20:0)	312.302848	C20H40O2	3.28E+08	1.13E+09	6.01E+08	2.00E-03	n.s.	n.s.	Biosynthesis of unsaturated fatty acids
335.295544	Docosadienoic acid (C22:2)	336.302820	C22H40O2	4.11E+07	1.96E+08	6.15E+07	2.10E-02	n.s.	n.s.	Biosynthesis of unsaturated fatty acids
419.353093	Cholestanetriol	420.360369	C27H48O3	1.65E+07	3.73E+07	1.41E+07	6.50E-03	n.s.	2.70E-03	Primary bile acid biosynthesis
417.337420	Dihydroxycholesterol	418.344696	C27H46O3	6.18E+07	1.26E+08	7.23E+07	1.10E-02	n.s.	n.s.	Primary bile acid biosynthesis; Steroid hormone biosynthesis
433.332347	Trihydroxycholestanal	434.339623	C27H46O4	6.37E+07	1.27E+08	6.35E+07	2.40E-02	n.s.	3.00E-02	Primary bile acid biosynthesis
399.326818	Hydroxycholestenone	400.334094	C27H44O2	3.14E+06	7.20E+06	3.75E+06	7.00E-03	n.s.	n.s.	Steroid biosynthesis; Primary bile acid biosynthesis
401.342490	Hydroxycholesterol	402.349766	C27H46O2	1.86E+07	7.74E+07	1.87E+07	5.20E-04	n.s.	5.45E-03	Primary bile acid biosynthesis; Steroid hormone biosynthesis
413.342482	no classification possible	414.349758	C28H46O2	1.87E+06	5.47E+06	2.32E+06	3.70E-03	n.s.	n.s.	Steroid biosynthesis

6.1.6 Metabolite classes impacted through baseline, HRS and LRS diet

6.1.6.1 Phosphatidic acids impacted through diet

Table 6.1-12: Phosphatidic acid altered in baseline diet.

List of significantly changed phosphatidic acids (PA) through baseline diet, analyzed in (+) FT-ICR-MS; Table contains averaged experimental mass, compound name, monoisotopic mass, molecular formula, obtained with NetCalc, arithmetic mean of the compared feeding groups and their respective p-values, obtained with *post hoc* Kruskal-Nemenyi test.

Mass (avg.)	Compound name	Monoisotopic mass	molecular formula	Mean B	Mean HRS	Mean LRS	p-value B vs. HRS	p-value B vs. LRS	p-value HRS vs. LRS
395.255942	LysoPA(P-16:0) PA(P-16:0)	394.248426	C ₁₉ H ₃₀ O ₈ P	4.28E+09	1.68E+09	9.13E+08	1.98E-02	4.60E-04	n.s.
397.271028	PA(O-16:0) LysoPA(O-16:0)	396.264076	C ₁₉ H ₄₁ O ₆ P	9.10E+08	2.78E+08	1.95E+08	6.70E-03	1.60E-03	n.s.
409.235058	PA(16:1)	408.227690	C ₁₉ H ₃₇ O ₇ P	6.30E+08	1.41E+08	2.54E+07	3.30E-02	6.80E-05	n.s.
423.287066	DHAP(18:0e) PA(P-18:0)	422.279726	C ₂₁ H ₄₃ O ₆ P	3.29E+08	7.94E+07	3.02E+07	1.68E-02	3.50E-04	n.s.
431.219655	PA(18:4)	430.212040	C ₂₁ H ₃₅ O ₇ P	8.33E+07	2.08E+06	3.08E+06	8.70E-03	6.40E-03	n.s.
433.234707	PA(18:3)	432.227690	C ₂₁ H ₃₇ O ₇ P	5.82E+08	6.71E+07	8.96E+06	2.54E-03	3.20E-04	n.s.
437.266379	PA(18:1) LysoPA(18:1) DHAP(18:0)	436.258990	C ₂₁ H ₄₁ O ₇ P	3.93E+08	7.44E+07	1.86E+07	4.70E-02	6.50E-05	n.s.
459.250989	PA(20:4), LysoPA(20:4)	458.243340	C ₂₃ H ₃₉ O ₇ P	4.36E+08	6.62E+07	3.57E+07	8.50E-03	1.70E-03	n.s.
461.266473	PA(20:3)	460.258990	C ₂₃ H ₄₁ O ₇ P	9.14E+08	1.17E+08	2.95E+07	1.14E-02	2.90E-04	n.s.
463.282064	PA(20:2)	462.274640	C ₂₃ H ₄₃ O ₇ P	8.08E+08	1.25E+08	2.94E+07	4.60E-03	2.00E-04	n.s.
481.292582	PA(20:0)	480.285205	C ₂₃ H ₄₅ O ₈ P	4.10E+07	1.70E+07	1.46E+07	3.10E-02	2.70E-02	n.s.
491.402369	PA(22:2)	490.305940	C ₂₅ H ₄₇ O ₇ P	8.87E+06	0.00E+00	0.00E+00	3.30E-02	3.70E-02	n.s.
649.489351	PA(32:0)	623.444051	C ₃₆ H ₆₄ O ₆ P	6.75E+07	3.11E+06	1.26E+06	3.10E-03	3.30E-03	n.s.
657.485838	PA(P-34:2) PA(O-34:3)	656.478091	C ₃₇ H ₆₉ O ₇ P	7.01E+09	3.70E+09	2.67E+09	3.90E-02	1.10E-02	n.s.
659.501346	PA(P-34:0) PA(O-34:1)	658.493941	C ₃₇ H ₇₁ O ₇ P	5.60E+09	3.28E+09	1.64E+09	3.20E-02	1.70E-02	n.s.
661.525607	PA(P-34:1) PA(O-34:2)	660.509391	C ₃₇ H ₇₃ O ₇ P	4.71E+08	5.83E+07	2.79E+07	6.70E-03	1.00E-03	n.s.
663.541240	PA(O-34:0)	662.525041	C ₃₇ H ₇₅ O ₇ P	1.08E+08	2.02E+07	7.43E+06	1.12E-02	4.30E-04	n.s.
675.504917	PA(34:1)	674.488656	C ₃₇ H ₇₁ O ₈ P	9.69E+07	9.20E+06	1.88E+07	1.20E-03	3.50E-03	n.s.
677.520665	PA(34:0)	676.504306	C ₃₇ H ₇₃ O ₈ P	2.42E+08	2.32E+07	5.01E+07	1.30E-03	2.10E-03	n.s.
685.525222	PA(P-36:2) PA(O-36:3)	684.509391	C ₃₉ H ₇₃ O ₇ P	6.87E+08	5.18E+07	1.49E+07	7.40E-04	9.80E-04	n.s.
687.541354	PA(P-36:1) PA(O-36:2)	686.525041	C ₃₉ H ₇₅ O ₇ P	1.14E+08	1.38E+07	3.13E+06	2.80E-03	1.80E-04	n.s.
701.520931	PA(36:2)	700.504306	C ₃₉ H ₇₃ O ₈ P	2.54E+08	1.83E+07	3.30E+06	8.50E-04	2.50E-04	n.s.
703.536355	PA(36:1)	702.519956	C ₃₉ H ₇₅ O ₈ P	5.46E+08	2.52E+07	1.14E+06	8.90E-04	1.30E-04	n.s.

Table 6.1-13: Phosphatidic acids altered through LRS diet.

List of significantly changed phosphatidic acids (PA) through LRS diet, analyzed in (+) FT-ICR-MS; Table contains averaged experimental mass, compound name, monoisotopic mass, molecular formula, obtained with NetCalc, arithmetic mean of the compared feeding groups and their respective p-values, obtained with *post hoc* Kruskal-Nemenyi test.

Mass (avg.)	Compound name	Monoisotopic mass	molecular formula	Mean B	Mean HRS	Mean LRS	p-value B vs. HRS	p-value B vs. LRS	p-value HRS vs. LRS
439.282129	PA(18:0) LPA(18:0)		C ₂₁ H ₄₃ O ₇ P	2.84E+08	6.17E+07	1.52E+09	1.36E-02	n.s.	6.60E-04
495.344785	PA(22:0)		C ₂₅ H ₅₁ O ₇ P	2.70E+07	5.67E+07	1.37E+09	n.s.	5.50E-07	2.80E-03
735.496474	PA(39:6)		C ₄₂ H ₇₁ O ₈ P	1.32E+07	1.74E+07	4.02E+07	n.s.	9.40E-03	n.s.
759.590345	PA(40:1)		C ₄₃ H ₈₃ O ₈ P	3.49E+06	8.00E+06	8.06E+07	n.s.	4.20E-03	n.s.

Table 6.1-14: Phosphatidic acids altered through dietary starch intake.

List of significantly changed phosphatidic acids (PA) through dietary starch intake, analyzed in (+) FT-ICR-MS; Table contains averaged experimental mass, compound name, monoisotopic mass, molecular formula, obtained with NetCalc, arithmetic mean of the compared feeding groups and their respective p-values, obtained with *post hoc* Kruskal-Nemenyi test.

Mass (avg.)	Compound name	Monoisotopic mass	molecular formula	Mean B	Mean HRS	Mean LRS	p-value B vs. HRS	p-value B vs. LRS	p-value HRS vs. LRS
629.417711	PA(31:3)		C34H61O8P	3.20E+07	8.08E+07	9.90E+07	6.40E-03	7.80E-03	n.s.
681.449484	PA(35:5)		C38H65O8P	4.50E+06	1.36E+07	1.87E+07	4.63E-02	3.60E-03	n.s.
683.501696	PA(P-36:3) PA(O-36:4)		C39H71O7P	8.77E+06	4.13E+07	5.72E+07	6.96E-03	3.40E-04	n.s.
685.480582	PA(35:3)		C38H69O8P	1.33E+07	2.09E+07	5.40E+07	n.s.	1.60E-04	n.s.
749.511478	PA(40:6)		C43H73O8P	3.06E+06	1.11E+07	9.86E+06	3.30E-03	4.45E-02	n.s.
761.548446	PA(P-42:6)		C45H77O7P	7.40E+06	1.65E+07	1.38E+07	1.70E-02	n.s.	n.s.
777.543152	PA(42:6)		C45H77O8P	2.99E+06	1.53E+07	1.19E+07	4.90E-04	1.03E-02	n.s.
779.558759	PA(42:5)		C45H79O8P	8.14E+06	2.93E+07	2.90E+07	1.90E-02	3.40E-02	n.s.
781.574725	PA(42:4)		C45H81O8P	6.39E+06	1.81E+07	1.89E+07	3.60E-02	4.00E-02	n.s.

Table 6.1-15: Cyclic phosphatidic acids altered in baseline diet.

List of significantly changed cyclic phosphatidic acids (PA) through baseline diet, analyzed in (+) FT-ICR-MS; Table contains averaged experimental mass, compound name, monoisotopic mass, molecular formula, obtained with NetCalc, arithmetic mean of the compared feeding groups and their respective p-values, obtained with *post hoc* Kruskal-Nemenyi test.

Mass (avg.)	Compound name	Monoisotopic mass	molecular formula	Mean B	Mean HRS	Mean LRS	p-value B vs. HRS	p-value B vs. LRS	p-value HRS vs. LRS
393.240023	CPA(16:0)	392.232776	C19H37O6P	6.75E+09	2.03E+09	1.74E+09	9.99E-03	8.40E-04	n.s.
417.239696	CPA(18:2)	416.232776	C21H37O6P	1.79E+10	2.30E+09	1.30E+08	4.15E-03	9.10E-04	n.s.
419.255352	CPA(18:1)	418.248426	C21H39O6P	5.61E+10	8.06E+09	5.77E+08	1.09E-02	5.30E-04	n.s.
421.271372	CPA(18:0)	420.264076	C21H41O6P	4.84E+09	8.24E+08	5.84E+07	2.24E-03	6.80E-04	n.s.

Table 6.1-16: Fatty acids altered through the baseline, HRS or LRS diet.

List of significantly changed fatty acids through baseline diet, HRS or LRS diet, analyzed in (-) FT-ICR-MS; Table contains averaged experimental mass, compound name, monoisotopic mass, molecular formula, obtained with NetCalc, arithmetic mean of the compared feeding groups and their log₂ fold change values, plus the respective p-values, obtained with *post hoc* Kruskal-Nemenyi test. From Maier, T. V.; Lucio, M.; Lee, L. H.; VerBerkmoes, N. C.; Brislawn, C. J.; Bernhardt, J.; Lamendella, R.; McDermott, J. E.; Bergeron, N.; Heinzmann, S. S.; Morton, J. T.; González, A.; Ackermann, G.; Knight, R.; Riedel, K.; Krauss, R. M.; Schmitt-Kopplin, P.; Jansson, J. K.: Impact of Dietary Resistant Starch on the Human Gut Microbiome, Metaproteome, and Metabolome. *mBio* vol. 8 no. 5 e01343-17 (2017). Data from Figure 2.4-18 and Figure 2.4-20, whose illustration and data depiction was modified from (Maier et al. 2017). Copyright (2017) Maier et al.

Mass (avg.)	Compound name	Monoisotopic mass	molecular formula	Mean B	Mean HRS	Mean LRS	log ₂ fc HRS to B	log ₂ fc LRS to B	log ₂ fc HRS vs LRS	p-value B vs. HRS	p-value B. vs LRS	p-value HRS vs. LRS
253.217286	Hexadecenoic acid (C16:1)	254.224562	C16H30O2	7.31E+08	3.07E+08	3.62E+08	-1.25	-1.01	-0.24	4.30E-03	n.s.	n.s.
279.232882	Octadecadienoic acid (C18:2)	280.240158	C18H32O2	6.49E+10	3.56E+10	4.39E+10	-0.87	-0.56	-0.3	3.10E-02	n.s.	n.s.
281.248559	Octadecenoic acid (C18:1)	282.255835	C18H34O2	9.91E+10	6.25E+10	5.31E+10	-0.66	-0.9	0.23	1.54E-02	1.10E-03	n.s.
269.248611	Heptadecanoic acid (C17:0)	270.255887	C17H34O2	4.02E+08	1.45E+09	8.18E+08	1.85	1.02	0.82	4.00E-02	n.s.	n.s.
283.264254	Octadecanoic acid (C18:0)	284.271530	C18H36O2	7.47E+09	1.78E+10	1.44E+10	1.26	0.94	0.31	3.40E-02	n.s.	n.s.
297.279855	Nonadecanoic acid (C19:0)	298.287131	C19H38O2	4.52E+07	1.14E+08	6.53E+07	1.33	0.53	0.8	2.30E-02	n.s.	n.s.
311.295572	Icosanoic acid (C20:0)	312.302848	C20H40O2	3.28E+08	1.13E+09	6.01E+08	1.79	0.87	0.91	2.00E-03	n.s.	n.s.
339.326858	Docosanoic acid (C22:0)	340.334134	C22H44O2	2.00E+08	4.04E+08	3.64E+08	1.01	0.86	0.15	4.60E-03	n.s.	n.s.
353.342498	Tricosanoic acid (C23:0)	354.349774	C23H46O2	2.70E+07	9.57E+07	4.55E+07	1.83	0.76	1.07	1.80E-03	n.s.	n.s.
367.358125	Tetracosanoic acid (C24:0)	368.365401	C24H48O2	6.11E+07	1.95E+08	1.34E+08	1.68	1.13	0.54	5.40E-03	n.s.	n.s.
381.373818	Pentacosanoic acid (C25:0)	382.381094	C25H50O2	5.97E+06	1.96E+07	1.05E+07	1.72	0.82	0.9	2.80E-03	n.s.	n.s.
395.389437	Hexacosanoic acid (C26:0)	396.396713	C26H52O2	8.29E+06	2.32E+07	1.71E+07	1.49	1.04	0.44	8.90E-03	n.s.	n.s.
301.217257	Icosapentanoic acid (C20:5)	302.224533	C20H30O2	3.66E+07	9.74E+07	3.01E+07	1.41	-0.29	1.7	n.s.	n.s.	2.00E-02
309.279850	Icosenoic acid (C20:1)	310.287126	C20H38O2	1.15E+09	1.87E+09	1.23E+09	0.7	0.09	0.6	4.00E-02	n.s.	n.s.
323.295503	Heneicosenoic acid (C21:1)	324.302779	C21H40O2	1.04E+07	2.35E+07	1.07E+07	1.18	0.05	1.14	4.50E-03	n.s.	1.29E-02
333.279906	Docosatrienoic acid (C22:3)	334.287182	C22H38O2	7.25E+07	2.02E+08	8.37E+07	1.48	0.21	1.27	6.70E-03	n.s.	n.s.
335.295544	Docosadienoic acid (C22:2)	336.302820	C22H40O2	4.11E+07	1.96E+08	6.15E+07	2.25	0.58	1.67	2.10E-02	n.s.	n.s.
337.311207	Docosenoic acid (C22:1)	338.318483	C22H42O2	1.40E+08	3.07E+08	1.33E+08	1.13	-0.08	1.21	6.30E-03	n.s.	n.s.
351.326838	Tricosenoic acid (C23:1)	352.334114	C23H44O2	2.97E+07	4.82E+07	2.37E+07	0.7	-0.33	1.02	4.40E-02	n.s.	n.s.
365.342500	Tetracosenoic acid (C24:1)	366.349776	C24H46O2	1.19E+08	3.08E+08	1.25E+08	1.38	0.07	1.3	3.60E-02	n.s.	n.s.
375.326727	Pentacosatrienoic acid (C25:3)	376.334003	C25H44O2	1.04E+07	4.68E+07	6.18E+06	2.17	-0.75	2.92	n.s.	n.s.	1.70E-03
389.342510	Hexacosatrienoic acid (C26:3)	390.349786	C26H46O2	1.94E+06	5.33E+06	2.66E+06	1.46	0.46	1	2.20E-03	n.s.	n.s.
391.358288	Hexacosadienoic acid (C26:2)	392.365564	C26H48O2	2.65E+06	6.22E+06	3.15E+06	1.23	0.25	0.98	2.00E-02	n.s.	n.s.
431.389434	Nonacosatrienoic acid (C29:3)	432.396710	C29H52O2	3.12E+06	1.13E+07	1.24E+06	1.86	-1.34	3.2	n.s.	n.s.	1.90E-03
241.217282	Pentadecanoic acid (C15:0)	242.224558	C15H30O2	2.99E+08	7.63E+08	9.51E+08	1.35	1.67	-0.32	n.s.	n.s.	n.s.
171.139046	Decanoic acid (C10:0)	172.146322	C10H20O2	5.84E+05	6.27E+05	1.47E+07	0.1	4.66	-4.55	n.s.	3.40E-04	8.20E-04
199.170355	Dodecanoic acid (C12:0)	200.177631	C12H24O2	4.16E+07	4.88E+07	2.00E+09	0.23	5.59	-5.36	n.s.	6.40E-05	2.00E-03
227.201651	Tetradecanoic acid (C14:0)	228.208927	C14H28O2	9.44E+07	1.87E+08	1.80E+09	0.99	4.25	-3.27	n.s.	9.20E-05	n.s.

Table 6.1-17: Dicarboxylic acids significantly increased in HRS diet samples.

List of significantly changed dicarboxylic acid through HRS diet, analyzed in (-) FT-ICR-MS; Table contains averaged experimental mass, compound name, monoisotopic mass, molecular formula, obtained with NetCalc, arithmetic mean of the compared feeding groups and their respective p-values, obtained with *post hoc* Kruskal-Nemenyi test.

Mass (avg.)	Compound name	Monoisotopic mass	molecular formula	Mean B	Mean HRS	Mean LRS	p-value B vs. HRS	p-value B. vs LRS	p-value HRS vs. LRS
227.128851	Dodecenedioic acid	228.136127	C12H20O4	5.99E+06	5.53E+07	1.10E+07	5.10E-04	n.s.	n.s.
297.207236	Heptadecenedioic acid	298.214512	C17H30O4	3.17E+06	7.90E+06	3.67E+06	4.80E-03	n.s.	2.05E-02
341.269716	Eicosanedioic acid	342.276992	C20H38O4	1.98E+07	5.75E+07	1.88E+07	4.40E-03	n.s.	2.80E-03
383.316672	Tricosanedioic acid	384.323948	C23H44O4	1.06E+07	3.89E+07	1.15E+07	3.70E-03	n.s.	1.04E-02

Table 6.1-18: Oxylipins, Hydroxy Fatty acids and Octadecanoids significantly increased in HRS diet samples.

List of significantly changed oxylipins through HRS diet, analyzed in (-) FT-ICR-MS; Table contains averaged experimental mass, compound name, monoisotopic mass, molecular formula, obtained with NetCalc, arithmetic mean of the compared feeding groups and their respective p-values, obtained with *post hoc* Kruskal-Nemenyi test.

Mass (avg.)	Compound name	Class	Monoisotopic mass	molecular formula	Mean B	Mean HRS	Mean LRS	p-value B vs. HRS	p-value B. vs LRS	p-value HRS vs. LRS
319.227841	Hydroxyeicosatetraenoic acid	Eicosanoids	320.235117	C20H32O3	2.49E+07	7.63E+07	3.64E+07	1.70E-04	n.s.	3.78E-02
353.233346	Trihydroxyeicosatrienoic acid	Eicosanoids	354.240622	C20H34O5	1.16E+07	5.77E+07	3.09E+07	2.20E-04	n.s.	n.s.
337.238417	Dihydroxyeicosatrienoic acid	Eicosanoids	338.245693	C20H34O4	1.69E+07	1.02E+08	2.57E+07	7.20E-04	n.s.	4.30E-02
335.222782	Dihydroxyeicosatetraenoic acid	Eicosanoids	336.230058	C20H32O4	9.07E+06	3.47E+07	1.59E+07	3.90E-05	n.s.	2.50E-02
351.217674	Trihydroxyeicosatetraenoic acid	Eicosanoids	352.22495	C20H32O5	6.85E+06	2.35E+07	1.26E+07	1.10E-04	n.s.	4.18E-02
325.202045	Oxo-dihydroxy-dinor-prostenoic acid	Eicosanoids	326.209321	C18H30O5	1.17E+07	3.82E+07	1.62E+07	3.00E-04	n.s.	1.36E-02
327.217677	Trihydroxyoctadecadienoic acid	Eicosanoids	328.224953	C18H32O5	2.56E+07	1.02E+08	3.04E+07	6.60E-04	n.s.	1.18E-02
327.290414	Hydroxyeicosanoic acid	Hydroxy fatty acids	328.29769	C20H40O3	7.28E+07	1.84E+08	6.84E+07	3.20E-03	n.s.	6.90E-03
371.316711	Dihydroxydocosanoic acid	Hydroxy fatty acids	372.323987	C22H44O4	4.45E+06	1.01E+07	4.56E+06	5.40E-03	n.s.	1.50E-02
347.24397	Tetrahydroxyoctadecanoic acid	Hydroxy fatty acids	348.251246	C18H36O6	4.32E+06	9.88E+06	5.06E+06	4.40E-02	n.s.	4.90E-02
287.222731	Dihydroxyhexadecanoic acid	Hydroxy fatty acids	288.230007	C16H32O4	1.68E+07	1.91E+08	2.27E+07	5.20E-03	n.s.	n.s.
309.207131	Hydroxyoctadecenoic acid	Hydroxy fatty acids	310.214407	C18H30O4	1.95E+07	8.62E+07	2.42E+07	5.00E-03	n.s.	2.20E-02
343.285361	Dihydroxyeicosanoic acid	Hydroxy fatty acids	344.292637	C20H40O4	9.50E+06	2.82E+07	9.37E+06	1.10E-03	n.s.	3.60E-03
331.249001	Trihydroxyoctadecanoic acid	Hydroxy fatty acids	332.256277	C18H36O5	1.18E+07	6.42E+07	1.50E+07	4.00E-03	n.s.	2.10E-02
313.238436	Dihydroxyoctadecenoic acid	Hydroxy fatty acids	314.245712	C18H34O4	2.09E+08	1.04E+09	1.97E+08	4.05E-03	n.s.	5.90E-04
329.233297	Trihydroxyoctadecenoic acid	Octadecanoids	330.240573	C18H34O5	5.81E+07	1.90E+08	5.35E+07	n.s.	n.s.	1.10E-02
311.222782	Dihydroxyoctadecadienoic acid	Octadecanoids	312.230058	C18H32O4	7.47E+07	2.63E+08	6.36E+07	9.10E-03	n.s.	1.10E-03

Table 6.1-19: Sulfated Oxylipins, Hydroxy Fatty acids and Octadecanoids significantly increased in HRS diet samples.

List of significantly changed sulfated oxylipins through HRS diet, analyzed in (-) FT-ICR-MS; Table contains averaged experimental mass, compound name, monoisotopic mass, molecular formula, obtained with NetCalc, arithmetic mean of the compared feeding groups and their respective p-values, obtained with *post hoc* Kruskal-Nemenyi test.

Mass (avg.)	Compound name	Class	Monoisotopic mass	molecular formula	Mean B	Mean HRS	Mean LRS	p-value B vs. HRS	p-value B. vs LRS	p-value HRS vs. LRS
399.184697	Hydroxyeicosatetraenoic acid sulfate	Eicosanoids	400.191973	C20H32O6S	1.47E+07	4.39E+07	3.69E+07	5.00E-03	4.40E-02	n.s.
417.195273	Dihydroxyeicosatrienoic acid sulfate	Eicosanoids	418.202549	C20H34O7S	2.84E+06	8.11E+06	4.69E+06	4.10E-03	n.s.	n.s.
415.179638	Dihydroxyeicosatetraenoic acid sulfate	Eicosanoids	416.186914	C20H32O7S	4.62E+06	1.55E+07	1.31E+07	5.90E-03	n.s.	n.s.
407.174533	Trihydroxyoctadecadienoic acid sulfate	Eicosanoids	408.181809	C18H32O8S	4.99E+05	4.35E+06	1.90E+06	3.70E-04	n.s.	n.s.
407.24727	Hydroxyeicosanoic acid sulfate	Hydroxy fatty acids	408.254546	C20H40O6S	1.86E+06	4.24E+06	1.70E+06	n.s.	n.s.	3.10E-02
393.195292	Dihydroxyoctadecenoic acid sulfate	Hydroxy fatty acids	394.202568	C18H34O7S	3.62E+06	3.19E+07	1.07E+07	5.90E-05	n.s.	n.s.
409.190153	Trihydroxyoctadecenoic acid sulfate	Octadecanoids	410.197429	C18H34O8S	1.18E+06	1.19E+07	5.11E+06	9.10E-05	n.s.	n.s.
391.179638	Dihydroxyoctadecadienoic acid sulfate	Octadecanoids	392.186914	C18H32O7S1	3.33E+06	1.29E+07	7.39E+06	1.20E-03	n.s.	n.s.

Table 6.1-20: SCFA profile in baseline, HRS and LRS diet samples.

List of SCFA, analyzed in UHPLC-(+)-ToF-MS; Table contains averaged experimental mass as AMP+ derivate, compound name, arithmetic mean of the compared feeding groups, including standard deviation and their respective p-values, obtained with *post hoc* Kruskal-Nemenyi test.

Mass (avg.) AMP+	Compound name	Mean B	Mean HRS	Mean LRS	p-value B vs. HRS	p-value B. vs LRS	p-value HRS vs. LRS
269.1654	Isovaleric acid	0.47 ± 0.27	0.40 ± 0.34	0.58 ± 0.42	n.s.	n.s.	n.s.
269.1654	Valeric acid	0.61 ± 0.54	0.66 ± 0.47	0.64 ± 0.40	n.s.	n.s.	n.s.
255.1496	Butyric acid	3.65 ± 1.99	5.39 ± 3.83	4.78 ± 2.70	n.s.	n.s.	n.s.
241.1341	Propionic acid	2.66 ± 1.09	3.65 ± 2.93	2.69 ± 0.70	n.s.	n.s.	n.s.

6.2 Tables of the InfantBio Study

6.2.1 Chemicals and other consumable material

Table 6.2-1: Chemicals

Name	Manufacturer	Details
MilliQ water	Merck Millipore Integral water purification system	18 MΩ, TOC < 5 ppb
Methanol	Sigma-Aldrich, St.Louis, USA	CHROMASOLV® for LC-MS, ≥99.9%
Acetonitril	Sigma-Aldrich, St.Louis, USA	CHROMASOLV® for LC-MS, ≥99.9%
Isopropanol	Sigma-Aldrich, St.Louis, USA	CHROMASOLV® for LC-MS, ≥99.9%
Formic acid	Sigma-Aldrich, St.Louis, USA	Eluent additive for LC-MS
Ammoniumacetate	Biosolve BV, Valkenswaard, Netherlands	ULC/MS
Propionic acid	Sigma-Aldrich, St.Louis, USA	≥99.5%
Butyric acid	Sigma-Aldrich, St.Louis, USA	≥99%
Valeric acid	Sigma-Aldrich, St.Louis, USA	≥99%
Isovaleric acid	Sigma-Aldrich, St.Louis, USA	99%
Lactic acid	Sigma-Aldrich, St.Louis, USA	>99%
Pyruvic acid	Sigma-Aldrich, St.Louis, USA	>99%
Hexanoic acid	Sigma-Aldrich, St.Louis, USA	≥99%
Heptanoic acid	Sigma-Aldrich, St.Louis, USA	96%
Octanoic acid	Sigma-Aldrich, St.Louis, USA	≥99.5%
Nonanoic acid	Sigma-Aldrich, St.Louis, USA	≥97%
Tetradecanoic acid	Sigma-Aldrich, St.Louis, USA	≥99.5%
Arachidonic acid	Sigma-Aldrich, St.Louis, USA	>95%
Decanoic acid	Fluka	>99%
Succinic acid	Sigma-Aldrich, St.Louis, USA	≥99.0%
Maleic acid	Sigma-Aldrich, St.Louis, USA	≥99.0%
Fumaric acid	Sigma-Aldrich, St.Louis, USA	≥99.0%
ESI Tune Mix	Agilent, Waldbronn, Germany	G1969-85000
α-Tauromuricholic acid, sodium salt	Steraloids Inc. Newport, USA	C1893-000
β-Tauromuricholic acid, sodium salt	Steraloids Inc. Newport, USA	C1899-000
ω-Tauromuricholic acid, sodium salt	Steraloids Inc. Newport, USA	C1889-000
Tauroursodeoxycholic acid, sodium salt	Calbiochem, San Diego, USA	580549-1GM
Taurocholic acid	Steraloids Inc. Newport, USA	C1965-000
Glycohyocholic acid, sodium salt	Steraloids Inc. Newport, USA	C1860-000
ω-Muricholic acid	Steraloids Inc. Newport, USA	C1888-000
Glycohyodeoxycholic acid	Abcam	sc-396740
Glycocholic acid	Steraloids Inc. Newport, USA	C1925-000
Taurochenodeoxycholic acid, sodium salt	Sigma-Aldrich, St.Louis, USA	T6260-100MG
α-Muricholic acid	Steraloids Inc. Newport, USA	C1890-000
β-Muricholic acid	Steraloids Inc. Newport, USA	C1895-000
Glycoursodeoxycholic acid	Sigma-Aldrich, St.Louis, USA	06863-1G

Taurodeoxycholic acid	Steraloids Inc. Newport, USA	C1160-000
Hyodeoxycholic acid	Sigma-Aldrich, St.Louis, USA	H3878-5G
Ursodeoxycholic acid	Sigma-Aldrich, St.Louis, USA	U5127-1G
Cholic acid	Sigma-Aldrich, St.Louis, USA	C1129-25G
Glycochenodeoxycholic acid, sodium salt	Sigma-Aldrich, St.Louis, USA	G0759-100MG
Glycodeoxycholic acid, sodium salt	Calbiochem	361311-5GM
Taurolithocholic acid, sodium salt	Sigma-Aldrich, St.Louis, USA	T7515-1G
5α-Cholanolic Acid-3α-ol-6-one	Steraloids Inc. Newport, USA	C0720-000
3α-Hydroxy-7 Ketolithocholic Acid	Steraloids Inc. Newport, USA	C1600-000
3α-Hydroxy-12 Ketolithocholic Acid	Steraloids Inc. Newport, USA	C1650-000
Apocholic acid	Steraloids Inc. Newport, USA	C2500-000
Chenodeoxycholic acid	Sigma-Aldrich, St.Louis, USA	C9377-100MG
6-Ketolithocholic acid	Steraloids Inc. Newport, USA	C1706-000
Deoxycholic acid	Sigma-Aldrich, St.Louis, USA	D2510-10G
Glycolithocholic acid, sodium salt	Santa Cruz Biotechnology, Inc., Heidelberg, Germany	sc-396741
Allolithocholic acid	Steraloids Inc. Newport, USA	C0700-000
Isolithocholic acid	Steraloids Inc. Newport, USA	C1475-000
Lithocholenic acid	Steraloids Inc. Newport, USA	C2700-000
Isodeoxycholic acid	Steraloids Inc. Newport, USA	C1170-000
Lithocholic acid	Sigma-Aldrich, St.Louis, USA	L6250-10G
Dehydrolithocholic acid	Steraloids Inc. Newport, USA	C1750-000

Table 6.2-2: Consumable material

Name	Manufacturer	Details
NucleoSpin® Bead Tubes with ceramic beads	Macherey Nagel, Düren, Germany	-
AMP+ Mass Spectrometry Kit	Caymen Chemicals, Ann Arbor, MI, USA	-

Table 6.2-3: Columns

Name	Manufacturer	Details
VisionHT C18 HL	W. R. Grace & Co, Columbia, USA	1.5 μ m 2.0 mm x 150 mm
BEH C8	Waters GmbH, Eschborn, Germany	1.7 μ m, 2.1 mm x 150 mm
BEH C18	Waters GmbH, Eschborn, Germany	1.7 μ m, 2.1 mm x 150 mm

6.2.2 Instrument Setup

6.2.2.1 UHPLC-ToF-MS conditions

For non-targeted metabolomics analyses and SCFA analyses a Waters ACQUITY UPLC® system (Waters GmbH, Eschborn, Germany) was used, including following devices: binary solvent manager (BSM), sample manager (SM), column manager (CM) and PDA detector, coupled to an Bruker UHR-qToF-MS (maXis™, Bruker Daltonik GmbH, Bremen, Germany). The used parameters are given in Table 6.2-4 (non-targeted metabolomics), Table 6.2-5 (SOP) and Table 6.2-6 (SCFA).

Table 6.2-4: Non-targeted metabolomics analyses of fecal samples

Parameter	(+) ToF-MS	(-) ToF-MS
LC		
Run time [min]	15.5	15.5
Flow rate [mL/min]	0.4	0.4
Injection volume [μ L]	5	5
Injection	Partial loop	Partial loop
Column temperature [$^{\circ}$ C]	40	40
ToF-MS		
Mass range in Da	50 – 1000	50 – 1100
Spectrum rate in Hz	1	1
Ion cooler RF	50 Vpp	50 Vpp
Ion cooler transfer time	75.0 μ s	75.0 μ s
Threshold Signal to Noise	500	500
Quadrupole [eV]	3.0	-3.0
Capillary [V]	4500	4000
End plate offset [V]	-500	-500
Nebulizer Gas Flow Rate [bar]	2	2
Drying Gas Flow rate [L/min]	8	8
Dry Gas Temperature [$^{\circ}$ C]	200	200

Table 6.2-5: SOP: Metabolite Profiling using RP- UHPLC-MS.

Parameter	(-) ToF-MS
LC	
Run time [min]	10
Flow rate [mL/min]	0.4
Injection volume [μ L]	5
Injection	Partial loop
Column temperature [$^{\circ}$ C]	40
ToF-MS	
Mass range in Da	100.0 – 1500
Spectrum rate in Hz	2
Ion cooler RF	75 Vpp
Ion cooler transfer time	75 μ s
Threshold Signal to Noise	500
Quadrupole [eV]	3
Capillary [V]	4000
End plate offset [V]	-500
Nebulizer Gas Flow Rate [bar]	2.0
Drying Gas Flow rate [L/min]	10.0
Dry Gas Temperature [$^{\circ}$ C]	200

Table 6.2-6: SCFA Analysis

Parameter	
LC	
Run time [min]	22
Flow rate [mL/min]	0.3
Injection volume [μ L]	1
Injection	Partial loop
Column temperature [$^{\circ}$ C]	40
(+) ToF-MS	
Mass range in Da	50.0 – 1200
Spectrum rate in Hz	1
Ion cooler RF	50 Vpp
Ion cooler transfer time	75 μ s
Threshold Signal to Noise	500
Quadrupole [eV]	3
Capillary [V]	4500
End plate offset [V]	-500
Nebulizer Gas Flow Rate [bar]	2.0
Drying Gas Flow rate [L/min]	8.0
Dry Gas Temperature [$^{\circ}$ C]	200

6.2.2.2 Other Instruments

Table 6.2-7: Other Instruments

Parameter	Manufacturer	Details
refrigerated Centrifuge	Eppendorf	5804R
ultrasonic bath	Bandelin Sonorex	RK100H
Vortex	Scientific Industry	Vortex Genie 2
10 mL Hamilton Glass Syringe	Hamilton	-

6.2.3 Extrapolated metabolites for the discrimination of feeding and over time

Table 6.2-8: Significant features for all exclusively breastfed infants changed over time.

Significant mass signals significantly changed in breast fed infants over time, including month 1, 3, 5, 7, 9 and 12, analyzed in UHPLC-(+)-ToF-MS; ordered with increased p-value of month 1. Mass signals were obtained through PLS-DA analysis of all month (based on Figure 3.4-3 (VIP score >0.8)). P-values were calculated with the two-sided Student's t-test (heteroscedastic). Table contains averaged experimental mass, retention time (in minutes), compound name, if possible, VIP score of PLS-DA analysis and respective p-values, obtained with Student's t-test comparing breast fed versus formula-fed infants of month 1, 3, 5, 7, 9 and 12.

m/z [M+H]	RT	Compound	VIP score	Month 1	Month 3	Month 5	Month 7	Month 9	Month 12	MS/MS
552.3367	5.00	Unknown	1.60835	5.09E-07	4.48E-07	3.45E-05	1.26E-05	3.58E-02	5.78E-02	x
694.2353	0.67	Unknown	1.33307	6.64E-05	3.64E-03	1.98E-02	1.24E-01	n.s.	5.43E-01	
548.2551	4.48	Unknown	1.87395	7.68E-05	1.90E-03	1.10E-02	1.09E-01	n.s.	n.s.	
721.2123	0.68	Unknown	1.71306	1.54E-04	6.79E-04	4.10E-02	n.s.	n.s.	n.s.	
775.2620	0.66	Unknown	1.41775	3.95E-04	3.23E-03	1.77E-01	n.s.	n.s.	n.s.	
512.1849	0.73	Unknown	1.34731	6.91E-04	1.16E-03	8.15E-02	5.88E-02	6.84E-01	8.83E-01	
462.3440	5.60	Unknown	1.33924	7.25E-04	4.39E-06	6.23E-05	3.09E-05	3.76E-02	6.24E-02	
343.1241	0.78	Unknown	1.33311	1.05E-03	1.43E-03	2.20E-02	9.77E-02	4.45E-01	5.48E-01	
617.2619	8.15	Unknown	1.67109	1.15E-03	8.12E-05	3.56E-05	1.11E-02	2.92E-01	3.03E-01	
419.2287	4.53	Unknown	1.32836	1.27E-03	3.00E-03	1.83E-02	6.27E-02	2.30E-01	8.94E-01	
497.1767	4.50	Unknown	1.51583	1.48E-03	6.94E-04	1.92E-02	4.28E-06	6.07E-02	8.96E-02	
375.2921	4.84	Unknown	1.57092	2.78E-03	5.55E-05	1.51E-04	6.76E-06	8.49E-02	5.41E-02	
357.2828	4.84	Unknown	1.60186	4.84E-03	3.19E-05	1.89E-04	1.54E-05	1.01E-01	3.96E-02	
412.3070	5.84	Unknown	1.30506	5.40E-03	1.99E-03	6.20E-03	5.80E-01	1.37E-01	1.33E-01	
945.4938	4.85	Unknown	1.63415	6.89E-03	1.68E-03	9.30E-04	1.66E-04	1.30E-01	8.81E-02	
201.1863	6.70	Dodecanoic acid	1.22607	1.06E-02	1.69E-04	1.88E-01	6.31E-01	1.26E-01	5.43E-01	
453.2159	4.41	Unknown	1.71581	1.77E-02	1.34E-03	1.38E-03	1.78E-05	7.09E-02	6.72E-02	
299.1412	8.15	Unknown	1.88622	1.83E-02	7.84E-05	5.91E-05	9.03E-04	9.33E-02	2.00E-01	

Table 6.2-9: Significant features for all exclusively formula-fed infants changed over time.

Significant mass signals significantly changed formula-fed infants over time, including month 1, 3, 5, 7, 9 and 12, analyzed in UHPLC-(+)-ToF-MS; ordered with increased p-value of month 1. Mass signals were obtained through PLS-DA analysis of all month (based on Figure 3.4-3 (VIP score >0.8)). P-values were calculated with the two-sided Student's t-test (heteroscedastic). Table contains averaged experimental mass, retention time (in minutes), compound name, if possible, VIP score of PLS-DA analysis and respective p-values, obtained with Student's t-test comparing breast fed versus formula-fed infants of month 1, 3, 5, 7, 9 and 12.

m/z [M+H]	RT	Compound	VIP score	Month 1	Month 3	Month 5	Month 7	Month 9	Month 12	MS/MS
407.2455	3.05	Unknown	1.602	1.77E-14	3.58E-15	1.38E-07	2.23E-05	4.55E-03	5.75E-01	x
386.7162	2.59	Unknown	1.524	3.42E-14	2.14E-09	3.83E-09	5.30E-07	3.80E-05	2.76E-01	
377.2296	3.10	Unknown	1.575	2.43E-13	2.00E-10	1.76E-09	6.00E-06	2.26E-03	2.72E-03	x
401.3094	9.56	Unknown	1.396	4.10E-13	7.27E-11	3.14E-11	4.86E-08	1.27E-05	4.94E-03	
427.3610	9.56	Unknown	1.550	5.02E-13	2.36E-09	2.39E-08	2.35E-06	1.36E-04	7.65E-03	
365.1393	1.20	Unknown	1.645	3.09E-12	4.62E-09	3.35E-05	1.61E-03	5.81E-02	n.s.	x
421.2190	3.12	Unknown	1.589	3.38E-12	1.54E-06	6.05E-04	7.87E-04	2.41E-02	3.96E-01	
383.1527	1.21	Unknown	1.662	6.97E-12	8.87E-09	9.75E-06	1.28E-03	3.49E-03	3.85E-01	x
417.3371	9.53	Unknown	1.493	1.26E-11	2.10E-07	3.41E-09	1.98E-05	1.97E-05	4.51E-01	
434.2285	0.76	Unknown	1.831	2.07E-11	1.47E-08	3.09E-06	4.18E-04	1.34E-02	5.45E-01	
323.1967	3.04	Unknown	1.697	4.53E-11	1.74E-09	5.68E-06	2.52E-04	3.03E-02	1.69E-01	
371.2214	3.04	Unknown	1.645	4.61E-11	7.02E-09	2.42E-05	4.70E-04	3.49E-02	8.69E-01	
569.3009	2.99	Unknown	1.846	1.46E-10	4.55E-06	3.58E-03	4.16E-02	1.06E-01	1.30E-01	
389.2328	3.04	Prostaglandine	1.659	3.99E-10	6.07E-09	6.20E-06	4.15E-04	1.86E-02	5.76E-01	x
303.1916	3.16	Unknown	1.567	4.14E-10	1.63E-08	3.69E-08	2.59E-04	4.83E-04	1.03E-02	x
521.2789	2.66	Unknown	1.439	8.43E-08	5.05E-05	2.03E-05	1.27E-04	2.73E-03	6.11E-01	
281.0847	0.67	Unknown	1.475	1.02E-07	9.79E-05	4.71E-01	1.17E-01	3.29E-01	4.10E-01	
262.0715	0.71	Unknown	1.403	1.37E-07	1.72E-04	1.82E-03	5.68E-02	5.55E-01	4.23E-01	
289.0718	0.67	Unknown	2.363	1.56E-07	2.22E-03	n.s.	n.s.	n.s.	n.s.	
551.2835	2.98	Unknown	2.337	1.84E-07	3.67E-05	3.32E-01	n.s.	n.s.	n.s.	
413.3421	8.68	Unknown	1.249	1.85E-07	9.66E-06	1.20E-06	1.75E-03	4.49E-02	1.83E-03	
176.1051	0.75	Unknown	1.444	2.02E-07	3.59E-02	4.81E-02	9.64E-01	7.49E-01	5.42E-01	
326.3105	7.32	Unknown	1.772	2.39E-07	6.63E-07	8.62E-06	6.43E-02	3.94E-02	9.52E-01	
806.4407	6.90	Unknown	1.563	2.50E-07	1.24E-05	1.02E-03	3.43E-02	1.04E-02	5.06E-01	
309.1655	0.71	Unknown	1.341	2.73E-07	1.90E-04	2.79E-02	1.60E-01	2.59E-01	3.55E-01	

248.1178	0.79	Unknown	1.306	8.21E-07	3.03E-04	4.30E-03	7.75E-02	1.18E-02	3.91E-01
813.4731	3.03	Unknown	1.388	1.15E-06	3.29E-05	2.74E-04	1.53E-02	1.13E-01	3.29E-01
255.0908	0.69	Unknown	1.423	1.24E-06	1.12E-03	6.05E-01	3.91E-01	1.41E-01	6.92E-02
493.1950	0.69	Unknown	2.087	1.84E-06	5.80E-04	3.32E-01	n.s.	n.s.	n.s.
471.2374	0.70	Unknown	1.405	1.86E-06	9.01E-04	4.55E-02	4.22E-01	1.47E-01	4.70E-01
553.2563	2.75	Unknown	2.133	2.05E-06	1.00E-03	n.s.	n.s.	n.s.	5.47E-01
459.1820	3.13	Unknown	1.594	2.14E-06	2.41E-06	2.56E-03	7.85E-03	7.07E-02	8.93E-01
229.1367	0.76	Unknown	1.754	4.24E-06	1.10E-01	4.27E-01	7.00E-01	5.39E-01	8.48E-02
572.2815	2.98	Unknown	2.066	5.49E-06	1.94E-04	n.s.	n.s.	n.s.	3.43E-01
683.3371	2.60	Unknown	2.142	2.19E-05	9.83E-04	2.07E-01	n.s.	n.s.	3.43E-01
246.1745	3.07	Unknown	1.352	4.60E-05	3.25E-05	9.99E-03	7.48E-02	3.45E-02	2.45E-01
778.3754	6.12	Unknown	1.582	4.77E-05	2.22E-02	1.31E-03	9.51E-02	9.68E-02	3.07E-01
764.4230	6.32	Unknown	1.475	1.09E-04	2.37E-02	9.00E-03	3.24E-01	3.29E-01	7.48E-01
254.2498	5.53	Unknown	1.534	1.12E-04	1.42E-05	1.79E-03	8.46E-03	3.73E-02	9.25E-02
408.2057	3.04	Unknown	1.380	1.39E-04	5.83E-08	3.37E-05	1.48E-03	5.20E-02	5.89E-01
762.4100	6.29	Unknown	1.466	3.32E-04	2.54E-05	5.85E-03	1.25E-01	1.39E-01	7.01E-01
545.2040	1.20	Unknown	1.990	6.16E-04	1.21E-03	n.s.	n.s.	n.s.	n.s.
273.2597	7.50	Unknown	1.391	1.33E-03	1.26E-05	6.73E-05	2.49E-05	1.87E-03	1.83E-01
469.4921	4.49	Unknown	1.695	2.81E-03	1.09E-03	2.87E-02	5.77E-03	4.09E-01	8.57E-01
418.3462	7.62	Unknown	1.237	5.47E-03	3.47E-04	5.06E-10	9.12E-09	8.89E-07	3.55E-02
427.2113	2.97	Unknown	1.391	7.40E-03	5.41E-03	1.33E-05	9.10E-04	8.51E-01	2.45E-01
427.3608	7.53	Unknown	1.435	8.14E-03	9.65E-06	5.78E-05	1.80E-06	1.68E-03	1.70E-03
445.3714	7.53	Unknown	1.378	1.04E-02	2.42E-06	1.15E-04	6.49E-06	3.52E-03	4.23E-03
539.2329	2.88	Unknown	1.268	4.47E-02	2.13E-01	3.60E-07	4.57E-04	3.14E-03	6.42E-01
338.3570	4.52	Unknown	1.670	5.99E-02	4.40E-05	1.50E-03	3.98E-02	1.02E-02	1.92E-01
431.3554	6.93	Unknown	1.698	6.25E-02	2.93E-06	1.24E-07	2.15E-07	1.15E-04	1.42E-03
417.3345	6.72	Unknown	1.585	1.60E-01	4.80E-08	6.05E-08	7.23E-08	3.50E-07	6.62E-03
447.3480	7.64	Unknown	1.410	1.77E-01	1.89E-02	3.04E-04	1.23E-05	2.08E-03	7.66E-03
405.2998	6.97	Unknown	1.313	4.42E-01	4.52E-04	5.09E-06	1.15E-03	1.58E-01	1.29E-02
547.4245	7.62	Unknown	1.385	4.81E-01	4.13E-02	1.60E-06	7.49E-06	2.84E-03	1.78E-02
348.2912	6.87	Unknown	1.281	7.57E-01	1.90E-08	3.64E-06	6.27E-02	2.23E-01	2.85E-01
429.3763	10.27	Unknown	1.316	8.72E-01	1.85E-02	2.21E-03	6.94E-03	1.67E-02	1.63E-01
459.3516	7.62	Unknown	1.467	n.s.	2.60E-02	1.86E-03	2.07E-04	3.36E-03	9.40E-02

Table 6.2-10: Significant features for all exclusively breastfed infants changed over time.

Significant mass signals significantly changed breast fed infants over time, including month 1, 3, 5, 7, 9 and 12, analyzed in UHPLC(-)-ToF-MS; ordered with increased p-value of month 1. Mass signals were obtained through PLS-DA analysis of all month (based on Figure 3.4-3 (VIP score >0.8)). P-values were calculated with the two-sided Student's t-test (heteroscedastic). Table contains averaged experimental mass, retention time (in minutes), compound name, if possible, VIP score of PLS-DA analysis and respective p-values, obtained with Student's t-test comparing breast fed versus formula-fed infants of month 1, 3, 5, 7, 9 and 12.

m/z [M-H]	RT	Compound	VIP score	Month 1	Month 3	Month 5	Month 7	Month 9	Month 12	MS/MS
550.3184	5.02	Glycerophospho- lipid	1.098	5.30E-06	1.13E-07	3.04E-08	3.39E-01	1.43E-01	6.21E-02	
353.1488	7.28	Unknown	1.193	4.61E-04	2.69E-04	8.96E-02	6.08E-02	2.42E-01	5.80E-01	
998.3454	0.86	Unknown	1.148	4.64E-04	4.75E-04	2.44E-02	2.37E-02	3.43E-01	3.63E-01	
167.0204	0.92	Unknown	1.155	3.46E-03	8.98E-03	4.58E-03	1.74E-02	2.76E-01	6.45E-01	
553.3342	5.04	Unknown	1.165	4.63E-03	2.41E-03	1.33E-02	5.04E-02	7.49E-01	1.84E-01	
531.2992	4.71	Cyprinolsulfate	1.008	9.55E-03	4.04E-04	9.26E-04	9.82E-06	5.70E-02	3.33E-01	x
303.2316	7.25	Eicosatetraenoic acid	1.097	1.08E-02	5.36E-04	1.17E-03	1.38E-03	3.14E-01	7.42E-01	x
943.487	4.87	Unknown	1.128	2.13E-02	6.65E-03	1.89E-03	3.42E-03	1.19E-01	2.93E-01	
247.5432	3.10	Unknown	1.182	2.66E-02	2.58E-03	7.35E-03	7.02E-05	3.44E-02	6.82E-02	
161.0452	0.94	Unknown	1.165	2.76E-02	1.37E-02	1.80E-02	4.87E-03	2.14E-01	2.71E-01	
181.0504	2.81	OH-phenyllactic acid	1.036	3.96E-02	6.55E-05	3.31E-04	1.04E-04	1.45E-01	1.12E-01	x
507.1503	0.87	Unknown	1.126	4.09E-02	7.84E-01	4.59E-02	1.20E-01	8.80E-01	5.13E-02	
199.1702	6.69	Dodecanoic acid	0.91	8.54E-02	5.24E-02	4.88E-01	9.50E-01	3.03E-01	2.89E-01	
469.2812	4.16	Unknown	1.165	9.03E-02	5.50E-01	9.32E-01	2.13E-01	1.09E-01	8.01E-02	
517.289	4.36	Unknown	1.243	9.24E-02	3.49E-04	1.17E-03	4.31E-01	3.26E-02	9.56E-01	
305.2006	4.09	Unknown	1.162	6.75E-01	2.89E-02	2.19E-04	5.86E-05	9.34E-02	1.97E-01	
487.2391	4.48	Sulfocholic acid	1.06	7.81E-01	2.85E-03	1.38E-03	2.89E-04	1.56E-01	4.99E-02	x

Table 6.2-11: Significant features for all exclusively formula-fed infants changed over time

Significant mass signals significantly changed formula-fed infants over time, including month 1, 3, 5, 7, 9 and 12, analyzed in UHPLC(-)-ToF-MS; ordered with increased p-value of month 1. Mass signals were obtained through PLS-DA analysis of all month (based on Figure 3.4-3 (VIP score >0.8)). P-values were calculated with the two-sided Student's t-test (heteroscedastic). Table contains averaged experimental mass, retention time (in minutes), compound name, if possible, VIP score of PLS-DA analysis and respective p-values, obtained with Student's t-test comparing breast fed versus formula-fed infants of month 1, 3, 5, 7, 9 and 12.

m/z [M-H]	RT	Compound	VIP score	Month 1	Month 3	Month 5	Month 7	Month 9	Month 12	MS/MS
312.0938	1.83	Unknown	1.274	4.84E-16	4.09E-11	7.69E-07	3.71E-06	1.36E-03	5.01E-02	
405.2261	3.11	Sterol Lipid	1.381	1.90E-12	2.67E-12	5.68E-07	3.25E-05	4.93E-03	6.32E-01	x
381.1331	1.28	Unknown	1.328	3.70E-12	7.54E-09	1.28E-05	2.18E-03	1.24E-02	1.84E-01	x
833.4319	3.10	Unknown	1.288	1.47E-11	6.24E-10	8.82E-06	2.79E-04	2.57E-02	n.s.	
315.1869	3.09	Unknown	1.337	2.06E-11	7.67E-11	3.22E-06	2.86E-04	8.10E-01	5.11E-01	
567.2789	3.05	Fatty Acyl	1.465	1.46E-09	8.56E-06	3.49E-03	3.36E-02	7.95E-02	1.72E-01	x
811.4568	3.10	Unknown	1.362	2.41E-09	3.90E-08	5.82E-05	5.39E-04	7.19E-02	5.22E-01	
973.4722	3.07	Unknown	1.733	4.80E-09	6.01E-06	n.s.	n.s.	n.s.	n.s.	
389.1916	2.84	Unknown	1.317	1.10E-08	9.75E-03	1.15E-03	7.30E-04	4.14E-03	1.79E-01	
804.3975	6.87	Unknown	1.192	4.01E-08	1.04E-06	2.19E-03	5.67E-03	1.00E-02	3.19E-02	
519.2658	2.72	Unknown	1.178	4.34E-08	1.78E-05	1.37E-05	1.44E-04	8.74E-03	3.81E-02	x
469.2039	0.82	Unknown	1.178	4.66E-08	5.55E-04	2.12E-01	3.11E-01	1.64E-01	2.91E-01	
585.3419	7.37	Tocotrienol glucuronide	1.189	6.56E-08	1.91E-07	8.06E-07	2.40E-03	2.44E-03	5.71E-02	x
375.1179	0.81	Unknown	1.505	1.15E-07	2.46E-05	1.50E-02	2.36E-02	6.93E-02	4.26E-01	
313.2365	5.64	Dihydroxyoleic acid	1.105	1.21E-07	3.68E-05	3.60E-04	3.45E-03	4.07E-03	1.20E-02	x
465.2845	6.57	Cholesterol sulfate	1.128	1.32E-07	4.41E-03	5.39E-02	4.71E-01	2.50E-01	5.55E-01	
607.3824	6.90	Sterol Lipid	1.092	3.58E-07	9.32E-06	1.38E-03	1.08E-01	4.17E-02	4.54E-01	
471.3311	7.46	Unknown	1.154	9.14E-07	6.44E-07	8.22E-05	1.68E-01	6.10E-01	8.45E-01	
681.3175	2.68	Unknown	1.145	2.47E-06	1.66E-02	n.s.	n.s.	n.s.	n.s.	
776.3722	6.12	Unknown	1.274	7.83E-06	1.05E-03	1.35E-03	7.79E-02	4.18E-02	1.04E-01	
776.404	6.12	Unknown	1.27	9.52E-06	1.20E-03	1.55E-03	8.23E-02	5.06E-02	9.21E-02	
577.3719	8.10	Unknown	1.081	1.27E-05	4.31E-05	1.95E-05	2.28E-05	1.81E-06	1.25E-03	
804.5673	6.82	Glycerophospho-lipid	1.153	1.64E-05	4.81E-03	3.19E-01	2.90E-01	1.05E-01	7.56E-01	
521.2616	5.37	Unknown	1.175	2.39E-05	5.40E-07	1.23E-06	2.53E-07	2.86E-04	3.46E-03	
242.012	2.64	Unknown	1.493	5.39E-05	5.95E-03	3.31E-01	n.s.	n.s.	8.56E-01	
543.185	1.27	Unknown	1.373	6.65E-05	1.16E-03	n.s.	n.s.	n.s.	3.29E-01	
591.3879	8.31	Tocopherol glucuronide	1.146	7.03E-05	9.50E-05	1.92E-05	1.30E-05	6.15E-07	2.77E-05	x
762.3968	6.31	Unknown	1.191	7.60E-05	1.16E-04	1.06E-02	4.62E-02	2.08E-01	1.88E-01	
760.3877	6.28	Unknown	1.211	1.17E-04	7.02E-06	8.64E-03	5.54E-02	1.11E-01	3.97E-02	
505.2635	6.48	Unknown	0.972	2.15E-04	5.73E-02	2.76E-02	3.19E-02	1.99E-01	8.23E-02	
427.1782	4.99	Unknown	1.09	2.95E-04	1.22E-05	7.96E-05	2.33E-05	3.81E-04	2.35E-02	
557.454	9.09	Unknown	1.173	3.05E-04	4.85E-05	2.53E-05	4.21E-04	1.65E-04	6.69E-01	
425.1905	3.01	Unknown	1.201	3.59E-04	3.95E-05	2.25E-01	9.08E-02	1.04E-01	3.44E-01	
527.3046	5.76	Unknown	1.098	4.79E-04	3.65E-06	7.56E-05	2.05E-05	7.00E-05	2.63E-02	
497.2926	7.45	Unknown	1.071	6.25E-04	3.95E-07	4.07E-07	2.38E-06	2.31E-07	2.66E-02	
377.0847	0.87	Unknown	1.182	7.56E-04	3.50E-03	8.31E-01	3.15E-01	2.40E-01	1.93E-02	
448.307	5.22	Glycochenodeoxy-cholic Acid	0.961	1.00E-03	2.86E-02	1.79E-03	6.55E-06	3.13E-01	5.46E-02	x
380.3132	7.54	Fatty Acyl	1.112	1.33E-03	4.71E-01	3.08E-03	7.85E-02	2.45E-02	1.08E-04	
599.3565	7.45	Unknown	1.103	1.51E-03	1.89E-02	9.00E-08	2.87E-04	9.00E-04	5.30E-01	
343.2617	6.29	Unknown	1.294	2.24E-03	1.12E-03	n.s.	n.s.	n.s.	2.59E-02	
401.2204	4.76	Unknown	1.293	4.36E-03	1.47E-03	2.23E-02	1.66E-01	8.40E-02	1.69E-01	
227.1281	5.16	Dodecenedioic acid	0.839	1.96E-02	2.62E-04	3.00E-05	6.77E-05	9.91E-05	3.70E-01	x
607.3835	7.42	Unknown	1.505	2.90E-02	2.10E-06	3.21E-05	1.92E-03	1.52E-03	3.60E-01	
489.2659	8.15	Unknown	1.146	3.16E-02	1.85E-02	7.79E-06	5.11E-06	1.50E-04	3.05E-01	
389.2685	6.74	Unknown	1.299	5.83E-02	1.10E-03	9.46E-07	6.97E-06	2.60E-04	2.28E-04	
513.3154	5.33	Unknown	1.095	1.89E-01	1.83E-06	8.62E-07	2.96E-08	2.65E-04	4.47E-02	
511.2943	5.25	Unknown	1.128	2.47E-01	4.88E-04	3.84E-01	1.31E-09	4.83E-04	1.73E-02	
511.3101	7.67	Unknown	1.059	7.88E-01	3.14E-03	1.22E-03	1.55E-03	1.26E-04	2.65E-04	

6.2.4 Impact on the bile acid metabolism through breast- and formula-feeding

Table 6.2-12: Bile acids altered through breast- and formula-feeding over time

Bile acids altered in breast fed and formula-fed infants over time, including month 1, 3, 5, 7, 9 and 12, analyzed in UHPLC(-)-ToF-MS; Table contains averaged experimental mass, compound name, monoisotopic mass, retention time (in minutes), molecular formula and respective p-values, obtained with Mann-Whitney test.

Mass (avg.)	Compound name	Monoisotopic mass	retention time [min]	molecular formula	Month	Mean B	Mean F	*p-value
407.2818	Cholic acid	408.2876	5.15	C ₂₄ H ₄₀ O ₅	Month 1	6.89E+05	6.94E+05	n.s.
					Month 3	6.55E+05	5.09E+05	n.s.
					Month 5	6.68E+05	6.00E+05	n.s.
					Month 7	6.76E+05	6.21E+05	n.s.
					Month 9	5.46E+05	6.50E+05	n.s.
					Month 12	7.50E+05	4.56E+05	n.s.
391.2852	Chenodeoxycholic acid	392.2927	5.85	C ₂₄ H ₄₀ O ₄	Month 1	1.16E+05	8.66E+04	n.s.
					Month 3	1.32E+05	8.74E+04	n.s.
					Month 5	1.38E+05	1.02E+05	n.s.
					Month 7	9.84E+04	1.27E+05	n.s.
					Month 9	1.04E+05	2.62E+05	n.s.
					Month 12	9.38E+04	5.09E+05	n.s.
464.3007	Glycocholic acid	465.3090	4.69	C ₂₆ H ₄₃ NO ₆	Month 1	2.90E+04	5.77E+04	7.26E-05
					Month 3	5.60E+03	5.50E+04	2.01E-04
					Month 5	4.57E+03	8.12E+03	5.16E-06
					Month 7	3.64E+03	8.14E+03	3.77E-04
					Month 9	2.16E+04	2.22E+04	n.s.
					Month 12	5.36E+03	6.08E+04	2.66E-02
448.3070	Glycochenodeoxycholic acid	449.3141	5.22	C ₂₆ H ₄₃ NO ₅	Month 1	5.87E+03	2.39E+04	8.77E-05
					Month 3	2.93E+03	6.44E+04	1.72E-07
					Month 5	3.30E+03	1.41E+04	2.48E-06
					Month 7	1.44E+03	1.28E+04	2.37E-06
					Month 9	1.05E+04	1.86E+04	2.76E-03
					Month 12	2.61E+03	3.67E+04	9.83E-04
531.2992	Cyprinolsulfate	532.3069	4.71	C ₂₇ H ₄₈ O ₈ S	Month 1	8.55E+04	1.92E+04	6.93E-05
					Month 3	1.16E+05	3.45E+04	1.28E-05
					Month 5	1.33E+05	3.65E+04	4.94E-06
					Month 7	8.99E+04	2.43E+04	5.44E-07
					Month 9	6.51E+04	2.10E+04	n.s.
					Month 12	8.78E+04	2.79E+04	n.s.
487.2391	Sulfocholic acid	488.2444	4.48	C ₂₄ H ₄₀ O ₈ S	Month 1	1.75E+05	1.91E+05	n.s.
					Month 3	3.63E+05	1.59E+05	1.85E-03
					Month 5	4.52E+05	1.77E+05	2.35E-04
					Month 7	3.81E+05	1.18E+05	4.50E-05
					Month 9	2.68E+05	1.19E+05	n.s.
					Month 12	3.56E+05	1.08E+05	1.51E-03
389.2686	6-Ketolithocholic Acid	390.2770	5.89	C ₂₄ H ₃₈ O ₄	Month 1	2.67E+02	4.17E+03	2.78E-03
					Month 3	1.93E+03	4.39E+03	n.s.
					Month 5	7.51E+03	7.13E+03	n.s.
					Month 7	9.15E+02	1.54E+04	7.06E-04
					Month 9	3.93E+03	3.97E+04	n.s.
					Month 12	2.50E+03	3.69E+04	2.36E-02
389.2682	5 α -Cholanic acid-3 α -ol-6-one 7-Ketolithocholic Acid	390.2770	5.45	C ₂₄ H ₃₈ O ₄	Month 1	2.24E+04	1.63E+04	n.s.
					Month 3	2.11E+04	2.91E+04	2.55E-02
					Month 5	7.57E+03	2.65E+04	2.79E-05
					Month 7	9.67E+03	3.36E+04	6.74E-06
					Month 9	2.36E+04	7.08E+04	n.s.
					Month 12	2.49E+04	1.17E+05	2.79E-02

Table 6.2-13: Bile acids differently altered through interventional formula and placebo formula.

Bile acids differently altered through interventional and placebo formula-fed infants, including month 1, 3, 5, 7, 9 and 12, analyzed in UHPLC(-)-ToF-MS; Table contains averaged experimental mass, compound name, arithmetic mean of compared groups and respective p-values, obtained with *post hoc* Kruskal-Nemenyi test.

Mass (avg.)	Compound name	Monoisotopic mass	retention time [min]	molecular formula	Month	Mean B	Mean F-	Mean F+	p-value B vs. F-	p-value B vs. F+	p-value F- vs. F+
391.2852	Chenodeoxycholic acid	392.2927	5.85	C ₂₄ H ₄₀ O ₄	Month 1	1.16E+05	5.37E+04	1.17E+05	n.s.	n.s.	0.015
					Month 3	1.32E+05	1.00E+05	7.47E+04	n.s.	n.s.	n.s.
					Month 5	1.38E+05	9.11E+04	1.13E+05	n.s.	n.s.	n.s.
					Month 7	9.84E+04	1.37E+05	1.18E+05	n.s.	n.s.	n.s.
					Month 9	1.04E+05	1.80E+05	3.44E+05	n.s.	n.s.	n.s.
					Month 12	9.38E+04	4.79E+05	5.34E+05	n.s.	n.s.	n.s.
464.3007	Glycocholic acid	465.3090	4.69	C ₂₆ H ₄₃ NO ₆	Month 1	2.90E+04	9.74E+04	2.16E+04	3.40E-04	0.014	n.s.
					Month 3	5.60E+03	1.00E+05	9.78E+03	3.50E-04	n.s.	n.s.
					Month 5	4.57E+03	8.08E+03	8.16E+03	3.00E-04	6.30E-04	n.s.
					Month 7	3.64E+03	7.16E+03	9.12E+03	1.10E-02	8.60E-03	n.s.
					Month 9	2.16E+04	1.73E+04	2.72E+04	n.s.	n.s.	n.s.
					Month 12	5.36E+03	1.17E+05	1.40E+04	n.s.	n.s.	n.s.
448.3070	Glycochenodeoxycholic acid	449.3141	5.22	C ₂₆ H ₄₃ NO ₅	Month 1	5.87E+03	3.11E+04	1.73E+04	6.70E-05	n.s.	n.s.
					Month 3	2.93E+03	1.05E+05	2.39E+04	6.90E-06	4.70E-04	n.s.
					Month 5	3.30E+03	1.65E+04	1.18E+04	5.20E-05	2.10E-03	n.s.
					Month 7	1.44E+03	1.30E+04	1.26E+04	4.80E-04	7.60E-04	n.s.
					Month 9	1.05E+04	1.80E+04	1.91E+04	1.40E-02	0.037	n.s.
					Month 12	2.61E+03	6.63E+04	1.20E+04	n.s.	n.s.	n.s.
531.2992	Cyprinolsulfate	532.3069	4.71	C ₂₇ H ₄₆ O ₈ S	Month 1	8.55E+04	1.42E+04	2.37E+04	5.90E-04	2.58E-02	n.s.
					Month 3	1.16E+05	3.17E+04	3.74E+04	3.00E-03	1.50E-03	n.s.
					Month 5	1.33E+05	2.72E+04	4.58E+04	2.90E-04	4.71E-03	n.s.
					Month 7	8.99E+04	2.41E+04	2.45E+04	3.30E-04	6.70E-04	n.s.
					Month 9	6.51E+04	1.89E+04	2.32E+04	n.s.	n.s.	n.s.
					Month 12	8.78E+04	2.87E+04	2.71E+04	n.s.	n.s.	n.s.

6.2.5 Intermediates of the tocopherol metabolism increased in formula fed infants

Table 6.2-14: Metabolites of the tocopherol metabolism altered in formula-fed infants.

Metabolites of the tocopherol metabolism significantly changed in formula-fed infants, including month 1, 3, 5, 7, 9 and 12, analyzed in UHPLC-(-)-ToF-MS; Table contains averaged experimental mass, compound name, monoisotopic mass, retention time (in minutes), molecular formula and respective p-values, obtained with *post hoc* Kruskal-Nemenyi test.

Mass (avg.)	Compound name	Monoisotopic mass	retention time [min]	molecular formula	Month	Mean B	Mean F	*p-value
585.3419	γ -tocotrienol glucuronide	586.3506	7.37	$C_{34}H_{50}O_8$	Month 1	5.16E+02	1.03E+05	9.78E-08
					Month 3	1.36E+03	1.17E+05	6.14E-08
					Month 5	4.15E+03	7.02E+04	6.32E-07
					Month 7	4.06E+03	4.71E+04	2.65E-06
					Month 9	3.13E+03	3.51E+04	0.000554
					Month 12	4.99E+03	1.57E+04	0.1381
591.3879	γ -tocopherol glucuronide	592.3975	8.31	$C_{34}H_{56}O_8$	Month 1	7.85E+03	5.08E+04	2.19E-05
					Month 3	8.25E+03	5.88E+04	1.99E-07
					Month 5	6.74E+03	3.99E+04	3.68E-08
					Month 7	5.63E+03	5.24E+04	6.56E-07
					Month 9	8.21E+03	4.72E+04	9.30E-07
					Month 12	6.84E+03	3.20E+04	0.004312
605.4029	α -tocopherol glucuronide	606.4132	8.48	$C_{35}H_{58}O_8$	Month 1	1.44E+04	1.02E+04	5.34E-01
					Month 3	3.10E+03	1.35E+04	1.55E-02
					Month 5	2.44E+03	4.38E+03	1.32E-01
					Month 7	2.39E+03	6.07E+03	1.15E-02
					Month 9	6.46E+02	6.01E+03	8.26E-04
					Month 12	7.44E+02	5.31E+03	2.06E-02
599.3565	α -tocotrienol glucuronide	600.3662	7.45	$C_{35}H_{52}O_8$	Month 1	67.80	2.41E+04	6.49E-06
					Month 3	2.99	4.56E+04	9.11E-08
					Month 5	0	4.54E+03	5.87E-08
					Month 7	11.00	2.97E+03	1.50E-04
					Month 9	0	2.18E+03	5.41E-03
					Month 12	1.15E+04	4.23E+03	0.79
577.3719	δ -tocopherol glucuronide	578.3819	8.10	$C_{33}H_{54}O_8$	Month 1	0	6.45E+03	4.37E-07
					Month 3	0	1.19E+04	4.85E-09
					Month 5	489.68	6.46E+03	5.61E-06
					Month 7	0	7.88E+03	5.40E-07
					Month 9	0	5.69E+03	6.98E-05
					Month 12	165.81	5.86E+03	6.98E-05

6.2.6 Fatty acids altered in breastfed and formula-fed infants

Table 6.2-15: Fatty acids altered between F+ and F- vs. breastfed

Fatty acids differently altered through breast feeding and formula, including month 1, 3, 5, 7, 9 and 12, analyzed in UHPLC-(-/+)-ToF-MS; Table contains averaged experimental mass, ionization mode, compound name, monoisotopic mass, retention time (in minutes), molecular formula, arithmetic mean of comrade groups and respective p-values, obtained with Mann-Whitney Test.

Mass (avg.)	ESI	Compound name	Monoisotopic mass	retention time [min]	molecular formula	Month	Mean B	Mean F-	Mean F+	p-value B vs. F-	p-value B vs. F+	p-value F- vs. F+
201.1863	(+)	Dodecanoic acid	200.1776	6.70	C ₁₂ H ₂₄ O ₂	Month 1	3.64E+04	3.73E+02	4.17E+02	2.00E-03	1.40E-03	n.s.
						Month 3	1.23E+04	1.64E+03	4.16E+02	9.20E-04	1.92E-03	n.s.
						Month 5	1.86E+04	0.00E+00	1.43E+04	1.20E-02	n.s.	n.s.
						Month 7	5.70E+03	9.86E+02	7.12E+03	n.s.	n.s.	n.s.
						Month 9	7.60E+03	0.00E+00	8.53E+02	n.s.	n.s.	n.s.
						Month 12	3.81E+03	2.85E+03	1.94E+03	n.s.	n.s.	n.s.
227.2007	(-)	Tetradecanoic acid	228.2089	7.22	C ₁₄ H ₂₈ O ₂	Month 1	5.49E+04	1.99E+02	0.00E+00	2.95E-02	9.40E-03	n.s.
						Month 3	1.55E+04	1.77E+04	0.00E+00	n.s.	5.60E-03	n.s.
						Month 5	6.99E+04	3.78E+02	1.27E+04	7.00E-03	2.90E-02	n.s.
						Month 7	8.29E+03	2.13E+03	5.55E+03	n.s.	n.s.	n.s.
						Month 9	2.16E+04	3.90E+03	5.41E+03	n.s.	n.s.	n.s.
						Month 12	2.93E+04	2.95E+04	1.86E+04	n.s.	n.s.	n.s.
255.2351	(+)	Hexadecenoic acid	254.2246	6.20	C ₁₆ H ₃₀ O ₂	Month 1	2.28E+05	1.33E+04	2.03E+04	1.50E-03	5.28E-02	n.s.
						Month 3	1.25E+05	1.06E+04	3.16E+04	1.30E-03	n.s.	n.s.
						Month 5	7.88E+04	1.89E+04	7.32E+04	1.20E-02	n.s.	2.30E-02
						Month 7	6.68E+04	2.84E+04	3.65E+04	n.s.	n.s.	n.s.
						Month 9	3.51E+05	4.03E+04	2.85E+04	n.s.	4.20E-02	n.s.
						Month 12	6.62E+04	6.06E+04	7.01E+04	n.s.	n.s.	n.s.
303.2316	(-)	Eicosatetraenoic acid	304.2402	7.25	C ₂₀ H ₃₂ O ₂	Month 1	1.50E+05	6.34E+04	5.90E+04	5.10E-02	2.10E-02	n.s.
						Month 3	7.39E+04	4.07E+04	2.88E+04	n.s.	3.10E-03	n.s.
						Month 5	8.40E+04	3.85E+04	4.06E+04	9.60E-03	2.66E-02	n.s.
						Month 7	6.59E+04	2.15E+04	2.17E+04	2.30E-02	2.30E-02	n.s.
						Month 9	8.38E+04	3.64E+04	2.01E+04	n.s.	n.s.	n.s.
						Month 12	1.62E+04	1.51E+04	1.54E+04	n.s.	n.s.	n.s.
301.2182	(-)	Icosapentaenoic acid	302.2246	6.97	C ₂₀ H ₃₀ O ₂	Month 1	4.82E+04	7.55E+03	8.20E+03	5.90E-03	3.08E-02	n.s.
						Month 3	1.14E+04	6.23E+03	2.87E+03	8.90E-03	2.70E-03	n.s.
						Month 5	1.23E+04	2.49E+03	4.51E+03	1.30E-02	n.s.	n.s.
						Month 7	9.06E+03	1.89E+03	1.73E+03	n.s.	n.s.	n.s.
						Month 9	1.74E+04	2.71E+03	4.40E+02	n.s.	n.s.	n.s.
						Month 12	1.68E+03	1.52E+02	6.40E+02	n.s.	n.s.	n.s.

6. Appendix

Table 6.2-16: Metabolites, altered between F+ and F- vs. breastfed.

Metabolites altered through interventional and placebo formula-fed infants, compared to breast-fed infants, including month 1, 3, 5, 7, 9 and 12, analyzed in UHPLC(-)-ToF-MS; Table contains averaged experimental mass, compound name, monoisotopic mass, arithmetic mean of compared groups and respective p-values, obtained with *post hoc* Kruskal-Nemenyi test.

Mass (avg.)	ESI	Compound name	Monoisotopic mass	retention time [min]	molecular formula	Month	Mean B	Mean F-	Mean F+	p-value B vs. F-	p-value B vs. F+	p-value F- vs. F+
181.0504	(-)	Hydroxyphenyl-lactic acid	182.0579	2.81	C ₉ H ₁₀ O ₄	Month 1	1.57E+05	7.30E+04	5.01E+04	n.s.	n.s.	n.s.
						Month 3	2.90E+05	2.93E+04	6.58E+04	5.80E-05	5.40E-03	n.s.
						Month 5	2.90E+05	5.27E+04	8.04E+04	2.10E-04	2.42E-02	n.s.
						Month 7	3.29E+05	2.73E+04	3.99E+04	2.50E-03	2.26E-02	n.s.
						Month 9	1.56E+05	3.22E+04	4.32E+04	n.s.	n.s.	n.s.
						Month 12	1.71E+05	6.11E+04	1.31E+04	n.s.	1.70E-03	n.s.
227.128	(-)	Dodecenedioic acid	228.1362	5.16	C ₁₂ H ₂₀ O ₄	Month 1	0.00E+00	1.26E+04	3.94E+03	7.00E-03	n.s.	n.s.
						Month 3	0.00E+00	8.70E+03	1.13E+04	1.30E-02	2.00E-03	n.s.
						Month 5	0.00E+00	2.02E+04	1.94E+04	3.10E-04	6.96E-03	n.s.
						Month 7	6.52E+02	1.87E+04	1.02E+04	2.90E-04	1.42E-02	n.s.
						Month 9	0.00E+00	2.54E+04	1.34E+04	3.50E-04	n.s.	n.s.
						Month 12	8.06E+03	3.06E+04	1.60E+04	n.s.	n.s.	n.s.
313.2365	(-)	Dihydroxyoleic acid	314.2457	5.64	C ₁₈ H ₃₄ O ₄	Month 1	5.28E+03	3.09E+04	3.25E+04	1.30E-03	6.50E-05	n.s.
						Month 3	1.21E+03	2.51E+04	1.67E+04	1.20E-05	4.10E-05	n.s.
						Month 5	3.00E+03	1.86E+04	1.77E+04	7.20E-04	1.79E-03	n.s.
						Month 7	8.42E+03	1.92E+04	3.18E+04	4.07E-02	8.30E-04	n.s.
						Month 9	9.12E+03	2.78E+04	2.23E+04	7.00E-03	n.s.	n.s.
						Month 12	1.60E+04	6.61E+04	3.17E+04	1.70E-02	n.s.	n.s.

6.2.7 Impact of different feeding types on the SCFA profile (breastfed vs. formula-fed)

Table 6.2-17: SCFA, pyruvic acid and lactic acid altered through either breastfeeding or formula feeding; *Mann-Whitney Test, ° *post hoc* Kruskal-Nemenyi test.

SCFA, lactic acid and pyruvic acid altered through, breast feeding, interventional and placebo formula-fed infants, including month 1, 3, 5, 7, 9 and 12, analyzed as AMP+ derivatives in HPLC-(+)-ToF-MS; Table contains averaged experimental mass, compound name, retention time (in minutes), arithmetic mean of compared groups and respective p-values, obtained with *post hoc* Kruskal-Nemenyi test.

Mass (avg.)	Compound name	retention time [min]	Month	Mean B	Mean F	*p-value B vs. F	Mean F-	Mean F+	°p-value B vs. F-	°p-value B vs. F+	°p-value F- vs. F+
255.1134	Pyruvic acid	4.10	Month 1	4.03	0.67	n.s.	0.46	0.87	n.s.	n.s.	n.s.
			Month 3	1.41	0.27	1.03E-02	0.29	0.26	n.s.	n.s.	n.s.
			Month 5	5.78	0.26	3.07E-04	0.04	0.47	3.00E-02	1.80E-02	n.s.
			Month 7	3.43	0.05	3.53E-05	0.10	0.00	2.17E-02	1.20E-03	n.s.
			Month 9	0.52	0.01	3.42E-03	0.00	0.02	n.s.	n.s.	n.s.
			Month 12	0.13	0.13	n.s.	0.00	0.26	n.s.	n.s.	n.s.
257.129	Lactic acid	3.60	Month 1	31.40	1.97	8.13E-03	2.09	1.86	4.10E-02	n.s.	n.s.
			Month 3	9.38	3.99	n.s.	7.06	0.92	n.s.	n.s.	n.s.
			Month 5	52.02	1.88	1.05E-03	0.49	3.27	2.40E-03	n.s.	n.s.
			Month 7	20.55	0.70	1.38E-04	0.97	0.43	2.04E-02	8.30E-04	n.s.
			Month 9	4.95	0.20	n.s.	0.27	0.14	n.s.	n.s.	n.s.
			Month 12	0.71	2.13	n.s.	4.33	0.12	n.s.	n.s.	n.s.
241.1341	Propionic acid	4.00	Month 1	4.71	20.57	1.30E-05	22.66	18.68	1.80E-04	1.60E-03	n.s.
			Month 3	10.08	13.93	n.s.	14.50	13.36	n.s.	n.s.	n.s.
			Month 5	10.34	19.48	1.54E-03	20.87	18.09	7.80E-03	n.s.	n.s.
			Month 7	11.38	18.41	n.s.	17.47	19.36	n.s.	n.s.	n.s.
			Month 9	11.77	16.84	n.s.	18.81	15.04	n.s.	n.s.	n.s.
			Month 12	17.22	19.85	n.s.	17.45	22.04	n.s.	n.s.	n.s.
255.1497	Butyric acid	4.60	Month 1	1.11	3.58	5.39E-04	4.26	2.97	9.90E-03	1.04E-02	n.s.
			Month 3	1.00	5.04	4.04E-03	6.53	3.54	1.30E-01	n.s.	n.s.
			Month 5	1.21	8.49	8.29E-05	11.00	5.99	4.50E-04	1.15E-02	n.s.
			Month 7	1.75	7.33	2.08E-03	7.89	6.77	1.50E-02	4.50E-02	n.s.
			Month 9	2.95	8.76	n.s.	11.89	5.91	3.80E-02	n.s.	n.s.
			Month 12	9.26	14.99	n.s.	13.98	15.90	n.s.	n.s.	n.s.
269.1654	Isovaleric acid	5.30	Month 1	0.00	0.40	1.30E-04	0.43	0.37	3.10E-03	1.18E-02	n.s.
			Month 3	0.17	0.51	1.25E-02	0.48	0.55	n.s.	n.s.	n.s.
			Month 5	0.07	0.76	2.49E-05	0.85	0.68	1.00E-03	1.30E-03	n.s.
			Month 7	0.16	0.73	1.97E-03	0.61	0.85	n.s.	2.10E-02	n.s.
			Month 9	0.52	1.28	n.s.	1.77	0.83	n.s.	n.s.	n.s.
			Month 12	1.07	1.75	n.s.	1.59	1.89	n.s.	n.s.	n.s.
269.1654	Valeric acid	5.50	Month 1	0.00	0.04	n.s.	0.09	0.00	n.s.	n.s.	n.s.
			Month 3	0.08	0.06	n.s.	0.09	0.03	n.s.	n.s.	n.s.
			Month 5	0.03	0.25	1.39E-02	0.34	0.17	2.50E-02	n.s.	n.s.
			Month 7	0.02	0.11	2.48E-03	0.08	0.15	4.70E-02	n.s.	n.s.
			Month 9	0.01	0.23	6.22E-03	0.40	0.08	1.30E-02	n.s.	n.s.
			Month 12	0.15	0.43	n.s.	0.53	0.34	n.s.	n.s.	n.s.

6.2.8 Differences in exclusively non-probiotic fed and probiotic fed infants

Table 6.2-18: Differences in exclusively non-probiotic fed and probiotic fed infants.

Mass signals altered in differently in interventional and placebo formula-fed infants, in UHPLC-(-/+)-ToF-MS; Table contains averaged experimental mass, ionization mode, monoisotopic mass, retention time (in minutes), arithmetic mean of compared groups and respective p-values, obtained with *post hoc* Kruskal-Nemenyi test.

Mass (avg.)	ESI	Monoisotopic mass	retention time [min]	Month	Mean B	Mean F-	Mean F+	*p-value B vs. F-	*p-value B vs. F+	*p-value F- vs. F+
440.2844	(+)	439.2771	6.12	Month 1	1.99E+04	1.60E+05	3.92E+04	3.30E-04	n.s.	n.s.
644.4008	(+)	643.3935	7.16	Month 1	7.34E+03	7.51E+04	1.37E+04	1.70E-04	n.s.	n.s.
644.4008	(+)	643.3935	7.16	Month 3	1.58E+04	7.84E+04	1.19E+04	9.00E-04	n.s.	2.70E-02
445.3707	(+)	444.3634	10.71	Month 1	1.11E+04	4.04E+04	1.09E+04	3.50E-03	n.s.	4.20E-02
510.3339	(+)	509.3266	4.49	Month 1	2.99E+03	1.96E+02	7.88E+03	n.s.	n.s.	4.20E-02
537.3863	(+)	536.3790	4.14	Month 1	2.62E+03	4.64E+03	2.64E+04	n.s.	2.20E-02	n.s.
438.2606	(-)	437.2533	6.1	Month 1	0.00E+00	1.23E+05	2.94E+04	2.30E-03	n.s.	n.s.
516.3154	(-)	515.3081	7.13	Month 1	4.73E+03	1.37E+04	2.24E+03	n.s.	n.s.	2.90E-02
573.3827	(-)	572.3754	7.86	Month 1	0.00E+00	4.60E+03	1.32E+03	2.10E-05	2.40E-02	n.s.
541.3335	(-)	540.3262	5.47	Month 1	2.84E+03	3.08E+03	4.37E+04	n.s.	3.40E-02	6.10E-02
403.2689	(-)	402.2616	4.47	Month 9	3.00E+03	1.61E+04	6.37E+03	1.00E-03	n.s.	3.80E-02
298.1122	(-)	297.1049	0.85	Month 12	4.71E+03	1.08E+04	3.78E+03	n.s.	n.s.	3.20E-02
378.2958	(-)	377.2885	7.21	Month 5	9.87E+02	2.36E+03	2.65E+04	9.00E-04	n.s.	3.30E-02

6.2.9 Correlations between OTUs and Metabolites

Table 6.2-19: Feeding Cohort Specific Metabolites and Correlation to OTUs of Month 1.

Correlated metabolites and OTUs of Breastfed (B), Interventional formula (F+) and placebo formula fed (F-) Infants, analyzed in UHPLC-(-/+)-ToF-MS Ranked from High to Low Importance (Order) by Significance on OPLS-DA loadings plot. *m/z* = mass-to-charge ratio of positive electrospray ionization. Molecular formula and classification assigned using the MassTRIX webserver with an error of 0.05 Da, assignment by LipidMaps and HMDB. From Bazanella, M., Maier, T. V., Clavel, T., Lagkouvardos, I., Lucio, M., Maldonado-Gómez, M. X., Autran, C., Walter, J., Bode, L., Schmitt-Kopplin, P., Haller, D.: Randomized controlled trial on the impact of early-life intervention with bifidobacteria on the healthy infant fecal microbiota and metabolome. *Am J Clin Nutr.* (2017), 106(5):1274-1286. Reproduced and adapted from (Bazanella et al. 2017) by permission of Oxford University Press. Copyright (2017) American Society for Nutrition.

	ID	Feed	Order	<i>m/z</i> or taxonomy	RT [min]	MS/MS	Lipid Maps classification	HMDB classification
MONTH 1	Cluster_4611	B	1	552.3367	5.00	x		
	Cluster_1816	B	2	621.7142	0.67			
	Cluster_5216	B	3	621.2105	0.68			
	Cluster_0644	B	4	256.0822	0.75			
	Cluster_5825	B	5	694.2353	0.67			
	Cluster_3214	B	6	376.2631	5.40			Benzopyrans
	Cluster_5970	B	7	713.2216	0.68			
	Cluster_5136	B	8	613.1922	0.66			
	Cluster_2992	B	9	341.2931	6.67			
	Cluster_2002	B	10	721.2123	0.68			
	Cluster_3467	F	1	407.2455	3.05	x		
	Cluster_3230	F	2	377.2296	3.10	x		Lipids
	Cluster_0971	F	3	386.7162	2.59			
	Cluster_3644	F	4	427.3610	9.56			Lipids
	Cluster_3593	F	5	421.2190	3.12			
	Cluster_3745	F-	1	440.2844	6.12			
	OTU_10	F-	2	<i>Bacteroides sp.</i>				
	Cluster_3789	F-	3	445.3707	10.71		Sterol Lipids [ST]	Prenol Lipids
	Cluster_5412	F-	4	644.4008	7.16			
	OTU_18	F-	5	<i>Bacteroides sp.</i>				
Cluster_5175	F-	6	616.3490	6.36				
Cluster_6345	F-	7	764.4230	6.32				
Cluster_0385	F+	1	510.3340	4.49				
Cluster_4506	F+	2	537.3864	4.14				
OTU_4	F+	3	<i>Bifidobacterium sp.</i>					
Cluster_6749	F+	4	813.5680	4.79		Glycerophospholipids [GP]		
OTU_142	F+	6	<i>Lactococcus sp.</i>					
Cluster_3067	F+	7	353.2507	4.88				
Cluster_2260	F+	8	144.0825	3.03				
Cluster_3573	F+	9	417.3345	6.72				

Table 6.2-20: Feeding Cohort Specific Metabolites and Correlation to OTUs of Month 7.

Correlated metabolites and OTUs of Breastfed (B) and Formula-fed (F) Infants, analyzed in UHPLC-(+)-ToF-MS, Ranked from High to Low Importance (Order) by Significance on OPLS-DA loadings plot. m/z = mass-to-charge ratio of positive electrospray ionization. Molecular formula and classification assigned using the MassTRIX webserver with an error of 0.05 Da, assignment by LipidMaps and HMDB. From Bazanella, M., Maier, T. V., Clavel, T., Lagkouvardos, I., Lucio, M., Maldonado-Gómez, M. X., Autran, C., Walter, J., Bode, L., Schmitt-Kopplin, P., Haller, D.: Randomized controlled trial on the impact of early-life intervention with bifidobacteria on the healthy infant fecal microbiota and metabolome. *Am J Clin Nutr.* (2017), 106(5):1274-1286. Reprinted and adapted from (Bazanella et al. 2017) by permission of Oxford University Press. Copyright (2017) American Society for Nutrition.

	ID	Feed	Order	m/z or taxonomy	RT [min]	MS/MS	Lipid Maps classification	HMDB classification
MONTH 7	Cluster_4141	B	1	491.3308	6.43			
	Cluster_4188	B	2	497.1767	4.50			
	Cluster_3864	B	3	453.2159	4.41			
	Cluster_4611	B	4	552.3367	5.00	x		
	Cluster_3207	B	5	375.2921	4.84		Sterol Lipids [ST]	Steroids and Steroid Derivatives
	Cluster_3088	B	6	357.2828	4.84			Fatty Acids and Conjugates
	Cluster_4029	B	7	473.2537	4.84		Sterol Lipids [ST]	Steroids and Steroid Derivatives
	Cluster_3946	B	8	462.3440	5.60		Sphingolipids [SP]	Sphingolipids
	Cluster_2277	B	9	162.1070	0.75			
	Cluster_3159	B	10	368.3898	10.04			
	Cluster_2614	B	11	279.1036	1.81		Polyketides	
	Cluster_0566	B	12	209.6185	3.70			
	Cluster_2524	B	13	261.1469	2.80		primary amine	
	Cluster_2352	B	14	206.0830	3.62			
	OTU_1	B	15	<i>Bifidobacterium sp.</i>				
	Cluster_3580	F	1	418.3462	7.62			
	Cluster_3425	F	2	401.3094	9.56		Sterol Lipids [ST]	Prenol Lipids
	Cluster_3573	F	3	417.3345	6.72			
	Cluster_0971	F	4	386.7162	2.59			
	Cluster_3493	F	5	410.3203	8.24			
	Cluster_3683	F	6	431.3554	6.93		Sterol Lipids [ST]	Prenol Lipids
	Cluster_3644	F	7	427.3610	9.56			Lipids
	Cluster_3230	F	8	377.2296	3.10	x		Lipids
	Cluster_4577	F	9	547.4245	7.62			
	Cluster_3803	F	10	447.3480	7.64			
	Cluster_3781	F	11	445.3714	7.53		Sterol Lipids [ST]	
	Cluster_2580	F	12	273.2597	7.50			
	Cluster_3467	F	13	407.2455	3.05	x		
	Cluster_3575	F	14	417.3371	9.53			
	OTU_29	F	15	<i>Flavonifractor sp.</i>				
	Cluster_3613	F	16	423.3296	8.51			

Table 6.2-21: Feeding Cohort Specific Metabolites and Correlation to OTUs of Month 12.

Correlated metabolites and OTUs of Breastfed (B) and Formula-fed (F) Infants, analyzed in UHPLC-(+)-ToF-MS, Ranked from High to Low Importance (Order) by Significance on OPLS-DA loadings plot. m/z = mass-to-charge ratio of positive electrospray ionization. Molecular formula and classification assigned using the MassTRIX webserver with an error of 0.05 Da, assignment by LipidMaps and HMDB. From Bazanella, M., Maier, T. V., Clavel, T., Lagkouvardos, I., Lucio, M., Maldonado-Gómez, M. X., Autran, C., Walter, J., Bode, L., Schmitt-Kopplin, P., Haller, D.: Randomized controlled trial on the impact of early-life intervention with bifidobacteria on the healthy infant fecal microbiota and metabolome. *Am J Clin Nutr.* (2017), 106(5):1274-1286. Reprinted and adapted from (Bazanella et al. 2017) by permission of Oxford University Press. Copyright (2017) American Society for Nutrition.

	ID	Feed	Order	m/z or taxonomy	RT [min]	MS/MS	Lipid Maps classification	HMDB classification
MONTH 12	Cluster_2524	B	1	261.1469	2.80		primary amine	Amino Acids and Derivatives
	Cluster_4871	B	2	583.2605	5.10			
	Cluster_2250	B	3	118.0880	0.81			
	Cluster_2352	B	4	206.0830	3.62			
	Cluster_3088	B	5	357.2828	4.84			Fatty Acids and Conjugates
	Cluster_4611	B	6	552.3367	5.00	x		
	OTU_29	F	1	<i>Flavonifractor sp.</i>				
	Cluster_3642	F	2	427.3608	7.53			Lipids
	Cluster_3613	F	3	423.3296	8.51			Fatty Acid Esters
	Cluster_3914	F	4	458.3999	10.11		Sterol Lipids [ST]	
	Cluster_4445	F	5	531.4156	10.11			
Cluster_3580	F	6	418.3462	7.62				
Cluster_3644	F	7	427.3610	9.56				
Cluster_3425	F	8	401.3094	9.56		Sterol Lipids [ST]		
Cluster_2771	F	9	303.1916	3.16	x			
Cluster_3803	F	10	447.3480	7.64				
OTU_125	F	11	<i>Coprobacillus sp.</i>					

Table 6.2-22: Feeding Cohort Specific Metabolites and Correlation to OTUs of Month 1.

Correlated metabolites and OTUs of Breastfed (B), Interventional formula (F+) and placebo formula fed (F-) Infants, analyzed in UHPLC-(-)-ToF-MS Ranked from High to Low Importance (Order) by Significance on OPLS-DA loadings plot. m/z = mass-to-charge ratio of positive electrospray ionization. Molecular formula and classification assigned using the MassTRIX webserver with an error of 0.05 Da, assignment by LipidMaps and HMDB.

	ID	Feed	Order	m/z or taxonomy	RT [min]	MS/MS	Lipid Maps classification	HMDB classification
MONTH 1	Cluster_1704	B	1	550.3184	5.02		GP	
	Cluster_3175	B	2	854.2985	0.90		GP	
	Cluster_3680	B	3	998.3454	0.86			
	Cluster_3376	B	4	909.2396	0.87			
	Cluster_3094	B	5	837.2976	0.88			
	Cluster_0020	B	6	727.3631	0.82			
	Cluster_3645	B	7	982.2628	0.82			
	Cluster_2619	B	8	726.2212	0.86			
	Cluster_3167	B	9	852.2956	0.87			
	Cluster_2468	B	10	695.2238	0.88		PK	
	Cluster_0435	F	1	312.0938	1.83			
	Cluster_0843	F	2	405.2260	3.11	x	ST	
	Cluster_0714	F	3	381.1331	1.28	x		Piperidines
	Cluster_0449	F	4	315.1869	3.09			
	Cluster_1814	F	5	567.2789	3.05	x	FA	Eicosanoids
	Cluster_3076	F	6	833.4319	3.10			
	Cluster_2973	F	7	811.4568	3.10			
	Cluster_3613	F	8	973.4721	3.07			
	Cluster_1937	F	9	585.3419	7.37		γ -Tocotrienol glucuronide	GP
	Cluster_0760	F	10	389.1916	2.84			
Cluster_1505	F-	1	516.3155	7.13				
OTU_10	F-	2	<i>Bacteroides sp.</i>					
Cluster_1850	F-	3	573.3827	7.86				
Cluster_2750	F-	4	762.3968	6.31				
Cluster_1026	F-	5	438.2606	6.10				
Cluster_1655	F+	1	541.3335	5.47				
Cluster_2982	F+	2	811.5762	4.82				
Cluster_1105	F+	3	451.2645	4.85				
Cluster_0841	F+	5	405.2655	4.82		ST	Steroids and Steroid Derivatives	
OTU_4	F+	6	<i>Bifidobacterium sp.</i>					

Table 6.2-23: Feeding Cohort Specific Metabolites and Correlation to OTUs of Month 7.

Correlated metabolites and OTUs of Breastfed (B) and Formula-fed (F) Infants, analyzed in UHPLC(-)-ToF-MS, Ranked from High to Low Importance (Order) by Significance on OPLS-DA loadings plot. m/z = mass-to-charge ratio of positive electrospray ionization. Molecular formula and classification assigned using the MassTRIX webserver with an error of 0.05 Da, assignment by LipidMaps and HMDB.

	ID	Feed	Order	m/z or taxonomy	RT [min]	MS/MS	Lipid Maps classification	HMDB classification
MONTH 7	Cluster_1596	B	1	531.2992	4.71	Cyprinolsulfate	ST	Steroids and Steroid Derivatives
	Cluster_0761	B	2	389.0971	3.70			Betalains
	Cluster_0072	B	3	305.2006	4.09			
	Cluster_0030	B	4	247.5431	3.10			
	Cluster_1327	B	5	487.2391	4.48	7-Sulfocholic acid	ST	
	Cluster_0179	B	6	181.0504	2.81	Hydroxyphenyllactic acid		
	Cluster_0017	B	7	389.241	3.50			
	Cluster_0064	B	8	297.1253	4.43			
	Cluster_2174	B	9	627.3722	4.78			
	Cluster_1671	B	10	544.2574	4.88			
Cluster_0448	F	1	315.2531	5.96				
OTU_29	F	2	<i>Flavonifractor sp.</i>					
Cluster_0237	F	3	227.1281	5.16	Traumatic acid	FA	Fatty Acids and Conjugates	
Cluster_1010	F	4	435.2754	5.46		PR		
Cluster_1523	F	5	519.2658	2.72	x			
Cluster_1651	F	6	541.3191	7.25				
Cluster_2020	F	7	599.3565	7.45				
Cluster_3076	F	8	833.4319	3.10				
Cluster_2973	F	9	811.4568	3.10				
Cluster_0760	F	10	389.1916	2.84				

Table 6.2-24: Feeding Cohort Specific Metabolites and Correlation to OTUs of Month 12.

Correlated metabolites and OTUs of Breastfed (B) and Formula-fed (F) Infants, analyzed in UHPLC(-)-ToF-MS, Ranked from High to Low Importance (Order) by Significance on OPLS-DA loadings plot. m/z = mass-to-charge ratio of positive electrospray ionization. Molecular formula and classification assigned using the MassTRIX webserver with an error of 0.05 Da, assignment by LipidMaps and HMDB.

	ID	Feed	Order	m/z or taxonomy	RT [min]	MS/MS	Lipid Maps classification	HMDB classification
MONTH 12	Cluster_0926	B	1	421.0659	0.87			
	Cluster_2156	B	2	624.3362	4.74		ST	
	Cluster_1182	B	3	464.1811	4.48			
	Cluster_1704	B	4	550.3184	5.02		GP	
	Cluster_1671	B	5	544.2574	4.88			
	Cluster_1327	B	6	487.2391	4.48	7-Sulfocholic acid	ST	
	Cluster_1222	B	7	469.2812	4.16			
	Cluster_0209	B	8	204.0662	3.69			
	Cluster_1677	B	9	546.1973	0.93			Trisaccharides
	Cluster_1914	B	10	583.2704	4.87			
OTU_14	B	11	<i>Enterococcus sp.</i>					
OTU_29	F	1	<i>Flavonifractor sp.</i>					
Cluster_0765	F	2	389.2686	5.89	6-Lithocholic acid	ST	Steroids and Steroid Derivatives	
Cluster_1973	F	3	591.3878	8.31	γ -Tocopherol glucuronide	ST		
Cluster_0766	F	4	389.2685	6.74		ST	Steroids and Steroid Derivatives	
Cluster_0827	F	5	403.2689	4.47				
Cluster_1154	F	6	459.3463	7.61		ST		
Cluster_0776	F	7	391.2852	5.85	Chenodeoxycholic acid	ST	Steroids and Steroid Derivatives	
Cluster_1475	F	8	511.3101	7.67				
Cluster_0764	F	9	389.2682	5.45	5 α -Cholanic acid-3 α -ol-6-one 7-Ketolithocholic Acid	ST	Steroids and Steroid Derivatives	

Chapter VII

Literature

Abdulkadir, B., Nelson, A., Skeath, T., Marrs, E. C., Perry, J. D., Cummings, S. P., Embleton, N. D., Berrington, J. E. and Stewart, C. J. (2016). "Routine Use of Probiotics in Preterm Infants: Longitudinal Impact on the Microbiome and Metabolome." *Neonatology* **109**(4): 239-247.

Alnouti, Y. (2009). "Bile Acid sulfation: a pathway of bile acid elimination and detoxification." *Toxicol Sci* **108**(2): 225-246.

Arrieta, M. C., Stiemsma, L. T., Amenyogbe, N., Brown, E. M. and Finlay, B. (2014). "The intestinal microbiome in early life: health and disease." *Front Immunol* **5**: 427.

Athenstaedt, K. and Daum, G. (1999). "Phosphatidic acid, a key intermediate in lipid metabolism." *Eur J Biochem* **266**(1): 1-16.

Aw, W. and Fukuda, S. (2015). "Toward the comprehensive understanding of the gut ecosystem via metabolomics-based integrated omics approach." *Semin Immunopathol* **37**(1): 5-16.

Backhed, F., Ding, H., Wang, T., Hooper, L. V., Koh, G. Y., Nagy, A., Semenkovich, C. F. and Gordon, J. I. (2004). "The gut microbiota as an environmental factor that regulates fat storage." *Proc Natl Acad Sci U S A* **101**(44): 15718-15723.

Backhed, F., Roswall, J., Peng, Y., Feng, Q., Jia, H., Kovatcheva-Datchary, P., Li, Y., Xia, Y., Xie, H., Zhong, H., Khan, M. T., Zhang, J., Li, J., Xiao, L., Al-Aama, J., Zhang, D., Lee, Y. S., Kotowska, D., Colding, C., Tremaroli, V., Yin, Y., Bergman, S., Xu, X., Madsen, L., Kristiansen, K., Dahlgren, J. and Wang, J. (2015). "Dynamics and Stabilization of the Human Gut Microbiome during the First Year of Life." *Cell Host Microbe* **17**(5): 690-703.

Ballard, O. and Morrow, A. L. (2013). "Human milk composition: nutrients and bioactive factors." *Pediatr Clin North Am* **60**(1): 49-74.

Balzer, M. and Deussen, O. (2005). Voronoi treemaps. *Information Visualization, INFOVIS 2005. IEEE Symposium on IEEE*.

Bazanella, M., Maier, T. V., Clavel, T., Lagkouvardos, I., Lucio, M., Maldonado-Gomez, M. X., Autran, C., Walter, J., Bode, L., Schmitt-Kopplin, P. and Haller, D. (2017). "Randomized controlled trial on the impact of early-life intervention with bifidobacteria on the healthy infant fecal microbiota and metabolome." *Am J Clin Nutr* **106**(5): 1274-1286.

Behall, K. M., Scholfield, D. J., Yuhaniak, I. and Canary, J. (1989). "Diets containing high amylose vs amylopectin starch: effects on metabolic variables in human subjects." *Am J Clin Nutr* **49**(2): 337-344.

Belenguer, A., Duncan, S. H., Calder, A. G., Holtrop, G., Louis, P., Lobley, G. E. and Flint, H. J. (2006). "Two routes of metabolic cross-feeding between *Bifidobacterium adolescentis* and butyrate-producing anaerobes from the human gut." *Appl Environ Microbiol* **72**(5): 3593-3599.

Beloborodova, N., Bairamov, I., Olenin, A., Shubina, V., Teplova, V. and Fedotcheva, N. (2012). "Effect of phenolic acids of microbial origin on production of reactive oxygen species in mitochondria and neutrophils." *J Biomed Sci* **19**: 89.

Benson, A. K., Kelly, S. A., Legge, R., Ma, F., Low, S. J., Kim, J., Zhang, M., Oh, P. L., Nehrenberg, D., Hua, K., Kachman, S. D., Moriyama, E. N., Walter, J., Peterson, D. A. and Pomp, D. (2010). "Individuality in gut microbiota composition is a complex polygenic trait shaped by multiple environmental and host genetic factors." *Proc Natl Acad Sci U S A* **107**(44): 18933-18938.

Bergeron, N., Williams, P. T., Lamendella, R., Faghihnia, N., Grube, A., Li, X., Wang, Z., Knight, R., Jansson, J. K., Hazen, S. L. and Krauss, R. M. (2016). "Diets high in resistant starch increase plasma levels of trimethylamine-N-oxide, a gut microbiome metabolite associated with CVD risk." *Br J Nutr* **116**(12): 2020-2029.

Bergmann, H., Rodriguez, J. M., Salminen, S. and Szajewska, H. (2014). "Probiotics in human milk and probiotic supplementation in infant nutrition: a workshop report." *Br J Nutr* **112**(7): 1119-1128.

Bernhardt, J., Funke, S., Hecker, M. and Siebourg, J. (2009). Visualizing Gene Expression Data via Voronoi Treemaps. *Voronoi Diagrams, ISVD '09. Sixth International Symposium on Copenhagen*, IEEE: 233-241.

Biasucci, G., Benenati, B., Morelli, L., Bessi, E. and Boehm, G. (2008). "Cesarean delivery may affect the early biodiversity of intestinal bacteria." *Journal of Nutrition* **138**(9): 1796s-1800s.

Bird, S. S., Marur, V. R., Sniatynski, M. J., Greenberg, H. K. and Kristal, B. S. (2011). "Lipidomics profiling by high-resolution LC-MS and high-energy collisional dissociation fragmentation: focus on characterization of mitochondrial cardiolipins and monolysocardiolipins." *Anal Chem* **83**(3): 940-949.

Birt, D. F., Boylston, T., Hendrich, S., Jane, J. L., Hollis, J., Li, L., McClelland, J., Moore, S., Phillips, G. J., Rowling, M., Schalinske, K., Scott, M. P. and Whitley, E. M. (2013). "Resistant starch: promise for improving human health." *Adv Nutr* **4**(6): 587-601.

Boersma, E. R., Offringa, P. J., Muskiet, F. A., Chase, W. M. and Simmons, I. J. (1991). "Vitamin E, lipid fractions, and fatty acid composition of colostrum, transitional milk, and mature milk: an international comparative study." *Am J Clin Nutr* **53**(5): 1197-1204.

Boulangé, C. L., Neves, A. L., Chilloux, J., Nicholson, J. K. and Dumas, M. E. (2016). "Impact of the gut microbiota on inflammation, obesity, and metabolic disease." *Genome Med* **8**(1): 42.

Bowen, B. P. and Northen, T. R. (2010). "Dealing with the unknown: metabolomics and metabolite atlases." *J Am Soc Mass Spectrom* **21**(9): 1471-1476.

Brown, I., Warhurst, M., Arcot, J., Playne, M., Illman, R. J. and Topping, D. L. (1997). "Fecal numbers of bifidobacteria are higher in pigs fed *Bifidobacterium longum* with a high amylose cornstarch than with a low amylose cornstarch." *Journal of Nutrition* **127**(9): 1822-1827.

Brown, I. L., Wang, X., Topping, D. L., Playne, M. J. and Conway, P. L. (1998). "High amylose maize starch as a versatile prebiotic for use with probiotic bacteria." *Food Australia* **50**(12): 603-610.

Bujak, R., Struck-Lewicka, W., Markuszewski, M. J. and Kaliszan, R. (2015). "Metabolomics for laboratory diagnostics." *J Pharm Biomed Anal* **113**: 108-120.

Bullen, C. L., Tearle, P. V. and Stewart, M. G. (1977). "The effect of "humanised" milks and supplemented breast feeding on the fecal flora of infants." **10**(4).

Cao, H., Huang, H., Xu, W., Chen, D., Yu, J., Li, J. and Li, L. (2011). "Fecal metabolome profiling of liver cirrhosis and hepatocellular carcinoma patients by ultra performance liquid chromatography-mass spectrometry." *Anal Chim Acta* **691**(1-2): 68-75.

Caporaso, J. G., Kuczynski, J., Stombaugh, J., Bittinger, K., Bushman, F. D., Costello, E. K., Fierer, N., Pena, A. G., Goodrich, J. K., Gordon, J. I., Huttley, G. A., Kelley, S. T., Knights, D., Koenig, J. E., Ley, R. E., Lozupone, C. A., McDonald, D., Muegge, B. D., Pirrung, M., Reeder, J., Sevinsky, J. R., Turnbaugh, P. J., Walters, W. A., Widmann, J., Yatsunencko, T., Zaneveld, J. and Knight, R. (2010). "QIIME allows analysis of high-throughput community sequencing data." *Nat Methods* **7**(5): 335-336.

Caporaso, J. G., Lauber, C. L., Walters, W. A., Berg-Lyons, D., Huntley, J., Fierer, N., Owens, S. M., Betley, J., Fraser, L., Bauer, M., Gormley, N., Gilbert, J. A., Smith, G. and Knight, R. (2012). "Ultra-high-throughput microbial community analysis on the Illumina HiSeq and MiSeq platforms." *ISME J* **6**(8): 1621-1624.

Caporaso, J. G., Lauber, C. L., Walters, W. A., Berg-Lyons, D., Lozupone, C. A., Turnbaugh, P. J., Fierer, N. and Knight, R. (2011). "Global patterns of 16S rRNA diversity at a depth of millions of sequences per sample." *Proc Natl Acad Sci U S A* **108** Suppl 1: 4516-4522.

Caricilli, A. M. and Saad, M. J. (2013). "The role of gut microbiota on insulin resistance." *Nutrients* **5**(3): 829-851.

Chang, S. H., Chen, M. C., Chien, N. H. and Wu, L. Y. (2016). "CE: Original Research: Examining the Links Between Lifestyle Factors and Metabolic Syndrome." *Am J Nurs* **116**(12): 26-36.

Chassard, C. and Lacroix, C. (2013). "Carbohydrates and the human gut microbiota." *Curr Opin Clin Nutr Metab Care* **16**(4): 453-460.

Chiang, J. Y. (2013). "Bile acid metabolism and signaling." *Compr Physiol* **3**(3): 1191-1212.

Chow, J., Panasevich, M. R., Alexander, D., Vester Boler, B. M., Rossoni Serao, M. C., Faber, T. A., Bauer, L. L. and Fahey, G. C. (2014). "Fecal metabolomics of healthy breast-fed versus formula-fed infants before and during in vitro batch culture fermentation." *J Proteome Res* **13**(5): 2534-2542.

Cockburn, D. W., Orlovsky, N. I., Foley, M. H., Kwiatkowski, K. J., Bahr, C. M., Maynard, M., Demeler, B. and Koropatkin, N. M. (2015). "Molecular details of a starch utilization pathway in the human gut symbiont *Eubacterium rectale*." *Mol Microbiol* **95**(2): 209-230.

Computing, R. F. f. S. (2014). R: A language and environment for statistical computing. R. C. Team.

Conlon, M. A. and Bird, A. R. (2014). "The impact of diet and lifestyle on gut microbiota and human health." *Nutrients* **7**(1): 17-44.

Conway, P. L. (2001). "Prebiotics and human health: The state-of-the-art and future perspectives " *Scandinavian Journal of Nutrition* **45**(1): 13-21.

Cummings, J. H. (1981). "Short chain fatty acids in the human colon." *Gut* **22**(9): 763-779.

de Hoffmann, E. and Stroobant, V. (2007). *Mass Spectrometry: Principles and Applications*.

Deda, O., Gika, H. G., Wilson, I. D. and Theodoridis, G. A. (2015). "An overview of fecal sample preparation for global metabolic profiling." *J Pharm Biomed Anal* **113**: 137-150.

Del Chierico, F., Vernocchi, P., Petrucca, A., Paci, P., Fuentes, S., Pratico, G., Capuani, G., Masotti, A., Reddel, S., Russo, A., Vallone, C., Salvatori, G., Buffone, E., Signore, F., Rigon, G., Dotta, A., Miccheli, A., de Vos, W. M., Dallapiccola, B. and Putignani, L. (2015). "Phylogenetic and Metabolic Tracking of Gut Microbiota during Perinatal Development." *PLoS One* **10**(9): e0137347.

Delzenne, N. M., Neyrinck, A. M., Backhed, F. and Cani, P. D. (2011). "Targeting gut microbiota in obesity: effects of prebiotics and probiotics." *Nat Rev Endocrinol* **7**(11): 639-646.

den Besten, G., van Eunen, K., Groen, A. K., Venema, K., Reijngoud, D. J. and Bakker, B. M. (2013). "The role of short-chain fatty acids in the interplay between diet, gut microbiota, and host energy metabolism." *J Lipid Res* **54**(9): 2325-2340.

Dettmer, K., Aronov, P. A. and Hammock, B. D. (2007). "Mass spectrometry-based metabolomics." *Mass Spectrom Rev* **26**(1): 51-78.

Diaz, S. O., Pinto, J., Barros, A. S., Morais, E., Duarte, D., Negrao, F., Pita, C., Almeida Mdo, C., Carreira, I. M., Spraul, M. and Gil, A. M. (2016). "Newborn Urinary Metabolic Signatures of Prematurity and Other Disorders: A Case Control Study." *J Proteome Res* **15**(1): 311-325.

Dominguez-Bello, M. G., Costello, E. K., Contreras, M., Magris, M., Hidalgo, G., Fierer, N. and Knight, R. (2010). "Delivery mode shapes the acquisition and structure of the initial microbiota across multiple body habitats in newborns." *Proc Natl Acad Sci U S A* **107**(26): 11971-11975.

Dunn, W. B., Bailey, N. J. and Johnson, H. E. (2005). "Measuring the metabolome: current analytical technologies." *Analyst* **130**(5): 606-625.

Edwards, C. A. and Parrett, A. M. (2002). "Intestinal flora during the first months of life: new perspectives." *Br J Nutr* **88 Suppl 1**: S11-18.

Edwards, C. A., Parrett, A. M., Balmer, S. E. and Wharton, B. A. (1994). "Faecal short chain fatty acids in breast-fed and formula-fed babies." *Acta Paediatr* **83**(5): 459-462.

Erickson, A. R., Cantarel, B. L., Lamendella, R., Darzi, Y., Mongodin, E. F., Pan, C., Shah, M., Halfvarson, J., Tysk, C., Henrissat, B., Raes, J., Verberkmoes, N. C., Fraser, C. M., Hettich, R. L. and Jansson, J. K. (2012). "Integrated metagenomics/metaproteomics reveals human host-microbiota signatures of Crohn's disease." *PLoS One* **7**(11): e49138.

Eyssen, H. and Parmentier, G. (1974). "Biohydrogenation of sterols and fatty acids by the intestinal microflora." *Am J Clin Nutr* **27**(11): 1329-1340.

Eyssen, H., van Eldere, J., Parmentier, G., Huijghebaert, S. and Mertens, J. (1985). "Influence of microbial bile salt desulfation upon the fecal excretion of bile salts in gnotobiotic rats." *Journal of Steroid Biochemistry* **22**(4): 547-554.

Fahy, E., Subramaniam, S., Brown, H. A., Glass, C. K., Merrill, A. H., Jr., Murphy, R. C., Raetz, C. R., Russell, D. W., Seyama, Y., Shaw, W., Shimizu, T., Spener, F., van Meer, G., VanNieuwenhze, M. S., White, S. H., Witztum, J. L. and Dennis, E. A. (2005). "A comprehensive classification system for lipids." *J Lipid Res* **46**(5): 839-861.

Fahy, E., Subramaniam, S., Murphy, R. C., Nishijima, M., Raetz, C. R., Shimizu, T., Spener, F., van Meer, G., Wakelam, M. J. and Dennis, E. A. (2009). "Update of the LIPID MAPS comprehensive classification system for lipids." *J Lipid Res* **50** Suppl: S9-14.

Faith, J. J., Ahern, P. P., Ridaura, V. K., Cheng, J. and Gordon, J. I. (2014). "Identifying gut microbe-host phenotype relationships using combinatorial communities in gnotobiotic mice." *Sci Transl Med* **6**(220): 220ra211.

Faith, J. J., Hayete, B., Thaden, J. T., Mogno, I., Wierzbowski, J., Cottarel, G., Kasif, S., Collins, J. J. and Gardner, T. S. (2007). "Large-scale mapping and validation of Escherichia coli transcriptional regulation from a compendium of expression profiles." *PLoS Biol* **5**(1): e8.

Fang, L., Jiang, X., Su, Y. and Zhu, W. (2014). "Long-term intake of raw potato starch decreases back fat thickness and dressing percentage but has no effect on the longissimus muscle quality of growing-finishing pigs." *Livestock Science* **170**: 116-123.

Fanos, V., Antonucci, R., Barberini, L. and Atzori, L. (2012). "Urinary metabolomics in newborns and infants." *Adv Clin Chem* **58**: 193-223.

Fassler, C., Arrigoni, E., Venema, K., Brouns, F. and Amado, R. (2006). "In vitro fermentability of differently digested resistant starch preparations." *Mol Nutr Food Res* **50**(12): 1220-1228.

Fauconnier, M. L., Welti, R., Blee, E. and Marlier, M. (2003). "Lipid and oxylipin profiles during aging and sprout development in potato tubers (*Solanum tuberosum* L.)." *Biochim Biophys Acta* **1633**(2): 118-126.

Fiehn, O. (2002). "Metabolomics – the link between genotypes and phenotypes." *Plant Molecular Biology* **48**(1/2): 155-171.

Fischer, S. M. (1997). "Prostaglandins and cancer." *Front Biosci* **2**(4): d482-500.

Flint, H. J., Scott, K. P., Duncan, S. H., Louis, P. and Forano, E. (2012). "Microbial degradation of complex carbohydrates in the gut." *Gut Microbes* **3**(4): 289-306.

Flint, H. J., Scott, K. P., Louis, P. and Duncan, S. H. (2012). "The role of the gut microbiota in nutrition and health." *Nat Rev Gastroenterol Hepatol* **9**(10): 577-589.

Fouhse, J. M., Ganzle, M. G., Regmi, P. R., van Kempen, T. A. and Zijlstra, R. T. (2015). "High Amylose Starch with Low In Vitro Digestibility Stimulates Hindgut Fermentation and Has a Bifidogenic Effect in Weaned Pigs." *J Nutr* **145**(11): 2464-2470.

Fuentes-Zaragoza, E., Sánchez-Zapata, E., Sendra, E., Sayas, E., Navarro, C., Fernández-López, J. and Pérez-Alvarez, J. A. (2011). "Resistant starch as prebiotic: A review." *Starch - Stärke* **63**(7): 406-415.

Gabbs, M., Leng, S., Devassy, J. G., Monirujjaman, M. and Aukema, H. M. (2015). "Advances in Our Understanding of Oxylipins Derived from Dietary PUFAs." *Adv Nutr* **6**(5): 513-540.

Gao, Z., Yin, J., Zhang, J., Ward, R. E., Martin, R. J., Lefevre, M., Cefalu, W. T. and Ye, J. (2009). "Butyrate improves insulin sensitivity and increases energy expenditure in mice." *Diabetes* **58**(7): 1509-1517.

Gareau, M. G., Sherman, P. M. and Walker, W. A. (2010). "Probiotics and the gut microbiota in intestinal health and disease." *Nat Rev Gastroenterol Hepatol* **7**(9): 503-514.

Geng, P., Harnly, J. M. and Chen, P. (2015). "Differentiation of Whole Grain from Refined Wheat (*T. aestivum*) Flour Using Lipid Profile of Wheat Bran, Germ, and Endosperm with UHPLC-HRAM Mass Spectrometry." *J Agric Food Chem* **63**(27): 6189-6211.

Gerard, P. (2013). "Metabolism of cholesterol and bile acids by the gut microbiota." *Pathogens* **3**(1): 14-24.

Gerritsen, J., Smidt, H., Rijkers, G. T. and de Vos, W. M. (2011). "Intestinal microbiota in human health and disease: the impact of probiotics." *Genes Nutr* **6**(3): 209-240.

Ghaste, M., Mistrik, R. and Shulaev, V. (2016). "Applications of Fourier Transform Ion Cyclotron Resonance (FT-ICR) and Orbitrap Based High Resolution Mass Spectrometry in Metabolomics and Lipidomics." *Int J Mol Sci* **17**(6).

Gibney, M. J., Walsh, M., Brennan, L., Roche, H. M., German, B. and van Ommen, B. (2005). "Metabolomics in human nutrition: opportunities and challenges." *Am J Clin Nutr* **82**(3): 497-503.

Gibson, G. R. and Roberfroid, M. B. (1995). "Dietary modulation of the human colonic microbiota: introducing the concept of prebiotics." *J Nutr* **125**(6): 1401-1412.

Glauser, G., Grata, E., Rudaz, S. and Wolfender, J. L. (2008). "High-resolution profiling of oxylipin-containing galactolipids in Arabidopsis extracts by ultra-performance liquid chromatography/time-of-flight mass spectrometry." *Rapid Commun Mass Spectrom* **22**(20): 3154-3160.

Gobel, C. and Feussner, I. (2009). "Methods for the analysis of oxylipins in plants." *Phytochemistry* **70**(13-14): 1485-1503.

Goodacre, R. (2005). "Metabolomics – the way forward." *Metabolomics* **1**(1): 1-2.

- Goodacre, R. (2007). "Metabolomics of a superorganism." *J Nutr* **137**(1 Suppl): 259S-266S.
- Gouveia-Figueira, S., Karimpour, M., Bosson, J. A., Blomberg, A., Unosson, J., Pourazar, J., Sandstrom, T., Behndig, A. F. and Nording, M. L. (2017). "Mass spectrometry profiling of oxylipins, endocannabinoids, and N-acyl ethanolamines in human lung lavage fluids reveals responsiveness of prostaglandin E2 and associated lipid metabolites to biodiesel exhaust exposure." *Anal Bioanal Chem* **409**(11): 2967-2980.
- Gouveia-Figueira, S., Spath, J., Zivkovic, A. M. and Nording, M. L. (2015). "Profiling the Oxylipin and Endocannabinoid Metabolome by UPLC-ESI-MS/MS in Human Plasma to Monitor Postprandial Inflammation." *PLoS One* **10**(7): e0132042.
- Gowda, G. A. and Djukovic, D. (2014). "Overview of mass spectrometry-based metabolomics: opportunities and challenges." *Methods Mol Biol* **1198**: 3-12.
- Grapov, D., Adams, S. H., Pedersen, T. L., Garvey, W. T. and Newman, J. W. (2012). "Type 2 diabetes associated changes in the plasma non-esterified fatty acids, oxylipins and endocannabinoids." *PLoS One* **7**(11): e48852.
- Gregory, K. E., Bird, S. S., Gross, V. S., Marur, V. R., Lazarev, A. V., Walker, W. A. and Kristal, B. S. (2013). "Method development for fecal lipidomics profiling." *Anal Chem* **85**(2): 1114-1123.
- Griffiths, W. J. and Wang, Y. (2009). "Mass spectrometry: from proteomics to metabolomics and lipidomics." *Chem Soc Rev* **38**(7): 1882-1896.
- Gronlund, M. M., Lehtonen, O. P., Eerola, E. and Kero, P. (1999). "Fecal microflora in healthy infants born by different methods of delivery: permanent changes in intestinal flora after cesarean delivery." *J Pediatr Gastroenterol Nutr* **28**(1): 19-25.
- Gross, J. H. (2011). *Mass Spectrometry: A textbook*. Berlin Heidelberg, Springer-Verlag
- Haenen, D., Zhang, J., Souza da Silva, C., Bosch, G., van der Meer, I. M., van Arkel, J., van den Borne, J. J., Perez Gutierrez, O., Smidt, H., Kemp, B., Muller, M. and Hooiveld, G. J. (2013). "A diet high in resistant starch modulates microbiota composition, SCFA concentrations, and gene expression in pig intestine." *J Nutr* **143**(3): 274-283.
- Hamer, H. M., Jonkers, D., Venema, K., Vanhoutvin, S., Troost, F. J. and Brummer, R. J. (2008). "Review article: the role of butyrate on colonic function." *Aliment Pharmacol Ther* **27**(2): 104-119.
- Hammons, J. L., Jordan, W. E., Stewart, R. L., Taulbee, J. D. and Berg, R. W. (1988). "Age and diet effects on fecal bile acids in infants." *J Pediatr Gastroenterol Nutr* **7**(1): 30-38.
- Han, X. and Gross, R. W. (2005). "Shotgun lipidomics: electrospray ionization mass spectrometric analysis and quantitation of cellular lipidomes directly from crude extracts of biological samples." *Mass Spectrom Rev* **24**(3): 367-412.
- Harmsen, H. J. M., Wildeboer-Veloo, A. C. M., Raangs, G. C., Wagendorp, A. A., Klijn, N., Bindels, J. G. and Welling, G. W. (2000). "Analysis of Intestinal Flora Development in Breast-Fed and Formula-

Fed Infants by Using Molecular Identification and Detection Methods." *Journal of pediatric gastroenterology and nutrition* **30**(1): 61-67.

Hascoet, J. M., Hubert, C., Rochat, F., Legagneur, H., Gaga, S., Emady-Azar, S. and Steenhout, P. G. (2011). "Effect of formula composition on the development of infant gut microbiota." *J Pediatr Gastroenterol Nutr* **52**(6): 756-762.

Hashizume, C., Kishimoto, Y., Kanahori, S., Yamamoto, T., Okuma, K. and Yamamoto, K. (2012). "Improvement effect of resistant maltodextrin in humans with metabolic syndrome by continuous administration." *J Nutr Sci Vitaminol (Tokyo)* **58**(6): 423-430.

Haug, M., Laubach, C., Burke, M. and Harzer, G. (1987). "Vitamin E in human milk from mothers of preterm and term infants." *J Pediatr Gastroenterol Nutr* **6**(4): 605-609.

He, B., Nohara, K., Ajami, N. J., Michalek, R. D., Tian, X., Wong, M., Losee-Olson, S. H., Petrosino, J. F., Yoo, S. H., Shimomura, K. and Chen, Z. (2015). "Transmissible microbial and metabolomic remodeling by soluble dietary fiber improves metabolic homeostasis." *Sci Rep* **5**: 10604.

Heintz-Buschart, A., May, P., Laczny, C. C., Lebrun, L. A., Bellora, C., Krishna, A., Wampach, L., Schneider, J. G., Hogan, A., de Beaufort, C. and Wilmes, P. (2016). "Integrated multi-omics of the human gut microbiome in a case study of familial type 1 diabetes." *Nature Microbiology* **2**(16180).

Higgins, J. A., Higbee, D. R., Donahoo, W. T., Brown, I. L., Bell, M. L. and Bessesen, D. H. (2004). "Resistant starch consumption promotes lipid oxidation." *Nutr Metab (Lond)* **1**(1): 8.

Holmes, E., Kinross, J., Gibson, G. R., Burcelin, R., Jia, W., Pettersson, S. and Nicholson, J. K. (2012). "Therapeutic modulation of microbiota-host metabolic interactions." *Sci Transl Med* **4**(137): 137rv136.

Holzappel, W. H., Haberer, P., Snel, J., Schillinger, U. and Huis in't Veld, J. H. (1998). "Overview of gut flora and probiotics." *Int J Food Microbiol* **41**(2): 85-101.

Horgan, R. P. and Kenny, L. C. (2011). "'Omic' technologies: genomics, transcriptomics, proteomics and metabolomics." *The Obstetrician & Gynaecologist* **13**(3): 189-195.

Hullar, M. A., Burnett-Hartman, A. N. and Lampe, J. W. (2014). "Gut microbes, diet, and cancer." *Cancer Treat Res* **159**: 377-399.

Hyde, M. J., Griffin, J. L., Herrera, E., Byrne, C. D., Clarke, L. and Kemp, P. R. (2009). "Delivery by Caesarean section, rather than vaginal delivery, promotes hepatic steatosis in piglets." *Clin Sci (Lond)* **118**(1): 47-59.

Ingerslev, A. K., Karaman, I., Bagcioglu, M., Kohler, A., Theil, P. K., Bach Knudsen, K. E. and Hedemann, M. S. (2015). "Whole Grain Consumption Increases Gastrointestinal Content of Sulfate-Conjugated Oxylipins in Pigs - A Multicompartmental Metabolomics Study." *J Proteome Res* **14**(8): 3095-3110.

Jenness, R. (1979). "The composition of human milk." *Semin Perinatol* **3**(3): 225-239.

- Jin, S. J. and Tserng, K. Y. (1990). "Metabolic origins of urinary unsaturated dicarboxylic acids." *Biochemistry* **29**(37): 8540-8547.
- Jonsson, G., Midtvedt, A. C., Norman, A. and Midtvedt, T. (1995). "Intestinal microbial bile acid transformation in healthy infants." *J Pediatr Gastroenterol Nutr* **20**(4): 394-402.
- Kabir, M., Rizkalla, S. W., Champ, M., Luo, J., Boillot, J., Bruzzo, F. and Slama, G. (1998). "Dietary amylose-amylopectin starch content affects glucose and lipid metabolism in adipocytes of normal and diabetic rats." *J Nutr* **128**(1): 35-43.
- Kanehisa, M., Araki, M., Goto, S., Hattori, M., Hirakawa, M., Itoh, M., Katayama, T., Kawashima, S., Okuda, S., Tokimatsu, T. and Yamanishi, Y. (2008). "KEGG for linking genomes to life and the environment." *Nucleic Acids Res* **36**(Database issue): D480-484.
- Kanehisa, M. and Goto, S. (2000). "KEGG: kyoto encyclopedia of genes and genomes." *Nucleic Acids Res* **28**(1): 27-30.
- Kanehisa, M., Goto, S., Sato, Y., Furumichi, M. and Tanabe, M. (2012). "KEGG for integration and interpretation of large-scale molecular data sets." *Nucleic Acids Res* **40**(Database issue): D109-114.
- Khakimov, B., Bak, S. and Engelsen, S. B. (2014). "High-throughput cereal metabolomics: Current analytical technologies, challenges and perspectives." *Journal of Cereal Science* **59**(3): 393-418.
- Khan, M. T., Duncan, S. H., Stams, A. J., van Dijk, J. M., Flint, H. J. and Harmsen, H. J. (2012). "The gut anaerobe *Faecalibacterium prausnitzii* uses an extracellular electron shuttle to grow at oxic-anoxic interphases." *ISME J* **6**(8): 1578-1585.
- Kobayashi, H., Kanno, C., Yamauchi, K. and Tsugo, T. (1975). "Identification of alpha-, beta-, gamma-, and delta-tocopherols and their contents in human milk." *Biochim Biophys Acta* **380**(2).
- Lattimer, J. M. and Haub, M. D. (2010). "Effects of dietary fiber and its components on metabolic health." *Nutrients* **2**(12): 1266-1289.
- Lederberg, J. (2003). "Of Men and Microbes." *New Perspectives Quarterly* **20**(3): 52-55.
- Lehmann, J. M., Moore, L. B., Smith-Oliver, T. A., Wilkison, W. O., Willson, T. M. and Kliewer, S. A. (1995). "An Antidiabetic Thiazolidinedione Is a High Affinity Ligand for Peroxisome Proliferator-activated Receptor γ (PPAR γ)." *Journal of Biological Chemistry* **270**(22): 12953-12956.
- Lei, Z., Huhman, D. V. and Sumner, L. W. (2011). "Mass spectrometry strategies in metabolomics." *J Biol Chem* **286**(29): 25435-25442.
- Lenz, E. M. and Wilson, I. D. (2007). "Analytical strategies in metabolomics." *J Proteome Res* **6**(2): 443-458.
- Lin, C. S., Chang, C. J., Lu, C. C., Martel, J., Ojcius, D. M., Ko, Y. F., Young, J. D. and Lai, H. C. (2014). "Impact of the gut microbiota, prebiotics, and probiotics on human health and disease." *Biomed J* **37**(5): 259-268.

Lin, L., Yu, Q., Yan, X., Hang, W., Zheng, J., Xing, J. and Huang, B. (2010). "Direct infusion mass spectrometry or liquid chromatography mass spectrometry for human metabonomics? A serum metabonomic study of kidney cancer." *Analyst* **135**(11): 2970-2978.

Lockyer, S. and Nugent, A. P. (2017). "Health effects of resistant starch." *Nutrition Bulletin* **42**(1): 10-41.

Louis, P., Young, P., Holtrop, G. and Flint, H. J. (2010). "Diversity of human colonic butyrate-producing bacteria revealed by analysis of the butyryl-CoA:acetate CoA-transferase gene." *Environ Microbiol* **12**(2): 304-314.

Love, M. I., Huber, W. and Anders, S. (2014). "Moderated estimation of fold change and dispersion for RNA-seq data with DESeq2." *Genome Biol* **15**(12): 550.

Lozupone, C. and Knight, R. (2005). "UniFrac: a new phylogenetic method for comparing microbial communities." *Appl Environ Microbiol* **71**(12): 8228-8235.

Lu, H., Yan, H., Almeida, V. V., Adeola, O. and Ajuwon, K. M. (2016). "Effects of dietary resistant starch content on nutrient and energy digestibility and fecal metabolomic profile in growing pigs." *American Society of Animal Science* **94**(7): 364-368.

Macfarlane, G. T. and Englyst, H. N. (1986). "Starch utilization by the human large intestinal microflora." *J Appl Bacteriol* **60**(3): 195-201.

MacIntyre, D. A., Chandiramani, M., Lee, Y. S., Kindinger, L., Smith, A., Angelopoulos, N., Lehne, B., Arulkumaran, S., Brown, R., Teoh, T. G., Holmes, E., Nicholson, J. K., Marchesi, J. R. and Bennett, P. R. (2015). "The vaginal microbiome during pregnancy and the postpartum period in a European population." *Sci Rep* **5**: 8988.

Mackie, R. I., Sghir, A. and Gaskins, H. R. (1999). "Developmental microbial ecology of the neonatal gastrointestinal tract." *Am J Clin Nutr* **69**(5): 1035S-1045S.

Maier, T. V., Lucio, M., Lee, L. H., VerBerkmoes, N. C., Brislawn, C. J., Bernhardt, J., Lamendella, R., McDermott, J. E., Bergeron, N., Heinzmann, S. S., Morton, J. T., Gonzalez, A., Ackermann, G., Knight, R., Riedel, K., Krauss, R. M., Schmitt-Kopplin, P. and Jansson, J. K. (2017). "Impact of Dietary Resistant Starch on the Human Gut Microbiome, Metaproteome, and Metabolome." *mBio* **8**(5): e01343-01317.

Maitra, S. and Yan, J. (2008). "Principle Component Analysis and Partial Least Squares: Two Dimension Reduction Techniques for Regression."

Marques, T. M., Wall, R., Ross, R. P., Fitzgerald, G. F., Ryan, C. A. and Stanton, C. (2010). "Programming infant gut microbiota: influence of dietary and environmental factors." *Curr Opin Biotechnol* **21**(2): 149-156.

Marshall, A. G. (2000). "Milestones in fourier transform ion cyclotron resonance mass spectrometry technique development." *International Journal of Mass Spectrometry* **200**(1-3): 331-356.

Marshall, A. G., Hendrickson, C. L. and Jackson, G. S. (1998). "Fourier transform ion cyclotron resonance mass spectrometry: a primer." *Mass Spectrom Rev* **17**(1): 1-35.

Martin, R., Langa, S., Reviriego, C., Jimenez, E., Marin, M. L., Xaus, J., Fernandez, L. and Rodriguez, J. M. (2003). "Human milk is a source of lactic acid bacteria for the infant gut." *J Pediatr* **143**(6): 754-758.

Martin, V., Maldonado-Barragan, A., Moles, L., Rodriguez-Banos, M., Campo, R. D., Fernandez, L., Rodriguez, J. M. and Jimenez, E. (2012). "Sharing of bacterial strains between breast milk and infant feces." *Journal of Human Lactation* **28**(1): 36-44.

Martysiak-Zurowska, D., Szlagatys-Sidorkiewicz, A. and Zagierski, M. (2013). "Concentrations of alpha- and gamma-tocopherols in human breast milk during the first months of lactation and in infant formulas." *Matern Child Nutr* **9**(4): 473-482.

Matysik, S., Le Roy, C. I., Liebisch, G. and Claus, S. P. (2016). "Metabolomics of fecal samples: A practical consideration." *Trends in Food Science & Technology* **57**: 244-255.

McDermott, J. E., Vartanian, K. B., Mitchell, H., Stevens, S. L., Sanfilippo, A. and Stenzel-Poore, M. P. (2012). "Identification and validation of Ifit1 as an important innate immune bottleneck." *PLoS One* **7**(6): e36465.

McMurdie, P. J. and Holmes, S. (2013). "phyloseq: an R package for reproducible interactive analysis and graphics of microbiome census data." *PLoS One* **8**(4): e61217.

McNiven, E. M., German, J. B. and Slupsky, C. M. (2011). "Analytical metabolomics: nutritional opportunities for personalized health." *J Nutr Biochem* **22**(11): 995-1002.

Mehlan, H., Schmidt, F., Weiss, S., Schuler, J., Fuchs, S., Riedel, K. and Bernhardt, J. (2013). "Data visualization in environmental proteomics." *Proteomics* **13**(18-19): 2805-2821.

Meng, C., Kuster, B., Culhane, A. C. and Gholami, A. M. (2014). "A multivariate approach to the integration of multi-omics datasets." *BMC Bioinformatics* **15**(162): 162.

Midtvedt, A. C. and Midtvedt, T. (1993). "Conversion of cholesterol to coprostanol by the intestinal microflora during the first two years of human life." *J Pediatr Gastroenterol Nutr* **17**(2): 161-168.

Mika, A. and Sledzinski, T. (2017). "Alterations of specific lipid groups in serum of obese humans: a review." *Obes Rev* **18**(2): 247-272.

Mileti, E., Matteoli, G., Iliev, I. D. and Rescigno, M. (2009). "Comparison of the immunomodulatory properties of three probiotic strains of Lactobacilli using complex culture systems: prediction for in vivo efficacy." *PLoS One* **4**(9): e7056.

Miquel, S., Leclerc, M., Martin, R., Chain, F., Lenoir, M., Raguideau, S., Hudault, S., Bridonneau, C., Northen, T., Bowen, B., Bermudez-Humaran, L. G., Sokol, H., Thomas, M. and Langella, P. (2015). "Identification of metabolic signatures linked to anti-inflammatory effects of *Faecalibacterium prausnitzii*." *mBio* **6**(2): 10.

Miquel, S., Martin, R., Rossi, O., Bermudez-Humaran, L. G., Chatel, J. M., Sokol, H., Thomas, M., Wells, J. M. and Langella, P. (2013). "Faecalibacterium prausnitzii and human intestinal health." *Curr Opin Microbiol* **16**(3): 255-261.

Muller, C., Dietz, I., Tziotis, D., Moritz, F., Rupp, J. and Schmitt-Kopplin, P. (2013). "Molecular cartography in acute Chlamydia pneumoniae infections--a non-targeted metabolomics approach." *Anal Bioanal Chem* **405**(15): 5119-5131.

Nicholson, J. K., Holmes, E., Kinross, J., Burcelin, R., Gibson, G., Jia, W. and Pettersson, S. (2012). "Host-gut microbiota metabolic interactions." *Science* **336**(6086): 1262-1267.

Nicholson, J. K., Lindon, J. C. and Holmes, E. (1999). "Metabonomics': understanding the metabolic responses of living systems to pathophysiological stimuli via multivariate statistical analysis of biological NMR spectroscopic data." *Xenobiotica* **29**(11): 1181-1189.

Nicholson, J. K. and Wilson, I. D. (2003). "Opinion: understanding 'global' systems biology: metabonomics and the continuum of metabolism." *Nat Rev Drug Discov* **2**(8): 668-676.

Nørskov, N. P., Hedemann, M. S., Theil, P. K. and Knudsen, K. E. B. (2012). "Erratum to: Oxylipins discriminate between whole grain wheat and wheat aleurone intake: a metabolomics study on pig plasma." *Metabolomics* **9**(2): 480-482.

Novakova, L., Solichova, D. and Solich, P. (2006). "Advantages of ultra performance liquid chromatography over high-performance liquid chromatography: comparison of different analytical approaches during analysis of diclofenac gel." *J Sep Sci* **29**(16): 2433-2443.

Noverr, M. C., Erb-Downward, J. R. and Huffnagle, G. B. (2003). "Production of eicosanoids and other oxylipins by pathogenic eukaryotic microbes." *Clin Microbiol Rev* **16**(3): 517-533.

Ogawa, K., Ben, R. A., Pons, S., de Paolo, M. I. and Bustos Fernandez, L. (1992). "Volatile fatty acids, lactic acid, and pH in the stools of breast-fed and bottle-fed infants." *J Pediatr Gastroenterol Nutr* **15**(3): 248-252.

Oishi-Tanaka, Y. and Glass, C. K. (2010). "A New Role for Cyclic Phosphatidic Acid as a PPAR γ Antagonist." *Cell Metab* **12**(3): 207-208.

Ordiz, M. I., May, T. D., Mihindukulasuriya, K., Martin, J., Crowley, J., Tarr, P. I., Ryan, K., Mortimer, E., Gopalsamy, G., Maleta, K., Mitreva, M., Young, G. and Manary, M. J. (2015). "The effect of dietary resistant starch type 2 on the microbiota and markers of gut inflammation in rural Malawi children." *Microbiome* **3**: 37.

Otto, A., Bernhardt, J., Meyer, H., Schaffer, M., Herbst, F. A., Siebourg, J., Mader, U., Lalk, M., Hecker, M. and Becher, D. (2010). "Systems-wide temporal proteomic profiling in glucose-starved *Bacillus subtilis*." *Nat Commun* **1**: 137.

Peironcely, J. E., Rojas-Cherto, M., Tas, A., Vreeken, R., Reijmers, T., Coulier, L. and Hankemeier, T. (2013). "Automated pipeline for de novo metabolite identification using mass-spectrometry-based metabolomics." *Anal Chem* **85**(7): 3576-3583.

Penders, J., Thijs, C., Vink, C., Stelma, F. F., Snijders, B., Kummeling, I., van den Brandt, P. A. and Stobberingh, E. E. (2006). "Factors influencing the composition of the intestinal microbiota in early infancy." *Pediatrics* **118**(2): 511-521.

Perez-Cobas, A. E., Gosalbes, M. J., Friedrichs, A., Knecht, H., Artacho, A., Eismann, K., Otto, W., Rojo, D., Bargiela, R., von Bergen, M., Neulinger, S. C., Daumer, C., Heinsen, F. A., Latorre, A., Barbas, C., Seifert, J., dos Santos, V. M., Ott, S. J., Ferrer, M. and Moya, A. (2013). "Gut microbiota disturbance during antibiotic therapy: a multi-omic approach." *Gut* **62**(11): 1591-1601.

Pohlert, T. (2014). "The Pairwise Multiple Comparison of Mean Ranks Package (PMCMR), R package. (Version 4.1). ." Retrieved from <http://CRAN.R-project.org/package=PMCMR>.

Pokusaeva, K., Fitzgerald, G. F. and van Sinderen, D. (2011). "Carbohydrate metabolism in Bifidobacteria." *Genes Nutr* **6**(3): 285-306.

Pop, M., Paulson, J. N., Chakraborty, S., Astrovskaia, I., Lindsay, B. R., Li, S., Bravo, H. C., Harro, C., Parkhill, J., Walker, A. W., Walker, R. I., Sack, D. A. and Stine, O. C. (2016). "Individual-specific changes in the human gut microbiota after challenge with enterotoxigenic *Escherichia coli* and subsequent ciprofloxacin treatment." *BMC Genomics* **17**: 440.

Preedy, V. R. and Watson, V. (2007). *The Encyclopedia of Vitamin E*.

Qin, J., Li, R., Raes, J., Arumugam, M., Burgdorf, K. S., Manichanh, C., Nielsen, T., Pons, N., Levenez, F., Yamada, T., Mende, D. R., Li, J., Xu, J., Li, S., Li, D., Cao, J., Wang, B., Liang, H., Zheng, H., Xie, Y., Tap, J., Lepage, P., Bertalan, M., Batto, J. M., Hansen, T., Le Paslier, D., Linneberg, A., Nielsen, H. B., Pelletier, E., Renault, P., Sicheritz-Ponten, T., Turner, K., Zhu, H., Yu, C., Li, S., Jian, M., Zhou, Y., Li, Y., Zhang, X., Li, S., Qin, N., Yang, H., Wang, J., Brunak, S., Dore, J., Guarner, F., Kristiansen, K., Pedersen, O., Parkhill, J., Weissenbach, J., Meta, H. I. T. C., Bork, P., Ehrlich, S. D. and Wang, J. (2010). "A human gut microbial gene catalogue established by metagenomic sequencing." *Nature* **464**(7285): 59-65.

Qin, J., Li, Y., Cai, Z., Li, S., Zhu, J., Zhang, F., Liang, S., Zhang, W., Guan, Y., Shen, D., Peng, Y., Zhang, D., Jie, Z., Wu, W., Qin, Y., Xue, W., Li, J., Han, L., Lu, D., Wu, P., Dai, Y., Sun, X., Li, Z., Tang, A., Zhong, S., Li, X., Chen, W., Xu, R., Wang, M., Feng, Q., Gong, M., Yu, J., Zhang, Y., Zhang, M., Hansen, T., Sanchez, G., Raes, J., Falony, G., Okuda, S., Almeida, M., LeChatelier, E., Renault, P., Pons, N., Batto, J. M., Zhang, Z., Chen, H., Yang, R., Zheng, W., Li, S., Yang, H., Wang, J., Ehrlich, S. D., Nielsen, R., Pedersen, O., Kristiansen, K. and Wang, J. (2012). "A metagenome-wide association study of gut microbiota in type 2 diabetes." *Nature* **490**(7418): 55-60.

Quigley, E. M. (2013). "Gut bacteria in health and disease." *Gastroenterol Hepatol (N Y)* **9**(9): 560-569.

Ramakrishna, B. S. (2013). "Role of the gut microbiota in human nutrition and metabolism." *J Gastroenterol Hepatol* **28 Suppl 4**: 9-17.

Ramsay, A. G., Scott, K. P., Martin, J. C., Rincon, M. T. and Flint, H. J. (2006). "Cell-associated alpha-amylases of butyrate-producing Firmicute bacteria from the human colon." *Microbiology* **152**(Pt 11): 3281-3290.

Rendleman, J. A., Jr. (2000). "Hydrolytic action of alpha-amylase on high-amylose starch of low molecular mass." *Biotechnol Appl Biochem* **31 (Pt 3)**: 171-178.

Rhodes, R., Gligorov, N. and Schwab, A. P. (2013). *The Human Microbiome: Ethical, Legal and Social Concerns*, Oxford University Press.

Robertson, M. D., Bickerton, A. S., Dennis, A. L., Vidal, H. and Frayn, K. N. (2005). "Insulin-sensitizing effects of dietary resistant starch and effects on skeletal muscle and adipose tissue metabolism." *Am J Clin Nutr* **82**(3): 559-567.

Robinson, M. and Warne, T. R. (1991). "Sources of diacylglycerols generated during cell growth and phorbol ester stimulation in Madin-Darby canine kidney cells." *Biochim Biophys Acta* **1085**(1): 63-70.

Russell, W. R., Duncan, S. H. and Flint, H. J. (2013). "The gut microbial metabolome: modulation of cancer risk in obese individuals." *Proc Nutr Soc* **72**(1): 178-188.

Ruttkies, C., Schymanski, E. L., Wolf, S., Hollender, J. and Neumann, S. (2016). "MetFrag relaunched: incorporating strategies beyond in silico fragmentation." *Journal of Cheminformatics* **8**(1): 3.

Saad, M. J., Santos, A. and Prada, P. O. (2016). "Linking Gut Microbiota and Inflammation to Obesity and Insulin Resistance." *Physiology (Bethesda)* **31**(4): 283-293.

Sacchi, C. T., Whitney, A. M., Mayer, L. W., Morey, R., Steigerwalt, A., Boras, A., Weyant, R. S. and Popovic, T. (2002). "Sequencing of 16S rRNA gene: a rapid tool for identification of *Bacillus anthracis*." *Emerg Infect Dis* **8**(10): 1117-1123.

Saeed, A. I., Bhagabati, N. K., Braisted, J. C., Liang, W., Sharov, V., Howe, E. A., Li, J., Thiagarajan, M., White, J. A. and Quackenbush, J. (2006). "TM4 microarray software suite." *Methods Enzymol* **411**: 134-193.

Salonen, A. and de Vos, W. M. (2014). Impact of Diet on Human Intestinal Microbiota and Health. *Annual Review of Food Science and Technology, Vol 5*. M. P. Doyle and T. R. Klaenhammer. Palo Alto, Annual Reviews. **5**: 239-262.

Samuelsson, L. M., Young, W., Fraser, K., Tannock, G. W., Lee, J. and Roy, N. C. (2016). "Digestive-resistant carbohydrates affect lipid metabolism in rats." *Metabolomics* **12**(5).

Schmitt-Kopplin, P., Gelencser, A., Dabek-Zlotorzynska, E., Kiss, G., Hertkorn, N., Harir, M., Hong, Y. and Gebefugi, I. (2010). "Analysis of the unresolved organic fraction in atmospheric aerosols with ultrahigh-resolution mass spectrometry and nuclear magnetic resonance spectroscopy: organosulfates as photochemical smog constituents." *Anal Chem* **82**(19): 8017-8026.

Schulze, B., Dabrowska, P. and Boland, W. (2007). "Rapid enzymatic isomerization of 12-oxophytodienoic acid in the gut of lepidopteran larvae." *Chembiochem* **8**(2): 208-216.

Scott, K. P., Duncan, S. H., Louis, P. and Flint, H. J. (2011). "Nutritional influences on the gut microbiota and the consequences for gastrointestinal health." *Biochem Soc Trans* **39**(4): 1073-1078.

Seo, J. and Shneiderman, B. (2002). "Interactively exploring hierarchical clustering results." *Computer* **35**(7): 80-+.

Shahidi, F. and de Camargo, A. C. (2016). "Tocopherols and Tocotrienols in Common and Emerging Dietary Sources: Occurrence, Applications, and Health Benefits." *Int J Mol Sci* **17**(10): 1745.

Shanik, M. H., Xu, Y., Skrha, J., Dankner, R., Zick, Y. and Roth, J. (2008). "Insulin resistance and hyperinsulinemia: is hyperinsulinemia the cart or the horse?" *Diabetes Care* **31 Suppl 2**: S262-268.

Shannon, P., Markiel, A., Ozier, O., Baliga, N. S., Wang, J. T., Ramage, D., Amin, N., Schwikowski, B. and Ideker, T. (2003). "Cytoscape: a software environment for integrated models of biomolecular interaction networks." *Genome Res* **13**(11): 2498-2504.

Shearer, G. C., Harris, W. S., Pedersen, T. L. and Newman, J. W. (2010). "Detection of omega-3 oxylipins in human plasma and response to treatment with omega-3 acid ethyl esters." *J Lipid Res* **51**(8): 2074-2081.

Shen, J., Obin, M. S. and Zhao, L. (2013). "The gut microbiota, obesity and insulin resistance." *Mol Aspects Med* **34**(1): 39-58.

Shneiderman, B. (1992). "Tree visualization with tree-maps: 2-d space-filling approach." *ACM Transactions on Graphics* **11**(1): 92-99.

Skoog, D. A., Holler, J. and Crouch, S. R. (2013). *Instrumentelle Analytik: Grundlagen - Geräte - Anwendungen*, Springer Spektrum.

Smirnov, K. S., Maier, T. V., Walker, A., Heinzmann, S. S., Forcisi, S., Martinez, I., Walter, J. and Schmitt-Kopplin, P. (2016). "Challenges of metabolomics in human gut microbiota research." *Int J Med Microbiol* **306**(5): 266-279.

Smith, C. A., O'Maille, G., Want, E. J., Qin, C., Trauger, S. A., Brandon, T. R., Custodio, D. E., Abagyan, R. and Siuzdak, G. (2005). "METLIN: a metabolite mass spectral database." *Ther Drug Monit* **27**(6): 747-751.

Song, S. J., Lauber, C., Costello, E. K., Lozupone, C. A., Humphrey, G., Berg-Lyons, D., Caporaso, J. G., Knights, D., Clemente, J. C., Nakielny, S., Gordon, J. I., Fierer, N. and Knight, R. (2013). "Cohabiting family members share microbiota with one another and with their dogs." *Elife* **2**: e00458.

Soto, A., Martin, V., Jimenez, E., Mader, I., Rodriguez, J. M. and Fernandez, L. (2014). "Lactobacilli and bifidobacteria in human breast milk: influence of antibiotherapy and other host and clinical factors." *J Pediatr Gastroenterol Nutr* **59**(1): 78-88.

Stotz, E. and Bessey, O. A. (1942). "The blood lactate-pyruvate relation and its use in experimental thiamine deficiency in pigeons." *J Biol Chem* **143**(625-631).

Strassburg, K., Esser, D., Vreeken, R. J., Hankemeier, T., Muller, M., van Duynhoven, J., van Golde, J., van Dijk, S. J., Afman, L. A. and Jacobs, D. M. (2014). "Postprandial fatty acid specific changes in circulating oxylipins in lean and obese men after high-fat challenge tests." *Mol Nutr Food Res* **58**(3): 591-600.

Strassburg, K., Huijbrechts, A. M., Kortekaas, K. A., Lindeman, J. H., Pedersen, T. L., Dane, A., Berger, R., Brenkman, A., Hankemeier, T., van Duynhoven, J., Kalkhoven, E., Newman, J. W. and Vreeken, R. J. (2012). "Quantitative profiling of oxylipins through comprehensive LC-MS/MS analysis: application in cardiac surgery." *Anal Bioanal Chem* **404**(5): 1413-1426.

Stryer, L. (1995). *Biochemistry*.

Suhre, K. and Schmitt-Kopplin, P. (2008). "MassTRIX: mass translator into pathways." *Nucleic Acids Res* **36**(Web Server issue): W481-484.

Sun, Y., Su, Y. and Zhu, W. (2016). "Microbiome-Metabolome Responses in the Cecum and Colon of Pig to a High Resistant Starch Diet." *Front Microbiol* **7**: 779.

Syvaöja, E. L., Piironen, V., Varo, P., Koivistoinen, P. and Salminen, K. (1985). "Tocopherols and tocotrienols in Finnish foods: human milk and infant formulas." *Int J Vitam Nutr Res* **55**(2): 159-166.

Szylit, O. and Andrieux, C. (1993). "Physiological and pathophysiological effects of carbohydrate fermentation." *world rev nutr diet* **74**: 88-122.

Tanaka, Y., Takami, K., Nishijima, T., Aoki, R., Mawatari, T. and Ikeda, T. (2015). "Short- and long-term dynamics in the intestinal microbiota following ingestion of *Bifidobacterium animalis* subsp. *lactis* GCL2505." *Biosci Microbiota Food Health* **34**(4): 77-85.

Tatusov, R. L., Galperin, M. Y., Natale, D. A. and Koonin, E. V. (2000). "The COG database: a tool for genome-scale analysis of protein functions and evolution." *Nucleic Acids Res* **28**(1): 33-36.

Thomas, L. V., Ockhuizen, T. and Suzuki, K. (2014). "Exploring the influence of the gut microbiota and probiotics on health: a symposium report." *Br J Nutr* **112 Suppl 1**: S1-18.

Topping, D. L., Fukushima, M. and Bird, A. R. (2007). "Resistant starch as a prebiotic and synbiotic: state of the art." *Proceedings of the Nutrition Society* **62**(01): 171-176.

Tsukahara, T., Tsukahara, R., Fujiwara, Y., Yue, J., Cheng, Y., Guo, H., Bolen, A., Zhang, C., Balazs, L., Re, F., Du, G., Frohman, M. A., Baker, D. L., Parrill, A. L., Uchiyama, A., Kobayashi, T., Murakami-Murofushi, K. and Tigyi, G. (2010). "Phospholipase D2-dependent inhibition of the nuclear hormone receptor PPARgamma by cyclic phosphatidic acid." *Mol Cell* **39**(3): 421-432.

Turnbaugh, P. J., Ridaura, V. K., Faith, J. J., Rey, F. E., Knight, R. and Gordon, J. I. (2009). "The effect of diet on the human gut microbiome: a metagenomic analysis in humanized gnotobiotic mice." *Sci Transl Med* **1**(6): 6ra14.

Tziotis, D., Hertkorn, N. and Schmitt-Kopplin, P. (2011). "Kendrick-analogous network visualisation of ion cyclotron resonance Fourier transform mass spectra: improved options for the assignment of elemental compositions and the classification of organic molecular complexity." *Eur J Mass Spectrom (Chichester, Eng)* **17**(4): 415-421.

Ursell, L. K., Haiser, H. J., Van Treuren, W., Garg, N., Reddivari, L., Vanamala, J., Dorrestein, P. C., Turnbaugh, P. J. and Knight, R. (2014). "The intestinal metabolome: an intersection between microbiota and host." *Gastroenterology* **146**(6): 1470-1476.

Ussar, S., Fujisaka, S. and Kahn, C. R. (2016). "Interactions between host genetics and gut microbiome in diabetes and metabolic syndrome." *Mol Metab* **5**(9): 795-803.

Verberkmoes, N. C., Russell, A. L., Shah, M., Godzik, A., Rosenquist, M., Halfvarson, J., Lefsrud, M. G., Apajalahti, J., Tysk, C., Hettich, R. L. and Jansson, J. K. (2009). "Shotgun metaproteomics of the human distal gut microbiota." *ISME J* **3**(2): 179-189.

Villas-Boas, S. G., Mas, S., Akesson, M., Smedsgaard, J. and Nielsen, J. (2005). "Mass spectrometry in metabolome analysis." *Mass Spectrom Rev* **24**(5): 613-646.

Vu, H. S., Tamura, P., Galeva, N. A., Chaturvedi, R., Roth, M. R., Williams, T. D., Wang, X., Shah, J. and Welti, R. (2012). "Direct infusion mass spectrometry of oxylipin-containing Arabidopsis membrane lipids reveals varied patterns in different stress responses." *Plant Physiol* **158**(1): 324-339.

Wagele, B., Witting, M., Schmitt-Kopplin, P. and Suhre, K. (2012). "MassTRIX reloaded: combined analysis and visualization of transcriptome and metabolome data." *PLoS One* **7**(7): e39860.

Wahlen, E. and Strandvik, B. (1994). "Effects of different formula feeds on the developmental pattern of urinary bile acid excretion in infants." *J Pediatr Gastroenterol Nutr* **18**(1): 9-19.

Walker, A., Pfitzner, B., Neschen, S., Kahle, M., Harir, M., Lucio, M., Moritz, F., Tziotis, D., Witting, M., Rothballer, M., Engel, M., Schmid, M., Endesfelder, D., Klingenspor, M., Rattei, T., Castell, W. Z., de Angelis, M. H., Hartmann, A. and Schmitt-Kopplin, P. (2014). "Distinct signatures of host-microbial meta-metabolome and gut microbiome in two C57BL/6 strains under high-fat diet." *ISME J* **8**(12): 2380-2396.

Walker, A. W., Ince, J., Duncan, S. H., Webster, L. M., Holtrop, G., Ze, X., Brown, D., Stares, M. D., Scott, P., Bergerat, A., Louis, P., McIntosh, F., Johnstone, A. M., Lobley, G. E., Parkhill, J. and Flint, H. J. (2011). "Dominant and diet-responsive groups of bacteria within the human colonic microbiota." *ISME J* **5**(2): 220-230.

Whiteside, S. A., Razvi, H., Dave, S., Reid, G. and Burton, J. P. (2015). "The microbiome of the urinary tract--a role beyond infection." *Nat Rev Urol* **12**(2): 81-90.

WHO and FAO (2002). "Guidelines for the Evaluation of Probiotics in Food."

Wikoff, W. R., Anfora, A. T., Liu, J., Schultz, P. G., Lesley, S. A., Peters, E. C. and Siuzdak, G. (2009). "Metabolomics analysis reveals large effects of gut microflora on mammalian blood metabolites." *Proc Natl Acad Sci U S A* **106**(10): 3698-3703.

Wishart, D. S., Jewison, T., Guo, A. C., Wilson, M., Knox, C., Liu, Y., Djombou, Y., Mandal, R., Aziat, F., Dong, E., Bouatra, S., Sinelnikov, I., Arndt, D., Xia, J., Liu, P., Yallou, F., Bjorn Dahl, T., Perez-Pineiro, R., Eisner, R., Allen, F., Neveu, V., Greiner, R. and Scalbert, A. (2013). "HMDB 3.0--The Human Metabolome Database in 2013." *Nucleic Acids Res* **41**(Database issue): D801-807.

Wishart, D. S., Knox, C., Guo, A. C., Eisner, R., Young, N., Gautam, B., Hau, D. D., Psychogios, N., Dong, E., Bouatra, S., Mandal, R., Sinelnikov, I., Xia, J., Jia, L., Cruz, J. A., Lim, E., Sobsey, C. A., Shrivastava, S., Huang, P., Liu, P., Fang, L., Peng, J., Fradette, R., Cheng, D., Tzur, D., Clements, M., Lewis, A., De Souza, A., Zuniga, A., Dawe, M., Xiong, Y., Clive, D., Greiner, R., Nazyrova, A.,

Shaykhtudinov, R., Li, L., Vogel, H. J. and Forsythe, I. (2009). "HMDB: a knowledgebase for the human metabolome." *Nucleic Acids Res* **37**(Database issue): D603-610.

Wishart, D. S., Tzur, D., Knox, C., Eisner, R., Guo, A. C., Young, N., Cheng, D., Jewell, K., Arndt, D., Sawhney, S., Fung, C., Nikolai, L., Lewis, M., Coutouly, M. A., Forsythe, I., Tang, P., Shrivastava, S., Jeroncic, K., Stothard, P., Amegbey, G., Block, D., Hau, D. D., Wagner, J., Miniaci, J., Clements, M., Gebremedhin, M., Guo, N., Zhang, Y., Duggan, G. E., Macinnis, G. D., Weljie, A. M., Dowlatabadi, R., Bamforth, F., Clive, D., Greiner, R., Li, L., Marrie, T., Sykes, B. D., Vogel, H. J. and Querengesser, L. (2007). "HMDB: the Human Metabolome Database." *Nucleic Acids Res* **35**(Database issue): D521-526.

Witting, M., Lucio, M., Tziotis, D., Wagele, B., Suhre, K., Voulhoux, R., Garvis, S. and Schmitt-Kopplin, P. (2015). "DI-ICR-FT-MS-based high-throughput deep metabotyping: a case study of the *Caenorhabditis elegans*-*Pseudomonas aeruginosa* infection model." *Anal Bioanal Chem* **407**(4): 1059-1073.

Witting, M., Maier, T. V., Garvis, S. and Schmitt-Kopplin, P. (2014). "Optimizing a ultrahigh pressure liquid chromatography-time of flight-mass spectrometry approach using a novel sub-2µm core-shell particle for in depth lipidomic profiling of *Caenorhabditis elegans*." *J Chromatogr A* **1359**: 91-99.

Wolfer, A. M., Gaudin, M., Taylor-Robinson, S. D., Holmes, E. and Nicholson, J. K. (2015). "Development and Validation of a High-Throughput Ultrahigh-Performance Liquid Chromatography-Mass Spectrometry Approach for Screening of Oxylipins and Their Precursors." *Anal Chem* **87**(23): 11721-11731.

Wong, A., Sagar, D. R., Ortori, C. A., Kendall, D. A., Chapman, V. and Barrett, D. A. (2014). "Simultaneous tissue profiling of eicosanoid and endocannabinoid lipid families in a rat model of osteoarthritis." *J Lipid Res* **55**(9): 1902-1913.

Wong, J. M., de Souza, R., Kendall, C. W., Emam, A. and Jenkins, D. J. (2006). "Colonic health: fermentation and short chain fatty acids." *J Clin Gastroenterol* **40**(3): 235-243.

Xie, G., Zhang, S., Zheng, X. and Jia, W. (2013). "Metabolomics approaches for characterizing metabolic interactions between host and its commensal microbes." *Electrophoresis* **34**(19): 2787-2798.

Xiong, W., Abraham, P. E., Li, Z., Pan, C. and Hettich, R. L. (2015). "Microbial metaproteomics for characterizing the range of metabolic functions and activities of human gut microbiota." *Proteomics* **15**(20): 3424-3438.

Young, J. C., Pan, C., Adams, R. M., Brooks, B., Banfield, J. F., Morowitz, M. J. and Hettich, R. L. (2015). "Metaproteomics reveals functional shifts in microbial and human proteins during a preterm infant gut colonization case." *Proteomics* **15**(20): 3463-3473.

Ze, X., Duncan, S. H., Louis, P. and Flint, H. J. (2012). "Ruminococcus bromii is a keystone species for the degradation of resistant starch in the human colon." *ISME J* **6**(8): 1535-1543.

Zhang, A., Sun, H., Wang, P., Han, Y. and Wang, X. (2012). "Modern analytical techniques in metabolomics analysis." *Analyst* **137**(2): 293-300.

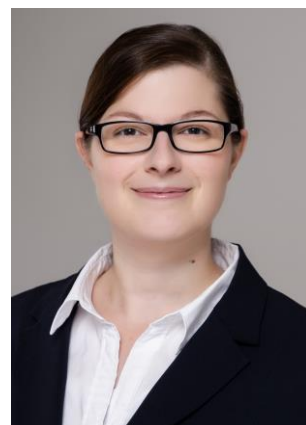
Zhou, A. L., Hergert, N., Rompato, G. and Lefevre, M. (2015). "Whole grain oats improve insulin sensitivity and plasma cholesterol profile and modify gut microbiota composition in C57BL/6J mice." *J Nutr* **145**(2): 222-230.

Zhou, Z., Zhang, Y., Zheng, P., Chen, X. and Yang, Y. (2013). "Starch structure modulates metabolic activity and gut microbiota profile." *Anaerobe* **24**: 71-78.

Curriculum vitae

Personal information

Name: Tanja Verena Maier
 Date and place of birth: September 22nd, 1986, Tübingen
 Nationality: German



Education and scientific work experience

- 11/2012 – 08/2016 **PhD candidate, Helmholtz Zentrum München GmbH, Research Unit Analytical BioGeoChemistry, Technische Universität München, Chair of Analytical Food Chemistry**
 Thesis: *Mass spectrometry based metabolomics to follow the prebiotic and probiotic impact on the human gut microbiome*
- 05/2015 Research stay, Pacific Northwest National Laboratory, Biological Sciences Division, Richland, WA, USA
- 10/2010 – 09/2012 **Master of Science in chemistry, Westfälische Wilhelms-Universität Münster**
 Grade: 1,9
 Thesis: Structure analysis for the elucidation of marker-substances of pathophysiological states in urine profiles, Grade: 1,0
- 03/2010 – 05/2010 Industrial placement, SAS Hagemann GmbH, Horb a. N., Germany
- 03/2009 – 08/2010 **Bachelor of Science in Applied Chemistry, Reutlingen University**
 Grade: 2,2
 Thesis: Alcoholysis of fatty acid ester with 2,2,2-Trichloroethanol for sensitive and direct detection by using GC-MS, Grade: 1,3
- 10/2006 – 02/2009 Eberhard Karls Universität, Tübingen, study programm: chemistry
- 09/2003 - 06/2006 **Abitur (University entrance qualification), Mathilde-Weber Schule, Tübingen**
 Grade: 2,5

Scientific Communications

Publications

Smirnov, K.S.; Maier, T. V.; Walker, A.; Heinzmann, S.S.; Forcisi, S.; Martinez, I.; Walter, J.; Schmitt-Kopplin, P.: *Challenges of metabolomics in human gut microbiota research*. Int J Med Microbiol. 306(5):266-79 (2016).

Witting, M.; Maier, T. V.; Garvis, S.; Schmitt-Kopplin, P.: *Optimizing an ultrahigh pressure liquid chromatography-time of flight-mass spectrometry approach using a novel sub-2 μ m core-shell particle for in depth lipidomic profiling of *Caenorhabditis elegans**.; J. Chromatogr. A 1359, 91-99 (2014).

Maier, T. V.; Schmitt-Kopplin, P.: *Capillary Electrophoresis in Metabolomics*, In: Capillary Electrophoresis – Methods and Protocols, Vol. 1483, 2016 (Book Chapter).

Bazanella, M., Maier, T. V., Clavel, T., Lagkouvardos, I., Lucio, M., Maldonado-Gómez, M. X., Aufran, C., Walter, J., Bode, L., Schmitt-Kopplin, P., Haller, D.: *Randomized controlled trial on the impact of early-life intervention with bifidobacteria on the healthy infant fecal microbiota and metabolome*. Am J Clin Nutr. 106(5):1274-1286 (2017).

Maier, T. V.; Lucio, M.; Lee, L. H.; VerBerkmoes, N. C.; Brislawn, C. J.; Bernhardt, J.; Lamendella, R.; McDermott, J. E.; Bergeron, N.; Heinzmann, S. S.; Morton, J. T.; González, A.; Ackermann, G.; Knight, R.; Riedel, K.; Krauss, R. M.; Schmitt-Kopplin, P.; Jansson, J. K.: *Impact of Dietary Resistant Starch on the Human Gut Microbiome, Metaproteome, and Metabolome*. mBio vol. 8 no. 5 e01343-17 (2017).

Oral presentations

Maier, T. V., Walker, A., Witting, M., Lucio, M., Heinzmann, S., Lamendella, R., Jansson, J., Schmitt-Kopplin, P.: *Lipidomics approach investigating the gut microbiome of insulin-resistant individuals by UHPLC-QToF-MS*; 30th International Symposium on Chromatography, 2014, Salzburg (A).

Posters

Maier, T. V., Bazanella, M., Clavel, T., Schmitt-Kopplin, P., Haller, D.: *Metabolomics approach investigating the fecal microbiota of breast-fed or formula-fed infants differentiating in probiotic and non-probiotic formula*. Department of Environmental Sciences (DES) Day 2016, Neuherberg, Germany.

Maier, T. V., Walker, A., Heinzmann, S., Lucio, M., Witting, M., Lamendella, R., Jansson, J., Schmitt-Kopplin, P.: *Comprehensive metabolomics of the gut microbiome applying different separation techniques coupled to mass spectrometry*; Analytical Tools for Cutting-edge Metabolomics – a joint meeting of the Analytical Division of the RSC and the International Metabolomics Society, 30th April 2014, London (UK).

Maier, T. V., Walker, A., Heinzmann, S., Lucio, M., Lamendella, R., Jansson, J., Schmitt-Kopplin, P.: *Effects of prebiotics on insulin resistance and the gut microbiome metabolism a non-targeted metabolomics study using FT-ICR-MS*; Metabolomics, 2013, Glasgow (UK).

Heinzmann, S.S., Walker, A., Maier, T. V., Smirnov, K.S., Lucio, M., Schmitt-Kopplin, P.: *Non-targeted Meta-Metabolomics approaches to study the importance of the gut microbiome on host metabolism*. Department of Environmental Sciences (DES) Day 2013, Neuherberg, Germany.

Eidesstattliche Erklärung

Ich erkläre an Eides statt, dass ich die bei der promotionsführenden Einrichtung Wissenschaftszentrum Weihenstephan für Ernährung, Landnutzung und Umwelt der Technischen Universität München zur Promotionsprüfung vorgelegte Arbeit mit dem Titel:

Mass spectrometry based metabolomics to follow the prebiotic and probiotic impact on the human gut microbiome

in Chemie am Lehrstuhl für Analytische Lebensmittelchemie unter der Anleitung und Betreuung durch apl. Prof. Dr. P. Schmitt-Kopplin ohne sonstige Hilfe erstellt und bei der Abfassung nur die gemäß § 6 Abs. 6 und 7 Satz 2 angegebenen Hilfsmittel benutzt habe.

- (x) Ich habe keine Organisation eingeschaltet, die gegen Entgelt Betreuerinnen und Betreuer für die Anfertigung von Dissertationen sucht, oder die mir obliegenden Pflichten hinsichtlich der Prüfungsleistungen für mich ganz oder teilweise erledigt.
- (x) Ich habe die Dissertation in dieser oder ähnlicher Form in keinem anderen Prüfungsverfahren als Prüfungsleistung vorgelegt.
- (x) Ich habe den angestrebten Doktorgrad noch nicht erworben und bin nicht in einem früheren Promotionsverfahren für den angestrebten Doktorgrad endgültig gescheitert.

Die öffentlich zugängliche Promotionsordnung der TUM ist mir bekannt, insbesondere habe ich die Bedeutung von § 28 (Nichtigkeit der Promotion) und § 29 (Entzug des Doktorgrades) zur Kenntnis genommen. Ich bin mir der Konsequenzen einer falschen Eidesstattlichen Erklärung bewusst.

Mit der Aufnahme meiner personenbezogenen Daten in die Alumni-Datei bei der TUM bin ich

- (x) einverstanden
- () nicht einverstanden

München, den

.....

Unterschrift